PLASTICITY CASCADES AND PLACE CELL ACTIVITY DIFFER IN NEW SPATIAL LEARNING BASED ON CONTEXT FAMILIARITY

ELLEN G. FRASER

Bachelor of Arts and Sciences, Quest University Canada, 2018

A thesis submitted

in partial fulfillment of the requirements for the degree of

MASTERS OF SCIENCE

In

NEUROSCIENCE

Department of Neuroscience

University of Lethbridge

LETHBRIDGE, ALBERTA, CANADA

PLASTICITY CASCADES AND PLACE CELL ACTIVITY DIFFER IN NEW SPATIAL LEARNING BY CONTEXT FAMILIARITY

ELLEN G. FRASER

Date of Defense: August 19th, 2020

Dr. Robert J. McDonald	Professor	Ph.D.
Thesis Supervisor		
Dr. Masami Tatsuno	Associate Professor	Ph.D.
Thesis Examination Committee Member		
Dr. David R. Euston	Associate Professor	Ph.D.
Thesis Examination Committee Member		
Dr. Robert Sutherland	Professor	Ph.D.
Chair, Thesis Examination Committee		

DEDICATION

To K. H., J. H, and K. C.

ABSTRACT

In these experiments I have studied the effects of context familiarity on new spatial learning on a protein, behavioural, and cellular scale. I found evidence that there is greater expression of plasticity products in MEC-connected regions of the HPC in novel context learning and LEC-connected regions of the HPC in familiar context learning. Also in this experiment I observed a greater effect in downstream proteins, supporting the convergence of these cascades. In the second set of experiments I introduced the dry-land contextual navigation task and demonstrated learning in it. Furthermore, I compared the results in this task with rats in a water-based task and found that win-stay tendencies differ between the two tasks. Finally, in the last experiment I assessed place-cell activity in dorsal CA1 in freely-behaving mice in the DCNT. I found evidence of global remapping but not encoding of the reward.

ACKNOWLEDGEMENTS

First and foremost, I'd like to thank my supervisor, Dr. Robert McDonald. He set a very high standard for academic supervision, and I'd like to thank him for taking a chance on me and this project. I'd also like to thank the many faculty members who I've had the privilege of learning from. Dr. Masami Tatsuno, thank you for your additional teaching and patience as I learned new methods for analyzing this data. Thank you, Dr. Robert Sutherland for welcoming me to lab meetings, and for chairing my defense committee. Thank you, Dr. David Euston for your thorough feedback as a member of my committee. I'd also like to thank Dr. Neal Melvin for his continued support of my scientific journey.

I have had the immense privilege of collaborating throughout these projects. I'd like to thank Dr. J. Quinn Lee, and Erin Falkenberg for their technical expertise, training, and support. Charithe Bonifacio, Tyler Trudel, Ty Marakowski, Deesha Apparaju, Keva Klamer, and Tyrone Moline, thank you all for your honours and independent study work which were direct contributions to the data presented here. This thesis would not have been possible without your time, thoughtful questions, and efforts. Dr. Maurice Needham, Nhung Hong, Isabelle Gauthier, Moira Holley, Karen Dow-Cazal, Di Shao, and Dr. Helen Kelley, thank you for your support of the services that were essential for this thesis. To my peers: Abby Nixon, Rebecca McHugh, and Surjeet Singh, thank you for being great friends and coffee-mates.

Finally, I have the utmost gratitude for my friends and family. To my family, Ming and John Fraser, thank you for your endless support and guidance. Kurtis Cridland, thank you for keeping me balanced. Carling Pang, Danielle Macina, and Kate Benner,

thank you all for the many long phone calls, for your patience and laughs along the way. Anissa Gamble, thank you for your thorough and honest feedback on this document.

TABLE OF CONTENTS

LIST OF FIGURES

CHAPTER 1: GENERAL INTRODUCTION

One of the central tenants of learning and memory function is synaptic plasticity, the theory that memory has a physical manifestation in our brains which allows for synapses to communicate more effectively as a result of stimulation (Hebb, 1949; Pavlov, 1927). Another dominant theory of learning and memory function is that different parts of the brain are functionally dissociable (Kandel et al., 2014). Studying how these two theories engage with one another requires interpolation from a cellular to a systems level. Furthermore, as a much of our systems-level understanding of learning and memory function is based in behavioural neuroscience, their processing styles are theoretical in nature. Therefore, studying this combination necessitates pairing the concrete functional understanding of plasticity mechanisms with the theoretical/conceptual understanding of memory systems.

The experiments included in this thesis target a learning and memory system thought to be centered on the hippocampus, and differences between familiar and novel context learning. By targeting the hippocampal system, this thesis draws upon the theory of Multiple Parallel Memory Systems (MPMS) (White & McDonald, 2002). The general introduction discusses MPMS, context learning, NMDA-LTP and plasticity cascades, NMDA receptors in the hippocampal system, and entorhinal cortex-hippocampus connectivity with respect to context learning. These subjects provide a background for context learning which spans from the protein to cellular to systems to behavioural levels.

Multiple Parallel Memory Systems

The MPMS idea was originally inspired by various double and triple dissociations of learning and memory function and (Packard, Hirsh, White, 1989; Sutherland and

McDonald, 1990; McDonald & White, 1993), and elaborated upon theoretically as multiple parallel memory systems that influence behaviour on their own or in some instances interact (White & McDonald, 2002). The theory identifies a model for information processing in which information is processed in parallel in multiple brain regions; the coherence of the information with the processing style of each region dictates that region's contribution to the memory's function. Furthermore, the theory postulates both key elements of the processing styles for each of the proposed regions, as well as how the parallel outputs from each of these regions interact with one another.

The basis for the models of each system are stimulus inputs, reinforcers, and response outputs (Figure 1.1). These components are the elements of a generalized learning situation and can be both internal as well as external. Stimuli include both external cues and reinforcers, as well as internal affective states. Responses include both observable (and therefore external) behaviours, as well as unobservable (or internal) autonomic responses and modulators. Unobservable autonomic responses include neural activity, neurotransmitter release, and hormonal changes. Modulators include whether the memory is strengthened or enhanced. Together, these elements and their relationships in the different memory systems illustrate their respective processing styles.

The models for each system demonstrate how these components interact in pure tasks; pure tasks for a given region are extremely coherent with the processing style of that region. The pure tasks identified in the 2002 review were applied to the 8-arm radial maze and include: win-shift for the hippocampus system, win-stay for the dorsal striatum system, and conditioned cue preference for the amygdala system. The experiments addressed in the review compared rats with fimbria-fornix, dorsal striatum, and/or lateral

nucleus of the amygdala lesions, to isolate the hippocampus, dorsal striatum, and amygdala systems, respectively, and demonstrated characteristics of their processing styles based on the requirements of each task.

While the proposed systems process in parallel, their outputs interact in a plethora of ways: cooperatively/competitively, within/between subsystems, as necessary or incidental processes, and their balance can be altered through systemic changes. As such, afferents and efferents for these systems can be indicators of their interactions. These interactions have been defined in the Interactive Memory Systems Theory (IMST) (McDonald, Devan, & Hong, 2004). These interactions influence behaviour, as different processing styles can result in different behavioural conclusions. Therefore, mediating the relationships between these systems is critical for appropriate responses, and altering the interactions between memory systems can explain a variety of psychiatric disorders.

Hippocampus System

The hippocampus system is thought to be involved in stimulus-stimulus learning. For this type of associative learning, each stimulus experienced during an event is associated with others present, independent of responses or behaviour (Figure 1.2). Evidence for this model is provided in a win-shift version of the radial arm maze, where an animal is required to retrieve a single food pellet from the end of each arm. This task required animals to *reference* previously entered arms, presumably using spatial information, and incorporate this memory throughout the trial. The importance of the hippocampal system for reference memory is consistent with other prominent theories of hippocampus function including: cognitive mapping theory (O'Keefe & Nadel, 1978), relational representation (Eichenbaum, 1994), and configural association theory

(Sutherland & Rudy, 1989). In each of these theories, there is a clear role of hippocampus in the flexible use of representations. Similarly, the hippocampal system, as outlined in MPMS is responsible for incorporating specific information about stimuli into subsequent behaviours, like which arms are depleted of food in the win-shift variation of the radial arm maze.

Structural data about the hippocampus supports its role in stimulus-stimulus learning. The hippocampus' structure is a trisynaptic circuit where information flows from entorhinal cortex, through the perforant path to the dentate gyrus, through mossy fibers to CA3, through Schaffer collaterals to CA1. This organization has been proposed to allow the hippocampus to act as an index (Buzsáki & Tingley, 2018; Teyler & DiScenna, 1986), through which representations can be separated or 'filled in' (completed) (Neunuebel & Knierim, 2014). The hippocampal formation includes entorhinal cortex, subiculum, and the traditional subfields of the hippocampus (dentate gyrus, CA3, and CA1). The formation has anatomical connections throughout cortical and subcortical regions (see Knierim, 2015 for review). Hippocampal afferents support its role generating associations between stimuli, as outputs are targeted to higher level structures that can regulate behaviour.

Striatum System

The dorsal striatal system is thought to be involved in stimulus-response learning. In this form of associative learning, a stimulus is associated with a specific response due to its temporal contiguity with a reinforcer (Figure 1.3). Evidence for this model is provided in a win-stay version of the radial arm maze. In this version, arms of the maze that were cued with a light indicated that there was a food reward at the end of the arm.

Unlike the win-shift version, this task required that animals associated lit arms with the reward, irrespective of the arm's spatial location or previously entered arms. The automatic response that an animal develops to the stimulus make this behaviour habitual, unlike stimulus-stimulus or stimulus-reinforcer learning in other systems.

The dorsal striatum primarily receives input from somatic sensorimotor subnetworks. The direct and predominant convergence of motor and sensory information in the dorsal striatum supports its role in stimulus-response learning (Hintiryan et al., 2016). Furthermore, stimulus-response associations are supported by a variety of feedback pathways from the superior colliculus, thalamus, and globus pallidius. Dopaminergic inputs from the midbrain and feedback pathways may also affect affective states and modulation. The primary striatal outputs are to the globus pallidius, thalamus, subthalamic nucleus, and the substantia nigra (see Dudman & Gerfen, 2015 for review). The thalamus also sends projections to the prefrontal cortex through the thalamo-cortical pathway, which supports the MPMS theory which incorporates parallel processes information at higher processing structures.

Amygdala System

The amygdala system has been implicated in stimulus-reinforcement learning (Figure 1.4). For this form of learning, a neutral stimulus becomes associated with reinforcement and this results in a conditioned affective response. This learning was demonstrated through a cued-context conditioning version of the radial arm maze. In this version rats were contained in two different arms, one that was supplied with food and another that wasn't. A cue (small light) was present in one of the two arms so that they were distinguishable. During stimulus-reinforcement learning, the neutral stimulus (arm)

becomes *conditioned* with the reinforcer (food) and can result in responses elicited by the reinforcer. This differs from stimulus-response learning because in S-R learning the reinforcer modulates the relationship between the stimulus and response, and therefore could modulate the relationship between any set of stimuli and responses. Meanwhile, in stimulus-reinforcement learning, the association is made between the stimulus and reinforcer. The reinforcer can modulate this relationship by virtue of its either appetitive or aversive nature, but any responses are unconditioned to the reinforcer.

Inputs to the amygdala are thought to be involved in emotional memories and motivation, while the outputs are thought to be involved in emotional behaviours. Inputs include olfactory bulb inputs, sensory inputs relayed through the thalamus, sensory cortices inputs, and endocrine inputs (see Olucha-Bordonau, Fortes-Marco, Otero-García, Lanuza, & Martínez-García, 2015 for review). The high level of input from sensory regions supports the integration of sensory information with reinforcement information in the amygdala. Furthermore, endocrine inputs provide enhancement of this learning in stressful conditions, and in the context of socio-sexual behaviours (Roozendaal & McGaugh, 1997). Amygdala efferents include: associative frontotemporal cortical areas, prefrontal cortex, perirhinal, insular, and hippocampal cortices, thalamus, and striatum (Olucha-Bordonau et al., 2015). The amygdala's diverse efferents support its role controlling the expression of stimulus-reinforcement associations. Furthermore, its efferents support the eventual convergence of information processed there in higher-order processing regions where it can be related to information processed in parallel in other systems.

Context

All learning takes place somewhere, in some context. One context is defined as, "a set of concurrent independent component features that potentially can be sampled by an individual" (Rudy, 2009). These component features include place, spatial cues, scent, and circumstances leading up to the event. Rudy has defined two properties that define a context: stability, and variation. Stability, a concept concerning context also supported by Nadel (2008), describes stable features of a context that make it identifiable and are unchanging regardless of if they are experienced. In our experiments, experience is defined by stimulus which incites a physiological response in the animal. The variation property of context suggests that cues and stimuli may change within a given context, and that this is an important factor when a subject is trying to learn contingencies related to that context. The variation concept of context, however, does not indicate when these changes constitute a new context. This becomes relevant when comparisons are made between context experiments and "morphing" experiments, wherein which one context is gradually changed into another (Leutgeb et al., 2005). The balance between contextual stability and variation on a physiological level may come down to pattern completion, which is the process by which an animal uses the similarity between a stimulus input and memory to appropriately predict, in this case, context.

Contexts and how they are represented in the brain, are an area of prominent research amongst systems neuroscientists, both the theory of context representations (McDonald & White, 1993; O'Keefe & Nadel, 1978; Sutherland & Rudy, 1989) and physiological basis of context representations (Alme et al., 2014; Knierim, 2002). In this literature, contexts appear to be represented in multiple brain regions including

neocortical system, entorhinal cortex, and hippocampal formation (Rudy, 2009). Despite being represented in multiple brain regions, these representations are evidently not equivalent. The hippocampus and its representations of space have been studied extensively with respect to context (Rudy, 2009). However, while deficits are observed in HPC lesion animals when context conditioning is trained rapidly, they are not observed when these representations are developed over distributed sessions (Lehmann et al., 2009). Therefore, while the hippocampus has been the centre of context research, it is not the only system involved or responsible, and the components of the context may be stored differently based on how the learning takes place.

For example, in the theory of multiple parallel memory networks (MPMN), regions such as the hippocampus, amygdala, perirhinal cortex, and dorsal striatum can all store components of a context (Fraser & McDonald, 2020). An example of how these systems process the same event is shown in Figure 1.5. The hippocampus network acquires and stores complex representations of the relationships of the stimuli that make up an event as well as the temporal order of events. The amygdala network acquires and stores environmental stimuli that signal the presence of reinforced events. The perirhinal system acquires and stores visual object and scene stimuli and participates in recognition using this information. Finally, the dorsal striatum acquires and stores associations between stimuli that are associated with a reinforced response. Therefore, all these regions store some kind of context information, and the dominance of these systems depends on the learning event that takes place.

The association between learned events and contexts has been studied rigorously in animal behaviour through tasks like fear conditioning to context. In this paradigm, an

animal is placed in a chamber for a minute or two and shocked. During the testing phase the animal is placed into that same chamber and without the shock they show the learned response through freezing behaviour (Blanchard et al., 1976). The learning in this task is easily measured and rapidly acquired, however the neural systems responsible for this learning differs based on how the experiment is conducted. If the hippocampus is lesioned prior to training, the animals shows few deficits during testing, but if the hippocampus is lesioned after training, the animals show significant deficits during testing (Maren et al., 1997). Therefore, the task is sensitive to hippocampal dysfunction in the retrograde but not anterograde directions. Furthermore, in retrograde experiments, the aforementioned Lehmann 2009 results demonstrated that distributed training sessions rendered context fear conditioning hippocampus independent. What research using context fear conditioning has demonstrated is that context learning can take place in multiple memory systems, is distributed to be hippocampus-independent with more training sessions, but that with a single-trial paradigm is preferentially dependent on a learning and memory system centered on the hippocampus.

A circumstance in which context is extremely important for learning is spatial navigation, because contextual information is used in this learning. In contrast with other forms of context learning, where stimuli is uses purely for identification or recognition. As such, a variety of tasks have addressed this type of learning including the Morris Water Task, 8-arm radial maze, and virtual environments (Harvey et al., 2009; McDonald and White, 1993; Morris et al., 1982). In research studying NMDA receptor antagonism in context learning, all of these tasks have been used (Bye & McDonald, 2019; Caramanos & Shapiro, 1994; Taylor et al., 2014).

Context representations

The importance of cellular representations of space originates from the theory of cognitive mapping. This theory originated prior to the many of the techniques we use today to examine how cells in numerous networks represent space when Tolman observed that rats, given the opportunity to freely explore, took shortcuts to a baited location in later trials (Tolman & Honzik, 1930). In another experiment, they also found that when parts of the maze were blocked, rats were able to selectively navigate new ones (Tolman et al., 1946). The prior exploratory period in the maze informed the rats' behaviour in the baited trials, prompting Tolman to hypothesize that the brain generated a representation of the space during the exploration to be used later. Later, this representation was applied literally in *The Hippocampus as a Cognitive Map*, where this theory argues that the spatial framework is generated in the hippocampus to represent space (O'Keefe & Nadel, 1978). Evidence for this spatial framework can be found across the hippocampus and entorhinal cortex, and notably in place cells in CA1 (O'Keefe & Dostrovsky, 1971).

In novel contexts, new cellular representations are developed through global remapping (Wilson & McNaughton, 1993). This new population code is made up of cells that fire when the animal is in a specific location, and as the animal moves around the context different cells fire to represent these areas. While there is chance overlap of active cells in distinct contexts, overlap is greater in CA1 than CA3 place fields (Leutgeb et al., 2004). In different shaped contexts, cellular representations differ, and with repeated exposure they continue to diverge (Lever et al., 2002). Furthermore, when context shapes are gradually morphed from one shape into another, incremental plastic changes are observed in the place representations at each morphed stage (Leutgeb et al., 2005).

Pattern separation and pattern completion are neural processes that may be key to accurately learning about different contexts, events associated with them, and the ability to elicit appropriate behaviours when re-encountered. Pattern separation is the process by which representations with similarity are discernable, and pattern completion is the process by which a complete representation can be recruited with an incomplete set of inputs (Sahay et al., 2011). These theories are, in part, based on physical patterns of cellular activity in the brain. It has been proposed that attractor networks are the mechanism underlying spatial maps. Attractor networks allow for an entire network to be activated when limited stimuli are present, allowing for context recognition. Furthermore, different contexts appear to have different attractor networks. This is further supported by another morphing experiment in which sharp changes in place fields were observed between morphed contexts (Wills et al., 2005). These data appear to contradict the previously cited Leutgeb experiments (2005), however this may not be the case. Attractors may not be discrete, but exist on a continuum (Tsodyks, 2005).

Other cellular representations of space have been found in the entorhinal cortex include border (Savelli et al., 2008; Solstad et al., 2008) and grid cells (Fyhn et al., 2004; Hafting et al., 2005). More recently, the hippocampal representations of other context features like objects (Høydal et al., 2018), other subjects (Danjo et al., 2018), goals (Sarel et al., 2017), and rewards (Gauthier & Tank, 2018) have been studied.

In summary, historical evidence of context representations comes from behavioural experiments and since, evidence of cellular representations of context and mechanistic theories about the storage and recruitment of these representations have made great advances. Contexts, and their contents are represented by populations of cells. A

dissimilar set of inputs can be distinguished through pattern separation, and with an incomplete set of inputs, these representations can be recruited through pattern completion and the attractor networks that support them.

NMDA-Long Term Potentiation

Early *in vivo* work isolated the memory trace in *Aplysia Californica* to modifications in a set of synapses (Kandel, 1976). This discovery, in combination with early *in vitro* studies, resulting in the discovery of long term potentiation (LTP) (T. V. P. Bliss & Lømo, 1973) have laid the groundwork for our basic understanding that learning and memory are based on long-term changes in synaptic efficacy. The study of memory at this level (molecular and synaptic) has not yet been applied to MPMS, however many studies have antagonized mechanisms responsible for LTP in the aforementioned systems. As such, this chapter focuses on one of the mechanisms for initiating LTP, NMDA receptors (Collingridge et al., 1983), and applies our understanding of the NMDAR-dependent LTP (NMDA-LTP) in specific memory systems to the greater MPMS theory.

NMDA receptors (NMDAR) are an ionotropic glutamate receptor whose activation results in the influx of calcium and sodium ions inside the cell. The work of Collingridge et al, studying *in vitro* LTP in Schaffer-collateral projections onto CA1 of the hippocampus, determined that NMDAR are necessary for the induction of LTP (1983). The influx of calcium ions through NMDAR allows for a plethora of post-synaptic biochemical cascades that lead to strengthening of synapses through physical changes to dendritic spines (Cingolani & Goda, 2008), and the increase of other glutamate receptors which increase the efficacy of these synapses with subsequent

stimulation (Bear & Malenka, 1994). Furthermore, NMDAR dependence is also demonstrated pre-synaptically, in CA3 excitatory post-synaptic potentials (e.p.s.cs) when stimulation was applied to mossy fibres (Weisskopf & Nicoll, 1995). Some pre-synaptic changes associated with LTP include increased concentrations of glutamate, transient increases in calcium concentrations at the pre-synaptic terminal which allow for greater responses in subsequent stimulations, and increased probabilities for vesicular fusion at potentiated synapses (see Bliss & Collingridge, 2013 for review). Changes at both pre-synaptic and post-synaptic sites are important for learning and memory function, as proposed by coincident signalling (Bourne & Nicoll, 1993), and NMDARs play an important role in the function at both sites.

NMDA-dependent function has been measured at both the cellular and behavioural levels. While previous *in vitro* work makes it clear that NMDA receptors are necessary for the induction but not maintenance of LTP (Collingridge et al., 1983), *in vivo* results at both the cellular and behavioural levels are less consistent. *In vivo* results are of relevance to MPMS, since currently, parallel multisensory processing cannot be studied *in vitro*, however dynamics of specific systems with NMDAR blockade *in vitro* my provide clues for what we observe *in vivo*.

Cellular dynamics have been defined in specific memory systems, like place fields in the hippocampus. Behavioural dynamics, as mentioned previously, exist as either pure tasks or impure tasks for a given memory system. For example, while MPMS demonstrates affirming results using variations of the radial arm maze, much of the NMDA-blocked behavioural literature is based on tasks such as the Morris water task (MWT), or fear conditioning, which have been shown be both dissociative between

different memory systems, and use combinations of these memory systems based on the specific procedures used and if lesions occur in the retrograde or anterograde directions (Antoniadis & McDonald, 2000; McDonald, Lo, King, Wasiak, & Hong, 2007; McDonald et al., 2010). Therefore, how the procedures used in these tasks specifically support or require stimulus-stimulus, stimulus-response, and/or stimulus-reinforcement associations is of importance for behavioural dynamics in experiments antagonizing the role of NMDAR in these memory systems. The role of NMDAR in a given memory system can be assessed either through specific infusion of the antagonist in that area, or through assessment in tasks whose performance is impaired with lesions of that area.

Plasticity Cascades downstream of NMDA-LTP

Current evidence suggests that lasting synaptic changes can be categorized into four sequential stages: generation, stabilization, consolidation, and maintenance (Lynch, Rex, & Gall, 2007). These stages are characterized by biochemical cascades that take place in the synapse and support the strengthening of these synapses. In chapter 2, we focused on five different proteins that have been identified in these cascades: NMDAR, calcium/calmodulin-dependent protein kinase II (CaMKII), cAMP response element-binding protein (CREB), and AMPAR subunits.

One requirement of LTP expression is that the influx of Ca^{2+} becomes translated into sustained changes in the synapse. CaMKII's autophosphorylation is believed to support sustained changes in the synapse because it is involved in both changing synaptic structure and enhancing the function of glutamate receptors (Shonesy et al., 2014). Thr286 autophosphorylation of CaMKII allows it to remain active beyond the Ca^{2+} signal window (Ohsako et al., 1991). CaMKII influences glutamate receptor activity by

increasing the trafficking of AMPAR to the post-synaptic terminal (Lisman et al., 2002), and synaptic structure by phosphorylating transcription factors like CREB (Ma et al., 2015). CREB is a transcription factor which is responsible for the transcription of many immediate early genes (IEGs) which have gained popularity as cellular indicators of activity (Greenberg et al., 1992). Genes whose transcription is supported by CREB, and support trace consolidation are associated with generating long lasting changes in dendritic spine shape, like Arc, or further regulate gene expression, like c-fos (Farris et al., 2017). Trace consolidation provides long-lasting structural support for the group of cells that make up the memory trace.

The synaptic changes that support learning are book-ended by AMPAR subunit dynamics. During generation, AMPAR containing the GluA1 subunit are trapped in the post-synaptic density. During maintenance, AMPAR containing the GluA2 subunit are trafficked into the post-synaptic density and replace the GluA1s (Shi et al., 1999). This increases Ca^{2+} permeability (Rudy, 2013).

Of the five proteins being studied in these experiments, all of them show either increased expression, or impairments when knocked out/blocked during spatial learning or during novel environment learning, when these experiments were conducted. These experiments were inspired by our previous work with NMDAR blockade where we demonstrated that the receptors were necessary for new learning in a novel context but not a familiar one (Bye & McDonald, 2019). In mice with mutated CaMKII, spatial memory impairments have been observed in the water task and Barnes maze (Bach et al., 1995; Silva et al., 1992), however no deficits were shown in contextual fear conditioning (Bach et al., 1995). Increases in pCREB expression have been observed in both the radial

arm maze and water task forms of spatial learning (Mizuno et al., 2002; Porte et al., 2008). Furthermore, open field tests have shown increased pCREB expression in novel contexts (Moncada & Viola, 2006). AMPAR show a combination of effects. In mice lacking GluA1 subunits, deficits were observed in non-matching to sample spatial learning tasks but not matching to sample spatial learning tasks (Reisel et al., 2002). In mice with a mutation that made GluA1 subunits unable to be phosphorylated, spatial learning deficits were observed (Lee et al., 2003). All together, these data demonstrate that the five proteins selected are important for spatial learning, however the story is incomplete.

Role of NMDA Receptors in the Hippocampus System

Experiments in the hidden-platform MWT, a hippocampus-dependent task (McDonald & White, 1994; Morris, Garrud, Rawlins, & O'Keefe, 1982; Sutherland, Whishaw, & Kolb, 1983; Sutherland, Kolb, & Whishaw, 1982), demonstrated that NMDAR are necessary for its acquisition (Morris et al., 1986). Similarly, in a hippocampus system pure task, NMDAR genetic knock outs (NMDAR-KO) result in performance deficits (Bannerman et al., 2012). These experiments not only provide key evidence for the role of hippocampal-LTP in learning, but it also that this learning was NMDA-LTP dependent. These results were replicated by Saucier and Cain, and this group also added a pre-trained condition (1995). In spatial navigation hippocampus-dependent tasks, pre-training appears to be key to NMDA-dependent learning. Saucier and Cain demonstrated this on both a cellular and behavioural level by recording e.p.s.ps in the dentate gyrus, and performance in a rapidly acquired hidden platform MWT (training time < 1 hr). Rats treated with an NMDAR antagonist show no increase in

e.p.s.p slope or population spike from baseline either 1 hour or 24 hours after high-frequency trains, whereas controls demonstrate increases in both. In behaviour, similarity was observed between pre-trained groups regardless of drug treatment, while a clear deficit was observed in later trials between naïve controls and naïve drug treated groups. The effect of pre-training is observed both when pre-training consists of hidden platform locations are pseudorandom (Saucier & Cain, 1995), and when they are consistent (McDonald et al., 2005). This effect is, however, only observed when pre-training takes place in the training context (Bye & McDonald, 2019).

There are many dominant theories of hippocampus function (Nadel & Moscovitch, 1997; O'Keefe & Nadel, 1978; Rudy & Sutherland, 1995; Teyler & DiScenna, 1986). While these theories differ significantly, every theory listed here agrees that spatial information is stored or referenced in the hippocampus, even if the representation is part of a larger set of sensory inputs. Our observations that NMDAR-dependent learning is pretraining context-specific (Bye & McDonald, 2019), are consistent with the activity of place cells in the presence of NMDAR antagonists (Kentros et al., 1998; Sheffield et al., 2017; Taverna et al., 2005). Kentros et al. determined that NMDAR are necessary at initial exposure for the stability of environment specific firing patterns (1998). This finding, that place field stability is NMDAR-dependent, has been supported further with a variety of techniques. In a virtual environment, the same effect is shown in somatic calcium transients. In a novel context, NMDAR-KO mice show significantly fewer transients during the last 8 laps of the environment than wild-type mice, while no significant is observed during the first 8 laps. Furthermore, of all active neurons in the novel environment, a significantly smaller fraction show place-specific

firing in NMDAR-KO mice than wild-type (Sheffield et al., 2017). Enhanced LTP, regulated by NMDA receptors in a nociceptor knockout mouse (Taverna et al., 2005), and in other models (McHugh et al., 1996; Nakazawa et al., 2002), also result in unstable place fields. Therefore, appropriate spatial representations in the hippocampus rely on the regulation of NMDAR activity and expression.

These behavioural and cellular phenomena can also be matched to our understanding of stimulus-stimulus learning in the hippocampal system. While NMDAR blockade impairs stimulus-stimulus learning, it does not impair modifications of the pre-established associations during learning (McDonald et al., 2005). Therefore, in the hippocampal system, NMDAR are necessary for stimulus-stimulus learning, and consolidation of the modulations to stimulus-stimulus associations.

Arguments that contradict these previous reports have also been made, that MWT learning in a novel environment is not NMDAR-dependent, however, it appears that major procedural differences in the MWT account for these results. While Bannerman et al. have shown that rats, pre-trained in a different context from which they were tested, do not exhibit NMDAR-dependent learning in the MWT, this testing was prolonged (1 trial per day for 8 days) (1995), rather than rapid (as exhibited by Saucier and Cain (1995), McDonald et al. (2005), and Bye & McDonald (2019)).

All together these results demonstrate that NMDAR-dependent hippocampus functions are: prolonged or rapid learning in a novel context, consolidation after rapid learning in a familiar context. Furthermore, in the stimulus-stimulus model of the hippocampus system proposed by MPMS, NMDAR are necessary for consolidating any

modulations to stimulus-stimulus associations, and encoding stimulus-stimulus associations.

Entorhinal Cortex-Hippocampal Projections and Context

Major input into the hippocampus comes from the entorhinal cortex (EC) via the perforant path. The entorhinal cortex is primarily split between its medial and lateral areas, MEC and LEC, respectively. These regions have been thought to have different functional significance, with the MEC attributed to 'where' and the LEC attributed to 'what'. The functional differences can be observed in both lesion, and cell activity literature. Lesions of the medial perforant path (MPP), but not lateral perforant path (LPP) impair place learning in the water task (Ferbinteanu, Holsinger, & McDonald, 1999). Furthermore, place cells have been recorded in the MEC (Quirk, Muller, Kubie, & Ranck, 1992), and lesions to the MEC impair the accuracy of firing fields in CA1 of the hippocampus (Brun et al., 2008). Not only are these two regions functionally dissociable, but their connections to other fields of the HPC also differ.

Highlighted by Cembrowski and Spruston (2019), there is molecular, circuit, and behavioural heterogeneity within subfields of the HPC. Of note, this heterogeneity exists in proximodistal anatomical connectivity to EC, and in trends in proximodistal recruitment for spatial learning. There is extensive literature regarding dentate gyrus – EC connectivity (Dolorfo & Amaral, 1998; Hjorth-Simonsen & Jeune, 1972; Köhler, 1985; Wyss, 1981). Generally, MEC and LEC preferentially project to enclosed and exposed dentate gyrus (DG), respectively, but has been previously reviewed (Amaral & Witter, 1995). Assessment of this functional heterogeneity, related to this anatomical heterogeneity has produced mixed results. For example, spatial exploration and brief

spatial experiences result in greater activation of the enclosed blade (Chawla et al., 2005; Chawla, Sutherland, Olson, McNaughton, & Barnes, 2018) of the DG. The functional relationship between spatial experience and the enclosed blade, and the anatomical relationship between MEC and the exposed blade contradict the extensive literature that highlights the spatial role of MEC.

In CA1 and CA3, the functional relationship between MEC and LEC connectivity and recruitment for spatial learning is consistent with anatomical trends. In CA1, this heterogeneity has been focused along the transverse axis to support spatial versus non-spatial tasks. The trends in CA1 show that there are preferential connections between proximal CA1 and MEC, and between distal CA1 and LEC (Knierim, Neunuebel, & Deshmukh, 2014). These anatomical trends are then mirrored in the recruitment of these areas for spatial and non-spatial tasks, respectively (Hartzell et al., 2013; Henriksen et al., 2010). It has been reported that there are no anatomical gradients between medial or lateral entorhinal cortex connectivity along the transverse axis of CA3 (Sun et al., 2017). Functional differences, however, have been reported. Distal CA3 is preferentially recruited in spatial learning tasks (Flasbeck, Atucha, Nakamura, Yoshida, & Sauvage, 2018), and this recruitment is correlated with activation of the MEC, measured by c-fos expression (Nakazawa, Pevzner, Tanaka, & Wiltgen, 2016). Whereas proximal CA3 is preferentially activated in non-spatial learning tasks (Nakamura, Flasbeck, Maingret, Kitsukawa, & Sauvage, 2013).

In addition to spatial versus non spatial learning, differences in the roles of LEC and MEC have been found within spatial learning tasks. In a recent commentary, Nilssen

et. al. (2019) highlight that changes to context, sensory input over time, are supported by LEC, while allocentric representations of context are supported by MEC.

Purpose and projects

In the present experiments I have assessed differences between novel and familiar context new learning on multiple scales. In the first set of experiments we have assessed differences in the expression of different plasticity proteins, measuring differences in context learning on the protein scale. In later analyses of these experiments we assessed how the patterns of expression differed along the transverse and long axes. We based our hypotheses on the connectivity patterns between MEC and LEC with HPC along these axes, measuring differences in context learning on a system level. In the next set of experiments, we introduced a novel spatial learning task in mice and assessed learning outcomes in it, as well as compared behaviour with that of rats in the MWT. This set of experiments measured differences in context learning on a behavioural scale. Finally, in the last experimental chapter we used miniature microscopes in the dry-land contextual navigation task. In this experiment we assessed encoding similarity between familiar and novel context learning, and the distribution of encoding properties within the population of cells we recorded from. All together, these experiments provide a multi-scale approach to understanding spatial learning in familiar or novel contexts.

CHAPTER 2: PLASTICITY CASCADES

Introduction

Neurobiologists believe that learning and memory has a physical basis and want to understand what properties of the brain allow it to acquire and maintain information generated by our experiences. A central theory of how learning takes place in the brain is based on the idea of synaptic plasticity, neurons that have correlated firing will strengthen their synaptic connections, allowing them to communicate more effectively with one another (Hebb, 1949; Pavlov, 1984). This plasticity in the ensemble of neurons activated during the original experience allows a representation of the information to persist and allow for retrieval under the right conditions.

Key experimental evidence for the idea that synaptic plasticity supports learning and memory processes in the mammal came from the work of Bliss and Lømo (1973) who studied the ways in which patterns of electrical activity in neurons can alter the way that brain regions communicate with one another. Their work focused on the hippocampus (HPC), in many ways an ideal system to study synaptic plasticity because of its unique intrinsic organization. One striking component of HPC anatomical organization is the trisynaptic circuit in which there are well delineated layers of neurons in subfields of the structure that project via large axon bundles to the dendritic trees of neurons in another subfield and then those neurons project to another subfield further down the circuit. This organization was of interest to neurophysiologists because it was possible to study neurons from one subfield that were connected to another subfield and to determine if you could artificially modify the strength of synapses connecting these regions.

These investigators stimulated an axon bundle, perforant path, originating from neurons in the entorhinal cortex and recorded from dentate gyrus neurons, the recipients of that input. Bliss and Lomo (1973) showed an increase in synaptic efficacy at monosynaptic junctions, occurring as the result of afferent fiber tetanization. This was an important discovery because it provided a way to study how synaptic strength can be modified by experience. This model system to study mechanisms of learning and memory was called Long Term Potentiation (LTP), the mechanism that strengthens synapses, by inducing a greater post-synaptic potential in response to a stimulus (Bliss & Lømo, 1973). In this form of LTP, an influx of CA^{2+} ions through N-methyl-D-aspartate receptors (NMDAR) triggers LTP mechanisms which induce both biochemical and structural changes in the activated synapses (Dunwiddie & Lynch, 1979). Tellingly, Lømo (2018) in the original presentation abstract of this effect in 1967 described the results as "…an example of plastic change in a neuronal chain…"

In the 1980s several key findings emerged implicating glutamate release as the presynaptic neurotransmitter, the discovery of post-synaptic glutamate receptors (NMDAR and α-amino-3-hydroxy-5-methyl-4-isoxazolepropionic acid (AMPAR)) whose activity were key drivers of LTP, and the development of pharmacological agents that can block different glutamate receptors (Bear & Malenka, 1994). This work led to the seminal experiments by Collingridge and colleagues (Collingridge, Kehl, & McLennan, 1983) showing that pharmacological blockade of AMPA receptors in HPC blocked LTP and that blocking NMDA receptors prevented induction of LTP but not expression. This work laid the foundations for the canonical idea that NMDA receptor activity was critical for

LTP induction and AMPA receptors were necessary for both induction and long-term maintenance of LTP.

Key evidence that LTP in the HPC was the mechanism underlying learning and memory functions also emerged from important behavioural pharmacology experiments led by Richard Morris in which his research group linked glutamate-based plasticity mechanisms to a form of learning dependent on the HPC. For these experiments, rats were administered an NMDA-antagonist intraventricularly throughout training on the spatial version of the Morris water task (MWT). The dose of the drug had been previously shown to block LTP induction in the HPC. The results showed that shutting down NMDA activity during acquisition of the spatial version of the MWT severely impaired spatial learning (Morris, Anderson, Lynch, & Baudry, 1986). These results strongly supported the idea that HPC NMDAR were crucial for the initial encoding of spatial information and was consistent with the demonstration that NMDAR activation were important for LTP induction (Collingridge et al., 1983). Taken together, this and other evidence made the important link between NMDAR-dependent LTP in HPC, and learning and memory functions supported by both the HPC and related neural circuits (Morris, 1989; Morris, Davis, & Butcher, 1990; Morris, Steele, Bell, & Martin, 2013; Morris, 2013).

Despite continued belief in this view of the role of NMDAR-dependent LTP in HPC some contrary evidence exists in the literature. This work emerged from a concern that peripheral or intraventricular administration of the NMDAR antagonists, techniques employed by Morris and colleagues, could impair the supports for learning and memory functions like sensory processing, motor control, and motivation as the neural systems mediating these processes also have NMDAR and their functions would be blocked using

these administration methods (Cain, 1997; Keith & Rudy, 1990). To assess this idea, researchers employed mitigation procedures like pre-training to try and reduce the impacts of these secondary effects of the pharmacological manipulation. A good example of this approach was a set of experiments (Saucier & Cain, 1995) in which a pre-training procedure was instituted before any pharmacological manipulation occurred. The pre-training consisted of letting the subjects swim in the pool with no escape platform available. On the following day, a similar procedure to those used by Morris was employed in which NMDAR antagonists were administered peripherally 1 hour before training on the spatial version of the MWT. Surprisingly, the results showed that if pre-training procedures were employed rats with their NMDAR blocked showed normal acquisition of a spatial learning task shown to be dependent on the HPC (Morris, Garrud, Rawlins, & O'Keefe, 1982; Sutherland, Whishaw, & Kolb, 1983; Sutherland, Kolb, & Whishaw, 1982). They concluded that their pre-training mitigation procedure reduced the impact of these pharmacological confounds allowing the subjects with blocked NMDAR function to show they had normal learning and memory functions.

This pattern of results was intriguing and a related report showing that the initial formation and short-term maintenance of place cells in HPC was not disrupted by NMDAR blockade (Kentros et al., 1998) but long-term stability of these place representations were compromised. Subsequently, a similar effect at a behavioural level showed that rats with intrahippocampal NMDAR blockade showed normal rapid acquisition of a new escape location in a testing environment in which those same subjects had received pre-training procedures to a different escape location in the pool (McDonald et al., 2005). Further, like the place cell report this experiment showed that

long-term consolidation processes were compromised following NMDAR blockade during acquisition training. Even though it indirectly replicated the Saucier and Cain experiments (1995), their hypothesis about why this effect happened was different. Based on these reports and other controverting evidence (Bannerman et al., 1995, 2012, 2008; Morris, Steele, Bell, & Martin, 2013; Morris, 2013) they hypothesized that HPC NMDARs might be essential for new learning with new spatial information but not new learning with familiar spatial information. To directly test this idea, the role of HPC NMDA receptors in new learning with novel versus familiar contexts was assessed. The design of the experiments were similar to those of the McDonald et al., (2005) experiments except that an additional group of rats were trained to asymptotic levels of performance (4 days, 8 trials per day) to escape to a static goal location and then given rapid acquisition training (one day, 16 trials) in an identical pool in a new training context. Intrahippocampal infusions of +/-CPP, at a dose shown to block LTP in HPC, dramatically impaired new learning with novel spatial information but had no impact on new learning with familiar spatial information. Further experiments assessed the impacts of new learning in familiar versus novel contexts on expression of an immediate early gene (IEG) linked to HPC LTP and learning. The experiments showed that new learning in a novel testing context increased Arc expression in certain sub-regions of the HPC while the expression of Arc did not increase following new learning in a familiar context. Finally, NMDAR blockade in either rapid acquisition condition (new or familiar testing room) resulted in long-term memory consolidation impairments (Bye & McDonald, 2019). These results are interesting because they provided a potential explanation for why pre-training procedures render new learning in the same training context NMDAR

independent and point to a potential idea about the specific role of this form of plasticity in HPC learning and memory processes.

The goal of the present experiments was to pursue some of the issues raised by this work and expand the scope of the research questions. ***These experiments are based on significant progress in our understanding of the biochemical and structural changes that occur in the post-synaptic region during events that induce LTP, and the complex projection patterns from the entorhinal cortex into the HPC.***

Lasting synaptic changes can be categorized into four sequential stages: generation, stabilization, consolidation, and maintenance, and allow for the persistence of memory (Lynch, Rex, & Gall, 2007). These stages are characterized by proteins that are expressed and activated to strengthen synapses. In the present three experiments, we focused on five different proteins that have been identified in these cascades: NMDAR, calcium/calmodulin-dependent protein kinase II (CaMKII), cAMP response element-binding protein (CREB), and AMPAR subunits.

LTP expression depends on the influx of Ca^{2+} becoming translated into sustained changes in the synapse. In *Experiment 2: pCaMKII and pCREB* we assessed the presence of phosphorylated CaMKII (pCaMKII), because the autophosphorylation of this protein allows it remain active beyond the influx of Ca^{2+} (Ohsako et al., 1991). We also assessed the presence of phosphorylated CREB (pCREB), as the phosphorylation of this transcription factor allows for the expression of proteins necessary for trace consolidation (Farris et al., 2017).

In experiment 3, we assessed how the ratio of GluA2:GluA1 receptors changed between two time points. Significant differences between time points would indicate that greater trafficking of GluA2 receptors to replace GluA1s. Synaptic changes that support learning are book-ended by AMPAR subunit dynamics, which increases Ca^{2+} permeability (Rudy, 2013).

Major input into the hippocampus comes from the entorhinal cortex (EC) via the perforant path. The entorhinal cortex is primarily split between its medial and lateral areas, MEC and LEC, respectively. Both the EC and the perforant path show functional differences between their medial and lateral portions. One description of these differences attributes 'where' functions to the MEC and 'what' functions to the LEC (Knierim et al., 2014). Similarly, lesions to the MPP but not LPP impair place learning (Ferbinteanu, Holsinger, & McDonald, 1999). Not only are these two regions functionally dissociable, but their connections to other fields of the HPC also differ.

There is heterogeneity within subfields of the HPC on the molecular, circuit, and behavioural scales (Cembrowski & Spruston, 2019). In this set of experiments, we took into account the heterogeneity in proximodistal anatomical connectivity to EC, and in trends in proximodistal recruitment for spatial learning. The implications of heterogeneous connectivity, and the differences between MEC and LEC function within spatial learning tasks (Nilssen et al., 2019) are the basis for our hypotheses in these experiments. These hypotheses will be explained further and have been depicted in Figure 2.1.

The impact of knocking out and blocking the proteins studied in this set of experiments has been reviewed in in general introduction. The involvement of these

proteins in spatial learning or context learning is evident, however, we do not understand the specific roles of these proteins, nor how their expression differs when spatial learning takes place in familiar versus novel contexts. The latter of these two questions will be explored in this chapter; how does expression differ in these plasticity proteins when spatial learning takes place and when this learning is either in a familiar or novel context.

The current experiments examine indicators of plasticity, downstream of NMDA-LTP, across proximodistal HPC following new learning in a familiar versus a novel training context. A ratio of GluA2 to GluA1 AMPA receptor subunits, as well as measures of pCaMKII, pCREB, and NMDAR expression were conducted and in some cases used as a measure of plasticity, based on previous findings that learning differs in its NMDA-dependence between familiar and novel contexts (Bye and McDonald, 2019). Furthermore, in *Experiment* 3, the ratio of GluA2:GluA1 receptors was measured at 70 and 180 minutes following new learning based on both in vivo and in vitro studies that demonstrate that GluA1 expression peaks at 70 minutes and GluA2 expression peaks at 180 minutes (Bhattacharya et al., 2017; Nayak, Zastrow, Lickteig, Zahniser, & Browning, 1998). We predict that new learning in a novel context will result in greater HPC plasticity related in subregions of HPC that receive significant input from MEC, while new learning in a familiar context HPC plasticity will be greatest in regions that receive significant input from LEC (Figure 2.1).

Methods consistent across experiments

Subjects

Subjects were 16 male Long Evans rats aged 90 days, weighing between 317- 420 g at the start of the task. Rats were housed in groups of 3 and were maintained on a 12-

hour light/dark cycle with *ad libitum* food and water access. Rats were acclimatized for 7 days prior to handling and handled for 5 minutes per day for the 5 days leading up to water task. All procedures were approved by the University of Lethbridge Animal Welfare Committee and in accordance with the Canadian Council of Animal Care.

Behavioural Apparatus and Analysis

Spatial learning in the water task was conducted in two rooms, each with a white fibreglass pool (height = 46 cm, diameter = 127 cm). Each pool was located in the center of a room, and each room had distinct extra-maze features. These features include the entry direction, inter-trial cage location, orientation of the experimenter, wall hangings, and furniture. Water was refreshed daily and mixed with ~ 50 mL of white non-toxic tempura paint. The hidden platform (square, 10 cm by 10 cm) was located ~ 3 cm below the water's surface and made of clear acrylic. Behavioural data was collected using an overhead camera and analyzed with Noldus Ethovision 11.5. Two-way ANOVAs and Bonferroni post-hoc comparisons were used on behavioural data using GraphPad Prism 8.

Contextual Navigation Water Task

Task procedure involved a 2-room, 2 phase version of the hidden-platform water task, shown in Figure 2.2. All phases took place between 08:00 and 12:00. 4 groups were run in the task, differing in room condition and time of sacrifice.

Phase 1: Pre-training

On each training day phase 1, rats were moved from their home cages into transport cages and transported on a wheeled cart to context A. Rats were trained over 8 trials per day for 4 days to find a hidden platform location in the SE quadrant of the pool

where they remained for 10 seconds after every trial. The starting location was randomized, and the maximum allowed time was 60 s after which the animal was placed on the platform for 10 seconds if they could not locate the platform. The average inter-trial interval was 5 minutes, during which the rat was in a transport cage.

Phase 2: Rapid new learning

During new learning, rats underwent rapid new learning in either the training context (same room condition) (n = 8), or a novel context (new room condition) (n = 8). Rats were trained over 16 trials in 45 minutes to find a hidden platform in either the NW quadrant (same room), or the SW quadrant (new room), where they remained for 10 seconds after every trial. The starting location was again, randomized and the maximum allowed time was 60 s after which the animal was placed on the platform for 10 s if they could not locate the platform.

Perfusion and Tissue Preparation

At either 15 (same room n = 4, new room n = 4) (pCaMKII), 70 (same room n = 4, new room n = 4) (NMDAR, GluA2, GluA1), or 180 minutes (same room n = 4, new room n = 4) (pCREB, GluA2, GluA1), rats were euthanized with an intracardiac injection of sodium pentobarbital (125 mg/mL). Rats were then perfused with 4% paraformaldehyde (PFA) and 0.1 M phosphate buffer saline (PBS) transcardially. Brains were extracted and stored in 4% PFA for 24 hours, after which they were transferred to 30% sucrose + 0.2% sodium azide for 3 days. Brains were sliced in 12 series at 40 µm on a freezing sliding microtome and stored in 0.1M PBS + 0.2% sodium azide.

Microscopy

Slides were imaged on an Olympus FV 1200 inverted microscope at 20x. Each slice was imaged with the 488 nm laser at 4.6% power. Images of DG, CA3 and CA1 from both hemispheres were captured and sorted across the long axis. For the CA1 region, both a distal and a proximal image was acquired. Images were acquired in a Z stack of 14 images, taken at a 2048 resolution, which allowed for a 0.31 μm pixel size, and a 634.57μm by 634.57μm sized area in the XY plane. Maximum value Z-projections were used for the analysis. Sample images are shown in Figure 2.3.

Analysis

Histology analysis was conducted using ImageJ (NIH) and MatLab routines. For overall expression in each sub-region, average pixel fluorescence was calculated in each image. For overall expression in each sub-region, average pixel fluorescence was calculated in each image. In DG, the image was rotated so that blade being analyzed (supra or infrapyramidal) was on the bottom. Then, a line was mapped parallel to the granule layer of the blade being analyzed, and another exclusionary line was drawn to exclude CA3 and the DG blade not being analyzed from the analysis. For CA3 and CA1, a line was mapped parallel to the granule layer, and if there were regions that were not a part of this subfield in the image, they were excluded in the same way that CA3 and the opposing blade were excluded in the DG analysis. 20 perpendicular bins were drawn in each sub-region, and 20 random lines were generated perpendicular to this axis within each bin. Average pixel fluorescence was calculated along each line, excluding the excluded region if there was one, and averaged to generate a matrix of pixel fluorescence values per HPC sub-region of each animal along both the long and transverse axes. For

the long axis, images were sorted from anterior to posterior based on dorsal hippocampus structure (i.e. most dorsal is most anterior dorsal hippocampus, and most ventral is most posterior dorsal hippocampus). This order became the basis for generating average pixel fluorescence along the long axis. This analysis was conducted identically between all stained samples. This method is shown in Figure 2.4. Linear and non-linear regressions, as well as ROUT tests for outliers were conducted using GraphPad Prism 8. Trend analyses between groups consisted of one-way ANOVAs of the aforementioned regressions.

Experiment 1: NMDAR

Methods specific to experiment 1

Immunohistochemistry

Immunohistochemistry was performed to detect NMDAR expression using a 3-day fluorescent immunohistochemical protocol.

On day 1, tissue was placed in 2000 µL of 0.1 M PBS + 0.2% Triton X (PBS TX-100). Tissue was incubated at a ratio of 1:100 for the primary antibody (Anit-NMDDAR1 antibody produced in rabbit, Sigma Aldrich). Tissue was then left to incubate on an orbital shaker, agitated gently, for 24 hours at room temperature.

On day 2, the tissue was washed in 0.1 M PBS 3 x 5 min. Tissue was again placed in 1000 µL of PBS TX-100. It was then incubated in secondary antibody at a concentration of 1:2000 (Alexa flour 488 anti-rabbit IgG , New England Biolabs Ltm.). The tissue was covered in tin foil to ensure no light exposure during incubation, and incubated on an orbital shaker, agitated gently, for 24 hours at room temperature.

On day three, the tissue was washed again in 0.1 M PBS 3 x 5 min. After the washes, the tissue was added to a large petri dish containing 0.1 M PBS and sorted from anterior to posterior and then mounted onto 1% gelatin and 0.2% chromatin coated slides. The slides were then cover slipped and placed in a refrigerator at 4°C.

Results

Pre-training behaviour

During pre-training of the Contextual Navigation Water Task, a clear learning effect was observed in rats sacrificed 70 minutes post new-learning (Figures 2.5A/B).

This was shown in linear regressions of both path length (Fig. 2.5A) and latency (Fig. 2.5B) in both room condition groups (path length SR-70: slope = -126.9, $F_{1, 126} = 24.34$, $p < 0.0001$; path length NR-70: slope = -105.8, $F_{1, 124} = 8.149$, $p = 0.0051$; latency SR-70: slope = -4.659, $F_{1, 126} = 27.96$, $p < 0.0001$; latency NR-70: slope = -7.459, $F_{1, 124} = 27.92$, $p < 0.0001$). Furthermore, we observed no significant interaction ($F_{3, 246} = 1.317$, $p = 0.2693$) or effect of room ($F_{1, 246} = 3.532$, $p = 0.0614$) in path length. Post-hoc comparisons of path length showed no significant differences were observed on any days (Day 1: $p = 0.9991$; Day 2: $p = 0.0582$; Day 3: $p = 0.9917$; Day 4: $p = 0.6802$). Therefore, the rats learned the pre-training escape platform location.

In latency during pre-training, we observed both a significant learning effect ($F_{3, 246} = 26.12$, $p < 0.0001$), and room condition effect ($F_{1, 246} = 20.42$, $p < 0.0001$). No significant interaction ($F_{3, 246} = 1.587$, $p = 0.1932$) was found. Post-hoc comparisons showed that significant differences between room conditions were only observed on days 1 and 2 (Day 1: $p = 0.0011$; Day 2: $p = 0.0236$; Day 3: $p = 0.8653$; Day 4: $p = 0.3247$). Therefore, by the end of pre-training the room condition effect was no longer significant.

New learning behaviour

During new learning we observed a significant learning effect in both room conditions, in both path length (Fig. 2.5C) (path length SR-70: slope = -31.60, $F_{1, 62} = 19.71$, $p < 0.0001$; path length NR-70: slope = -19.16, $F_{1, 62} = 15.94$, $p = 0.0002$) and latency (Fig. 2.5D) (latency SR-70: slope = -1.275, $F_{1, 62} = 25.62$, $p < 0.0001$; latency NR-70: slope = -0.6975, $F_{1, 62} = 10.99$, $p = 0.0015$). In both path length and latency, a significant room effect was also observed (path length: $F_{1, 96} = 20.66$, $p < 0.0001$; latency: $F_{1, 96} = 4.036$, $p = 0.0474$). Post hoc comparisons show that these effects are limited to

early trials during new learning, trials 1 and 2 for path length (Trial 1: $p = 0.0332$; Trial 2: $p = 0.0455$), and trial 2 for latency (Trial 2: $p = 0.0452$). No significant interactions were shown in either measurement (path length: $F_{15, 96} = 0.7356$, $p = 0.7429$; latency: $F_{15, 96} = 1.199$, $p = 0.2857$). Therefore, rats learned the new escape platform location in both the same and new room conditions.

NMDAR expression across hippocampal subfields

In NMDAR expression, I hypothesize that there will be no difference in NMDAR expression between room conditions across hippocampal subfields.

When NMDAR expression was averaged within hippocampal subfields in each condition, a 2-way ANOVA illuminated significant effects of subfield ($F_{3, 36} = 4.333$, $p = 0.0105$) and room ($F_{2, 36} = 27.06$, $p < 0.0001$) (Figure 2.6). Post-hoc comparisons did not show any significant differences within room conditions between hippocampal subfields. Additionally, no significant interactions were observed ($F_{6, 36} = 0.1692$, $p = 0.9834$), or outliers ($Q = 1\%$).

Consistent with the hypothesis, in NMDAR expression we did not observe greater average pixel fluorescence in the new room group than the same room group. However, we did observe greater expression in control groups than experimental animals.

NMDAR expression between room conditions along the transverse axis within subfields

Unlike other proteins that are measured in this chapter, we did not expect to see any differences in the patterns of NMDAR expression in differing room conditions like those hypothesized in experiments 2 and 3.

We observed in the suprapyramidal blade, concave trends in same-room animals (R square = 0.2640, $Y = 60.92 - 0.02124X - 0.024569X^2$), and convex trends in new-room and control animals (NR-70: R square = 0.4740, $Y = 65.76 - 0.8335X + 0.009814X^2$; CTR: R square = 0.5635, $Y = 79.31 - 1.113X + 0.01697X^2$). These results are shown in Figure 2.7A, and are consistent with MEC connectivity patterns in the new room condition and LEC connectivity patterns in the same room condition. Our results from the infrapyramidal blade, however, were not consistent with those connectivity patterns. In the infrapyramidal blade, we observed significant positive expression patterns across all 3 groups (same room: R square = 0.3153, , $F_{1, 78} = 35.92$, $p < 0.0001$; new room: R square = 0.6077, $F_{1, 78} = 120.8$, $p < 0.0001$; cage CTR: R square = 0.6105, , $F_{1, 78} = 122.3$, $p < 0.0001$) (Figure 2.7B).

In CA3, we observed patterns of NMDAR expression that matched MEC connectivity in both the new room and same room group (Fig. 2.7C). All three conditions showed significant positive expression patterns (same room: R square = 0.05510, , $F_{1, 77} = 4.490$, $p = 0.0373$; new room: R square = 0.08936, $F_{1, 70} = 6.869$, $p = 0.0108$; cage CTR: R square = 0.2384 , $F_{1, 77} = 24.11$, $p < 0.0001$). In CA1, we also observed patterns of NMDAR expression that matched MEC connectivity in the new room group (R square = 0.1633, $F_{1, 76} = 14.83$, $p = 0.0002$) (Fig. 2.7D). Patterns of expression in the same room group and cage controls were insignificant (same room: R square = 0.04264, $F_{1, 76} = 3.385$, $p = 0.0697$; cage CTR: R square = 0.0003395, $F_{1, 76} = 0.02581$, $p = 0.8728$).

<u>NMDAR expression between room conditions along the long axis within subfields</u>

From dorsal to ventral, we also hypothesized that no significant trends would be observed in NMDAR expression. Largely, this was the case (Figure 2.8). In the

suprapyramidal blade of the DG, a significant negative trend was observed in cage controls (R square = 0.07816, $F_{1, 83} = 7038$, p = 0.0096), and both experimental groups showed insignificant trends (same room: R square = 0.0002359, $F_{1, 82} = 0.01935$, p = 0.8897; new room: R square = 0.007335, $F_{1, 103} = 0.7610$, p = 0.3850) (Fig. 2.8A). This result was the same in the infrapyramidal blade (same room: R square = 0.0006205, $F_{1, 82}$ = 0.05091, p = 0.8220; new room: R square = 0.01639, $F_{1, 103} = 1.716$, p = 0.1931; cage CTR: R square = 0.07158, $F_{1, 83} = 6.399$, p = 0.0133) (Fig. 2.8B).

In CA3, no significant relationship was found between NMDAR expression and the long axis in experimental groups (same room: R square = 0.01520, $F_{1, 55} = 0.8487$, p = 0.3609; new room: R square = 0.01627, $F_{1, 68} = 1.124$, p = 0.2927) (Fig. 2.8C). In cage controls, a significant positive relationship was observed (R square = 0.1583, $F_{1, 52}$ = 9.781, p = 0.0029). In CA1, no groups showed significant trends in NMDAR expression along the long axis (same room: R square = 0.0009873, $F_{1, 72} = 0.07116$, p = 0.7904; new room: R square = 0.007468, $F_{1, 72} = 0.5418$, p = 0.4641; cage CTR: R square = 0.00304, $F_{1, 62} = 0.3933$, p = 0.5329) (Fig. 2.8D).

Between groups analysis of NMDAR expression trends along the transverse axis

To assess if the patterns found in NMDAR expression were significantly different between groups, we conducted one-way ANOVAs on the slopes of the regressions. We hypothesized that there would be no significant differences between room conditions.

In the suprapyramidal blade, we observed that the same room condition was more concave than the new room and control conditions, and similarly, the new room condition was more convex than the same room condition but not the control conditions. These results, however, were not statistically significant (SR-70 vs. NR-70: mean difference = -

0.03437, p = 0.3072; SR-70 vs. CTR: mean difference = -0.04153, p = 0.1799; NR-70 vs. CTR: mean difference = -0.007156, p = 0.9497) (Fig. 2.9A). In the infrapyramidal blade, we observed no significant differences between the two room conditions or between the new room condition and controls, however the slope of NMDAR expression in the transverse axis was significantly greater in control animals than same room animals (SR-70 vs. NR-70: mean difference = -0.2033, p = 0.1761; SR-70 vs. CTR: mean difference = -0.2877, p = 0.0323; NR-70 vs. CTR: mean difference = -0.08440, p = 0.7388) (Fig. 2.9B).

In CA3, no significant differences were observed between any of the groups (SR-70 vs. NR-70: mean difference = -0.1004, p = 0.8459; SR-70 vs. CTR: mean difference = -0.2699, p = 0.2846; NR-70 vs. CTR: mean difference = -0.1695, p = 0.6215) (Fig. 2.9C). In CA1, the differences between the new room group and other two groups were significant (SR-70 vs. NR-70: mean difference = -0.4152, p = 0.0009; NR-70 vs. CTR: mean difference = -0.2735, p = 0.0435) (Fig. 2.9D). No significant differences were observed between the same room group and controls (SR-70 vs. CTR: mean difference = -0.1417, p = 0.4250).

Between groups analysis of NMDAR expression trends along the long axis

Along the long axis we hypothesized that the slopes of NMDAR expression trends would not differ between groups. We did observed this, shown in Figure 2.10, as in all regions we observed no significant differences in the slopes between any conditions.

Summary

In NMDAR expression, we largely did not observe patterns that either differed by room condition or matched MEC or LEC connectivity, consistent with our hypotheses.

We did, however, observe differences in patterns of NMDAR expression along the transverse axis that differed by room condition and matched MEC and LEC connectivity as hypothesized for the other proteins measured. This is to say that we observed an increasing trend along the transverse axis in the new room group and a decreasing trend along the transverse axis in the same room group.

Experiment 2: pCamKII, pCREB

Methods specific to experiment 2

Immunohistochemistry

Immunohistochemistry was performed to detect pCamKII expression in the 15 minute group, and pCREB expression in the 180 minute group using a 3-day fluorescent immunohistochemical protocol.

On day 1, tissue was placed in 1000 µL of 0.1 M PBS + 0.2% Triton X (PBS TX-100). Tissue being stained for pCamKII was incubated at a ratio of 1:200 for the primary antibody (Phospho-CaMKII (Thr286) (D21E4) Rabbit mAb, Cell Signaling Technology). Tissue stained for pCREB was incubated at a ratio of 1:400 for the primary antibody (Phospho-CREB (Ser133) (87G3) Rabbit mAb, New England BioLabs). Once the appropriate volume of antibody was added to the tissue, the trays were left to incubate on an orbital shaker, agitated gently, for 24 hours at room temperature.

On day 2, the tissue was washed in 0.1 M PBS 3 x 5 min. Tissue was again placed in 1000 µL of PBS TX-100. Tissue being stained for pCamKII was incubated in secondary antibody at a concentration of 1:2000 (Alexa flour 488 anti-rabbit IgG, New

England Biolabs Ltm.), and pCREB had a concentration of 1:1250 (Alexa flour 488 anti-rabbit IgG, New England Biolabs Ltm.). The tissue was covered in tin foil to ensure no light exposure during incubation, and incubated on an orbital shaker, agitated gently, for 24 hours at room temperature.

On day three, the tissue was washed again in 0.1 M PBS 3 x 5 min. After the washes, the tissue was added to a large petri dish containing 0.1 M PBS and sorted from anterior to posterior and then mounted onto 1% gelatin and 0.2% chromatin coated slides. The slides were then cover slipped and placed in a refrigerator at 4°C.

Results

Pre-training behaviour

In rats sacrificed 15 minutes (pCaMKII) post new-learning, a clear learning effect was observed in path length during pre-training behaviour in both room conditions (same room: slope = -135.7, $F_{1, 126} = 25.22$, $p < 0.0001$; new room: slope = -207.5, $F_{1, 126} = 27.20$, $p < 0.0001$) (Figure 2.11A). Similarly, in latency a significant learning effect was observed in pre-training (same room: slope = -5.002, $F_{1, 126} = 26.53$, $p < 0.0001$; new room: slope = -10.24, $F_{1, 126} = 57.05$, $p < 0.0001$) (Figure 2.11B). In a 2-way ANOVA, significant learning effects and room condition effects were observed under both measures (path length learning: $F_{3, 248} = 17.91$, $p < 0.0001$; path length room: $F_{1, 248} = 29.18$, $p < 0.0001$; latency learning: $F_{3, 248} = 30.09$, $p < 0.0001$; latency room: $F_{1, 248} = 50.23$, $p < 0.0001$). Post hoc analyses showed that these differences were only significant on days 2 and 3 for path length (Day 1: $p = 0.0535$; Day 2: $p < 0.0001$; Day 3: $p = 0.0344$; Day 4: $p = 0.8193$), and days 1, 2, and 3 for latency (Day 1: $p < 0.0001$; Day 2: $p < 0.0001$; Day 3: $p = 0.0186$; Day 4: $p = 0.7370$).

In rats sacrificed 180 minutes (pCREB) post new-learning, a clear learning effect was observed in path length during pre-training behaviour in both room conditions (same room: slope = -156.3, $F_{1, 126} = 34.39$, $p < 0.0001$; new room: slope = -129.4, $F_{1, 126} = 21.12$, $p < 0.0001$) (Figure 2.12A). Similarly, in latency a significant learning effect was observed in pre-training (same room: slope = -5.862, $F_{1, 126} = 30.50$, $p < 0.0001$; new room: slope = -6.511, $F_{1, 126} = 39.66$, $p < 0.0001$) (Figure 2.12B). In a 2-way ANOVA, significant learning effects were observed under both measures (path length learning: $F_{3, 248} = 19.86$, $p < 0.0001$; latency learning: $F_{3, 248} = 27.86$, $p < 0.0001$). No significant effect of room was shown in either measure (path length room: $F_{1, 248} = 1.386$, $p = 0.2401$; latency room: $F_{1, 248} = 0.9239$, $p = 0.3374$). Post hoc analyses showed no significant differences on any days between the room conditions in path length (Day 1: $p = 0.9559$; Day 2: $p = 0.6288$; Day 3: $p = 0.5487$; Day 4: $p = 0.9914$), or latency (Day 1: $p = 0.9680$; Day 2: $p = 0.9373$; Day 3: $p = 0.8663$; Day 4: $p = 0.9997$).

New learning behaviour

In rats sacrificed 15 minutes post new learning, significant learning effects were shown in new learning in both room conditions in both path length (same room: slope = -41.18, $F_{1, 62} = 25.31$, $p < 0.0001$; new room: slope = -23.83, $F_{1, 62} = 17.52$, $p < 0.0001$) (Figure 2.11C) and latency (same room: slope = -1.876, $F_{1, 62} = 30.04$, $p < 0.0001$; new room: slope = -1.079, $F_{1, 62} = 11.56$, $p = 0.0012$) (Figure 2.11D). A 2-way ANOVA of these behaviour showed both a significant learning effect ($F_{15, 96} = 4.371$, $p < 0.0001$) and room effect ($F_{1, 96} = 11.50$, $p = 0.0010$) in path length, and a significant learning effect in latency ($F_{15, 96} = 3.810$, $p < 0.0001$). No significant room effect was observed in latency ($F_{1, 96} = 1.725$, $p = 0.1922$). Post-hoc comparisons of path length between room

conditions showed that significant differences were limited to trial 1 (Trial 1: $p = 0.0069$). In latency, no trials showed any significant differences between the room conditions.

In rats sacrificed 180 minutes post new learning, significant learning effects were shown in new learning in both room conditions in both path length (same room: slope = -58.16, $F_{1, 62} = 66.72$, $p < 0.0001$; new room: slope = -20.43, $F_{1, 62} = 8.353$, $p = 0.0053$) (Figure 2.12C) and latency (same room: slope = -2.587, $F_{1, 62} = 55.39$, $p < 0.0001$; new room: slope = -0.5173, $F_{1, 62} = 2.647$, $p = 0.0017$) (Figure 2.12D). A 2-way ANOVA of these behaviour showed both a significant learning effect ($F_{15, 96} = 7.632$, $p < 0.0001$) and room effect ($F_{1, 96} = 23.67$, $p < 0.0001$) in path length. Similarly, a significant learning effect ($F_{15, 96} = 6.721$, $p < 0.0001$), room effect ($F_{1, 96} = 14.53$, $p = 0.0002$) was observed in latency during new learning. Post-hoc comparisons of path length between room conditions showed that significant differences were limited to trials 1, 2, and 5 (Trial 1: $p = 0.0005$; Trial 2: $p = 0.0498$; Trial 5: $p = 0.0074$). In latency, significant differences were also observed between the room conditions in trials 1, 2, and 5 (Trial 1: $p = 0.0002$; Trial 2: $p = 0.0476$; Trial 5: $p = 0.0399$).

pCaMKII and pCREB expression across hippocampal subfields

When pCaMKII expression was averaged within hippocampal subfields in each condition, a 2-way ANOVA illuminated significant effects of subfield ($F_{3, 36} = 5.451$, $p = 0.0034$) but not room ($F_{2, 36} = 3.103$, $p = 0.0571$) (Figure 2.13). Post-hoc comparisons did not show any significant differences within room conditions between hippocampal subfields. pCREB expression showed significant effects of both subfield and room (subfield: $F_{3, 36} = 3.844$, $p = 0.0174$; room: $F_{2, 36} = 22.27$, $p < 0.0001$). Significant differences between subfields were not observed in post hoc analyses in any conditions.

Contrary to our hypothesis, in pCREB expression we did not observe greater average pixel fluorescence in the new room group than the same room group (Figure 2.14). However, we did observe greater expression in control groups than experimental animals. These results mirror those found in *Experiment 1: NMDAR*.

pCaMKII and pCREB expression between room conditions along the transverse axis within subfields

We hypothesized that we'd observe convex trends in the suprapyramidal blade of the DG, no significant trends in the infrapyramidal blade of DG, a positive trend in CA3, and a negative trend in CA1, all from distal to proximal, in rats who underwent the same-room condition. We hypothesized that we'd observe concave trends in the suprapyramidal blade of DG, no significant trends in the infrapyramidal blade of DG, a negative trend in CA3, and a positive trend in CA1, all from distal to proximal, in rats who underwent the new-room condition. We hypothesized that we'd observe these same patterns in both pCaMKII and pCREB expression.

We observed in the suprapyramidal blade, concave trends in pCaMKII expression in both same-room animals (R square = 0.2333, $Y = 2.242 - 0.5469X - 0.02779X^2$), and new room animals (R square = 0.1776, $Y = 3.712 - 0.9055X + 0.04601X^2$). Convex trends were observed in control animals (R square = 0.3328, $Y = 2.073 - 0.5058X + 0.02570X^2$). The results shown in Figure 2.15A in new room animals were consistent with our hypothesis, however the results in same room animals were not. Our results from the infrapyramidal blade, shown in Figure 2.15B, were also inconsistent with our hypotheses. In the infrapyramidal blade, we observed significant positive expression patterns across all 3 groups (same room: R square = 0.5227, , $F_{1, 78} = 85.44$, $p < 0.0001$;

new room: R square = 0.5126, $F_{1, 78} = 82.05$, $p < 0.0001$; cage CTR: R square = 0.4479, $F_{1, 78} = 63.27$, $p < 0.0001$).

In pCREB expression we observed effects in the suprapyramidal blade that were similar to those observed in pCaMKII expression in the two experimental groups (Figure 2.16A). All three groups showed concave trends in pCREB expression along the transverse axis (same room: R square = 0.5545, $Y = 67.77 - 0.6793X - 0.01539X^2$; new room: R square = 0.3152, $Y = 61.28 - 0.4437X - 0.01143X^2$; cage CTR: R square = 0.4573, $Y = 78.12 - 0.6444X - 0.001266X^2$). Also similar to pCaMKII, significant positive pCREB expression was observed in the infrapyramidal blade in all three conditions (same room: R square = 0.6067, $F_{1, 78} = 120.3$, $p < 0.0001$; new room: R square = 0.4192, $F_{1, 78} = 56.29$, $p < 0.0001$; cage CTR: R square = 0.5808, $F_{1, 78} = 108.1$, $p < 0.0001$) (Figure 2.16B).

In CA3, we did not observe significant trends in pCaMKII expression along the transverse axis in either experimental condition (same room: R square = 0.03828, $F_{1, 68} = 2.707$, $p = 0.1045$; new room: R square = 0.004109, $F_{1, 63} = 0.2599$, $p = 0.6120$) (Figure 2.15C). In pCREB expression, however we did observe a significant positive trend in same room animals, consistent with our hypothesis (same room: R square = 0.4728, $F_{1, 69} = 61.88$, $p < 0.0001$), and no significant trend in new room animals (new room: R square = 0.0009170, $F_{1, 78} = 0.07159$, $p = 0.7897$) (Figure 2.16C). In control animals we observed significant positive trends along the transverse axis in both pCaMKII and pCREB expression (pCaMKII: R square = 0.3767, $F_{1, 68} = 41.10$, $p < 0.0001$; pCREB: R square = 0.1492, $F_{1, 72} = 12.63$, $p = 0.0007$).

In CA1, non=significant trends were observed in all conditions in both pCaMKII and pCREB expression other than significantly negative relationship between pCaMKII expression and the transverse axis in cage controls (pCaMKII same room: same room: R square = 0.006822, $F_{1, 77} = 0.5289$, p = 0.4693; pCaMKII new room: R square = 0.01887, $F_{1, 76} = 1.462$, p = 0.2304; pCaMKII CTR: cage CTR: R square = 0.05391, $F_{1, 77} = 0.0395$, p = 0.0395; pCREB same room: R square = 0.01182, $F_{1, 78} = 0.9326$, p = 0.3372; pCREB new room: R square = 0.0001450, $F_{1, 78} = 0.01131$, p = 0.9156; pCREB CTR: R square = 0.01925, $F_{1, 78} = 1.531$, p = 0.2197) (Figures 2.15D, 2.16D).

<u>pCaMKII and pCREB expression between room conditions along the long axis within subfields</u>

From dorsal to ventral, we hypothesized that trends in NMDAR expression would be negative in experimental groups. Results that confirm our hypothesis were found more so in pCaMKII expression than pCREB expression trends. In the suprapyramidal blade, pCaMKII expression trends were significant and negative in both experimental groups (same room: R square = 0.09113, $F_{1, 72} = 7.219$, p = 0.0090; new room: R square = 0.05531, $F_{1, 72} = 4.216$, p = 0.0437), and insignificant in controls (R square = 0.02192, $F_{1, 86} = 1.928$, p = 0.1686) (Figure 2.17A). pCREB expression trends along the long axis of the suprapyramidal blade were insignificant in all groups (same room: R square = 0.0003526, $F_{1, 93} = 0.03280$, p = 0.8567; new room: R square = 0.001981, $F_{1, 82} = 0.1628$, p = 0.6877; cage CTR: R square = 0.02108, $F_{1, 83} = 1.788$, p = 0.1849) (Figure 2.18A). In the infrapyramidal blade, this same pattern was found (Figures 2.17B, 2.18B). Significant negative patterns of expression of pCaMKII were observed in both experimental groups (same room: R square = 0.08939, $F_{1, 72} = 7.067$, p = 0.0097; new room: R square =

0.1107, $F_{1, 72} = 8.962$, p = 0.0038), while insignificant trends were observed in controls (cage CTR: R square = 0.004840, $F_{1, 86} = 0.4183$, p = 0.5195). Insignificant patterns of pCREB expression were observed along the long axis of the infrapyramidal blade in all three conditions (same room: R square = 3.140e-005, $F_{1, 93} = 0.002920$, p = 0.9570; new room: R square = 0.02410, $F_{1, 90} = 2.223$, p = 0.1395; cage CTR: R square = 0.03117, $F_{1, 83} = 2.670$, p = 0.1060).

In contrast to the observations made in the DG, and our hypotheses, we observed non-significant patterns of pCaMKII expression in both experimental conditions in CA3 (same room: R square = 0.03743, $F_{1, 55} = 2.139$, p = 0.1493; new room: R square = 0.01733, $F_{1, 52} = 0.9172$, p = 0.3426), and a significant positive trend in controls (R square = 0.2775, $F_{1, 52} = 19.97$, $p < 0.0001$) (Figure 2.17C). In pCREB expression, we observed patterns of expression that contradicted our hypotheses in both experimental conditions (Figure 2.18C). Significant positive patterns of pCREB expression were observed in both room conditions (same room: R square = 0.1416, $F_{1, 61} = 10.06$, p = 0.0024; new room: R square = 0.073333, $F_{1, 54} = 4.273$, p = 0.0435), and insignificant trends were observed in controls (R square = 0.005017, $F_{1, 54} = 0.2723$, p = 0.6040).

In CA1, shown in Figures 2.17D and 2.18D, we observed non-significant trends in pCaMKII and pCREB expression along the long axis in all conditions (pCaMKII same room: R square = 0.01223, $F_{1, 58} = 0.7183$, p = 0.4002; pCaMKII new room: R square = 0.006155, $F_{1, 50} = 0.3096$, p = 0.5804; pCaMKII CTR: R square = 0.006615, $F_{1, 70} = 0.4661$, p = 0.4970; pCREB same room: R square = 0.01352, $F_{1, 73} = 1.000$, p = 0.3206; pCREB new room: R square = 0.05940, $F_{1, 62} = 3.915$, p = 0.0523; pCREB CTR: R square = 0.01530, $F_{1, 64} = 0.9942$, p = 0.3225).

Between groups analysis of pCaMKII and pCREB expression trends along the transverse axis

To assess if the patterns found in pCaMKII and pCREB expression were significantly different between groups, we conducted one-way ANOVAs on the slopes of the regressions. We hypothesized that the same room condition would differ from controls and new room conditions in the following ways: in the suprapyramidal blade of the DG slopes would be more concave, in the infrapyramidal blade slopes would not differ, in CA3 slopes would be more positive, and in CA1 slopes would be more negative. We also hypothesized that the new room condition would differ from the same room condition and controls in the following ways: in the suprapyramidal blade of the DG slopes would be more convex, in the infrapyramidal blade slopes would not differ, in CA3 slopes would be more negative, and in CA1 slopes would be more positive.

The differences in pCaMKII expression patterns between room conditions in the suprapyramidal blade were inconsistent with our hypotheses. The only significant differences observed in the expression patterns between room conditions was between new room and control groups, and this difference contradicted our hypothesis (SR-15 vs. NR-15: mean difference = -0.06242, p = 0.4061; SR-15 vs. CTR mean difference = -0.07274, p = 0.2950; NR-15 vs. CTR: mean difference = -0.1352, p = 0.0162) (Figure 2.19A). We observed no significant differences in pCREB expression patterns between room conditions in the suprapyramidal blade (SR-180 vs. NR-180: mean difference = -0.003960, p = 0.9889; SR-180 vs. CTR: mean difference = -0.01412, p = 0.8682; NR-180 vs. CTR: mean difference = -0.01016, p = 0.9294) (Figure 2.20A). In the infrapyramidal blade in both pCaMKII and pCREB between-groups analyses we observed no significant

differences between expression patterns in all three groups (pCaMKII SR-15 vs. NR-15: mean difference = -0.3030, p = 0.2181; pCaMKII SR-15 vs. CTR: mean difference = 0.02730, p = 0.9876; pCaMKII NR-15 vs. CTR: mean difference = 0.3303, p = 0.1644; pCREB SR-180 vs. NR-180: mean difference = 0.2571, p = 0.1365; SR-180 vs. CTR: mean difference = 0.2202, p = 0.2307; NR-180 vs. CTR: mean difference = -0.03690, p = 0.9592) (Figures 2.19B, 20B).

In CA3, pCaMKII expression pattern differences between new room animals and controls support our hypotheses (mean difference = -0.7595, p = 0.0006), and so do the differences in pCREB expression patterns between new room animals and both same room and control groups (SR-180 vs. NR-180: mean difference = 0.8890, p < 0.0001; NR-180 vs. CTR: mean difference = -0.5007, p = 0.0184) (Figure 2.19C, 2.20C). Otherwise the only significant result was a significant difference in pCaMKII expression patterns between same room and control animals which contradicted our hypotheses (mean difference = -0.5294, p = 0.0208). All other findings were insignificant (pCaMKII SR-15 vs. NR-15: mean difference = 0.2301, p = 0.4848; pCREB SR-180 vs. CTR: mean difference = 0.3883, p = 0.1006).

In CA1, no significant differences were observed in either pCaMKII or pCREB expression trends along the transverse axis between any of the groups (pCaMKII SR-15 vs. NR-15: mean difference = 0.05226, p = 0.9318; pCaMKII SR-15 vs. CTR: mean difference = 0.1825, p = 0.4225; pCaMKII NR-15 vs. CTR: mean difference = 0.1302, p = 0.6457; pCREB SR-180 vs. NR-180: mean difference = 0.1035, p = 0.8543; SR-180 vs. CTR: mean difference = -0.04700, p = 0.9680; NR-180 vs. CTR: mean difference = -0.1505, p = 0.7171) (Figures 2.19D, 2.20D).

Between groups analysis of pCaMKII and pCREB expression trends along the long axis

Along the long axis we hypothesized that the slopes of pCaMKII and pCREB expression trends would be greater in the cage control group than the experimental groups. Much like the results from *Experiment 1: NMDAR*, we observed no significant differences in pCREB expression trends between any of the room conditions along the long axis of any of the subfields (Figure 2.22).

In pCaMKII expression however, some significant differences were observed. In the suprapyramidal blade, supporting our hypotheses, the control group had a significantly more positive trend than either of the experimental groups (SR-15 vs. NR-15: mean difference = -0.04100, p = 0.9911; SR-15 vs. CTR mean difference = -0.8334, p = 0.0200; NR-15 vs. CTR: mean difference = -0.7924, p = 0.0288) (Figure 2.21A). Similarly, in the infrapyramidal blade we observed a significant difference between new room and control groups that supports our hypothesis (SR-15 vs. NR-15: mean difference = 0.1869, p = 0.8311; SR-15 vs. CTR mean difference = -0.7248, p = 0.0520; NR-15 vs. CTR: mean difference = -0.9117, p = 0.0098) (Figure 2.21B).

Like the suprapyramidal blade, in CA3 we observed significant differences between experimental conditions and the control group that support our hypothesis that spatial learning shifts trends in pCaMKII expression along the long axis in patterns that mirror MEC connectivity. In CA3 we observed that the slope of pCaMKII expression in controls was significantly more positive than either room condition (SR-15 vs. NR-15: mean difference = -0.1621, p = 0. 9115; SR-15 vs. CTR mean difference = -1.651, p = 0.0001; NR-15 vs. CTR: mean difference = -1.489, p = 0.0006) (Figure 2.21C).

In CA1, we observed no significant differences in trends of pCaMKII expression along the long axis between any of the groups (SR-15 vs. NR-15: mean difference = 0.008000, p = 0. 9997; SR-15 vs. CTR mean difference = 0.05110, p = 0.9869; NR-15 vs. CTR: mean difference = 04310, p = 0.9914 (Figure 2.21D).

Summary

In pCaMKII expression, we did not observe patterns that either differed by room condition or matched MEC or LEC connectivity. We did, however, observe differences in patterns of pCaMKII expression in CA3 along the transverse axis that differed by spatial learning as hypothesized. This is to say that we observed increased pCaMKII in the experimental condition in comparison with the cage control group. In pCREB expression, we observed more patterns that differed by room condition and by spatial learning. In CA3, we observed significant differences in the patterns of expression between room conditions which matched MEC and LEC connectivity. In the DG, we observed increased pCREB in the experimental condition and therefore showed a spatial learning effect.

Experiment 3: GluA2:GluA1

Methods specific to experiment 3

Immunohistochemistry

Immunohistochemistry was performed to detect GluA1 and GluA2 expression using a 3-day fluorescent immunohistochemical protocol.

On day 1, tissue was washed in 0.1 M PBS 3 x 10 min and placed in 1000 µL of 0.1 M PBS + 0.2% Triton X (PBS TX-100). Tissue being stained for GluA1 was incubated at a ratio of 1:200 for the primary antibody (AMPA Receptor 1 (GluA1), Cell Signaling Technology). Tissue stained for GluA2 was incubated at a ratio of 1:500 for the primary antibody (Anti-Glutamate Receptor 2, EMD Millipore Corp.). Once the appropriate volume of antibody was added to the tissue, the trays were left to incubate on an orbital shaker, agitated gently, for 24 hours at room temperature.

On day 2, the tissue was washed in 0.1 M PBS 3 x 5 min. Tissue was again placed in 1000µL of PBS TX-100. Tissue being stained for GluA1 was incubated in secondary antibody at a concentration of 1:1000 (Alexa flour 488 anti-rabbit IgG, New England Biolabs Ltm.), and GluA2 had a concentration of 1:500 (Alexa flour 488 anti-mouse, Sigma Aldrich). The tissue was covered in tin foil to ensure no light exposure during incubation, and incubated on an orbital shaker, agitated gently, for 24 hours at room temperature.

On day three, the tissue was washed again in 0.1 M PBS 3 x 5 min. After the washes, the tissue was added to a large petri dish containing 0.1 M PBS and sorted from

anterior to posterior and then mounted onto 1% gelatin and 0.2% chromatin coated slides. The slides were then cover slipped and placed in a refrigerator at 4°C.

Analysis

In addition to the analysis procedure used identically in all 3 experiments, a ratio of GluA2 sample average pixel fluorescence, to GluA1 sample average pixel fluorescence was recorded as a measure of plastic expression in this experiment.

Results

Pre-training behaviour

Figure 2.23A shows the mean path length (cm) taken by rats that would undergo either same room or new room new learning to find a fixed, hidden escape platform during each of the four days of acquisition training on the spatial version of the Morris water task. Subjects swam longer distances early in training to find the hidden platform, and eventually find the platform more efficiently by the end of training. A two-way repeated-measures ANOVA for day by group showed a significant path length decrease over days of training ($F_{3, 820} = 43.08$, $p < 0.001$), and post hoc multiple comparison demonstrated no group difference ($0.0748 < p > 0.9999$). Latency over days showed the same effects, that latency decreased significantly over days (two-way ANOVA, $p < 0.0001$), and post hoc analyses show no significant differences between groups over days of training ($0.0727 < p > 0.9999$) (Figure 2.23B). Therefore, a learning effect over days of training was observed in both path length and latency to reach the target, regardless of group.

This learning was also reflected across trials, as the average path length from the fifth to the final trial was less than 274 cm during training. In contrast, the average path length from the first to the fourth trial was 464 cm, as seen in Figure S1. Two-way repeated-measures ANOVA for trial by group showed a significant path length decrease over trials of training ($F_{7, 752} = 7.473$, $p < 0.0001$). A Bonferroni-corrected post hoc multiple comparison test demonstrated no significant difference over training trials between groups ($0.2577 < p > 0.9999$). Similarly, latency was analyzed using a two-way repeated-measures ANOVA for trial by group, and significant decreases in latency to platform over trials of training ($F_{7, 752} = 8.768$, $p < 0.0001$). Post hoc analyses also demonstrated no significant difference over training trials between groups ($0.0705 < p > 0.9999$).

When the groups are divided by the time they would be sacrificed (70 or 180 minutes), the learning effect and lack of group effect are also observed in path length (learning: $F_{3, 514} = 8.768$, $p < 0.0001$; group: $F_{1, 514} = 0.9190$, $p = 0.3382$) and latency (Fig. S2) (learning: $F_{3, 514} = 57.11$, $p < 0.0001$; group: $F_{1, 514} = 2.973$, $p = 0.0853$).

New learning behaviour

Path length during new learning, in Figure 2.23C, shows a significant learning effect over all 16 trials, and the first 6 trials, but not the last 10. A two-way repeated measures ANOVA across all 16 trials by group shows significant path length decrease over all new learning trials ($F_{15, 352} = 23.42$, $p < 0.0001$), significant effects are also observed over the first 6 trials ($F_{5, 132} = 18.91$, $p < 0.0001$), however the learning effects plateau in the final 10 trials of new learning, as no significant decreases in path length are observed ($F_{9, 220} = 1.417$, $p = 0.1817$). Between groups comparisons also show significant

differences during new learning across all trials ($F_{1, 352} = 80.79$, $p < 0.0001$), as well as the first 6 trials ($F_{1, 132} = 52.93$, $p < 0.0001$). Post hoc analyses of the last 10 trials, however, show no significant effect of group ($0.1939 < p < 0.9999$), demonstrating that animals, regardless of group, reach an equal level of performance on during this phase of learning.

Latency during new learning shows a learning effect across all trials (Fig. 2.23D). Significant decreases in latency were observed over 16 ($F_{15, 352} = 15.71$, $p < 0.0001$), the first 6 ($F_{5, 132} = 11.66$, $p < 0.0001$), and the last 10 trials ($F_{9, 220} = 2.645$, $p = 0.0063$). Significant group effects were observed, with deficits in same room new learning, across all 16 trials ($F_{1, 352} = 18.03$, $p < 0.0001$). These group effects were also observed in the first 6 trials ($F_{1, 132} = 20.34$, $p < 0.0001$), but not in the last 10 trials ($F_{1, 220} = 0.4076$, $p = 0.05238$). Post hoc analyses of the last 10 trials further support the results, that animals regardless of group reach an equal level of performance on this phase of learning ($0.6769 < p > 0.9999$).

Once again, when groups were divided by the time that animals would be sacrificed, a significant learning effect was observed in path length and latency (Fig. S2) (path length learning: $F_{15, 96} = 8.861$, $p < 0.0001$; latency learning: $F_{15, 96} = 14.86$, $p < 0.0001$). While there was an effect of group in both path length and latency, these effects were isolated to either trial 3 in path length ($p = 0.0490$), or trials 2 and 3 in latency (Trial 2: $p = 0.0096$; Trial 3: $p = 0.0046$), out of the 16 trials undergone during the new learning phase.

GluA2:GluA1 Expression across hippocampal subfields

Figure 2.24 depicts the effects of new learning in a same-room or new-room condition on the ratio of GluA2:GluA1 expression in different subfields at different times. The within group comparison shows a significant effect of subfield ($F_{1.1378, 19.98} = 52.86$, $p < 0.0001$). This subfield effect is shown in the significantly greater GluA2:GluA1 expression in DG and CA3 than CA1 in both new room conditions, but not in the same room condition (post-hoc, $0.0089 < p > 0.0387$). Furthermore, there was a significant effect of subfield factor by group (room condition and sacrifice time) ($F_{8, 29} = 2.957$, $p = 0.0151$), and Chi-square results show significant relationship between subfield and group ($\chi^2 = 42.98$, $p < 0.0001$). Specifically, significant differences were observed between subfields in post hoc analyses in the new room but not same room animals (NR-70: DG vs. CA1, $p = 0.0223$, CA3 vs. CA1, $p = 0.0089$; NR-180: DG vs. CA1, $p = 0.0229$, CA3 vs. CA1, $p = 0.0387$). A ROUT outlier test (Q =1 %) identified no outliers. Therefore, there are both significant trends in subfield expression within groups, and significant differences observed across room condition and sacrifice time between groups.

GluA2:GluA1 expression between 70 and 180 minute groups, in same room and new room new learning along the transverse axis, within subfields.

Based on the connectivity patterns of the MEC and LEC with subfields of the hippocampus, either linear or non-linear models were used to analyze trends of GluA2:GluA1 expression. A linear model was used in CA3, and CA1 since connectivity with either MEC or LEC in these regions was polarized towards either the distal or proximal regions. A linear model was also used in the infrapyramidal blade of the DG since connectivity with the MEC and LEC is laminar. In the suprapyramidal blade of the

DG, however, MEC and LEC connectivity shifts in the middle third of the subfield so in this case we used a non-linear model. These models are shown in Figure 2.25. In the suprapyramidal blade of the dentate gyrus, a non-linear model was used. Concave trends were observed along the transverse axis at both time periods in new room animals, and cage controls (70 minutes: R square = 0.1670, $Y = 0.7942 + 0.01374X – 0.0003419X^2$; 180 minutes: R square = 0.06406, $Y = 0.9174 + 0.02720X – 0.001058X^2$; CTR: R square = 0.02546, , $Y = 0.9590 + 0.02367X – 0.001050X^2$). In contrast, same room animals showed only a slight concave trend in the 70-minute group, and a convex trend in the 180 minute group (70 minutes: R square = 0.004501, , $Y = 0.7460 + 0.001370X – 7.312e\text{-}005X^2$; 180 minutes: R square = 0.04783, , $Y = 0.9026 - 0.003634X + 0.0002648X^2$). Therefore, in the suprapyramidal blade we observed expression patterns that matched LEC connectivity in new room animals, cage controls, and the 70-minute same room groups, while we observed expression patterns that matched MEC connectivity in the same room 180-minute group. In the infrapyramidal blade of the dentate gyrus, a linear model was used (Fig. 2.25B). Significant positive trends were observed from distal to proximal in new room animals at both 70 and 180 minutes, and control animals 70 minutes: R square = 0.4373, $F_{1, 18} = 13.99$, $p = 0.0015$; 180 minutes: R square = 0.4498, $F_{1, 18} = 14.72$, $p = 0.0012$; CTR: R square = 0.4702, $F_{1, 18} = 15.97$, $p = 0.0008$). No significant effect was observed in same room animals (70 minutes: R square = 0.06732, $F_{1, 18} = 1.299$, $p = 0.2693$; 180 minutes: R square = 3.149e-005, $F_{1, 18} = 0.0005668$, $p = 0.9813$). Therefore, in the infrapyramidal blade, we observed trends that match entorhinal-cortex connectivity in all non-significant groups (same room animals), however we did not observe trends that matched in either of the new room groups or the control group. In CA3, same room 180 minute animals showed a significant negative

trend, while controls showed a significant positive trend (SR-180 minutes: R square = 0.5974, $F_{1, 18} = 26.71$, $p < 0.0001$; CTR : R square = 0.2366, $F_{1, 18} = 5.579$, $p = 0.0296$) (Fig. 2.25C). All other groups showed no significant trends(NR-70 minutes: R square = 0.5312, $F_{1, 18} = 0.5312$, $p = 0.4755$; NR-180 minutes: R square = 0.1637, $F_{1, 18} = 3.524$, p = 0768; SR-70 minutes: R square = 0.1725, $F_{1, 18} = 3.753$, $p = 0.0686$). Therefore, we observed significant trends which match MEC connectivity in the same room 180-minute group, and we observed significant trends which matched LEC connectivity in the control group. Finally, in CA1, a significant negative trend was observed in the same room 180-minute group, and significant positive trends were observed in all other group. (SR-70 minutes: R square = 0.5825, $F_{1, 18} = 25.12$, $p < 0.0001$; SR-180 minutes: R square = 0.3301, $F_{1, 18} = 8.868$, $p = 0.0081$; NR-70 minutes: R square = 0.3084, $F_{1, 18} = 8.027$, $p = 0.0110$; NR-180 minutes: R square = 0.5007, $F_{1, 18} = 18.05$, $p = 0.0005$; CTR: R square = 0.3140, $F_{1, 18} = 8.240$, $p = 0.0102$) (Fig. 2.25D). Therefore, we observed trends which matched LEC connectivity in the same room 180-minute group, and trends which matched MEC connectivity in the same room 70-minute, new room 70-minute, new room 180-minute, and control groups.

<u>GluA2:GluA1 expression in 70 and 180 minute groups, in same room and new room new learning along the long axis, within subfields.</u>

Linear regressions along the long axis, from dorsal to ventral of the ventral hippocampus in all subfields. In the dentate gyrus, significant positive trends from dorsal to ventral were observed in same room animals at both time points, as well as controls (SR-70 minutes: R square = 0.8853, $F_{1, 8} = 61.77$, $p < 0.0001$; SR-180 minutes: R square = 0.6167, $F_{1, 8} = 12.87$, $p = 0.0071$; CTR: R square = 0.4869, $F_{1, 8} = 7.592$, $p = 0.0249$) (Fig.

2.26A). In contrast, significant negative trends were observed in new room animals at 180 minutes, but not 70 minutes (NR-70 minutes: R square = 0.0340, $F_{1, 8} = 0.2509$, p = 0.6300; NR-180 minutes: R square = 0.7165, $F_{1, 8} = 20.22$, p = 0.0020). Therefore, in the dentate gyrus we observed expression patterns in same room animals that matched LEC connectivity, and expression patterns in new room animals that matched MEC connectivity.

In CA3, significant positive trends were observed in both room conditions at 70 minutes, but no significant trends were observed at 180 minutes or in controls (SR-70 minutes: R square = 0.8185, $F_{1, 8} = 36.06$, p = 0.0003; NR-70 minutes: R square = 0.6926, $F_{1, 8} = 18.03$, p = 0.0028; SR-180 minutes: R square = 0.3459, $F_{1, 8} = 4.230$, p = 0.0737; NR-180 minutes: R square = 0.3965, $F_{1, 8} = 5.256$, p = 0.0511; CTR: R square = 0.01138, $F_{1, 8} = 0.09209$, p = 0.7693) (Fig. 2.26B). Therefore, in CA3, expression patterns do not differ by room condition, but both 70 minute group's expression patterns match LEC connectivity patterns.

Finally, in CA1, no significant trends were observed in any room condition or time point along the long axis (same room 70 minutes: R squared = 0.3507, $F_{1, 8} = 4.320$, p = 0.0713; same room 180 minutes: R squared = 0.3881, $F_{1, 8} = 5.074$, p = 0.0544; new room 70 minutes: R square = 0.06583, $F_{1, 8} = 0.5637$, p = 0.4743; new room 180 minutes: R square = 0.07164, $F_{1, 8} = 0.6173$, p = 0.4547; CTR: R square = 0.3212, $F_{1, 8} = 3.786$, p = 0.0876) (Fig. 2.26C). Therefore, none of the expression patterns in any of the room conditions matched MEC or LEC connectivity patterns.

Between groups analysis of GluA2:GluA1 expression trends along the transverse axis.

One-way ANOVAs were conducted on the slopes of the aforementioned regressions to assess the significance of differences between the GluA2:GluA1 expression patterns along the transverse axis in each of the hippocampal subfields. This between group analysis is shown in Figure 2.27. In the suprapyramidal blade of the dentate gyrus, since a non-linear model was used, the third coefficient was compared in the ANOVA to assess if the largest contributor to the trends were significantly different between room conditions. No significant differences in expression trends were observed between any groups (SR-70 vs. SR-180: mean difference = -0.0003379, p = 0.9878; SR-70 vs. NR-70: mean difference = 0.0002688, p = 0.9949; SR-70 vs. NR-180: mean difference = 0.0009849, p = 0.6057; SR-70 vs CTR: mean difference = 0.0009769, p = 0.6132; SR-180 vs. NR-70: mean difference = 0.0006067, p = 0.9017; SR-180 vs. NR-180: mean difference = 0.001323, p = 0.3093; SR-180 vs. CTR: mean difference = 0.1315, p = 0.3153; NR-70 vs. NR-180: mean difference = 0.0007161, p = 0.8338; NR-70 vs. CTR: mean difference = 0.0007081, p = 0.8394; NR-180 vs. CTR: mean difference = -8.000e-006, p > 0.9999) (Fig. 2.27A). Therefore, no significant differences in patterns of GluA2:GluA1 expression was observed between any groups. In the infrapyramidal blade, significant differences were observed between the control group and all other groups, but no significant difference were observed between any of the experimental groups (SR-70 vs. SR-180: mean difference = -0.0004154, p = 0.9973; SR-70 vs. NR-70: mean difference = -0.002800, p = 0.1744; SR-70 vs. NR-180: mean difference = -0.002565, p = 0.2499; SR-70 vs. CTR: mean difference = -0.007206, p <0.0001; SR-180 vs. NR-70: mean difference = -0.002385, p = 0.3205; SR-180 vs. NR-180: mean difference = -0.002150, p = 0.4270; SR-180 vs. CTR: mean difference = -0.006791, p <0.0001; NR-70

vs. NR-180: mean difference = 0.0002350, p = 0.9997; NR-70 vs. CTR: mean difference = -0.004406, p = 0.0059; NR-180 vs. CTR: mean difference = -0.004641, p = 0.0032) (Fig. 2.27B). Therefore, undergoing a spatial learning task significantly alters expression patterns, however room condition does not have an effect. In CA3, significant differences were observed in the trends of GluA2:GluA1 expression from distal to proximal between the same room 180-minute group and all other groups. Significant differences were not observed in any other conditions (SR-70 vs. SR-180: mean difference = 0.004312, p = 0.0068; SR-70 vs. NR-70: mean difference = 0.0001408, p >0.9999; SR-70 vs. NR-180: mean difference = -0.002595, p = 0.2315; SR-70 vs. CTR: mean difference = -0.0005329, p = 0.9928; SR-180 vs. NR-70: mean difference = -0.004171, p = 0.0096; SR-180 vs. NR-180: mean difference = -0.006907, p <0.0001; SR-180 vs. CTR: mean difference = -0.004845, p = 0.0016; NR-70 vs. NR-180: mean difference = -0.002736, p = 0.1861; NR-70 vs. CTR: mean difference = -0.0006737, p = 0.9834; NR-180 vs. CTR: mean difference = 0.002062, p = 0.4610) (Fig. 2.27C). Therefore, in CA3, a significant change occurs in same room animals from 70 to 180 minutes, however this difference is not shown in new room animals. This change reflects expression patterns that match LEC connectivity shifting to match MEC connectivity. Significant difference were only observed in CA1 between the same room 70 minute group and the new room 180 group, the same room 180 minute group and the new room 180 minute group, and the same room 180 minute group and controls (SR-70 vs. SR-180: mean difference = 0.004621, p = 0.1942; SR-70 vs. NR-70: mean difference = -0.0005270, p = 0.9991; SR-70 vs. NR-180: mean difference = -0.006107, p = 0.0379; SR-70 vs. CTR: mean difference = -0.002038, p = 0.8704; SR-180 vs. NR-70: mean difference = -0.005148, p = 0.1153; SR-180 vs. NR-180: mean difference = -0.01073, p = 0.0716; SR-180 vs. CTR: mean difference = -

0.006659, p = 0.0716; NR-70 vs. NR-180: mean difference = -0.005580, p = 0.1861; NR-70 vs. CTR: mean difference = 0.004069, p = 0.9526; NR-180 vs. CTR: mean difference = 0.002062, p = 0.3116) (Fig. 2.27D). Therefore, in CA1 we observed a significant difference in expression patterns at 180 minutes between room conditions. In the same room condition, these patterns favour LEC-connected regions, while in the new room condition, these patterns favour MEC-connected regions.

Between groups analysis of GluA2:GluA1 expression trends along the long axis.

Similar to the transverse axis, one-way ANOVAs were conducted to determine the significant differences in GluA2:GluA1 expression trends from dorsal to ventral in the dorsal hippocampus and these analyses are shown in Figure 2.28. In the dentate gyrus, significant differences in the trends of expression were observed in 3 cases: between the new room 180 minute group, and the same room 70, same room 180, and control groups (SR-70 vs. SR-180: mean difference = 0.008554, p = 0.8467; SR-70 vs. NR-70: mean difference = 0.01912, p = 0.1761; SR-70 vs. NR-180: mean difference = 0.03893, p = 0.0004; SR-70 vs. CTR: mean difference = -0.004780, p = 0.9790; SR-180 vs. NR-70: mean difference = 0.0156, p = 0.7202; SR-180 vs. NR-180: mean difference = 0.03038, p = 0.0072; SR-180 vs. CTR: mean difference = -0.01333, p = 0.5166; NR-70 vs. NR-180: mean difference = 0.01981, p = 0.1499; NR-70 vs. CTR: mean difference = -0.02390, p = 0.0523; NR-180 vs. CTR: mean difference = -0.04371, p <0.0001) (Fig. 2.28A). Therefore, we observed that while a significant change occurred in expression patterns in the new room condition, no significant change occurred in the same room condition. The changes in the new room condition show a stronger preference for MEC-connected regions. In CA3, significant differences were observed in 6 cases, between the same room

70 minute group and same room 180 minute, new room 180 minute, and control groups, and between the new room 70 minute group and same room 180 minute, new room 180 minute, and control groups (SR-70 vs. SR-180: mean difference = 0.03415, p = 0.0004; SR-70 vs. NR-70: mean difference = 0.003160, p = 0.9928; SR-70 vs. NR-180: mean difference = 0.03873, p <0.0001; SR-70 vs. CTR: mean difference = 0.02880, p = 0.0032; SR-180 vs. NR-70: mean difference = -0.03099, p = 0.0014; SR-180 vs. NR-180: mean difference = 0.004583, p = 0.9712; SR-180 vs. CTR: mean difference = -0.005374, p = 0.9501; NR-70 vs. NR-180: mean difference = 0.03557, p = 0.0002; NR-70 vs. CTR: mean difference = 0.02564, p = 0.0107; NR-180 vs. CTR: mean difference = -0.009930, p = 0.6677) (Fig. 2.28B). Therefore, in CA3 we observed significant changes in expression patterns in both room conditions, but not significant differences in these changes between room conditions. In both room conditions the changes show at 70 minutes that expression patterns matched LEC-connected regions, which at 180 minutes match MEC-connected regions. Finally, in CA1, no significant differences were found in the trends of GluA2:GluA1 expression along the long axis of CA1 (SR-70 vs. SR-180: mean difference = 0.006240, p = 0.9866; SR-70 vs. NR-70: mean difference = 0.01285, p = 0.8373; SR-70 vs. NR-180: mean difference = 0.01150, p = 8848; SR-70 vs. CTR: mean difference = 0.006210, p = 0.9869; SR-180 vs. NR-70: mean difference = 0.006611, p = 0.9834; SR-180 vs. NR-180: mean difference = 0.005259, p = 0.9930; SR-180 vs. CTR: mean difference = -3.000e-005, p >0.9999; NR-70 vs. NR-180: mean difference = -0.001352, p >0.999; NR-70 vs. CTR: mean difference = -0.006641, p = 0.9831; NR-180 vs. CTR: mean difference = -0.005289, p = 0.9928) (Fig. 2.28C). Therefore, spatial learning did not affect the long-axis patterns of GluA2:GluA1 expression to favor either the MEC or LEC-connected regions.

Summary

In GluA2:GluA1 expression, we largely observe patterns that either differed by room condition or matched MEC or LEC connectivity or differed by spatial learning. In the infrapyramidal blade we observed an effect of spatial learning. This is to say that we observed increased GluA2:GluA1 expression in MEC-connected regions in the experimental groups. Furthermore, in CA3 and CA1 we observed an affect of room condition, and therefore the new room condition's GluA2:GluA1 expression matched MEC connectivity patterns while the same room condition's GluA2:GluA1 expression matched LEC connectivity patterns.

Discussion

In this experiment, we trained rats to rapidly learn a new escape location in a familiar versus a novel context and assessed the expression of five different plasticity cascade proteins across the HPC. These proteins were NMDAR, pCaMKII, pCREB, GluA2 and GluA1. For pCaMKII, and pCREB, the average pixel fluorescence was used as a measure of plasticity. NMDAR expression was assessed given previous work which has demonstrated their differing roles in new learning between novel and familiar contexts (Bye & McDonald, 2019). For AMPAR subunits, GluA2 and GluA1, however, we employed a different strategy. During the consolidation stage of LTP, GluA2 receptors replace GluA1 receptors in the post synaptic membrane (Shi et al., 1999), and therefore we used a ratio of GluA2:GluA1 expression as a measure of plasticity. Previous work has indicated that NMDA receptors are necessary to encode new spatial learning in a novel context, however NMDA receptors are not necessary to encode new spatial learning in the same training context (Bye & McDonald, 2019). The proteins we assessed are activated or trafficked in later stages of NMDA-LTP, and therefore by measuring their expression, we could measure mechanisms that should be recruited for new learning in new-room versus same-room conditions. Our hypotheses were that new spatial learning in the new-room condition would result in greater indicators of plasticity, like pCaMKII and pCREB, than new learning in the same-room condition. We hypothesized that there would not differences in NMDAR expression between groups. In *Experiment 3* we also hypothesized that there would be a greater ratio of GluA2:GluA1 expression at the 180 minute time point than 70 minutes.

In our GluA2:GluA1 analysis, regardless of room condition and hippocampal subfield, we observed greater GluA2:GluA1 expression 180 minutes post-new learning than 70 minutes post-new learning. Our understanding of AMPAR subunit trafficking during the generation and maintenance stages of LTP consistent with this finding (Lynch, Rex, & Gall, 2007). During the generation of LTP, GluA1s are inserted into the post-synaptic membrane and during maintenance, GluA2s replace GluA1s. This receptor trafficking increases synaptic efficacy, thereby generating the structural changes widely accepted to be necessary for learning.

In the average pixel fluorescence we observed both room and subfield effects in all proteins other than pCaMKII (Fig. 2.13). Furthermore, when we assessed significant differences between specific room conditions, in NMDAR, pCREB, and pCaMKII we did not observe significant differences between the two experimental groups. Instead, we observed greater average pixel fluorescence in control groups in NMDAR (Fig. 2.6) and pCREB (Fig. 2.14). One reason for this could be a buffering effect of experience. In cage controls, experiences could have increased salience due to a lack of stimulus otherwise. In GluA2:GluA1, we observed a greater ratio of average pixel fluorescence in new room animals than same room animals (Fig. 2.24). The effects of sub-region were also greater in the new room condition than the same room condition suggesting that the recruitment of HPC subfields during new spatial learning has an early onset. Furthermore, the greater ratio at 180-minute time points from the 70 minute time points for the respective room conditions demonstrates the shift in receptor expression during consolidation.

In our analyses of protein expression along both the long and transverse axes of the HPC, we used regressions of this expression to demonstrate that this ratio is not

consistent within the subfields. Furthermore, we used one-way ANOVAs of these regressions to highlight where these patterns change significantly and thereby are indicative of an effect of room condition on patterns of expression. Therefore, the significant differences highlighted by the one-way ANOVA between group analyses reflect the effect of either, spatial learning through significant differences between experimental and control groups, or room condition through significant differences between room conditions, in these subfields.

Transverse connectivity between EC and HPC is predictive of results

As indicated in the introduction, recent reviews have stated a role for LEC when changes within a context occur, while the role of MEC might be more involved in allocentric context representation. This distinction is supported by functional cell types in these regions, with grid cells found in MEC, coherence between MEC and CA1 during spatial navigation, sparse spatially modulated cells in LEC, and cells responsible for olfactory processing and object representation found in the LEC (reviewed by Nilssen, Doan, Nigro, Ohara, & Witter, 2019). Therefore, in the new spatial learning in the same room condition, the LEC is hypothesized to be recruited to update the pre-existing representation. Based on these dissociable differences in function, we predicted that HPC regions with greater structural connectivity to LEC would be recruited more in the same room condition, while regions with greater structural connectivity to MEC would be recruited more in the new room condition. Therefore, we predicted that in the new room condition plasticity would increase from distal to proximal CA1, proximal to distal CA3, and from suprapyramidal to infrapyramidal blade of the DG. We also predict the opposite trends in the same room condition. *Dentate Gyrus:* DG inputs from EC originate

primarily from layer II, a population which constitutes the major source of fibres that make up the perforant path (Caballero-Bleda & Witter, 1994). Due to the strong input of EC to the DG, the lack of significant trends along the axis in both the supra and infrapyramidal blades is surprising. We analyzed the trends in the suprapyramidal blade differently than the infrapyramidal blade based on previously reported patterns of LEC and MEC connectivity to the suprapyramidal DG (Amaral & Witter, 1995). These reports state that fibres in the outer two thirds of the molecular layer of the DG originate in the MEC, while the fibres in the middle third of the molecular layer of DG originate in the LEC. Therefore, we explored if a non-linear, quadratic fit for the data would show the difference between the outer and inner thirds of the suprapyramidal DG. In contrast, EC connectivity with the infrapyramidal blade is uniform and therefore the null and the expected hypothesis are indistinguishable.

For the infrapyramidal DG, unlike the suprapyramidal blade, these same accounts do not highlight any preferential connectivity in LEC or MEC to distal or proximal portions of the blade (Amaral & Witter, 1995). LEC and MEC projections to the infrapyramidal blade have a laminar pattern, with LEC projections more superficial to MEC projections.

In the suprapyramidal blade we observed the predicted concave trend in NMDAR, pCaMKII, and pCREB in the same room group, and the predicted convex trend in the NMDAR new room group (Figures 2.7A, 2.15A, 2.16A). We therefore observed convex trends in the GluA2:GluA1 condition in the same room group, and concave trends in the pCaMKII, pCREB, and GluA2:GluA1 conditions (also Figures 2.7A, 2.15A, 2.16A, 2.25A). Based on the functional roles of MEC vs. LEC and their patterns of connectivity

with the suprapyramidal blade, some of the patterns of expression contradict our hypotheses. Notably, GluA2:GluA1 cage controls and new room 180-minute animals show similar expression patterns, and same room 180-minute and new room 70-minute animals show similar expression patterns (Figure 2.25A). One caveat to these findings, however, is that no significant differences were found between the third coefficients of these trends based on sacrifice time or room condition (Fig. 2.27A). Similarly, no significant differences were found between the third coefficients of the suprapyramidal blade nonlinear regressions in NMDAR, pCREB, or between the experimental conditions in pCaMKII (Figures 2.9A, 2.19A, 2.20A). Therefore, while the trends themselves were significant, the differences between them were not.

In the infrapyramidal blade, we hypothesized that we'd observe no significant non-zero slope along the transverse axis. Instead, we observed significant positive trends in NMDAR, pCaMKII, and pCREB in all groups (Figures 2.7B, 2.15B, 2.16B). In GluA2:GluA1 we observed significant positive slopes in both new room conditions (Figure 2.25B). In GluA2:GluA1 same room conditions, however, no significant effects were observed, consistent with our hypothesis because MEC and LEC connectivity in the infrapyramidal blade differ in a laminar fashion, from superficial to deep, rather than along the transverse axis (Fig. 2.25B). Largely, these slopes were not significantly different from one another. In pCaMKII and pCREB expression patterns we observed no significant differences between groups (Figures 2.19B, 2.20B). In NMDAR and GluA2:GluA1, however we did observe significant differences between the experimental groups and cage controls (Figures 2.9B, 2.27B). In GluA2:GluA1, these differences supported our hypothesis, but in NMDAR the significant difference between new room

and control groups contradicted it. Furthermore, while we did not observe a significant difference in the slopes of pCREB expression along the transverse axis, the effect of spatial is evident in the overall decrease in expression in the experimental groups (Figure 2.16B). Therefore, along the transverse axis of the infrapyramidal blade we observed an effect of learning on patterns of GluA2:GluA1 and pCREB expression.

It is possible that the plasticity recruited in the portions of the DG that receive input from LEC is because on the first trial of new room learning it appears that rats retrieve a representation from the original room training that provides an early strategy that can transfer to different contexts (Clark et al., 2015) but does not provide a solution in the new room (using a head-direction and pool geometry representation to calculate vectors to the platform position). The subjects quickly abandon strategy this strategy as it takes them to the wrong quadrant of the pool, and they start searching for the new escape location. According to this analysis, the original representation is recalled and used initially in the new room but soon a new representation is formed of the new allocentric environment.

In many HPC models, pattern separation, the ability for representations with significant overlap to be dissociated and discernable, takes place in the DG. Pattern separation is considered a 'preprocessing' stage for EC inputs to the HPC (Leutgeb, Leutgeb, Moser, & Moser, 2007; Neunuebel & Knierim, 2014). Based on this functional role of the DG, it is possible that preferential plasticity in the middle third (and therefore LEC-connected) suprapyramidal DG in the new-room condition is based on the rat's previous experience in the original training context. This previous training is the most similar and only task experience undergone by the animals. Therefore, it's likely that

during new learning, animals draw upon this experience.*CA3:* In CA3, while there are no reported gradients in connectivity with EC, there are reported gradients in function, with distal CA3 being favored for spatial tasks. We observed the predicted significantly positive effects in all groups in NMDAR, cage controls in pCaMKII, same room and control conditions in pCREB, and same room 180-minutes in GluA2:GluA1 (Figures 2.7C, 2.15C, 2.16C, 2.25C). All other findings were insignificant. When we compared trends in CA3, we expected that an effect of spatial learning would show more positive trends in the experimental groups. We also expected that an effect of room condition would show more positive trends in new room than same room conditions. We observed no significant differences between groups in NMDAR expression along the transverse axis (Fig. 2.9C). We observed contradicting evidence to our hypothesis in pCaMKII, with an effect of room but controls had a significantly more positive slope (Fig. 2.19C). In pCREB we also observed contradicting evidence to our hypothesis, as same room and controls had slopes significantly greater than the new room condition (Fig. 2.20C). Conversely, the GluA2:GluA1 between groups analysis supported our hypotheses by demonstrating significant differences between the slope of expression patterns over time in the same room condition. Over room conditions in 180 minute-sacrificed animals, the significant difference between the slopes of these two groups demonstrates that novel context learning significant alters the expression pattern, although the pattern does not significantly favor distal or proximal CA3 (Fig. 2.27C). This significant shift, which decreases the absolute preference, and shifts it towards MEC regions. All together, the results from CA3 support our hypotheses inconsistently. We observed that the effects increased from no effects to spatial learning effects to room effects as cascades converged. This is shown through the lack of effect in NMDAR, the spatial learning

effect in pCaMKII, and the room effects in pCREB and GluA2:GluA1. In other words, proteins that are affected later in the cascade were more sensitive to a room effect and proteins earlier in the cascade showed no effect. One reason why this may be the case, is that plasticity cascades converge. There are a number of biochemical pathways which are triggered by the influx of Ca^{2+} and result in the phosphorylation of CREB, like the PKA and ERK pathways (Thomas & Huganir, 2004; Waltereit & Weller, 2003). Therefore, it is likely that proteins later in the cascade are more sensitive to the trends we hypothesized than proteins earlier in the cascade due to a converging effect.

Therefore, in CA3, unlike DG, we observed our predicted pattern. This difference between patterns that support the role of MEC in new-room learning and LEC in same-room learning may be evidence of pattern separation. Pattern separation in this case is demonstrated by the initial recruitment of all relevant information from LEC, and the subsequent dissociation from the familiar context, which recruits MEC to encode the novel context.

Previous reports that DG NMDAR are necessary for pattern separation provide an interesting link between the experiments that inspired this project, and the present results (McHugh et al., 2007). Animals with NMDAR blockade may demonstrate deficits encoding new learning in the MWT due to an inability to discriminate between contexts. The partial input of relevant information to DG from LEC, proposed here, may result in the recruitment of that population, and the inability to encode novel contexts and new learning using that representation.

CA1: In CA1, MEC connectivity increases from distal to proximal. We therefore hypothesized that we'd observe a positive trend in expression in new room animals and a

negative trend in expression in same room animals. We observed no significant results that contradicted our hypotheses and we observed clear evidence that supported our hypotheses in NMDAR and GluA2:GluA1. In NMDAR we observed significant positive trends in new room groups, and statistically insignificant results in same room and control groups (Figure 2.7D). In GluA2:GluA1, we observed similar positive trends in controls, all new room animals, as well as same room animals at 70 minutes. Furthermore, a significant negative trend was observed in same room animals at 180 minutes (Figure 2.25D). In pCaMKII and pCREB expression, we observed no significant trends in any experimental groups (Figures 2.15D, 2.16D). The between groups analysis we conducted further supported the significant linear regressions that we observed. In NMDAR and GluA2:GluA1 between groups comparisons we observed significant differences between room conditions in NMDAR, and between 180 minute room conditions in GluA2:GluA1 (Figures 2.9D, 2.27D). The GluA2:GluA1 between groups analysis further supports our hypothesis by showing no significant differences in the slope of expression patterns between the two 70-minute conditions, which shifts to a significant difference in the slope of expression patterns between the two 180 minute conditions. Additionally, we observed significant differences between the slopes of NMDAR expression in new room and control groups (Figure 2.9D). In groups where no significant trends were observed, pCaMKII and pCREB, we observed no significant differences between groups (Figures 2.19D, 2.20D). These CA1 trends in plasticity protein expression, and the differences between these trends demonstrate an effect of room condition in both NMDAR and GluA2:GluA1 (Figures 2.29, 2.32), and no effects in pCaMKII and pCREB (Figures 2.30, 2.31).

Dorsal and ventral HPC connectivity patterns with EC, plasticity, and new spatial learning in a familiar versus new context

Along the long axis, because there is greater MEC connectivity with dorsal HPC than ventral HPC and the opposite is true of LEC, we predicted that in the new room condition there would be greater recruitment of dorsal regions of dorsal HPC and in the same room condition there would be greater recruitment of ventral regions of dorsal HPC. We largely did not observe this effect, however. We observed that this was only the case in the dentate gyrus of pCaMKII and GluA2:GluA1 expression patterns (Figures 2.17A, 2.17B, 2.26A). Furthermore, in the between groups analysis we that the effects differed between the proteins. An effect of spatial learning was found in the differences between pCaMKII expression trends and an effect of room was found in the differences between GluA2:GluA1 expression trend (Figures 2.21A, 2.28A). This is somewhat consistent with our results from the transverse axis of CA3, where we observed a greater effect of experimental condition downstream than upstream in the plasticity cascade.

The lack of significance in the pattern of effects might be explained by recent changes in our understanding of the dorsal and ventral HPC contributions to place learning. Early work suggested that ventral HPC had little or no role in place learning in the water task (Moser et al., 1993; Moser et al., 1995; Bannerman et al., 1999; Bannerman et al., 2002). However, later work showed that although dorsal HPC was more efficient at place learning in the water maze, the ventral HPC did make a contribution and could in fact compensate for the dorsal HPC in the right training conditions (Ferbinteanu and McDonald, 2000; Ferbinteanu, Ray and McDonald, 2003). More recently a report showed that the ventral HPC was fundamentally involved in the

early stages and the dorsal HPC in the later stages of place learning (Ruediger et al., 2012). These new findings suggest that both dorsal and ventral HPC are important for place learning.

Trying to understand the current pattern of results through the lens of this new view of the functions of the long axis of the HPC might be illuminating. Our analysis of the task we used in the present experiments is that in both the familiar and novel context new learning conditions the ventral HPC would be heavily recruited early in training and then the precise place navigational processes mediated by the dorsal HPC would become involved. Why do we make this prediction? Recently, we have hypothesized (Gruber and McDonald, 2012) that during the early stages of place learning a learning and memory network centered on the ventral HPC, but also involving the ventral striatum, medial prefrontal cortex, and amygdala. This network is thought to be an early triaging system during learning and crucial for responses to stimuli based on their associated affective value in a context. Early in learning in situations where specific stimuli are associated with positive rewards or negative reinforcement, this network rapidly acquire responses to these stimuli promoting arousal, attention and general approach responses towards cues predictive for the regions of the training context predictive of the reward. These behaviours allow the subjects to keep approaching the general region of the escape platform and allow the dorsal HPC and related circuits to acquire representations that support spatially specific navigational behaviours to the exact region of the platform.

Based on this analysis, we may have observed enhanced plasticity in the ventral HPC than initially predicted because of the need for ventral HPC circuits during the early stages of new learning in both familiar and novel contexts.

Interference effects during new learning in the same context

While the central hypotheses for this experiment are based in GluA2:GluA1 expression, interesting results were also observed in new spatial learning in the familiar versus novel contexts. There were no overall statistically significant differences between groups during pre-training, however, deficits were observed in early phases of new learning in the same room condition in comparison to the new room condition (Figures 2.5C/D, 2.11C/D, 2.12C/D, 2.23C/D). In the last 10 trials of new learning, however, rats reached the same level of performance based on both path length and latency to find the escape platform. We hypothesize that these deficits are due to retroactive interference. This is to say that when rats enter the water task in the same context as original training and must learn a new escape location, they must overwrite the previous platform location memory or learn to inhibit approach to the old location. Our previous work showed that it is probably the latter (McDonald et al., 2005). This claim is based on the demonstration, in that report, that following phase 2 mass training procedures control rats swim and spend more time in the new platform location in the first 10 seconds of a 30 second probe trial and then approach and spend more time in the original platform location in the second 10 seconds. This bin analysis of the probe trial following rapid new learning in a familiar context suggests that the memory for the original escape location is not erased but behaviour to that location is inhibited or dominated by a more recent representation.

CHAPTER 3: DRY-LAND CONTEXTUAL NAVIGATION TASK

Introduction

Contexts and how they are represented in the brain, are an area of prominent research amongst systems neuroscientists, both the theory of context representations (McDonald & White, 1993; O'Keefe & Nadel, 1978; Sutherland & Rudy, 1989) and physiological basis of context representations (Alme et al., 2014; Knierim, 2002). In spatial navigation, context is extremely important, as it provides spatial information to orient and navigate. Previous reports have used a variety of tasks to address the intersection between context and spatial learning, including the previous chapter which used the Morris Water Task (MWT) (Morris et al., 1982). Additionally, the reports that this thesis is based on have also used the MWT (McDonald et al., 2005; Bye & McDonald, 2019).

In the present experiments I wanted to develop a task that also assessed contextualized spatial learning, but also differed from the MWT versions used in previous experiments due to a few limitations. First, while the water task is an extremely efficient navigation learning task, its efficiency is based on its aversive nature for rodents (Golob & Taube, 2002). Furthermore, since animals can become submerged in the task it is not an option for cellular imaging studies. Therefore, I wanted to developed a task which is appetitively-motivated, on dry-land, and allows for free behaviour to test spatial navigation in two contexts.

The context in which learning occurs is intricately tied to a particular experience. We have been interested in examining how spatial learning in novel or familiar contexts influences the expression of proteins involved in synaptic strengthening (reviewed in the

previous chapter). Furthermore, in this research we observed that how the expression of these proteins matched with entorhinal cortex connectivity that differs by hippocampal subfield. I argued that pattern separation and pattern completion play a role in the recruitment of different subfields. As previously stated, pattern separation and completion are neural processes that may be key to accurately learning about different contexts, events associated with them, and the ability to elicit appropriate behaviours when re-encountered. (Rudy, 2009; Fraser and McDonald, 2020). In the contextual navigation water task we demonstrated (in the previous chapter) that regions responsible for this function have less distinct plastic expression based on context. The Dry Land Contextual Navigation Task (DCNT), is another such task in which we expect to see this pattern of results.

In the DCNT, we similarly dissociate between encoding and consolidation, and between environment familiarity, like the water task. The development of this new task also allowed us to look at different aspects of spatial learning in water or dry-land in mice or rats. One of the initial comparisons that we performed was an analysis of win-stay tendencies. This is based on previous work demonstrating that in similar tasks, behaviour differs greatly if a rat is swimming or in an open field (Whishaw & Pasztor, 2000). These data highlight that in a dry task rats are more likely to employ foraging behaviours, and not return to a previously baited area. In a water task, rats are more likely to return to the reinforced location. I hypothesized that the same observation could be made in a comparison between the DCNT and water task, that rats in the water task, unlike mice in the dry task, would show win-stay behaviours. This idea, that animals demonstrate a behavioural pattern of alternating place, was proposed by O'Keefe and Nadel to be

caused by the locale system (1978). This system is also thought to be responsible for the formation of a spatial representation and navigation.

In the present experiments we hypothesize that in the DCNT we will observe differences in new learning between familiar and novel context learning conditions. I hypothesize that in the familiar context, new spatial learning will be negatively impacted by the interference of the recently acquired old location. In the probe trial, I hypothesize that in the familiar context mice will visit the new location more frequently than the old one. In the comparative analysis, we expect to see similar results in path length, that animals show a clear learning effect, but that while win-stay tendencies decrease over learning in the water task, this is not true in the DCNT. We propose that this last hypothesis is due to dry-land tasks recruiting natural foraging behaviours which are not recruited in the water task.

I also included an assessment of stress hormone levels during different phases of training on the different tasks to determine if differences in the neurobiological mechanisms supporting new learning in a familiar versus a new context are due to differences in stress responses in the novel versus familiar condition (Bye and McDonald, 2019). This is based on previous experiments which used forced exposures to novel contexts as a stressor for mice (Bartolomucci et al., 2003).

Experiment 1: Dry land contextual navigation task

Methods

Subjects

Subjects were 24 male C57BL/6 mice aged 30 days at the start of the task. Mice were housed in pairs, and maintained on a 12-hour light/dark cycle with *ad libitum* food access. Until otherwise stated, mice also had *ad libitum* access to water. All subjects were acclimatized for 7 days prior to handling and handled for 5 minutes per day for the 5 days leading up to their respective tasks.

During the behavioural task mice were maintained under a standard water restriction protocol. Mice were water restricted for the three days prior to the start of pre-task training. On the first day of water restriction, mice had no access to water for 22 hours. On the second day of water restriction mice had no access to water for 23 hours, and on the third day of water restriction mice had no access to water for 23.5 hours. For the entirety of the task, mice were maintained on no water access for 23.5 hours, and *ad libitum* access for 30 minutes. During the task, this 30 minute period commenced at least 2 hours after the completion of the last trial.

All procedures were approved by the University of Lethbridge Animal Welfare Committee and in accordance with the Canadian Council of Animal Care.

Dry-land Contextual Navigation Task

Mice underwent the Dry-land Contextual Navigation Task. The training and new learning context were counter-balanced, and consisted of either a hexagon or octagon arena. Both arenas were 2000 cm^2, had 28 cm tall clear acrylic walls, and a base made of

a white wood-composite peg board. The walls were covered (on the outside of the arena) with either a white or black layer, as well as local cues. The end of a syringe cap was cut to less than $1/8^{th}$ of an inch (the thickness of the peg board) and the water reward was placed in this cap, inside the peg board holes.

Pre-task Training

Prior to pre-task training, plasma samples were taken from subjects through sub-mandibular collection. Pre-task training was conducted in the training context and consisted of two phases, each of which lasted for two days. During the first phase of pre-task training, mice were placed in the arena for 6 two-minute trials per day during which 8 random locations in the arena were baited with a water reward. The baited locations were randomized for each trial. During the second phase of pre-task training, mice were placed in the arena for 6 trials per day. Each trial lasted until the mouse located the single, baited reward location, which was randomized for each trial.

Phase 1: Pre-training

On the first 5 days of pre-training, mice were trained to find a single water reward in a consistent location, in the same context in which pre-task training occurred. 6 trials were conducted per day and each trial's maximum length was 2 minutes long. After the completion of this phase, mice were split into either same room- same location, same room- new location, or new room- new location groups. The differences in their procedures are listed below:

Phase 2: Rapid New Learning

Same Room- Same location condition: 8 of the subjects underwent rapid new learning in the same training context with the water reward located in the same location as during Phase 1. During rapid new learning, mice underwent 10 trials in the span of one hour. 30 minutes following new learning, a second plasma sample was retrieved from subjects through sub-mandibular collection.

Same Room- New location condition: 8 of the subjects underwent rapid new learning in the same training context with the water reward relocated to the opposite side of the arena, equidistant from the wall as the phase 1 water reward location. During rapid new learning, mice underwent 10 trials in the span of 1 hour. 30 minutes following new learning, a second plasma sample was retrieved from subjects through sub-mandibular collection.

New Room- New location condition: 8 of the subjects underwent rapid new learning in a new training context which differed in arena shape, colour, local and global cues, and orientation of the entrance. During rapid new learning, mice underwent 10 trials in the span of 1 hour to find the water reward. The water reward was in a different location, relative to cues and absolute coordinates, than the phase 1 water reward location. 30 minutes following new learning, a second plasma sample was retrieved from subjects through sub-mandibular collection.

Phase 3: Probe

Animals who underwent either of the same room conditions (n = 16) underwent a 20 second probe 24 hours after Phase 1. During the probe, animals were placed in the arena with no water reward.

Corticosterone Assay

A corticosterone in vitro competitive ELISA kit (ab108821 Corticosterone ELISA Kit, Abcam, Toronto, Canada) was used to measure corticosterone concentration in the plasma samples collected before the task and after rapid new learning. The assay was conducted according to the manufacturer's kit protocol and analyzed with a BioTek Instruments SynergyHT-I plate reader. All samples were run in either duplicate or quadruplicate.

Analysis

Behavioural data for both the Dry-land Contextual Navigation Task was collected using an overhead camera and analyzed with Noldus Ethovision 11.5. This allowed us to visualize the animal's trajectory. Trials 2-6 during Phase 1, and trials 2-10 during Phase 2 were analyzed for "win-stay tendencies" by three different experimenters who were blind to the animal's condition and the other experimenter's scoring. Win-stay was scored positively if the animal deviated by less than 35 degrees while locating the goal location. If the animal deviated by more than 35 degrees, the animal was not given a win-stay score for that trial.

Two-way ANOVAs and post-hoc comparisons were used on behavioural data using GraphPad Prism 8.

Results

Behaviour: pretraining

The dry land contextual navigation task is a spatial learning paradigm in which experimental conditions differ by new learning context familiarity. We observed a

learning effect over days but not over trails. During the pre-training phase of the DCNT we observed a significant effect of days but not a significant group effect, in a 2-way ANOVA of path length (Day: $F_{4, 733} = 19.26$, $p < 0.0001$; room condition: $F_{2, 733} = 0.9197$, $p = 0.3991$) and latency (Day: $F_{4, 733} = 20.27$, $p < 0.0001$; room condition: $F_{2, 733} = 0.8800$, $p = 0.4152$). This learning effect is demonstrated again in a linear regression of these data in path length (SR-S: slope = -26.20, $F_{1, 237} = 39.58$, $p < 0.0001$; SR-N: slope = -22.85, $F_{1, 237} = 19.98$, $p < 0.0001$; NR-N: slope = -22.06, $F_{1, 268} = 21.44$, $p < 0.0001$), and latency (SR-S: slope = -2.492, $F_{1, 237} = 33.91$, $p < 0.0001$; SR-N: slope = -2.350, $F_{1, 237} = 23.94$, $p < 0.0001$; NR-N: slope = -2.449, $F_{1, 268} = 25.40$, $p < 0.0001$) (Figures 3.2A and 3.2B). Similarly, in path length across trials we observed a significant effect of trial but not group (Trials: $F_{5, 730} = 8.775$, $p < 0.0001$; room condition: $F_{2, 730} = 0.9080$, $p = 0.4038$) (Figure 3.2C). The same observation was made in latency (Trials: $F_{5, 730} = 3.847$, $p = 0.0019$; room condition: $F_{2, 730} = 0.8335$, $p = 0.4349$) (Figure 3.2D). In linear regressions of these data, however, a learning effect was less evident. In path length we observed only a significant negative slope in the same room same location and same room new location groups, furthermore, the slopes observed were much smaller than those observed over days (SR-S: slope = -14.29, $F_{1, 237} = 15,72$, $p < 0.0001$; SR-N: slope = -9.591, $F_{1, 237} = 4.826$, $p = 0.0290$; NR-N: slope = -5.221, $F_{1, 268} = 1.632$, $p = 0.2026$). In latency we observed no significant slopes (SR-S: slope = -0.3254, $F_{1, 237} = 0.7414$, $p = 0.3901$; SR-N: slope = -0.5100, $F_{1, 237} = 1.501$, $p = 0.2217$; NR-N: slope = 0.1049, $F_{1, 268} = 0.06210$, $p = 0.8034$), demonstrating a lack of learning effect over trials.

Behaviour: new learning and probe

During new learning, the procedure differed between room conditions, as they took place in either the same room with the water reward relocated or not, or they took place in a new room entirely. During new learning we observed a significant effect of both trial and room condition in path length (Trial: $F_{9, 219} = 2.820$, $p = 0.0037$; room condition: $F_{2, 219} = 13.58$, $p < 0.0001$), and no significant interaction ($F_{18, 219} = 1.054$, $p = 0.4009$) (Figure 3.3A). In latency we observed the same effects, significance in trial and room condition (Trial: $F_{9, 219} = 2.677$, $p = 0.0057$; room condition: $F_{2, 219} = 8.877$, $p = 0.0002$), and a lack of significant interaction ($F_{18, 219} = 1.121$, $p = 0.3328$) (Figure 3.3C). We also took the average path length and latency across all trials in each group and performed a one-way ANOVA, shown in figures 3.3B and 3.3D. We observed significant differences between the same room same location group and both other groups in path length (SR-S vs. SR-N: mean difference = -39.17, $p = 0.0266$; SR-S vs. NR-N: mean difference = -73.56, $p < 0.0001$; SR-N vs. NR-N: mean difference = -34.40, $p = 0.0510$). In latency we only observed a significant difference between the same room same location group and the new room new location group (SR-S vs. SR-N: mean difference = -2.399, $p = 0.1326$; SR-S vs. NR-N: mean difference = -4.898, $p = 0.0002$; SR-N vs. NR-N: mean difference = -2.498, $p = 0.0989$).

On the 7th day we conducted a 20 second probe to assess the animal's preferences, and we show this data in figure 3.5. We measured the frequency with which the animal visited the old and new reward locations in both same room groups. We observed a significant interaction between conditions ($F_{1, 28} = 10.43$, $p = 0.0032$), and a significant difference in the frequency of old location visits between conditions (mean difference =

3.125, p = 0.0058). These data show that the same room same location animals show a preference for the old location and the same room new location animals show a preference for the new location. In the post-hoc analysis, the only significant difference was observed between the frequency of old location visits in the two groups (Old SR-S vs. old SR-N: mean difference = 3.125, p = 0.0058; old SR-S vs. new SR-S: mean difference = 2.250, p = 0.0757; old SR-N vs. new SR-N: mean difference = -1.625, p = 0.3350; new SR-S vs. new SR-N: mean difference = -0.7500, p = 0.9455). Therefore, we demonstrated a significant difference in the frequency of old location visits between the two same room conditions, demonstrating that the new learned location was retained 24 hours later.

Plasma corticosterone

We measured plasma corticosterone levels before pre-training and after new learning in all three conditions. We showed that there was a significant increase between the two days but not between room conditions (Fig. 3.5). We observed no significant differences between room conditions, but we did observe an effect of task (room condition: $F_{2, 50} = 0.8359$, p = 0.4394; task: $F_{1, 50} = 26.40$, $p < 0.0001$). No significant interaction was observed ($F_{2, 50} = 0.8977$, p = 0.4140).

Experiment 2: Comparison of mouse DCNT learning versus rat water task learning

Purpose

In this experiment we compared path length and win-stay tendencies between mice in the DCNT, and rats in the contextualized water task studied in previous chapter. These analyses were performed as an assessment of the new task, and as a comparison based on some hypothesized behavioural differences between it and the water task. ***This experiment is based on developments in our understanding of animal behaviour during spatial learning and therefore allows us to further understand context learning in a variety of contextualized spatial learning tasks.***

Methods

Subjects

Subjects were 16 male Long Evans rats aged 90 days, weighing between 317- 420 g at the start of the task, and 24 male C57BL/6 mice aged 30 days at the start of the task. Rats were housed in groups of 3, and mice were housed in pairs. Unless otherwise stated, both were maintained on a 12-hour light/dark cycle with *ad libitum* food and water access. All subjects were acclimatized for 7 days prior to handling and handled for 5 minutes per day for the 5 days leading up to their respective tasks.

During the behavioural task mice were maintained under a standard water restriction protocol. Mice were water restricted for the three days prior to the start of pre-task training. On the first day of water restriction, mice had no access to water for 22 hours. On the second day of water restriction mice had no access to water for 23 hours, and on the third day of water restriction mice had no access to water for 23.5 hours. For

the entirety of the task, mice were maintained on no water access for 23.5 hours, and *ad libitum* access for 30 minutes. During the task, this 30 minute period commenced at least 2 hours after the completion of the last trial.

All procedures were approved by the University of Lethbridge Animal Welfare Committee and in accordance with the Canadian Council of Animal Care.

Behavioural Apparatus and Analysis

Rats underwent a Contextual Navigation Water Task (also referred to in *Chapter 2*), while mice underwent the Dry-land Contextual Navigation Task. A comparison of these two tasks is shown in Figure 3.6.

Contextual Navigation Water Task

Spatial learning in the water task was conducted in two rooms, each with a white fibreglass pool (height = 46 cm, diameter = 127 cm). Each pool was located in the center of a room, and each room had distinct extra-maze features. These features include the entry direction, inter-trial cage location, orientation of the experimenter, wall hangings, and furniture. Water was refreshed daily and mixed with ~ 50 mL of white non-toxic tempura paint. The hidden platform (square, 10 cm by 10 cm) was located ~ 3 cm below the water's surface and made of clear acrylic.

Task procedure involved a 2-room, 2 phase version of the hidden-platform water task. All phases took place between 08:00 and 12:00. 4 groups were run in the task, differing in room condition and time of sacrifice.

Phase 1: Pre-training

On each training day phase 1, rats were moved from their home cages into transport cages and transported on a wheeled cart to context A. Rats were trained over 8 trials per day for 4 days to find a hidden platform location in the SE quadrant of the pool where they remained for 10 seconds after every trial. The starting location was randomized, and the maximum allowed time was 60 s after which the animal was placed on the platform for 10 seconds if they could not locate the platform. The average inter-trial interval was 5 minutes, during which the rat was in a transport cage.

Phase 2: Rapid new learning

During new learning, rats underwent rapid new learning in either the training context (same room condition) (n = 8), or a novel context (new room condition) (n = 8). Rats were trained over 16 trials in 45 minutes to find a hidden platform in either the NW quadrant (same room), or the SW quadrant (new room), where they remained for 10 seconds after every trial. The starting location was again, randomized and the maximum allowed time was 60 s after which the animal was placed on the platform for 10 s if they could not locate the platform.

Dry-land Contextual Navigation Task

Mice underwent the Dry-land Contextual Navigation Task. The training and new learning context were counter-balanced for, and consisted of either a hexagon or octagon arena. Both arenas were 2000 cm^2, had 28 cm tall clear acrylic walls, and a base made of a white wood-composite peg board. The walls were covered (on the outside of the arena) with either a white or black layer, as well as local cues. The end of a syringe cap was cut to less than $1/8^{th}$ of an inch (the thickness of the peg board) and the water reward was placed in this cap, inside the peg board holes.

Pre-task Training

Prior to pre-task training, plasma samples were taken from subjects through sub-mandibular collection. Pre-task training was conducted in the training context and consisted of two phases, each of which lasted for two days. During the first phase of pre-task training, mice were placed in the arena for 6 two-minute trials per day during which 8 random locations in the arena were baited with a water reward. The baited locations were randomized for each trial. During the second phase of pre-task training, mice were placed in the arena for 6 trials per day. Each trial lasted until the mouse located the single, baited reward location, which was randomized for each trial.

Phase 1: Pre-training

On the first 5 days of the task, mice were trained to find a single water reward in a consistent location, in the same context in which pre-task training occurred. 6 trials were conducted per day and each trial's maximum length was 2 minutes long. After the completion of this phase, mice were split into either same room- same location, same room- new location, or new room- new location groups. The differences in their procedures are listed below:

Phase 2: Rapid New Learning

Same Room- Same location: 8 of the subjects underwent rapid new learning in the same training context with the water reward located in the same location as during Phase 1. During rapid new learning, mice underwent 10 trials in the span of one hour. 30 minutes following new learning, a second plasma sample was retrieved from subjects through sub-mandibular collection.

Same Room- New location: 8 of the subjects underwent rapid new learning in the same training context with the water reward relocated to the opposite side of the arena, equidistant from the wall as the phase 1 water reward location. During rapid new learning, mice underwent 10 trials in the span of 1 hour. 30 minutes following new learning, a second plasma sample was retrieved from subjects through sub-mandibular collection.

New Room- New location: 8 of the subjects underwent rapid new learning in a new training context which differed in arena shape, colour, local and global cues, and orientation of the entrance. During rapid new learning, mice underwent 10 trials in the span of 1 hour to find the water reward. The water reward was in a different location, relative to cues and absolute coordinates, than the phase 1 water reward location. 30 minutes following new learning, a second plasma sample was retrieved from subjects through sub-mandibular collection.

Phase 3: Probe

Animals who underwent either of the same room conditions (n = 16) underwent a 20 second probe 24 hours after Phase 1. During the probe, animals were placed in the arena with no water reward.

Analysis

Behavioural data for both the Water and Dry-land Contextual Navigation Task was collected using an overhead camera and analyzed with Noldus Ethovision 11.5. Trials 2-6 during pre-training, and trials 2-10 during new learning were analyzed for "win-stay tendencies" by three different experimenters who were blind to the animal's

condition and the other experimenter's scoring. Win-stay was scored positively if the animal deviated by less than 35 degrees while locating the goal location. If the animal deviated by more than 35 degrees, win-stay was scored negatively.

Two-way ANOVAs and post-hoc comparisons were used on behavioural data using GraphPad Prism 8.

Results

Comparison of win-stay tendencies and path length

I assessed win-stay tendencies across days of both the dry-land and water-based spatial navigation tasks. We also compared these tendencies with path length, the traditional measure of learning, to show how this measure differs learning. In the DCNT, we observed learning over days through both a significant effect of day, as well as a significant interaction (Day: $F_{5, 718} = 6.173$, $p < 0.0001$; interaction: $F_{10, 718} = 3.156$, $p = 0.0006$). No significant effect of room was observed ($F_{2, 718} = 26.40$, $p = 0.4396$) (Figure 3.7A). In a linear regression of win stay tendencies over days of pre-training, no significant slopes were observed in either the same room new location group or the new room new location group (SR-N: slope = -0.003056, $F_{1, 170} = 0.01952$, $p = 0.8890$; NR-N: slope = 0.03683, $F_{1, 197} = 3.438$, $p = 0.0652$). The slope of win stay tendencies was significantly positive in the same room same location group during pre-training (SR-S: slope = 0.05578, $F_{1, 165} = 6.510$, $p = 0.0116$). In path length, we observed a clear learning effect over days of pre training, shown through both a 2-way ANOVA, and linear regressions in Figure 3.7B. In the 2-way ANOVA we demonstrated a significant learning effect ($F_{5, 979} = 16.87$, $p < 0.0001$), a significant room effect ($F_{2, 979} = 3.857$, $p = 0.0215$), and a significant interaction ($F_{10, 979} = 1.885$, $p = 0.0435$). The linear regression was

conducted on pre-training days, and demonstrated a significant negative slope in all conditions (SR-S: slope = -26.20, $F_{1, 237} = 39.58$, $p < 0.0001$; SR-N: slope = -22.85, $F_{1, 237} = 19.98$, $p < 0.0001$; NR-N: slope = -22.06, $F_{1, 268} = 21.44$, $p < 0.0001$). The results demonstrated that the pattern of win-stay tendencies and path length differ during the dry-land task. While we observed no trends in win-stay tendencies, there was a significant decreasing trend in path length, and these trends did not differ by room condition.

In the contextual navigation water task, we conducted the same analysis. Unlike the dry-land task, in the water-based task we observed a positive trend in win-stay tendencies over pre-training days. In win-stay tendencies we found a significant effect of day, room condition, and interaction (Day: $F_{4, 756} = 5.058$, $p = 0.0005$; room condition: $F_{1, 756} = 20.44$, $p < 0.0001$; interaction: $F_{4, 756} = 9.685$, $p < 0.0001$) (Figure 3.7C). The linear regression showed that the slopes in both room conditions were significantly positive, therefore showing that over days in this task there was an increase in win-stay tendencies (SR-N: slope = 0.04662, $F_{1, 328} = 4.191$, $p = 0.0414$; NR-N: slope = 0.09277, $F_{1, 328} = 12.85$, $p = 0.0004$). In rats that underwent the water task, we observed significant effects of day and significant interaction (Day: $F_{4, 842} = 33.33$, $p < 0.0001$; interaction: $F_{4, 842} = 5.298$, $p = 0.0003$). No significant effect of room condition was found ($F_{1, 842} = 1.179$, $p = 0.2778$). In the linear regression of pre training path length we observed a significant learning effect, shown through significant negative slopes in both groups (SR-N: slope = -46.15, $F_{1, 442} = 46.15$, $p < 0.0001$; NR-N: slope = -149.1, $F_{1, 382} = 51.05$, $p < 0.0001$) (Figure 3.7D). Therefore, in the water task we showed significant changes over days in both win-stay tendencies and path length. These increased in the former and decreased in the latter throughout pre-training.

Comparison of DCNT and water task in new learning

We compared win-stay tendencies between the two tasks in new learning and found that rats in the new room condition had greater win-stay tendencies than any of the other groups. We observed a significant effect of both task/species, and room condition (Task/species: $F_{1, 400} = 6.816$, $p = 0.0094$; room condition: $F_{1, 400} = 7.910$, $p = 0.0052$). No significant interaction was observed ($F_{1, 400} = 2.005$, $p = 0.1575$). In the post-hoc analyses we observed the same trends in the two tasks, that win-stay tendencies were greater in the new room new location groups than the same room new location groups. This difference was only significant between the rat water task new room new location group and all other groups (DCNT NR-N vs. CNWT NR-N: mean difference = -0.1659, $p = 0.0324$; CNWT SR-N vs. CNWT NR-N: mean difference = -0.1742, $p = 0.0027$; DCNT SR-N vs. CNWT NR-N: mean difference = -0.2235, $p = 0.0024$). It was insignificant in all other pairings (DCNT SR-N vs. DCNT NR-N: mean difference = -0.05754, $p = 0.8187$; DCNT SR-N vs. CNWT SR-N: mean difference = -0.04922, $p = 0.8150$; DCNT NR-N vs. CNWT SR-N: mean difference = 0.008315, $p = 0.9986$) (Figure 3.8). In this comparative analysis, I showed that there was no significant difference in the average win-stay tendency in same room conditions but there was a significant difference between the tasks in the new room conditions.

Discussion

In these experiments I presented a novel spatial learning paradigm and have compared the performance of mice in this task with the more commonly used rats in the water task. The DCNT assesses two main learning variables, encoding vs. consolidation, and novel vs. familiar context, shown in figure 3.1. If animals' performance improves during the new-learning phase, this demonstrates encoding. If animals continue to show a preference for the new-learning location in the probe trial, this demonstrates consolidation. Furthermore, as new-learning is split into same and new-room conditions, we can distinguish between learning in these conditions. We found that mice learned both the pre-training and new learning reward regions, and that they retained the memory 24 hours after new learning.

Learning is observed in the DCNT

We hypothesized that in the DCNT we would observe differences in new learning between familiar and novel context learning conditions. Furthermore, we hypothesized that in the familiar context, new learning would be negatively impacted by the interference of an old learned location. In the probe trial, we hypothesized that familiar context mice would visit the new location more frequently than the old one. In the comparative analysis, we expected to see similar results in path length, that animals showed a clear learning effect, but that while win-stay tendencies decreased over learning in the water task, this would not be true in the DCNT. A design comparison of these two tasks can be found in figure 3.6. Largely we found evidence that supported these hypotheses except for interference in the same-room new location condition.

In experiment 1, we demonstrated a clear learning effect over pre-training days, however a learning effect was not evident over pre-training trials (Fig. 3.2). Since the DCNT is an appetitive task and relies on animals to be water-restricted, the lack of learning effect over trials may be due to animals becoming more satiated over trails. During the new learning phase, we showed that all mice reached a asymptotic level over the 10 trials (Fig. 3.3). We did not observe, however evidence of memory interference in the same room new location group. We expected this group to have the greatest path length and latency, however the condition with the greatest path length and latency was the new room new location group. There are a few reasons why this might be the case including an anxiogenic response in the new context or the effects of establishing the place representation.

No significant stress response in novel context new spatial learning

Also, in experiment 1, I assessed corticosterone levels in the plasma of mice who underwent the DCNT to test if differences in the behaviour between room conditions could be due to a stress response. I took samples while mice were water restricted, before pre-training and after new-learning and observed elevated plasma corticosterone levels in the initial measure, and further elevated levels in the second measure (Fig. 3.5). In non-stressed mice, plasma corticosterone levels are approximately 50 ng/mL (Song et al., 2006). In the initial test, the average corticosterone level was 140.2274 ng/mL across all conditions. This is reflective stress experienced during the water restriction protocol and has been reported in rats (Heiderstadt et al., 2000). In the second measure, I observed significantly increased corticosterone levels relative to both the average non-stressed level and the elevated water-restricted level I measured. The average corticosterone level

across all groups after new learning was 383.4044 ng/mL, 243.1770 ng/mL greater than the initial measurement. Furthermore, we did not observe significant differences between room conditions. This assay demonstrated that the behavioural differences between groups was not due to a stress response caused by new learning in the new room condition. We did observe, however, an increased stress response between task naïve and mice who had undergone new learning. This data is consistent with other, but aversive, spatial learning tasks such as the water task and the Barnes maze (Harrison et al., 2009).

Different effects are observed in win-stay tendencies between dry-land and water-based tasks

In experiment 2, we compared the behavioural results from experiment 1 with the behavioural data from rats who underwent the contextual navigation water task across all experiments of chapter 2 (Figure 3.6). We did this to compare this novel spatial learning task with another spatial learning task in which it has been demonstrated that neurochemical mechanisms differ between familiar and novel context groups (Bye & McDonald, 2019). Furthermore, the locale system, the system proposed by O'Keefe and Nadel to represent space and is responsible for spatial navigation, is also proposed to generate win-shift (alternating) behaviour (1978). Further research has shown that while this is true in dry-land tasks it is not true in water (Whishaw & Pasztor, 2000). Therefore, we hypothesized that if we measured win-stay tendencies, or the frequency with which the animal returns directly to a learned location, we would observe win-stay frequencies that increased over days in the water task but not in the DCNT. This comparison was imperfect, as it lacked a mouse water task group and a rat DCNT group. Its purpose, however, was to compare the behavioural tasks being used throughout this thesis.

Furthermore, previous reports reviewing the differences between mouse and rat behaviour give us confidence in this comparison (Stranahan, 2011).

Figure 3.8 shows the win-stay and path length measures in both the DCNT and water task over all days of the tasks, including new learning. The first analysis was only done on the first 5 days for the DCNT, and the first 4 days for the water task. In the first pre-training analysis, I observed no significant trend over days in win-stay tendencies in the DCNT, while I observed a clear learning effect in path length. In pre-training of the water task, I observed a significant positive trend in the linear analysis of win-stay tendencies and a significant learning effect in path length. This difference, that in the DCNT significant trends were only observed in path length, and that in the water task opposing trends were observed, suggests that the win-stay measure increases with learning in the water task but is not a measure of learning in the DCNT. Furthermore, based on our hypothesis that this is due to alternating behaviour, established by the locale systems based on foraging behaviour, we can identify two major forces that might contribute to win-stay tendencies in the DCNT. First, over days the mice are exposed to a single reward location and therefore there is decreased incentive for alternating behaviour. Second, over days the representation of the pre-training context is strengthened, encouraging foraging behaviour. These two forces work in opposition to diminish any trend in win-stay tendencies over days of pre-training.

In the comparison of win-stay tendencies between groups in the two tasks we observed greater win-stay tendencies in the new room new location groups than the same room new location groups, however these differences were only significant in the water task. There are two notes to be made on this. First, as we have noted in chapter 2, the

water task is a highly aversive task, and in early stages of learning recruits a learning and memory network that includes the ventral HPC, the ventral striatum, medial prefrontal cortex, and amygdala. This network has been proposed to serve as a triaging system for stimuli to assess their value in promoting responses (Gruber & McDonald, 2012). Therefore, unlike in foraging behaviour, the ventral hippocampal triaging system encourages consistent responses prompted by specific stimuli. In the water task, our two new learning conditions differ in the extent of new learning that is taking place. In the same room new location condition, rats learn a new location of the escape platform, however all other aspects of the context are identical. In the new room new location condition, all of the spatial cues are being learned in addition to the new location of the escape platform. Therefore, it appears that the early stages of learning which recruit the triaging system are prompted by the new room condition, and result in greater win-stay tendencies. In the same room condition, it is likely that this same system promoted early consistent behaviour, making rats swim to the old location, and that in new learning either this routine is established enough that rats continue to return to the old location (not win-stay behaviour) or, rats have learned the context well enough that less consistent behaviour starts to take place leaning from the ventral hippocampal network to the dorsal hippocampal network.

In contrast, in the DCNT we observed no difference in win-stay tendencies during new learning between room conditions. In this task we also observed less win-stay tendencies than the new room condition of the water task. These data support our hypothesis that in this task there is greater alternating behaviour, as suggested by O'Keefe and Nadel (1978), and there is greater foraging behaviour, as suggested by Whishaw and

Pasztor (2000), in the new room condition. However, we did not observe significant differences in win-stay tendencies between the two same-room conditions in the two tasks. I expect that no significant difference was observed, however, because in the same room new location water task group, there was interference of the old location memory, and this confounded our measure of win-stay tendencies. The alternating behaviour that was observed is indicative that triaging is not as involved as an integrated representation of stimuli for learning this task, and this integrated representation takes place in the dorsal hippocampus.

In summary, in this chapter we presented a novel spatial learning task with the purpose of assessing spatial learning based on context familiarity. Using this task, we observed reliable learning outcomes over days but not trials. Furthermore, we measured plasma corticosterone and found a stress effect of task but not room condition. In comparison with previous reports, we also found a stress effect of water restriction. In contrast with the water task, we observed differences in win-stay tendencies between the new room conditions in these tasks. Furthermore, we observe differences between the same and new room groups in the water task. These data indicate that while learning is taking place over days, win-stay tendencies, as a measurement, may be used as a tool to demonstrate how the specific behaviours involved may serve as a window into the systems responsible for learning in each task. We have proposed that a ventral hippocampal network may be necessary for triaging stimuli and learning in early stages of the water task, while a dorsal hippocampal network is necessary for an integrated representation of stimuli in the DCNT.

CHAPTER 4: PLACE CELL ACTIVITY IN DCNT

Introduction

In previous chapters I examined the differences between spatial learning in familiar and novel contexts at a biochemical and behavioural scale. In this chapter I examined these differences at a cellular activity scale. The importance of cellular representations of space originates from the theory of cognitive mapping. This theory originated prior to the many of the techniques we use today to examine how cells in numerous networks represent space when Tolman observed that rats, given the opportunity to freely explore, took shortcuts to a baited location in later trials (Tolman & Honzik, 1930). In another experiment, they also found that when parts of the maze were blocked, rats were able to selectively navigate new ones (Tolman et al., 1946). The prior exploratory period in the maze informed the rats' behaviour in the baited trials, prompting Tolman to hypothesize that the brain generated a representation of the space during the exploration to be used later. Later, this representation was applied literally in *The Hippocampus as a Cognitive Map*, where this theory argues that the spatial framework is generated in the hippocampus to represent space (O'Keefe & Nadel, 1978). Evidence for this spatial framework can be found across the hippocampus and entorhinal cortex, and notably in place cells in CA1 (O'Keefe & Dostrovsky, 1971).

In novel contexts, new cellular representations are developed through global remapping (Wilson & McNaughton, 1993). This new population code is made up of cells that fire when the animal is in a specific location, and as the animal moves around the context different cells fire to represent these areas. While there is chance overlap of active cells in distinct contexts, overlap is greater in CA1 than CA3 place fields (Leutgeb et al.,

2004). In different shaped contexts, cellular representations differ, and with repeated exposure they continue to diverge (Lever et al., 2002).

In the previous chapters we have briefly discussed that pattern separation and pattern completion are neural processes that may be key to accurately learning about different contexts, events associated with them, and the ability to elicit appropriate behaviours when re-encountered. These theories are, in part, based on physical patterns of cellular activity in the brain. It has been proposed that attractor networks are the mechanism underlying spatial maps. Attractor networks allow for an entire network to be activated when limited stimuli are present, allowing for context recognition. Furthermore, different, distinct contexts appear to have different attractor networks (Tsodyks, 2005).

Other cellular representations of space have been found in the entorhinal cortex include border (Savelli et al., 2008; Solstad et al., 2008) and grid cells (Fyhn et al., 2004; Hafting et al., 2005). More recently, the hippocampal representations of other context features like objects (Høydal et al., 2018), other subjects (Danjo et al., 2018), goals (Sarel et al., 2017), and rewards (Gauthier & Tank, 2018) have been studied.

In our previous work, we have observed that while rats in the water task are able to learn a new reward location in a familiar context under NMDAR blockade, rats in a novel context are unable to (Bye & McDonald, 2019). In the present experiment, we wanted to provide preliminary evidence that NMDAR blockade disrupted global remapping. What this experiment assesses is how cellular representations differ in the dry-land contextual navigation task between familiar and novel context conditions. We have established this task in the previous chapter, and in this experiment we conduct the

task using miniaturized microscopes as to allow for the animals' free movement while imaging cells in dorsal CA1 of the hippocampus.

Experiment 1: Place cell activity based on environment familiarity

Methods

Subjects

Subjects were 4 Thy1-GCaMP6s mice (2 males, 2 females) which were bred on site. Mice were aged 4 months prior to surgery. They were housed in pairs with a perforated divider between subjects and maintained on a 12-hour light/dark cycle. Prior to and following the task, mice were given access to *ad libitum* food and water, and during the task were maintained with *ad libitum* food access and were water restricted.

During the behavioural task mice were maintained under a standard water restriction protocol. Mice were water restricted for the three days prior to the start of pre-task training. On the first day of water restriction, mice had no access to water for 22 hours. On the second day of water restriction mice had no access to water for 23 hours, and on the third day of water restriction mice had no access to water for 23.5 hours. For the entirety of the task, mice were maintained on no water access for 23.5 hours, and *ad libitum* access for 30 minutes. During the task, this 30 minute period commenced at least 2 hours after the completion of the last trial.

All procedures were approved by the University of Lethbridge Animal Welfare Committee and in accordance with the Canadian Council of Animal Care.

Surgery

All animals underwent GRIN lens implant in dorsal CA1 of the hippocampus. 30 minutes prior to surgery, animals were injected with buprenorphine (Temgesic, 0.03 mg/kg, sc.; Schering-Plough, Hertforshire, UK). Mice were then induced with 4%

isoflurane in 1 L/min oxygen to the surgical anaesthetic plane and maintained at 1-2% during the surgery. Post-surgery, mice were injected with meloxicam (Metacam, 5 mg/mL, 0.2 mg.kg, s.c. ; Buehringer Integelheim, Burlington, ON, Canada). Once animals were anaesthetized, their scalps were shaved and cleaned with 4% stanhexidine chloride and 70% EtOH. A circular section of scalp was cut out and two screws into the frontal bone (opposite side of the lens implant) and the interparietal bone. These screws were secured with Krazy glue. A hole was then drilled at -1.8 AP, and -1.5 ML. This whole was expanded using a dental drill by hand until it reached a diameter of just over 1.8 mm. Then, an aspirator was used to remove the cortex in the region below this hole until fibres over the hippocampus were visible (approximately -1.3 DV). The hole was flushed with and cleared of ACSF until bleeding stopped, and the GRIN lens was lowered into the hole. The lens was initially secured with Krazy glue and then the open scalp area was covered with dental acrylic, leaving a few millimeters of the GRIN lens exposed.

7 days after the GRIN lens implant, animals were anaesthetized, again, with 4% isoflurane in 1 L/min oxygen, and maintained with 1-2% isoflurane. The miniaturized microscope was attached to a base plate and held with a stereotaxic arm over the GRIN lens until there were visible cells in the field of view. At this point the base plate was secured with Krazy glue and allowed to dry before the stereotaxic arm was removed and the plate was further secured with dental acrylic.

Behavioural Apparatus and Analysis

Recordings were conducted throughout the three phases of the Dry-land Contextual Navigation Task. Mice underwent the Dry-land Contextual Navigation Task. The training and new learning context were counter-balanced for, and consisted of either

a hexagon or octagon arena. Both arenas were 2000 cm^2, had 28 cm tall clear acrylic walls, and a base made of a white wood-composite peg board. The walls were covered (on the outside of the arena) with either a white or black layer, as well as local cues. The end of a syringe cap was cut to less than $1/8^{th}$ of an inch (the thickness of the peg board) and the water reward was placed in this cap, inside the peg board holes.

Dry-land Contextual Navigation Task

Pre-task training was conducted in the training context and consisted of two phases, each of which lasted for two days. During the first phase of pre-task training, mice were placed in the arena for 6 two-minute trials per day during which 8 random locations in the arena were baited with a water reward. The baited locations were randomized for each trial. During the second phase of pre-task training, mice were placed in the arena for 6 trials per day. Each trial lasted until the mouse located the single, baited reward location, which was randomized for each trial.

Phase 1: Pre-training

On the first 5 days of the task, mice were trained to find a single water reward in a consistent location, in the same context in which pre-task training occurred. 6 trials were conducted per day and each trial's maximum length was 2 minutes long. After the completion of this phase, mice were split into either same room- same location, same room- new location, or new room- new location groups. The differences in their procedures are listed below:

Phase 2: Rapid New Learning

Same Room- New location: Rapid new learning for these subjects (n = 2) took place in the same training context with the water reward relocated to the opposite side of the arena, equidistant from the wall as the phase 1 water reward location. During rapid new learning, mice underwent 10 trials in the span of 1 hour.

New Room- New location: Rapid new learning for these subjects (n = 2) took place in a new training context which differed in arena shape, colour, local and global cues, and orientation of the entrance. During rapid new learning, mice underwent 10 trials in the span of 1 hour to find the water reward. The water reward was in a different location, relative to cues and absolute coordinates, than the phase 1 water reward location.

Phase 3: Probe

Same room animals (n = 2) underwent a 20 second probe 24 hours after Phase 1. During the probe, animals were placed in the arena with no water reward.

Place Cell Analysis

Analysis of cellular activity was conducted using MatLab routines. Analysis of calcium transients was conducted using previously established methods. Motion correction was conducted using Normcorre (Pnevmatikakis & Giovannucci, 2017), source extraction was conducted using CNMFE (Zhou et al., 2018), and cell registration was conducted using CellReg (Sheintuch et al., 2017).

A similar method was employed to determine place fields as stated by Ziv et. al (2013). Path was divided into 10 cm^2 bins, and the sum of calcium transients in a given bin was divided by the mouse's occupancy of the bin. The peak of this value was identified as the place field. Cells with non-place specific activity (greater than 6 bins)

were not included in further analyses. Each place field's position was determined by the centroid of its peak activity.

We defined a distinct place field by its radius. If the radius of the place field was less than 11.28 cm, making the place field less than $1/5^{th}$ of the entire arena, the place field was considered distinct. We then mapped place fields over days in the same animals to determine if/how they changed over days and between pre-training and new learning.

Since the mice were freely behaving in the DCNT task, there were limitations to the analyses we could conduct. Mice were not consistently in the same locations, their starting locations were randomized and therefore their trajectories were inconsistent, and as they were learning throughout the task their trial times were also inconsistent. Therefore, we used cell commonality to assess population activity on different days of the task. Cell commonality was calculated by taking a ratio of the number of cells active in both of two days, divided by the total number of cells active on those days.

The Z-score was calculated using the "zscore" function in MATLAB. In these analyses, the centre of the distribution was shifted to the centre of the cell commonality on pre-training days.

Perfusion and tissue preparation

Mice were euthanized with an intracardiac injection of sodium pentobarbital (125 mg/mL). Mice were then perfused with 4% paraformaldehyde (PFA) and 0.1 M phosphate buffer saline (PBS) transcardially. Brains were extracted and stored in 4% PFA for 24 hours, after which they were transferred to 30% sucrose + 0.2% sodium azide. Brains were sliced at 40 μm on a cryostat starting from the beginning of the implant to the

end of the implant. Sections were transferred onto slides and cresyl violet staining was completed.

Volumetric analysis

Volumetric analysis was conducted using Stereo Investigator, using the Cavaleri Estimator function. The parameters used were: 120 µm grid spacing and 40 µm slice width. Both hemispheres of the hippocampus were analyzed, and the volume of each hemisphere has been reported.

Results

Behaviour

In the DCNT we observed learning. No effect of room, but an effect of days was observed (Day: $F_{5, 148} = 11.96$, $p < 0.0001$; room condition: $F_{1, 148} = 2.017$, $p = 0.1577$) (Figure 4.4). Additionally, a learning effect was observed during pretraining days (SR-N: slope = -39.27, $F_{1, 58} = 16.35$, $p = 0.0002$; NR-N: slope = -30.69, $F_{1, 58} = 13.72$, $p = 0.0005$). These results suggest that mice outfitted with miniaturized microscopes were able to perform the DCNT task.

Histology

In a comparison of hippocampal volume between implanted and non-implanted hemispheres we observed no significant effect of implant ($F_{1, 56} = 3.589$, $p = 0.0633$). Therefore, the hippocampal formation was left largely intact for the task.

Cell Commonality

We registered active place cells in each animal over all days of the task and measured a ratio of the number of cells active in both of the two days being compared to

the total number of cell active in each of the days. We used a z score of these data to demonstrate significant differences in this ratio in each of the mice. While we observed z scores below -2 between the new learning phase and pre-training days in the new room condition (025: NR-N vs. T-1: z = -2.167; 026: NR-N vs. T-3: z = -2.251, NR-N vs. T-4: z = -2.208) (Fig. 4.6, upper panels), we observed either no significant differences or a z score greater than 2 in the same room conditions (031: SR-N vs. T-2: z = 2.384) (Fig. 4.6, lower panels). These data indicate that cell commonality between the same room condition new learning and pre-training was either not significantly different, or it was significantly greater. In the new room condition, cell commonality was significantly less between the new room condition new learning and pre-training.

Reward encoding

Based on previous reports that water rewards are represented in dorsal CA1 (Gauthier & Tank, 2018), we also plotted place fields over days to assess if representations of these rewards transferred contexts. I analyzed place cells that were registered over multiple days, and whose place fields overlapped with reward regions on both pre-training and new learning days. I did not observe this to be the case. On average, between all animals recorded from, we found 683 place cells. 30.7% of these cells were registered over multiple days (mean = 209.5, SEM = 85.39), 9.33% of these cells had place fields that overlapped with the reward zone during multiple days of pre-training (mean = 63.75, SEM = 24.69), 0.952% of these cells had place fields that overlapped with the reward zone for 1 day (mean = 6.5, SEM = 1.707), and only 0.037% of these cells had place fields that overlapped with both the pre-training and new learning reward zone (mean = 0.25, SEM = 0.25). This last 0.037% amounts to a single cell out of the total

2732 cells recorded across all four animals, and was recorded from a same room condition mouse. Therefore, we found no cells whose place fields overlapped with both reward zones in the new room condition, and only one cell whose place field overlapped with both reward zones in the same room condition, indicating that there was no significant encoding of reward in the cells that were recorded.

Discussion

In this chapter I examined cellular activity in the dry-land contextual navigation task. I showed that mice outfitted with miniaturized microscopes were able to perform the DCNT, that there were significant differences in the cell commonality between room conditions, and there was no significant transfer of reward region encoding between pre-training and new learning. All together, these data further validate the use of the DCNT in context-based spatial learning, demonstrate a global remapping effect between contexts, and do not provide evidence of reward encoding in dorsal CA1.

In our behavioural analysis, we showed that the Thy1-GCaMP6s mice with miniaturized microscopes were able to perform the DCNT. Interestingly, we observed greater path length during new learning in same room animals although it was not statistically significant. This is in contrast with the previous chapter in which we observed significantly greater path length during new learning in the new room animals. These behavioural differences come from a very small sample, however, and therefore we do not expect that they are a true representation of stereotypical behaviour in the task.

In our histological analysis we demonstrated that there was no significant loss of hippocampal volume between implanted and intact hemispheres. This data was collected to ensure that any behaviour and cellular activity observed was not a result of hippocampal damage. One of the greatest limitations of implantation in imaging is cortical loss. While this limitation could not be avoided, performance in this task is thought to be based on hippocampus function. Therefore, it was important to demonstrate that our surgical techniques did not damage the hippocampal formation. Furthermore,

based on the behavioural performance of the mice it appears that the task is independent of the cortical region aspirated during surgery.

We introduced a new analysis to assess population activity in the DCNT due to some of the valuable, but confounding, variables introduced with freely-behaving mice. Unlike previous reports which are able to correlate time with space by running mice on a linear track (Skocek et al., 2018), in this task mice underwent a learning task. Therefore, the mice had randomized starting points, trajectories, varying trial lengths, and did not evenly explore every area of the apparatus. To demonstrate the population differences throughout the task in a way that minimized how it was confounded with behavioural differences, we created the measure of cell commonality. Cell commonality is the ratio of cells active in both sessions to all cells active in each session. Using this measure, we demonstrated significant differences in cell commonality between new learning and pre-training in the two room conditions. We showed greater commonality in the same room condition between new learning and pre-training days and less commonality in the new room condition between new learning and pre-training days. These data indicate that there are differences in the population activated between the room conditions, and is consistent with the idea that global remapping occurs when rodents are trained in one context and then switched to another for further learning.

Finally, I analyzed the distribution of place cells that were registered over multiple days, and whose place fields overlapped with reward regions. In this analysis, we aimed to identify a population of cells in dorsal CA1 whose place fields overlapped with the reward region in pre-training and new learning despite the spatial shift between these phases. We aimed to identify cells that encoded the reward. This has been previously

reported in both a consistent and two different contexts (Gauthier & Tank, 2018). We, however, did not observe a population of cells whose activity followed this pattern. One key difference between the Tank experiment and the present experiment is repetition/alternation. The previous report used an alternating procedure in which animals experienced one reward location, followed by the other, and so on. In the present experiment, mice had multiple exposures over many days to one reward location, and a day later were exposed to the new reward location. It is possible that when reward exposure is conducted in an alternating manner it promotes the integrated representation, whereas when reward exposure is conducted with longer inter-exposure periods and without repetition representations are distinct.

Taken together, the data presented here demonstrate the versatility of the DCNT for freely behaving learning experiments and the exploration of the nature of the neural representations and neurobiological mechanisms underlying this spatial learning and memory. This was demonstrated with my demonstration of reliable learning with a significant surgical manipulation (head-mounted microendoscope), evidence of global remapping between learning contexts, and distribution of cellular representations. Global remapping in novel context and the lack of global remapping in familiar contexts is consistent with attractor network theory. Exposure and training day after day in familiar contexts recruited similar cellular representations while these same experiences in the novel context condition did not. Finally, while we did not find evidence of cellular representations of reward, we propose that these representations may be based on a more integrated learning process, unlike the distinct learning experiences presented in this experiment.

CHAPTER 5: GENERAL DISCUSSION

The experiments described in this thesis were conducted to enrich our understanding of the role of context in spatial learning. Contexts are inextricably tied to spatial learning, as their components are what distinguishes one space from another (Rudy, 2009). The experiments were designed to compare different forms of contextualized spatial learning on the protein scale (*Chapter 2: Plasticity Cascades*), the cellular scale (*Chapter 4: Place Cell Activity in the DCNT*), and the behavioural scale (*Chapter 3: Dry-land Contextual Navigation Task*).

Hypotheses

In *Chapter 2: Plasticity Cascades*, we hypothesized that there would be greater expression of plasticity products in hippocampus following new spatial learning in a new context versus new spatial learning in a familiar context. Furthermore, based on distinguishable role of the MEC and LEC in spatial learning (Nilssen et al., 2019), further supported by a functional dissociation of MPP and LPP in spatial learning (Ferbinteanu et al., 1999), we'd observe differences in plasticity product expression that matched connectivity patterns between these regions and the HPC. We hypothesized that new spatial learning in a familiar context would recruit the LEC, while new spatial learning in a novel context would recruit the MEC. These differences would then be reflected in the expression of pCaMKII, pCREB, and a shift in the ratio of GluA2:GluA1 receptors. In addition, previous reports have demonstrated a difference in the role of NMDAR in new spatial learning based on context (Bye & McDonald, 2019), and therefore we were also interested in if expression patterns of this receptor differed by context familiarity.

Anatomically, based on entorhinal cortex projection patterns to the HPC across the distal to proximal axis, we hypothesized that we'd observe convex trends in the suprapyramidal blade of the DG, no significant trends in the infrapyramidal blade of DG, a positive trend in CA3, and a negative trend in CA1, all from distal to proximal, in rats who underwent the same-room condition. We hypothesized that we'd observe concave trends in the suprapyramidal blade of DG, no significant trends in the infrapyramidal blade of DG, a negative trend in CA3, and a positive trend in CA1, all from distal to proximal, in rats who underwent the new-room condition. We hypothesized that the same room condition would differ from controls and new room conditions in the following ways: in the suprapyramidal blade of the DG slopes would be more concave, in the infrapyramidal blade slopes would not differ, in CA3 slopes would be more positive, and in CA1 slopes would be more negative. We also hypothesized that the new room condition would differ from the same room condition and controls in the following ways: in the suprapyramidal blade of the DG slopes would be more convex, in the infrapyramidal blade slopes would not differ, in CA3 slopes would be more negative, and in CA1 slopes would be more positive.

In *Chapter 3: Dry-Land Contextual Navigation Task*, our purpose was to develop a novel spatial learning task which measured encoding and consolidation in novel or familiar contexts. This task was based on the previously used water-based task and was designed with the intent of using it for cellular imaging studies in mice. I hypothesized that in the task we would observe differences in new learning between novel and familiar context learning conditions. I hypothesized that interference of the pre-training learning would negatively impact new spatial learning in the familiar context but not the novel

one. Furthermore, in the probe trial I hypothesized that familiar context mice would visit the new location more frequently than the old one. In this chapter I also conducted a second analysis of win-stay tendencies between the dry-land and water-based tasks. In this analysis I expected to see similar results in the traditional measure of learning, path length, but differing results in win-stay tendencies. I hypothesized that there would be greater win-stay tendencies in the water-based task due to the recruitment of alternating and foraging behaviour in the dry-land task.

In *Chapter 4: Place Cell Activity in DCNT* I assessed how cellular representations differ in the DCNT between familiar and novel context conditions. I utilized the task established in the previous chapter and to complete calcium imaging using miniature microscopes to allow for the animals' free movement while imaging cells in dorsal CA1 of the hippocampus. I hypothesized that I would observe global remapping in the analysis of cell commonality and reward representations in the analysis of the distribution of cellular representations.

Summary of results

In *Chapter 2: Plasticity Cascades*, the results showed mixed support for the hypotheses. Mostly, I did not observe increased expression of plasticity products in the novel context new learning. One case where we did observe increased expression was in the ratio of GluA2:GluA1. In this case we observed greater expression between the 180-minute novel and familiar context groups, but not the 70-minute groups. It was previously stated that the synaptic changes that support learning are book-ended by AMPAR dynamics, and the 180-minute ratio we measured was the closing book end. Therefore, while I did not observe evidence that there is greater expression of NMDAR, pCaMKII,

or pCREB in novel context new learning, I did observe evidence of an increase of the ratio of GluA2:GluA1 expression in this group, which supports an increase in calcium and sodium ion permeability (Doble, 1995).

Also in these experiments, we observed evidence in every protein in at least one region, that supported our hypotheses that there would be increase expression of plasticity products in regions of the HPC with greater connectivity to recruited sub-regions of the EC (Figures 2.29 to 2.31). In NMDAR expression patterns, we only observed an effect of context familiarity in CA1. In pCaMKII expression patterns, we only observed an effect of spatial learning in CA3. In pCREB expression patterns, we only observed an effect of spatial learning in the infrapyramidal blade, and an effect of context familiarity in CA3. Finally, in GluA2:GluA1 expression patterns, we observed an effect of spatial learning in the infrapyramidal blade, and an effect of context familiarity in CA1 and CA3.

In *Chapter 3: Dry-land Contextual Navigation Task*, I observed that mice learn during both the pre-training and the new learning phases of the task. Furthermore, rapid new learning is retained 24 hours later in the probe trial. I did not observe, however, an interference effect in new learning resulting in increased path lengths or latencies in the familiar context condition. In the comparison between the dry-land and water-based tasks I observed similar learning effects in path length, but when we compared win-stay tendencies I observed some major differences. In rats in the water-based task I observed a clear increase in win-stay tendencies over days. In mice in the dry-land task we observed no significant trend. These differences are similar to previous reports which compared, specifically, the medium in which rats perform a spatial learning task and found alternating or foraging behaviour in dry but not wet tasks (Whishaw & Pasztor, 2000). In

this chapter I also measured plasma corticosterone levels in the DCNT to assess if new learning in a novel context caused a significant stress response. We did not observe this to be the case. The only significant effect on stress responses was observed across all room conditions.

Finally, in *Chapter 4: Place Cell Activity in DCNT*, I observed a couple of phenomenon in cellular activity. First, in cell commonality, I observed that evidence of global remapping though a significant lack of cell commonality in novel context new learning in comparison to pre-training. Furthermore, in the distribution of cellular representations we observe a high population of cells that encode place, over multiple days, and that encode one of the reward locations but nearly no cells that represent the reward. This was surprising given recent reports that demonstrated this effect (Gauthier & Tank, 2018).

Novel contributions

A number of novel contributions have been made in the aforementioned experiments and have been discussed in their respective discussions. In each chapter, however, there have also been critical ideas introduced that will be discussed more generally here. Additionally, some novel methodology has been contributed in these experiments.

Novel methods

Analysis of protein expression along transverse axis

In *Chapter 2: Plasticity Cascades*, I developed a novel analysis to assess the patterns of protein expression along the transverse axis of the hippocampus. In this

analysis, I mapped a line along the granule layer of the hippocampus and bins perpendicular to this axis were mapped. Then, 20 lines, also perpendicular to the axis were mapped at random locations along the axis in each bin and the average pixel fluorescence was measured along each line. This method allowed me to develop a matrix of average pixel fluorescence in each bin by slice by animal.

Dry-land contextual navigation task

In *Chapter 3: Dry-land Contextual Navigation Task*, I developed a novel behavioural task for measuring spatial learning in familiar or novel contexts. This task not only showed a clear learning effect over days, but I also demonstrated through the behavioural analysis in *Chapter 4* that the task is compatible with miniature microscope imaging techniques.

Cell commonality

In *Chapter 4: Place Cell activity in the DCNT* I had to create a novel measure for population activity at different stages of the task. We had to create a novel measure because the behaviour in the task was so variable by trial and by day, as animals were freely behaving and learning throughout. Therefore, we calculated the ratio of cells active in both sessions to all cells active in each session. This measure demonstrated gross changes in the overlap between the population of cells active from one day to the next, allowing us to work around the free-behaving variables I had encountered.

Converging biochemical cascades

In *Chapter 2: Plasticity Cascades* I measured the expression of pCaMKII, NMDAR, GluA2:GluA1, and pCREB. These proteins are part of a set of biochemical

cascades that support synaptic strengthening by changing the physical structure of synapses and increase the efficacy of communication between neurons. One phenomenon that I noticed in the results was that support for the hypotheses increased the further downstream a protein was in the cascade. Perhaps the convergence of biochemical cascades allows for proteins further downstream to be more sensitive to the behavioural manipulations we were studying than proteins further upstream.

This conclusion is logical based on the interactions between proteins in the cascade. An accumulation of effect as these cascades converge has been modeled computationally (Blackwell & Jedrzejewska-Szmek, 2013). Convergence as a signal integrator has also been previously reviewed (Adams & Sweatt, 2002). Based on this information, I would expect proteins at similar stages in the biological cascade to show a similar effect. Finally, I would also expect that the effect of context familiarity on IEG expression would be greater than what I observed in any of the proteins measured in these experiments.

Comparison between rats and mice

In *Chapter 3: Dry-land Contextual Navigation Task* I performed a comparison between the dry-land task and the water-based task. Primarily, this comparison was conducted to assess some differences between the tasks given I was working under the assumption that they measured the same thing. In recent history, a shift has taken place in rodent neuroscience research marked by the increased use of mice as an experimental model (Ellenbroek & Youn, 2016). In behavioural neuroscience, this has often translated into the use of mice in tasks initially designed for rats (Stranahan, 2011). There are some marked differences between the behaviour in the two species, but largely acquisition of

information is consistent. Retention, however, appears to differ between species (Stranahan, 2011). One notable difference between species is observed in the MWT, rats learn markedly better and unlike mice their learning was not limited to a single place task (Whishaw, 1995). This result was replicated with the addition of a comparison on the radial arm maze in which the species had matched performances (Whishaw & Tomie, 1996). Therefore, considering the scope of experiments in this thesis I performed an analysis comparing learning in rats in the water task and mice in a dry-land task. While I did not compare both types of rodents on water and dry-land spatial tasks, based on previous reports I was confident in using both of these species-task pairings. We also are confident that differences in alternating behaviour, or as we measured, the opposite of win-stay tendencies, are generalizable to mice as well.

Repetition, alternation, and reward representations

We did not observe reward representations in *Chapter 4: Place Cell Activity in DCNT*. This was surprising given previous reports of reward representations in multiple contexts (Gauthier & Tank, 2018). One explanation for this discrepancy in results is based on the behavioural design of the Tank experiment in comparison to the DCNT used in this thesis. In the Tank experiment, animals were subject to a repetitive and alternating sequence of contexts and rewards. In the DCNT, contexts and rewards were exposed repetitively but not in an alternating fashion. I have proposed that by using an alternating procedure, these reward experiences are integrated in way that does not occur in the DCNT because there is a 24 hour interval between pre-training and rapid new-learning.

In a discussion on attractor networks, Tsodyks (2005) compares the differences found in CA3 representations between two morphing environment experiments (Leutgeb

et al., 2005; Wills et al., 2005) in a way that I think is similar to the differences observed between the Tank and our experiments. When the rats were exposed to the two distinguishable context, the representations were highly decorrelated, but when the rats were exposed to the gradually morphing context, the representations were much more similar and shifted towards the initial context (Tsodyks, 2005). Therefore, I propose that when context experiences become increasingly distinguishable through time, shape, or other stimuli, their cellular representations are also increasingly decorrelated.

Limitations

One of the primary concerns in the experiments presented in these experiments, is the level of individual variation, particularly in the plasticity cascade and place cell activity experiments. In a number of these experiments we used a small sample size (n = 4) and still observed notable effects. In future experiments, a more robust effect may be observed with a greater sample size.

In *Chapter 3: Dry-land Contextual Navigation Task*, I observed a learning effect over days but not trials. This was surprising since in rats in the water task show a learning effect over both days and trials. During pilots of this task, we limited the number of trials per day as after the 6th trial, mice ceased exploratory behaviour and instead would groom in the corner of the arena. This apparent lack of motivation to the reward, we interpreted as satiety. When we measured plasma corticosterone, we found an increase in our baseline compared to previous reports (Song et al., 2006). Therefore, I do not recommend adjusting the water-restriction protocol, but maybe extending pre-training for another day to lower stress levels. A lack of learning effect over trials is not necessarily a limitation, however satiety is definitely a confounding factor for behavioural measures in this task.

In *Chapter 4: Place Cell Activity in the DCNT*, I took recordings of cellular activity in dorsal CA1 of freely-behaving animals during a spatial learning task. In the analyses I encountered significant variation within an animal between days. While we addressed this in the design of our analyses, one limitation is the absolute number of active cells on subsequent days decreases as mice learn the reward location. Therefore, our sample size decreases throughout the task and we have fewer representations with which to compare one day to another.

Future directions

The experiments in this thesis were initiated due to previous work done in this lab which showed key differences in the role of NMDAR in familiar versus novel context spatial learning (Bye & McDonald, 2019). In these experiments, they showed that NMDAR are necessary for new learning in a novel context but not a familiar context in a water-based contextual navigation task. Therefore, a few key future experiments would replicate those here, but include the use +/- CPP to block NMDAR. These experiments could examine the differences in protein expression in animals with NMDAR blockade during a contextual spatial learning task, examine if the same effect is found in mice with NMDAR blockade in the DCNT, and examine how place cell activity differs during the DCNT in animals with NMDAR blockade.

In the first experiment an NMDAR blockade group would be added to the experiments in *Chapter 2: Plasticity Cascades*. I hypothesize that in the familiar context condition, we would observe the same patterns of expression in proteins earlier in the cascade like pCaMKII, but that we would not observe the same patterns of expression in later proteins like pCREB or GluA2:GluA1. This is because in the familiar context

condition rats show a learning effect, but do not demonstrate consolidation of this learning in a probe trial 24 hours later (McDonald et al., 2005). In the novel context condition, I hypothesize that we would observe no similar effects in any of the proteins since we do not observe a learning effect in this group (Bye & McDonald, 2019).

In the second experiment, an NMDAR blockade group would be added to the experiments in *Chapter 3: Dry-land Contextual Navigation Task* and I hypothesize that we would replicate the results reported previously in 2005 and 2019 (Bye & McDonald, 2019; McDonald et al., 2005). This means that in the familiar context condition we would observe that mice would learn the new reward location, however in the probe trial 24 hours later they would not show evidence of consolidation. Furthermore, in the novel context condition I hypothesize that we would not observe any learning effect during the rapid new learning phase.

Finally, in the third experiment, an NMDAR blockade group would be added to the experiments in *Chapter 4: Place Cell Activity in the DCNT*. Previous reports which used virtual environments and 2-photon calcium imaging have shown that there is a lack of stability in place fields when mice were treated with an NMDAR blockade (Sheffield et al., 2017). Other reports have also highlighted that NMDAR are necessary at the initial exposure to a context for the stability of the context-specific firing patterns (Kentros et al., 1998). This same report found that NMDAR are not necessary for the generation or short-term maintenance of new firing fields, but they were necessary for their long-term stability. Previously, I have discussed that pattern separation is the process by which an animal can distinguishing between contexts, and pattern completion is the process by which an animal can effectively predict a context with limited information (Leutgeb &

Leutgeb, 2007). Other reports which have selectively knocked-out a NMDAR subunit in granule cells of the dentate gyrus have found that this disrupts pattern separation (McHugh et al., 2007). Therefore, I expect that NMDAR blockade in the DCNT would disrupt pattern separation in the hippocampus by disrupting the stability of context-specific firing patterns.

Summary

In these experiments I have studied the effects of context familiarity on new spatial learning on a protein, behavioural, and cellular scale. In the process we developed a few novel methods including a novel analysis of protein expression along the transverse axis, the Dry-land Contextual Navigation Task, and the assessment of cell commonality in freely behaving mice. A number of novel contributions were made throughout these experiments. I observed increased support for my hypotheses in proteins further downstream in the plasticity cascades that support synaptic strengthening, suggesting that the converging effect of these cascades makes proteins downstream more sensitive to the context manipulations I was studying versus proteins upstream. I also completed experiments throughout this thesis that assessed contextual spatial learning in both rats and mice, and in both dry-land and water-based tasks. As such, I compared the behaviour in these two tasks and between these two species to demonstrate that both tasks were effective learning paradigms. We also compared a parameter that we thought would differ between the two tasks, alternating behaviour as measured as the opposite of win-stay tendencies. We observed that win-stay tendencies showed no significant trends over days in the dry-land task, while they showed a marked increase over days in the water-based task. Finally, we studied place cell activity in the DCNT and observed evidence of global

remapping in the novel context new spatial learning condition. We conducted this experiment in freely-behaving mice and used miniature microscopes. When we assessed reward representations in dorsal CA1, we did not find evidence of cells that encoded the reward. Instead, we propose that an alternating procedure, in contrast to our distinct phases, would result in a more integrated representation which would encode rewards similarly in different contexts.

The study of context through spatial learning is important because context is used for more than recognition, its components are essential for navigation and cuing salient features. I have studied contextual spatial learning in these experiments, as it requires a more thorough understanding of the context being navigated through, rather than a more simple understanding required for recognition. Hopefully these novel contributions will encourage the study of context in this way, as it appears that there is plenty of room for thorough investigation and discoveries of how context familiarity affects new spatial learning.

REFERENCES

Adams, J. P., & Sweatt, J. D. (2002). Molecular Psychology: Roles for the ERK MAP Kinase Cascade in Memory. *Annual Review of Pharmacology and Toxicology*, *42*(1), 135–163. https://doi.org/10.1146/annurev.pharmtox.42.082701.145401

Alme, C. B., Miao, C., Jezek, K., Treves, A., Moser, E. I., & Moser, M.-B. (2014). Place cells in the hippocampus: Eleven maps for eleven rooms. *Proceedings of the National Academy of Sciences*, *111*(52), 18428–18435. https://doi.org/10.1073/pnas.1421056111

Amaral, D. G., & Witter, M. P. (1995). Hippocampal Formation. In *The Rat Nervous System* (2nd ed., Vol. 65, pp. 477–479). Academic Press. https://onlinelibrary.wiley.com/doi/abs/10.1046/j.1471-4159.1995.65010471.x

Antoniadis, E. A., & McDonald, R. J. (2000). Amygdala, hippocampus and discriminative fear conditioning to context. *Behavioural Brain Research*, *108*(1), 1–19. https://doi.org/10.1016/s0166-4328(99)00121-7

Bach, M. E., Hawkins, R. D., Osman, M., Kandel, E. R., & Mayford, M. (1995). Impairment of spatial but not contextual memory in CaMKII mutant mice with a selective loss of hippocampal LTP in the range of the theta frequency. *Cell*, *81*(6), 905–915. https://doi.org/10.1016/0092-8674(95)90010-1

Bannerman, D. M., Deacon, R. M. J., Offen, S., Friswell, J., Grubb, M., & Rawlins, J. N. P. (2002). Double dissociation of function within the hippocampus: Spatial memory and hyponeophagia. *Behavioral Neuroscience*, *116*(5), 884–901. https://doi.org/10.1037//0735-7044.116.5.884

Bannerman, D. M., Good, M. A., Butcher, S. P., Ramsay, M., & Morris, R. G. M. (1995). Distinct components of spatial learning revealed by prior training and NMDA receptor blockade. *Nature*, *378*(6553), 182–186. https://doi.org/10.1038/378182a0

Bannerman, D. M., Yee, B. K., Good, M. A., Heupel, M. J., Iversen, S. D., & Rawlins, J. N. (1999). Double dissociation of function within the hippocampus: A comparison of dorsal, ventral, and complete hippocampal cytotoxic lesions. *Behavioral Neuroscience*, *113*(6), 1170–1188. https://doi.org/10.1037//0735-7044.113.6.1170

Bannerman, David M., Bus, T., Taylor, A., Sanderson, D. J., Schwarz, I., Jensen, V., Hvalby, Ø., Rawlins, J. N. P., Seeburg, P. H., & Sprengel, R. (2012). Dissecting spatial knowledge from spatial choice by hippocampal NMDA receptor deletion. *Nature Neuroscience*, *15*(8), 1153–1159. https://doi.org/10.1038/nn.3166

Bannerman, David M., Niewoehner, B., Lyon, L., Romberg, C., Schmitt, W. B., Taylor, A., Sanderson, D. J., Cottam, J., Sprengel, R., Seeburg, P. H., Köhr, G., & Rawlins, J. N. P. (2008). NMDA Receptor Subunit NR2A Is Required for Rapidly Acquired Spatial Working Memory But Not Incremental Spatial Reference Memory. *Journal of Neuroscience*, *28*(14), 3623–3630. https://doi.org/10.1523/JNEUROSCI.3639-07.2008

Bear, M. F., & Malenka, R. C. (1994). Synaptic plasticity: LTP and LTD. *Current Opinion in Neurobiology*, *4*(3), 389–399. https://doi.org/10.1016/0959-4388(94)90101-5

Bhattacharya, S., Kimble, W., Buabeid, M., Bhattacharya, D., Bloemer, J., Alhowail, A., Reed, M., Dhanasekaran, M., Escobar, M., & Suppiramaniam, V. (2017). Altered AMPA receptor expression plays an important role in inducing bidirectional synaptic plasticity during contextual fear memory reconsolidation. *Neurobiology of Learning and Memory*, *139*, 98–108. https://doi.org/10.1016/j.nlm.2016.12.013

Blackwell, K., & Jedrzejewska-Szmek, J. (2013). Molecular mechanisms underlying neuronal synaptic plasticity: Systems biology meets computational neuroscience in the wilds of synaptic plasticity. *Wiley Interdisciplinary Reviews. Systems Biology and Medicine*, *5*(6), 717–731. https://doi.org/10.1002/wsbm.1240

Blanchard, R. J., Fukunaga, K. K., & Blanchard, D. C. (1976). Environmental control of defensive reactions to footshock. *Bulletin of the Psychonomic Society*, *8*(2), 129–130. https://doi.org/10.3758/BF03335103

Bliss, T. V., & Collingridge, G. L. (2013). Expression of NMDA receptor-dependent LTP in the hippocampus: Bridging the divide. *Molecular Brain*, *6*(1), 5. https://doi.org/10.1186/1756-6606-6-5

Bliss, T. V. P., & Lømo, T. (1973). Long-lasting potentiation of synaptic transmission in the dentate area of the anaesthetized rabbit following stimulation of the perforant path. *The Journal of Physiology*, *232*(2), 331–356. https://doi.org/10.1113/jphysiol.1973.sp010273

Bourne, H. R., & Nicoll, R. (1993). Molecular machines integrate coincident synaptic signals. *Cell*, *72*, 65–75. https://doi.org/10.1016/S0092-8674(05)80029-7

Brun, V. H., Leutgeb, S., Wu, H.-Q., Schwarcz, R., Witter, M. P., Moser, E. I., & Moser, M.-B. (2008). Impaired spatial representation in CA1 after lesion of direct input from entorhinal cortex. *Neuron*, *57*(2), 290–302. https://doi.org/10.1016/j.neuron.2007.11.034

Buzsáki, G., & Tingley, D. (2018). Space and Time: The Hippocampus as a Sequence Generator. *Trends in Cognitive Sciences*, *22*(10), 853–869. https://doi.org/10.1016/j.tics.2018.07.006

Bye, C. M., & McDonald, R. J. (2019). A Specific Role of Hippocampal NMDA Receptors and Arc Protein in Rapid Encoding of Novel Environmental Representations and a More General Long-Term Consolidation Function. *Frontiers in Behavioral Neuroscience*, *13*. https://doi.org/10.3389/fnbeh.2019.00008

Caballero-Bleda, M., & Witter, M. P. (1994). Projections from the presubiculum and the parasubiculum to morphologically characterized entorhinal-hippocampal projection neurons in the rat. *Experimental Brain Research*, *101*(1), 93–108. https://doi.org/10.1007/bf00243220

Cain, D. P. (1997). LTP, NMDA, genes and learning. *Current Opinion in Neurobiology*, *7*(2), 235–242. https://doi.org/10.1016/S0959-4388(97)80012-8

Caramanos, Z., & Shapiro, M. L. (1994). Spatial memory and N-methyl-D-aspartate receptor antagonists APV and MK-801: Memory impairments depend on familiarity with the environment, drug dose, and training duration. *Behavioral Neuroscience*, *108*(1), 30–43. https://doi.org/10.1037/0735-7044.108.1.30

Cembrowski, M. S., & Spruston, N. (2019). Heterogeneity within classical cell types is the rule: Lessons from hippocampal pyramidal neurons. *Nature Reviews. Neuroscience*, *20*(4), 193–204. https://doi.org/10.1038/s41583-019-0125-5

Chawla, M. K., Guzowski, J. F., Ramirez-Amaya, V., Lipa, P., Hoffman, K. L., Marriott, L. K., Worley, P. F., McNaughton, B. L., & Barnes, C. A. (2005). Sparse, environmentally selective expression of Arc RNA in the upper blade of the rodent fascia dentata by brief spatial experience. *Hippocampus*, *15*(5), 579–586. https://doi.org/10.1002/hipo.20091

Chawla, M. K., Sutherland, V. L., Olson, K., McNaughton, B. L., & Barnes, C. A. (2018). Behavior-driven arc expression is reduced in all ventral hippocampal subfields compared to CA1, CA3, and dentate gyrus in rat dorsal hippocampus. *Hippocampus*, *28*(2), 178–185. https://doi.org/10.1002/hipo.22820

Cingolani, L. A., & Goda, Y. (2008). Actin in action: The interplay between the actin cytoskeleton and synaptic efficacy. *Nature Reviews Neuroscience*, *9*(5), 344–356. https://doi.org/10.1038/nrn2373

Clark, B. J., Hong, N. S., Bettenson, D. J., Woolford, J., Horwood, L., & McDonald, R. J. (2015). Maintained directional navigation across environments in the Morris water task is dependent on vestibular cues. *Journal of Experimental Psychology: Animal Learning and Cognition*, *41*(3), 301–308. https://doi.org/10.1037/xan0000066

Collingridge, G. L., Kehl, S. J., & McLennan, H. (1983). Excitatory amino acids in synaptic transmission in the Schaffer collateral-commissural pathway of the rat hippocampus. *The Journal of Physiology*, *334*, 33–46.

Danjo, T., Toyoizumi, T., & Fujisawa, S. (2018). Spatial representations of self and other in the hippocampus. *Science*, *359*(6372), 213–218. https://doi.org/10.1126/science.aao3898

Doble, A. (1995). Excitatory amino acid receptors and neurodegeneration. *Therapie*, *50*(4), 319–337.

Dolorfo, C. L., & Amaral, D. G. (1998). Entorhinal cortex of the rat: Topographic organization of the cells of origin of the perforant path projection to the dentate gyrus. *The Journal of Comparative Neurology*, *398*(1), 25–48.

Dombeck, D. A., Harvey, C. D., Tian, L., Looger, L. L., & Tank, D. W. (2010). Functional imaging of hippocampal place cells at cellular resolution during virtual navigation. *Nature Neuroscience*, *13*(11), 1433–1440. https://doi.org/10.1038/nn.2648

Dudman, J. T., & Gerfen, C. R. (2015). Chapter 17—The Basal Ganglia. In G. Paxinos (Ed.), *The Rat Nervous System (Fourth Edition)* (pp. 391–440). Academic Press. https://doi.org/10.1016/B978-0-12-374245-2.00017-6

Dunwiddie, T. V., & Lynch, G. (1979). The relationship between extracellular calcium concentrations and the induction of hippocampal long-term potentiation. *Brain Research*, *169*(1), 103–110. https://doi.org/10.1016/0006-8993(79)90377-9

Eichenbaum, H. (1994). The Hippocampal System and Declarative Memory. In *Memory Systems 1994* (1st ed., pp. 147–201). MIT Press.

Ellenbroek, B., & Youn, J. (2016). Rodent models in neuroscience research: Is it a rat race? *Disease Models & Mechanisms*, *9*(10), 1079–1087. https://doi.org/10.1242/dmm.026120

Farris, S., Dynes, J. L., & Steward, O. (2017). 4.06—MRNA Trafficking to Synapses and Memory Formation☆. In J. H. Byrne (Ed.), *Learning and Memory: A Comprehensive Reference (Second Edition)* (pp. 153–178). Academic Press. https://doi.org/10.1016/B978-0-12-809324-5.21108-5

Ferbinteanu, J, Holsinger, R. M. D., & McDonald, R. J. (1999). Lesions of the medial or lateral perforant path have different effects on hippocampal contributions to place learning and on fear conditioning to context. *Behavioural Brain Research*, *101*(1), 65–84. https://doi.org/10.1016/S0166-4328(98)00144-2

Ferbinteanu, Janina, Ray, C., & McDonald, R. J. (2003). Both dorsal and ventral hippocampus contribute to spatial learning in Long-Evans rats. *Neuroscience Letters*, *345*(2), 131–135. https://doi.org/10.1016/s0304-3940(03)00473-7

Flasbeck, V., Atucha, E., Nakamura, N. H., Yoshida, M., & Sauvage, M. M. (2018a). Spatial information is preferentially processed by the distal part of CA3: Implication for memory retrieval. *Behavioural Brain Research*, *347*, 116–123. https://doi.org/10.1016/j.bbr.2018.02.046

Flasbeck, V., Atucha, E., Nakamura, N. H., Yoshida, M., & Sauvage, M. M. (2018b). Spatial information is preferentially processed by the distal part of CA3: Implication for memory retrieval. *Behavioural Brain Research*, *347*, 116–123. https://doi.org/10.1016/j.bbr.2018.02.046

Fraser, E., & McDonald, R. (2020). NMDA receptor mediated plasticity in learning and memory. *Oxford Research Encyclopedia*, *(in press)*.

Fyhn, M., Molden, S., Witter, M. P., Moser, E. I., & Moser, M.-B. (2004). Spatial representation in the entorhinal cortex. *Science (New York, N.Y.)*, *305*(5688), 1258–1264. https://doi.org/10.1126/science.1099901

Gauthier, J. L., & Tank, D. W. (2018). A Dedicated Population for Reward Coding in the Hippocampus. *Neuron*, *99*(1), 179-193.e7. https://doi.org/10.1016/j.neuron.2018.06.008

Ghosh, K. K., Burns, L. D., Cocker, E. D., Nimmerjahn, A., Ziv, Y., Gamal, A. E., & Schnitzer, M. J. (2011). Miniaturized integration of a fluorescence microscope. *Nature Methods*, *8*(10), 871–878. https://doi.org/10.1038/nmeth.1694

Golob, E. J., & Taube, J. S. (2002). Differences between appetitive and aversive reinforcement on reorientation in a spatial working memory task. *Behavioural Brain Research*, *136*(1), 309–316. https://doi.org/10.1016/s0166-4328(02)00184-5

Greenberg, M. E., Thompson, M. A., & Sheng, M. (1992). Calcium regulation of immediate early gene transcription. *Journal of Physiology, Paris*, *86*(1–3), 99–108. https://doi.org/10.1016/s0928-4257(05)80013-0

Gruber, A. J., & McDonald, R. J. (2012). Context, emotion, and the strategic pursuit of goals: Interactions among multiple brain systems controlling motivated behavior. *Frontiers in Behavioral Neuroscience*, *6*, 50. https://doi.org/10.3389/fnbeh.2012.00050

Hafting, T., Fyhn, M., Molden, S., Moser, M.-B., & Moser, E. I. (2005). Microstructure of a spatial map in the entorhinal cortex. *Nature*, *436*(7052), 801–806. https://doi.org/10.1038/nature03721

Hargreaves, E. L., Rao, G., Lee, I., & Knierim, J. J. (2005). Major dissociation between medial and lateral entorhinal input to dorsal hippocampus. *Science (New York, N.Y.)*, *308*(5729), 1792–1794. https://doi.org/10.1126/science.1110449

Harrison, F. E., Hosseini, A. H., & McDonald, M. P. (2009). Endogenous anxiety and stress responses in water maze and Barnes maze spatial memory tasks. *Behavioural Brain Research*, *198*(1), 247–251. https://doi.org/10.1016/j.bbr.2008.10.015

Hartzell, A. L., Burke, S. N., Hoang, L. T., Lister, J. P., Rodriguez, C. N., & Barnes, C. A. (2013). Transcription of the Immediate-Early Gene Arc in CA1 of the Hippocampus Reveals Activity Differences along the Proximodistal Axis That Are Attenuated by Advanced Age. *The Journal of Neuroscience*, *33*(8), 3424–3433. https://doi.org/10.1523/JNEUROSCI.4727-12.2013

Harvey, C. D., Collman, F., Dombeck, D. A., & Tank, D. W. (2009). Intracellular dynamics of hippocampal place cells during virtual navigation. *Nature*, *461*(7266), 941–946. https://doi.org/10.1038/nature08499

Hebb, D. O. (1949). *The organization of behavior* (Vol. 65). Wiley.

Heiderstadt, K. M., McLaughlin, R. M., Wright, D. C., Walker, S. E., & Gomez-Sanchez, C. E. (2000). The effect of chronic food and water restriction on open-field behaviour and serum corticosterone levels in rats. *Laboratory Animals*, *34*(1), 20–28. https://doi.org/10.1258/002367700780578028

Helmchen, F., Fee, M. S., Tank, D. W., & Denk, W. (2001). A Miniature Head-Mounted Two-Photon Microscope: High-Resolution Brain Imaging in Freely Moving Animals. *Neuron*, *31*(6), 903–912. https://doi.org/10.1016/S0896-6273(01)00421-4

Henriksen, E. J., Colgin, L. L., Barnes, C. A., Witter, M. P., Moser, M.-B., & Moser, E. I. (2010a). Spatial Representation along the Proximodistal Axis of CA1. *Neuron*, *68*(1), 127–137. https://doi.org/10.1016/j.neuron.2010.08.042

Henriksen, E. J., Colgin, L. L., Barnes, C. A., Witter, M. P., Moser, M.-B., & Moser, E. I. (2010b). Spatial representation along the proximodistal axis of CA1. *Neuron*, *68*(1), 127–137. https://doi.org/10.1016/j.neuron.2010.08.042

Hintiryan, H., Foster, N. N., Bowman, I., Bay, M., Song, M. Y., Gou, L., Yamashita, S., Bienkowski, M. S., Zingg, B., Zhu, M., Yang, X. W., Shih, J. C., Toga, A. W., & Dong, H.-W. (2016). The mouse cortico-striatal projectome. *Nature Neuroscience*, *19*(8), 1100–1114. https://doi.org/10.1038/nn.4332

Hjorth-Simonsen, A., & Jeune, B. (1972). Origin and termination of the hippocampal perforant path in the rat studied by silver impregnation. *Journal of Comparative Neurology*, *144*(2), 215–231. https://doi.org/10.1002/cne.901440206

Hok, V., Poucet, B., Duvelle, É., Save, É., & Sargolini, F. (2016). Spatial cognition in mice and rats: Similarities and differences in brain and behavior. *Wiley Interdisciplinary Reviews. Cognitive Science*, *7*(6), 406–421. https://doi.org/10.1002/wcs.1411

Høydal, Ø. A., Skytøen, E. R., Moser, M.-B., & Moser, E. I. (2018). Object-vector coding in the medial entorhinal cortex. *BioRxiv*, 286286. https://doi.org/10.1101/286286

Ito, H. T., & Schuman, E. M. (2012). Functional division of hippocampal area CA1 via modulatory gating of entorhinal cortical inputs. *Hippocampus*, *22*(2), 372–387. https://doi.org/10.1002/hipo.20909

Kandel, E. R. (1976). *Cellular basis of behavior: An introduction to behavioral neurobiology*. W. H. Freeman.

Kandel, E. R., Dudai, Y., & Mayford, M. R. (2014). The Molecular and Systems Biology of Memory. *Cell*, *157*(1), 163–186. https://doi.org/10.1016/j.cell.2014.03.001

Keith, J. R., & Rudy, J. W. (1990). Why NMDA-receptor-dependent long-term potentiation may not be a mechanism of learning and memory: Reappraisal of the NMDA-receptor blockade strategy. *Psychobiology*, *18*(3), 251–257. https://doi.org/10.3758/BF03327238

Kentros, C., Hargreaves, E., Hawkins, R. D., Kandel, E. R., Shapiro, M., & Muller, R. V. (1998). Abolition of long-term stability of new hippocampal place cell maps by NMDA receptor blockade. *Science (New York, N.Y.)*, *280*(5372), 2121–2126.

Knierim, J. J. (2002). Dynamic Interactions between Local Surface Cues, Distal Landmarks, and Intrinsic Circuitry in Hippocampal Place Cells. *Journal of Neuroscience*, *22*(14), 6254–6264. https://doi.org/10.1523/JNEUROSCI.22-14-06254.2002

Knierim, J. J. (2015). The hippocampus. *Current Biology*, *25*(23), R1116–R1121. https://doi.org/10.1016/j.cub.2015.10.049

Knierim, J. J., Neunuebel, J. P., & Deshmukh, S. S. (2014). Functional correlates of the lateral and medial entorhinal cortex: Objects, path integration and local–global reference frames. *Philosophical Transactions of the Royal Society B: Biological Sciences*, *369*(1635). https://doi.org/10.1098/rstb.2013.0369

Köhler, C. (1985). A projection from the deep layers of the entorhinal area to the hippocampal formation in the rat brain. *Neuroscience Letters*, *56*(1), 13–19. https://doi.org/10.1016/0304-3940(85)90433-1

Lee, H.-K., Takamiya, K., Han, J.-S., Man, H., Kim, C.-H., Rumbaugh, G., Yu, S., Ding, L., He, C., Petralia, R. S., Wenthold, R. J., Gallagher, M., & Huganir, R. L. (2003). Phosphorylation of the AMPA receptor GluR1 subunit is required for synaptic plasticity and retention of spatial memory. *Cell*, *112*(5), 631–643. https://doi.org/10.1016/s0092-8674(03)00122-3

Lehmann, H., Sparks, F. T., Spanswick, S. C., Hadikin, C., McDonald, R. J., & Sutherland, R. J. (2009). Making context memories independent of the hippocampus. *Learning & Memory*, *16*(7), 417–420. https://doi.org/10.1101/lm.1385409

Leutgeb, J. K., Leutgeb, S., Moser, M.-B., & Moser, E. I. (2007). Pattern Separation in the Dentate Gyrus and CA3 of the Hippocampus. *Science*, *315*(5814), 961–966. https://doi.org/10.1126/science.1135801

Leutgeb, J. K., Leutgeb, S., Treves, A., Meyer, R., Barnes, C. A., McNaughton, B. L., Moser, M.-B., & Moser, E. I. (2005a). Progressive Transformation of Hippocampal Neuronal Representations in "Morphed" Environments. *Neuron*, *48*(2), 345–358. https://doi.org/10.1016/j.neuron.2005.09.007

Leutgeb, J. K., Leutgeb, S., Treves, A., Meyer, R., Barnes, C. A., McNaughton, B. L., Moser, M.-B., & Moser, E. I. (2005b). Progressive Transformation of Hippocampal Neuronal Representations in "Morphed" Environments. *Neuron*, *48*(2), 345–358. https://doi.org/10.1016/j.neuron.2005.09.007

Leutgeb, S., & Leutgeb, J. K. (2007). Pattern separation, pattern completion, and new neuronal codes within a continuous CA3 map. *Learning & Memory*, *14*(11), 745–757. https://doi.org/10.1101/lm.703907

Leutgeb, S., Leutgeb, J. K., Barnes, C. A., Moser, E. I., McNaughton, B. L., & Moser, M.-B. (2005). Independent codes for spatial and episodic memory in hippocampal neuronal ensembles. *Science (New York, N.Y.)*, *309*(5734), 619–623. https://doi.org/10.1126/science.1114037

Leutgeb, S., Leutgeb, J. K., Treves, A., Moser, M.-B., & Moser, E. I. (2004). Distinct Ensemble Codes in Hippocampal Areas CA3 and CA1. *Science*, *305*(5688), 1295–1298. https://doi.org/10.1126/science.1100265

Lever, C., Wills, T., Cacucci, F., Burgess, N., & O'Keefe, J. (2002). Long-term plasticity in hippocampal place-cell representation of environmental geometry. *Nature*, *416*(6876), 90–94. https://doi.org/10.1038/416090a

Lisman, J., Schulman, H., & Cline, H. (2002). The molecular basis of CaMKII function in synaptic and behavioural memory. *Nature Reviews. Neuroscience*, *3*(3), 175–190. https://doi.org/10.1038/nrn753

Lømo, T. (2018). Discovering long-term potentiation (LTP) – recollections and reflections on what came after. *Acta Physiologica*, *222*(2), e12921. https://doi.org/10.1111/apha.12921

Lynch, G., Rex, C. S., & Gall, C. M. (2007). LTP consolidation: Substrates, explanatory power, and functional significance. *Neuropharmacology*, *52*(1), 12–23. https://doi.org/10.1016/j.neuropharm.2006.07.027

Ma, H., Li, B., & Tsien, R. W. (2015). Distinct roles of multiple isoforms of CaMKII in signaling to the nucleus. *Biochimica et Biophysica Acta*, *1853*(9), 1953–1957. https://doi.org/10.1016/j.bbamcr.2015.02.008

Maren, S., Aharonov, G., & Fanselow, M. S. (1997). Neurotoxic lesions of the dorsal hippocampus and Pavlovian fear conditioning in rats. *Behavioural Brain Research*, *88*(2), 261–274. https://doi.org/10.1016/s0166-4328(97)00088-0

McDonald, R. J., & White, N. M. (1993). A triple dissociation of memory systems: Hippocampus, amygdala, and dorsal striatum. *Behavioral Neuroscience*, *107*(1), 3–22.

McDonald, R. J., & White, N. M. (1994). Parallel information processing in the water maze: Evidence for independent memory systems involving dorsal striatum and hippocampus. *Behavioral and Neural Biology*, *61*(3), 260–270. https://doi.org/10.1016/s0163-1047(05)80009-3

McDonald, Robert J., Devan, B. D., & Hong, N. S. (2004). Multiple memory systems: The power of interactions. *Neurobiology of Learning and Memory*, *82*(3), 333–346. https://doi.org/10.1016/j.nlm.2004.05.009

McDonald, Robert J., Hong, N. S., Craig, L. A., Holahan, M. R., Louis, M., & Muller, R. U. (2005). NMDA-receptor blockade by CPP impairs post-training consolidation of a rapidly acquired spatial representation in rat hippocampus. *The European Journal of Neuroscience*, *22*(5), 1201–1213. https://doi.org/10.1111/j.1460-9568.2005.04272.x

McDonald, Robert J., Lo, Q., King, A. L., Wasiak, T. D., & Hong, N. S. (2007). Empirical tests of the functional significance of amygdala-based modulation of hippocampal representations: Evidence for multiple memory consolidation pathways. *European Journal of Neuroscience*, *25*(5), 1568–1580. https://doi.org/10.1111/j.1460-9568.2007.05397.x

McDonald, Robert J., Yim, T. T., Lehmann, H., Sparks, F. T., Zelinski, E. L., Sutherland, R. J., & Hong, N. S. (2010). Expression of a conditioned place preference or spatial navigation task following muscimol-induced inactivations of the amygdala or dorsal hippocampus: A double dissociation in the retrograde direction. *Brain Research Bulletin*, *83*(1), 29–37. https://doi.org/10.1016/j.brainresbull.2010.06.001

McHugh, T. J., Blum, K. I., Tsien, J. Z., Tonegawa, S., & Wilson, M. A. (1996). Impaired hippocampal representation of space in CA1-specific NMDAR1 knockout mice. *Cell*, *87*(7), 1339–1349.

McHugh, Thomas J., Jones, M. W., Quinn, J. J., Balthasar, N., Coppari, R., Elmquist, J. K., Lowell, B. B., Fanselow, M. S., Wilson, M. A., & Tonegawa, S. (2007a). Dentate gyrus NMDA receptors mediate rapid pattern separation in the hippocampal network. *Science (New York, N.Y.)*, *317*(5834), 94–99. https://doi.org/10.1126/science.1140263

McHugh, Thomas J., Jones, M. W., Quinn, J. J., Balthasar, N., Coppari, R., Elmquist, J. K., Lowell, B. B., Fanselow, M. S., Wilson, M. A., & Tonegawa, S. (2007b). Dentate Gyrus NMDA Receptors Mediate Rapid Pattern Separation in the Hippocampal Network. *Science*, *317*(5834), 94–99. https://doi.org/10.1126/science.1140263

Mizuno, M., Yamada, K., Maekawa, N., Saito, K., Seishima, M., & Nabeshima, T. (2002). CREB phosphorylation as a molecular marker of memory processing in the hippocampus for spatial learning. *Behavioural Brain Research*, *133*(2), 135–141. https://doi.org/10.1016/S0166-4328(01)00470-3

Moncada, D., & Viola, H. (2006). Phosphorylation state of CREB in the rat hippocampus: A molecular switch between spatial novelty and spatial familiarity? *Neurobiology of Learning and Memory*, *86*(1), 9–18. https://doi.org/10.1016/j.nlm.2005.12.002

Morris, R. G. (1989a). Synaptic plasticity and learning: Selective impairment of learning rats and blockade of long-term potentiation in vivo by the N-methyl-D- aspartate receptor

antagonist AP5. *Journal of Neuroscience*, *9*(9), 3040–3057. https://doi.org/10.1523/JNEUROSCI.09-09-03040.1989

Morris, R. G. (1989b). Synaptic plasticity and learning: Selective impairment of learning rats and blockade of long-term potentiation in vivo by the N-methyl-D- aspartate receptor antagonist AP5. *Journal of Neuroscience*, *9*(9), 3040–3057. https://doi.org/10.1523/JNEUROSCI.09-09-03040.1989

Morris, R. G., Anderson, E., Lynch, G. S., & Baudry, M. (1986a). Selective impairment of learning and blockade of long-term potentiation by an N-methyl-D-aspartate receptor antagonist, AP5. *Nature*, *319*(6056), 774–776. https://doi.org/10.1038/319774a0

Morris, R. G., Anderson, E., Lynch, G. S., & Baudry, M. (1986b). Selective impairment of learning and blockade of long-term potentiation by an N-methyl-D-aspartate receptor antagonist, AP5. *Nature*, *319*(6056), 774–776. https://doi.org/10.1038/319774a0

Morris, R. G., Davis, S., & Butcher, S. P. (1990). Hippocampal synaptic plasticity and NMDA receptors: A role in information storage? *Philosophical Transactions of the Royal Society of London. Series B, Biological Sciences*, *329*(1253), 187–204. https://doi.org/10.1098/rstb.1990.0164

Morris, R. G., Garrud, P., Rawlins, J. N., & O'Keefe, J. (1982). Place navigation impaired in rats with hippocampal lesions. *Nature*, *297*(5868), 681–683. https://doi.org/10.1038/297681a0

Morris, R. G. M., Anderson, E., Lynch, G. S., & Baudry, M. (1986). Selective impairment of learning and blockade of long-term potentiation by an N-methyl-D-aspartate receptor antagonist, AP5. *Nature*, *319*(6056), 774–776. https://doi.org/10.1038/319774a0

Morris, R. G. M., Garrud, P., Rawlins, J. N. P., & O'Keefe, J. (1982). Place navigation impaired in rats with hippocampal lesions. *Nature*, *297*(5868), 681–683. https://doi.org/10.1038/297681a0

Morris, R. G. M., Steele, R. J., Bell, J. E., & Martin, S. J. (2013). N-methyl-d-aspartate receptors, learning and memory: Chronic intraventricular infusion of the NMDA receptor antagonist d-AP5 interacts directly with the neural mechanisms of spatial learning. *The European Journal of Neuroscience*, *37*(5), 700–717. https://doi.org/10.1111/ejn.12086

Morris, Richard G. M. (2013). NMDA receptors and memory encoding. *Neuropharmacology*, *74*, 32–40. https://doi.org/10.1016/j.neuropharm.2013.04.014

Moser, E., Moser, M. B., & Andersen, P. (1993). Spatial learning impairment parallels the magnitude of dorsal hippocampal lesions, but is hardly present following ventral lesions. *The Journal of Neuroscience: The Official Journal of the Society for Neuroscience*, *13*(9), 3916–3925.

Moser, M. B., Moser, E. I., Forrest, E., Andersen, P., & Morris, R. G. (1995). Spatial learning with a minislab in the dorsal hippocampus. *Proceedings of the National Academy of Sciences*, *92*(21), 9697–9701. https://doi.org/10.1073/pnas.92.21.9697

Murphy, D. D., & Segal, M. (1997). Morphological plasticity of dendritic spines in central neurons is mediated by activation of cAMP response element binding protein.

Proceedings of the National Academy of Sciences, *94*(4), 1482–1487. https://doi.org/10.1073/pnas.94.4.1482

Nadel, L., & Moscovitch, M. (1997). Memory consolidation, retrograde amnesia and the hippocampal complex. *Current Opinion in Neurobiology*, *7*(2), 217–227.

Nadel, Lynn. (2008). The hippocampus and context revisited. In *Hippocampal place fields: Relevance to learning and memory* (pp. 3–15). Oxford University Press. https://doi.org/10.1093/acprof:oso/9780195323245.003.0002

Nakamura, N. H., Flasbeck, V., Maingret, N., Kitsukawa, T., & Sauvage, M. M. (2013). Proximodistal Segregation of Nonspatial Information in CA3: Preferential Recruitment of a Proximal CA3-Distal CA1 Network in Nonspatial Recognition Memory. *The Journal of Neuroscience*, *33*(28), 11506–11514. https://doi.org/10.1523/JNEUROSCI.4480-12.2013

Nakazawa, K., Quirk, M. C., Chitwood, R. A., Watanabe, M., Yeckel, M. F., Sun, L. D., Kato, A., Carr, C. A., Johnston, D., Wilson, M. A., & Tonegawa, S. (2002). Requirement for Hippocampal CA3 NMDA Receptors in Associative Memory Recall. *Science (New York, N.Y.)*, *297*(5579), 211–218. https://doi.org/10.1126/science.1071795

Nakazawa, Y., Pevzner, A., Tanaka, K. Z., & Wiltgen, B. J. (2016a). Memory retrieval along the proximodistal axis of CA1. *Hippocampus*, *26*(9), 1140–1148. https://doi.org/10.1002/hipo.22596

Nakazawa, Y., Pevzner, A., Tanaka, K. Z., & Wiltgen, B. J. (2016b). Memory retrieval along the proximodistal axis of CA1. *Hippocampus*, *26*(9), 1140–1148. https://doi.org/10.1002/hipo.22596

Nayak, A., Zastrow, D. J., Lickteig, R., Zahniser, N. R., & Browning, M. D. (1998a). Maintenance of late-phase LTP is accompanied by PKA-dependent increase in AMPA receptor synthesis. *Nature*, *394*(6694), 680–683. https://doi.org/10.1038/29305

Nayak, A., Zastrow, D. J., Lickteig, R., Zahniser, N. R., & Browning, M. D. (1998b). Maintenance of late-phase LTP is accompanied by PKA-dependent increase in AMPA receptor synthesis. *Nature*, *394*(6694), 680–683. https://doi.org/10.1038/29305

Neunuebel, J. P., & Knierim, J. J. (2014a). CA3 Retrieves Coherent Representations from Degraded Input: Direct Evidence for CA3 Pattern Completion and Dentate Gyrus Pattern Separation. *Neuron*, *81*(2), 416–427. https://doi.org/10.1016/j.neuron.2013.11.017

Neunuebel, J. P., & Knierim, J. J. (2014b). CA3 Retrieves Coherent Representations from Degraded Input: Direct Evidence for CA3 Pattern Completion and Dentate Gyrus Pattern Separation. *Neuron*, *81*(2), 416–427. https://doi.org/10.1016/j.neuron.2013.11.017

Nilssen, E. S., Doan, T. P., Nigro, M. J., Ohara, S., & Witter, M. P. (2019). Neurons and networks in the entorhinal cortex: A reappraisal of the lateral and medial entorhinal subdivisions mediating parallel cortical pathways. *Hippocampus*. https://doi.org/10.1002/hipo.23145

Ohsako, S., Nakazawa, H., Sekihara, S., Ikai, A., & Yamauchi, T. (1991). Role of Threonine-286 as Autophosphorylation Site for Appearance of Ca2+-Independent Activity of

Calmodulin-Dependent Protein Kinase II α Subunit. *The Journal of Biochemistry*, *109*(1), 137–143. https://doi.org/10.1093/oxfordjournals.jbchem.a123334

O'Keefe, J., & Dostrovsky, J. (1971). The hippocampus as a spatial map. Preliminary evidence from unit activity in the freely-moving rat. *Brain Research*, *34*(1), 171–175. https://doi.org/10.1016/0006-8993(71)90358-1

O'Keefe, John, & Nadel, L. (1978). *The Hippocampus as a Cognitive Map*. Oxford: Clarendon Press. http://arizona.openrepository.com/arizona/handle/10150/620894

Olucha-Bordonau, F. E., Fortes-Marco, L., Otero-García, M., Lanuza, E., & Martínez-García, F. (2015). Chapter 18 - Amygdala: Structure and Function. In G. Paxinos (Ed.), *The Rat Nervous System (Fourth Edition)* (pp. 441–490). Academic Press. https://doi.org/10.1016/B978-0-12-374245-2.00018-8

Packard, M. G., Hirsh, R., & White, N. M. (1989). Differential effects of fornix and caudate nucleus lesions on two radial maze tasks: Evidence for multiple memory systems. *The Journal of Neuroscience: The Official Journal of the Society for Neuroscience*, *9*(5), 1465–1472.

Pavlov, I. P. (1927). *Conditioned reflexes: An investigation of the physiological activity of the cerebral cortex*. Oxford Univ. Press.

Pavlov, Ivan P. (1984). *Conditioned Reflexes* (G. P. Anrep, Ed.; reprint edition). Dover Pubns.

Pnevmatikakis, E. A., & Giovannucci, A. (2017). NoRMCorre: An online algorithm for piecewise rigid motion correction of calcium imaging data. *Journal of Neuroscience Methods*, *291*, 83–94. https://doi.org/10.1016/j.jneumeth.2017.07.031

Porte, Y., Buhot, M. C., & Mons, N. E. (2008). Spatial memory in the Morris water maze and activation of cyclic AMP response element-binding (CREB) protein within the mouse hippocampus. *Learning & Memory*, *15*(12), 885–894. https://doi.org/10.1101/lm.1094208

Quirk, G. J., Muller, R. U., Kubie, J. L., & Ranck, J. B. (1992). The positional firing properties of medial entorhinal neurons: Description and comparison with hippocampal place cells. *Journal of Neuroscience*, *12*(5), 1945–1963. https://doi.org/10.1523/JNEUROSCI.12-05-01945.1992

Reisel, D., Bannerman, D. M., Schmitt, W. B., Deacon, R. M. J., Flint, J., Borchardt, T., Seeburg, P. H., & Rawlins, J. N. P. (2002). Spatial memory dissociations in mice lacking GluR1. *Nature Neuroscience*, *5*(9), 868–873. https://doi.org/10.1038/nn910

Roozendaal, B., & McGaugh, J. L. (1997). Glucocorticoid receptor agonist and antagonist administration into the basolateral but not central amygdala modulates memory storage. *Neurobiology of Learning and Memory*, *67*(2), 176–179. https://doi.org/10.1006/nlme.1996.3765

Rudy, J. W., & Sutherland, R. J. (1995). Configural association theory and the hippocampal formation: An appraisal and reconfiguration. *Hippocampus*, *5*(5), 375–389. https://doi.org/10.1002/hipo.450050502

Rudy, Jerry W. (2009). Context representations, context functions, and the parahippocampal–hippocampal system. *Learning & Memory*, *16*(10), 573–585. https://doi.org/10.1101/lm.1494409

Rudy, Jerry W. (2013). *The Neurobiology of Learning and Memory* (2 edition). Sinauer Associates is an imprint of Oxford University Press.

Ruediger, S., Spirig, D., Donato, F., & Caroni, P. (2012). Goal-oriented searching mediated by ventral hippocampus early in trial-and-error learning. *Nature Neuroscience*, *15*(11), 1563–1571. https://doi.org/10.1038/nn.3224

Sarel, A., Finkelstein, A., Las, L., & Ulanovsky, N. (2017). Vectorial representation of spatial goals in the hippocampus of bats. *Science*, *355*(6321), 176–180. https://doi.org/10.1126/science.aak9589

Saucier, D., & Cain, D. P. (1995). Spatial learning without NMDA receptor-dependent long-term potentiation. *Nature*, *378*(6553), 186–189. https://doi.org/10.1038/378186a0

Savelli, F., Yoganarasimha, D., & Knierim, J. J. (2008). Influence of boundary removal on the spatial representations of the medial entorhinal cortex. *Hippocampus*, *18*(12), 1270–1282. https://doi.org/10.1002/hipo.20511

Sheffield, M. E. J., Adoff, M. D., & Dombeck, D. A. (2017). Increased Prevalence of Calcium Transients across the Dendritic Arbor during Place Field Formation. *Neuron*, *96*(2), 490-504.e5. https://doi.org/10.1016/j.neuron.2017.09.029

Sheintuch, L., Rubin, A., Brande-Eilat, N., Geva, N., Sadeh, N., Pinchasof, O., & Ziv, Y. (2017). Tracking the Same Neurons across Multiple Days in Ca2+ Imaging Data. *Cell Reports*, *21*(4), 1102–1115. https://doi.org/10.1016/j.celrep.2017.10.013

Shi, S. H., Hayashi, Y., Petralia, R. S., Zaman, S. H., Wenthold, R. J., Svoboda, K., & Malinow, R. (1999). Rapid spine delivery and redistribution of AMPA receptors after synaptic NMDA receptor activation. *Science (New York, N.Y.)*, *284*(5421), 1811–1816. https://doi.org/10.1126/science.284.5421.1811

Shonesy, B. C., Jalan-Sakrikar, N., Cavener, V. S., & Colbran, R. J. (2014). Chapter Three - CaMKII: A Molecular Substrate for Synaptic Plasticity and Memory. In Z. U. Khan & E. C. Muly (Eds.), *Progress in Molecular Biology and Translational Science* (Vol. 122, pp. 61–87). Academic Press. https://doi.org/10.1016/B978-0-12-420170-5.00003-9

Silva, A. J., Paylor, R., Wehner, J. M., & Tonegawa, S. (1992). Impaired spatial learning in alpha-calcium-calmodulin kinase II mutant mice. *Science*, *257*(5067), 206–211. https://doi.org/10.1126/science.1321493

Skocek, O., Nöbauer, T., Weilguny, L., Traub, F. M., Xia, C. N., Molodtsov, M. I., Grama, A., Yamagata, M., Aharoni, D., Cox, D. D., Golshani, P., & Vaziri, A. (2018). High-speed volumetric imaging of neuronal activity in freely moving rodents. *Nature Methods*, *15*(6), 429–432. https://doi.org/10.1038/s41592-018-0008-0

Solstad, T., Boccara, C. N., Kropff, E., Moser, M.-B., & Moser, E. I. (2008). Representation of geometric borders in the entorhinal cortex. *Science (New York, N.Y.)*, *322*(5909), 1865–1868. https://doi.org/10.1126/science.1166466

Song, L., Che, W., Min-wei, W., Murakami, Y., & Matsumoto, K. (2006). Impairment of the spatial learning and memory induced by learned helplessness and chronic mild stress. *Pharmacology Biochemistry and Behavior*, *83*(2), 186–193. https://doi.org/10.1016/j.pbb.2006.01.004

Stranahan, A. M. (2011). Similarities and differences in spatial learning and object recognition between young male C57Bl/6J mice and Sprague-Dawley rats. *Behavioral Neuroscience*, *125*(5), 791–795. https://doi.org/10.1037/a0025133

Sun, Q., Sotayo, A., Cazzulino, A. S., Snyder, A. M., Denny, C. A., & Siegelbaum, S. A. (2017). Proximodistal Heterogeneity of Hippocampal CA3 Pyramidal Neuron Intrinsic Properties, Connectivity, and Reactivation during Memory Recall. *Neuron*, *95*(3), 656-672.e3. https://doi.org/10.1016/j.neuron.2017.07.012

Sutherland, R. J., & McDonald, R. J. (1990). Hippocampus, amygdala, and memory deficits in rats. *Behavioural Brain Research*, *37*(1), 57–79. https://doi.org/10.1016/0166-4328(90)90072-m

Sutherland, R. J., & Rudy, J. W. (1989). Configural association theory: The role of the hippocampal formation in learning, memory, and amnesia. *Psychobiology*, *17*(2), 129–144. https://doi.org/10.3758/BF03337828

Sutherland, R. J., Whishaw, I. Q., & Kolb, B. (1983). A behavioural analysis of spatial localization following electrolytic, kainate- or colchicine-induced damage to the hippocampal formation in the rat. *Behavioural Brain Research*, *7*(2), 133–153. https://doi.org/10.1016/0166-4328(83)90188-2

Sutherland, Robert J., Kolb, B., & Whishaw, I. Q. (1982). Spatial mapping: Definitive disruption by hippocampal or medial frontal cortical damage in the rat. *Neuroscience Letters*, *31*(3), 271–276. https://doi.org/10.1016/0304-3940(82)90032-5

Taverna, F. A., Georgiou, J., McDonald, R. J., Hong, N. S., Kraev, A., Salter, M. W., Takeshima, H., Muller, R. U., & Roder, J. C. (2005). Defective place cell activity in nociceptin receptor knockout mice with elevated NMDA receptor-dependent long-term potentiation. *The Journal of Physiology*, *565*(Pt 2), 579–591. https://doi.org/10.1113/jphysiol.2004.081802

Taylor, A. M., Bus, T., Sprengel, R., Seeburg, P. H., Rawlins, J. N., & Bannerman, D. M. (2014). Hippocampal NMDA receptors are important for behavioural inhibition but not for encoding associative spatial memories. *Philosophical Transactions of the Royal Society of London. Series B, Biological Sciences*, *369*(1633), 20130149–20130149. https://doi.org/10.1098/rstb.2013.0149

Teyler, T. J., & DiScenna, P. (1986). The hippocampal memory indexing theory. *Behavioral Neuroscience*, *100*(2), 147–154.

Thomas, G. M., & Huganir, R. L. (2004). MAPK cascade signalling and synaptic plasticity. *Nature Reviews Neuroscience*, *5*(3), 173–183. https://doi.org/10.1038/nrn1346

Tolman, E. C., & Honzik, C. H. (1930). Introduction and removal of reward, and maze performance in rats. *University of California Publications in Psychology*, *4*, 257–275.

Tolman, E. C., Ritchie, B. F., & Kalish, D. (1946). Studies in spatial learning. I. Orientation and the short-cut. *Journal of Experimental Psychology*, *36*(1), 13–24. https://doi.org/10.1037/h0053944

Tsodyks, M. (1999). Attractor neural network models of spatial maps in hippocampus. *Hippocampus*, *9*(4), 481–489. https://doi.org/10.1002/(SICI)1098-1063(1999)9:4<481::AID-HIPO14>3.0.CO;2-S

Tsodyks, M. (2005). Attractor neural networks and spatial maps in hippocampus. *Neuron*, *48*(2), 168–169. https://doi.org/10.1016/j.neuron.2005.10.006

Waltereit, R., & Weller, M. (2003). Signaling from cAMP/PKA to MAPK and synaptic plasticity. *Molecular Neurobiology*, *27*(1), 99–106. https://doi.org/10.1385/MN:27:1:99

Weisskopf, M. G., & Nicoll, R. A. (1995). Presynaptic changes during mossy fibre LTP revealed by NMDA receptor-mediated synaptic responses. *Nature*, *376*(6537), 256–259. https://doi.org/10.1038/376256a0

Whishaw, I. Q. (1995). A comparison of rats and mice in a swimming pool place task and matching to place task: Some surprising differences. *Physiology & Behavior*, *58*(4), 687–693. https://doi.org/10.1016/0031-9384(95)00110-5

Whishaw, I. Q., & Pasztor, T. J. (2000). Rats alternate on a dry-land but not swimming-pool (Morris task) place task: Implications for spatial processing. *Behavioral Neuroscience*, *114*(2), 442–446. https://doi.org/10.1037//0735-7044.114.2.442

Whishaw, I. Q., & Tomie, J. A. (1996). Of mice and mazes: Similarities between mice and rats on dry land but not water mazes. *Physiology & Behavior*, *60*(5), 1191–1197. https://doi.org/10.1016/s0031-9384(96)00176-x

White, N. M., & McDonald, R. J. (2002). Multiple Parallel Memory Systems in the Brain of the Rat. *Neurobiology of Learning and Memory*, *77*(2), 125–184. https://doi.org/10.1006/nlme.2001.4008

Wills, T. J., Lever, C., Cacucci, F., Burgess, N., & O'Keefe, J. (2005). Attractor dynamics in the hippocampal representation of the local environment. *Science (New York, N.Y.)*, *308*(5723), 873–876. https://doi.org/10.1126/science.1108905

Wilson, M. A., & McNaughton, B. L. (1993). Dynamics of the hippocampal ensemble code for space. *Science (New York, N.Y.)*, *261*(5124), 1055–1058. https://doi.org/10.1126/science.8351520

Witter, M. P. (2007). The perforant path: Projections from the entorhinal cortex to the dentate gyrus. *Progress in Brain Research*, *163*, 43–61. https://doi.org/10.1016/S0079-6123(07)63003-9

Wyss, J. M. (1981). An autoradiographic study of the efferent connections of the entorhinal cortex in the rat. *The Journal of Comparative Neurology*, *199*(4), 495–512. https://doi.org/10.1002/cne.901990405

Zhou, P., Resendez, S. L., Rodriguez-Romaguera, J., Jimenez, J. C., Neufeld, S. Q., Giovannucci, A., Friedrich, J., Pnevmatikakis, E. A., Stuber, G. D., Hen, R., Kheirbek, M.

A., Sabatini, B. L., Kass, R. E., & Paninski, L. (2018). Efficient and accurate extraction of in vivo calcium signals from microendoscopic video data. *ELife*, *7*, e28728. https://doi.org/10.7554/eLife.28728

Ziv, Y., Burns, L. D., Cocker, E. D., Hamel, E. O., Ghosh, K. K., Kitch, L. J., El Gamal, A., & Schnitzer, M. J. (2013). Long-term dynamics of CA1 hippocampal place codes. *Nature Neuroscience*, *16*(3), 264–266. https://doi.org/10.1038/nn.3329

APPENDIX 1: FIGURES

Chapter 1 Figures:

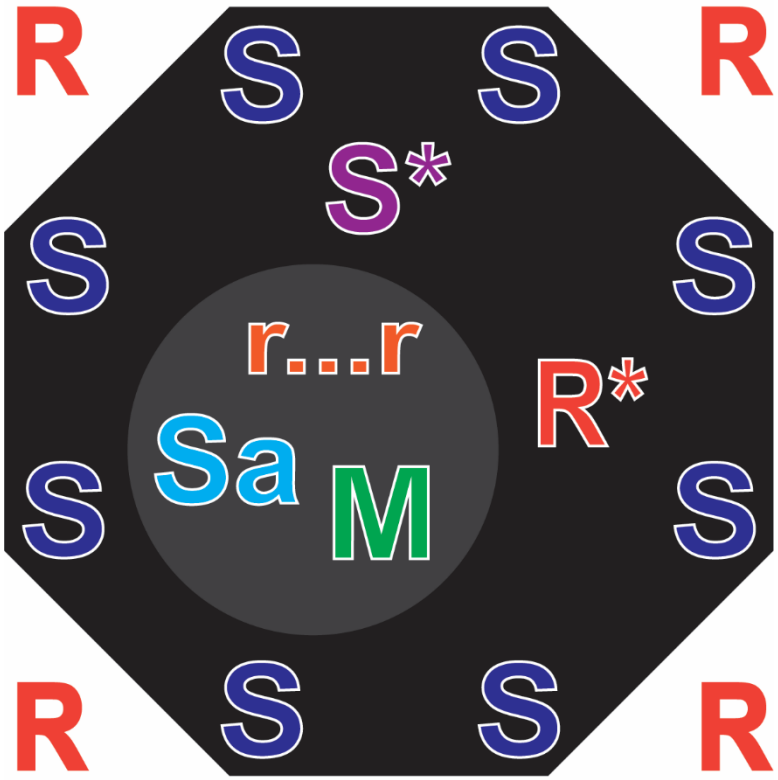

Figure 1.1: Blank learning model showing elements of learning situations. The learning model includes neutral cues (S), reinforcers (S*), escape or approach responses (R*), autonomic responses (r…r), affective states (Sa), memory modulation (M).

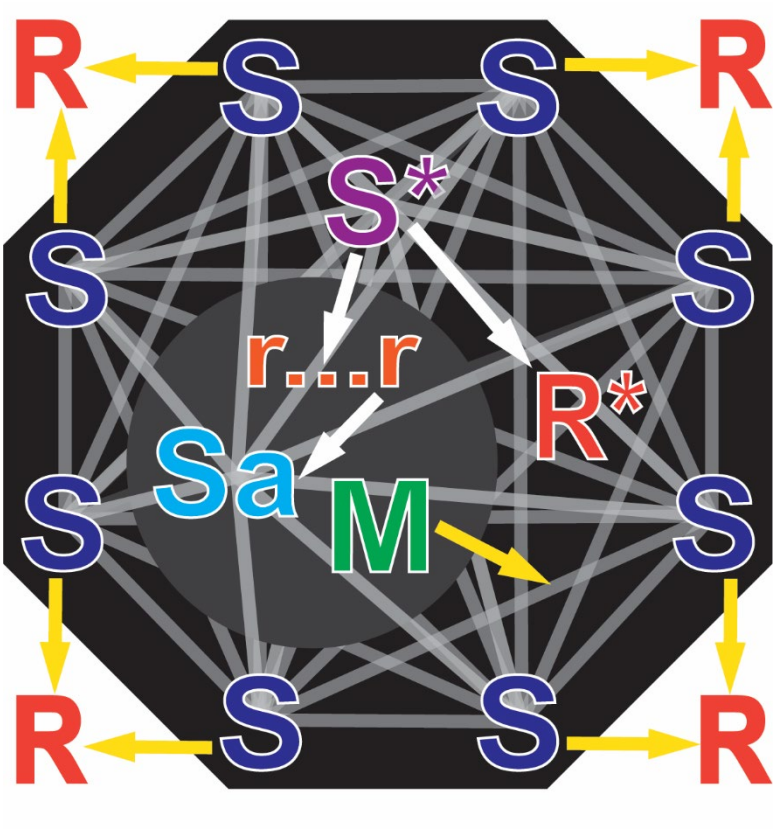

Figure 1.2: Stimulus-stimulus learning in the hippocampal system. In the hippocampal system, information is processed to create associations between stimuli. Multiple associations are made between stimuli (S) and other stimuli, including the reinforcer (S*) and the internal affective state (Sa). The modulatory response (M) influences the associations between stimuli. Gray lines represent the associations made by the hippocampal system. Yellow arrows highlight unidirectional relationship between elements that are unique to they system, while white arrows represent the unidirectional relationship between elements that are consistent across all systems.

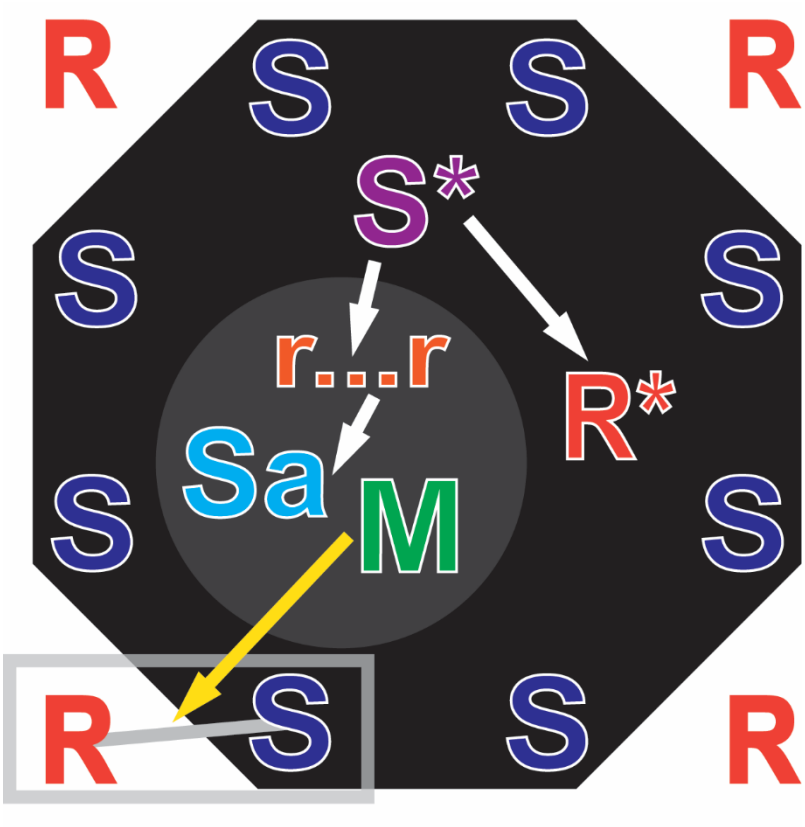

Figure 1.3: Stimulus-response learning in the striatum system. Associations are made between a stimulus (S) and a response (R). These associations are influenced by the modulatory response (M). Gray lines represent the associations made by the striatum system. Yellow arrows highlight unidirectional relationship between elements that are unique to they system, while white arrows represent the unidirectional relationship between elements that are consistent across all systems.

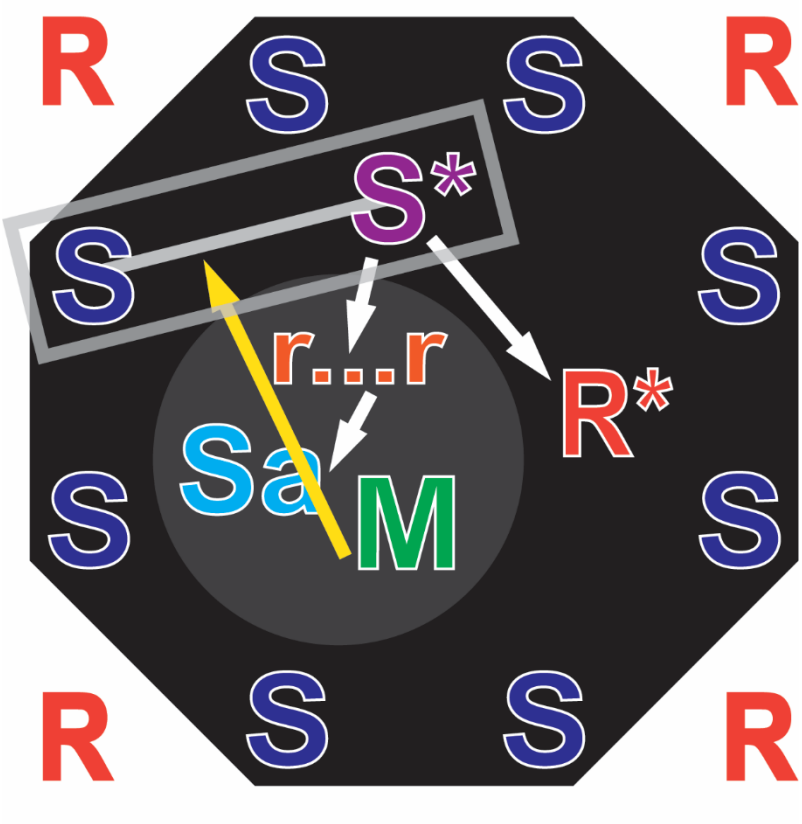

Figure 1.4: Stimulus-reinforcer learning in the amygdala system. Learning is processed in this system through associations between stimulus (S) and reinforcers (S*). These associations are also influence by the modulatory response (M). Gray lines represent the associations made by the amygdala system. Yellow arrows highlight unidirectional relationship between elements that are unique to they system, while white arrows represent the unidirectional relationship between elements that are consistent across all systems.

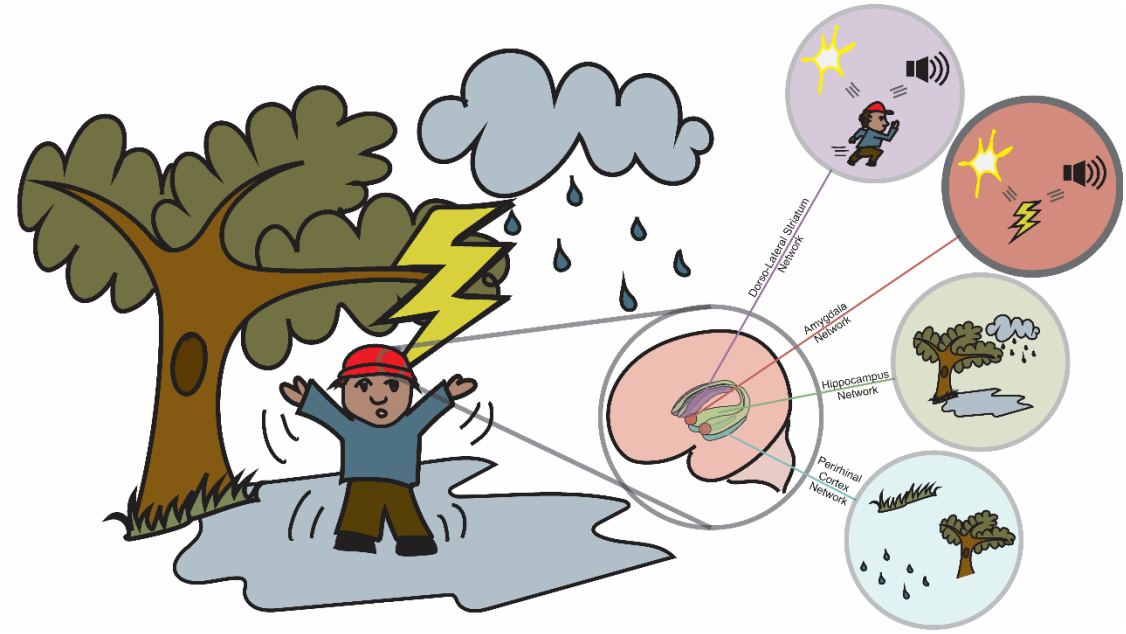

Figure 1.5: Example of multiple parallel memory systems. In this example, the person gets shocked in a thunderstorm and they learn that they'll be shocked in that environment. This learning experience is processed by the striatum, amygdala, hippocampus, and perirhinal cortex networks. The coherence between the information being processed, in this example, the lightning and environmental stimuli, and the amygdala network's processing style, dictates its responsibility over the learning event. In other systems, such as the perirhinal cortex, object stimuli, like grass, raindrops, and the person's hat are processed, however this system is not responsible for the learning event. Similarly, the hippocampus has a processing style that generates associations between stimuli, such as the clouds, puddle, and tree, however this style is not coherent with the information involved in the learning event and therefore this network is not responsible. Furthermore, the striatum network's processing style generates associations between stimuli and the response, like the environment and the person jumping. Since the striatum's processing

style is not coherent with the information it is not responsible for the learning event. Each of these networks processes the information at hand and provides parallel outputs. Since the information in this example, the lightning and environmental stimuli, matches well with the amygdala's stimulus-reinforcer processing style, this region is responsible for the learning event.

Chapter 2 Figures:

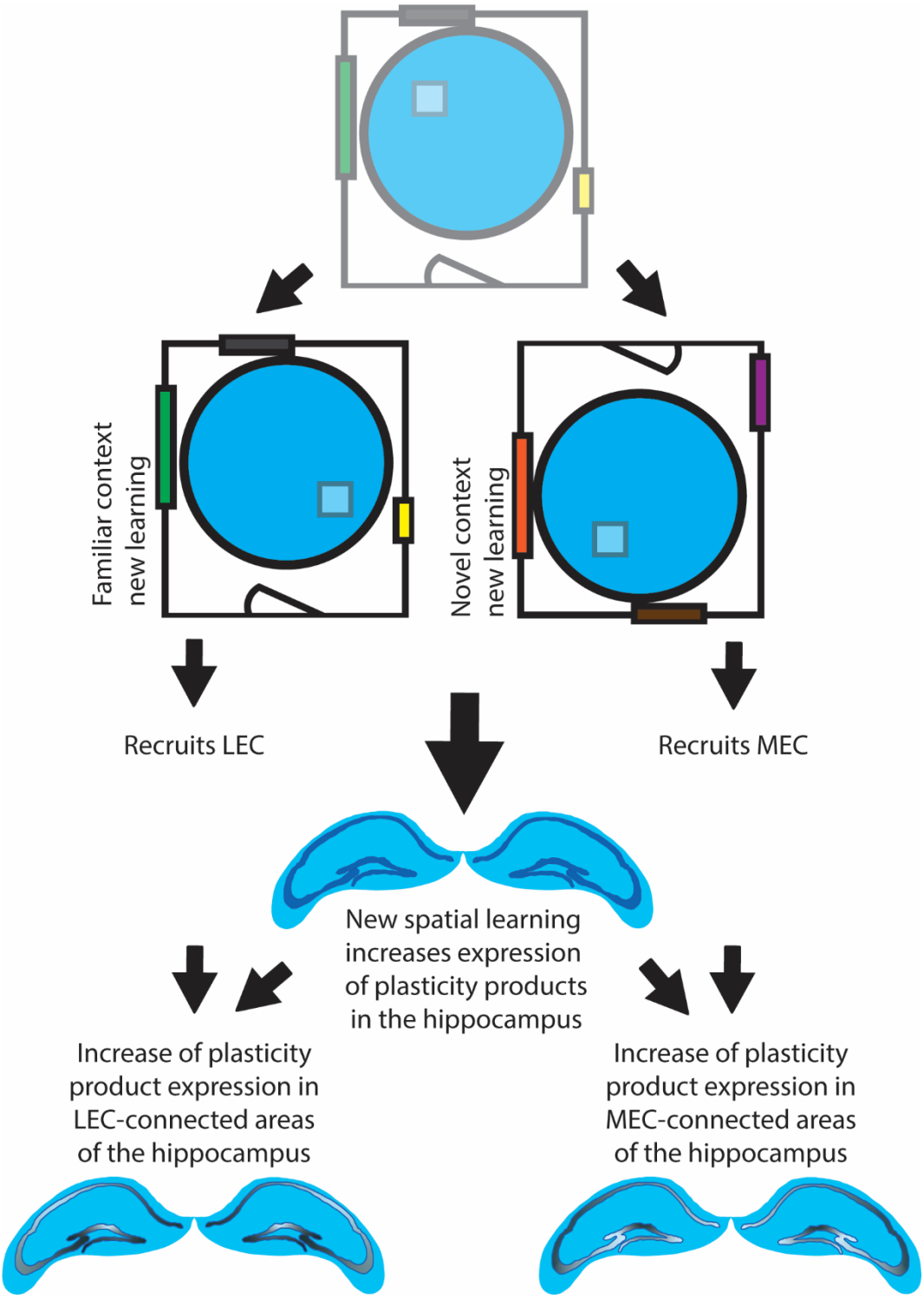

Figure 2.1: Generalized hypothesis for experiments. Our hypothesis is that familiar context new spatial learning recruits the LEC, while novel context new spatial learning

recruits the MEC and these differences in recruitment will be observed in patterns of plasticity product expression in the hippocampus that match either the connectivity patterns of LEC or MEC for familiar and novel contexts, respectively.

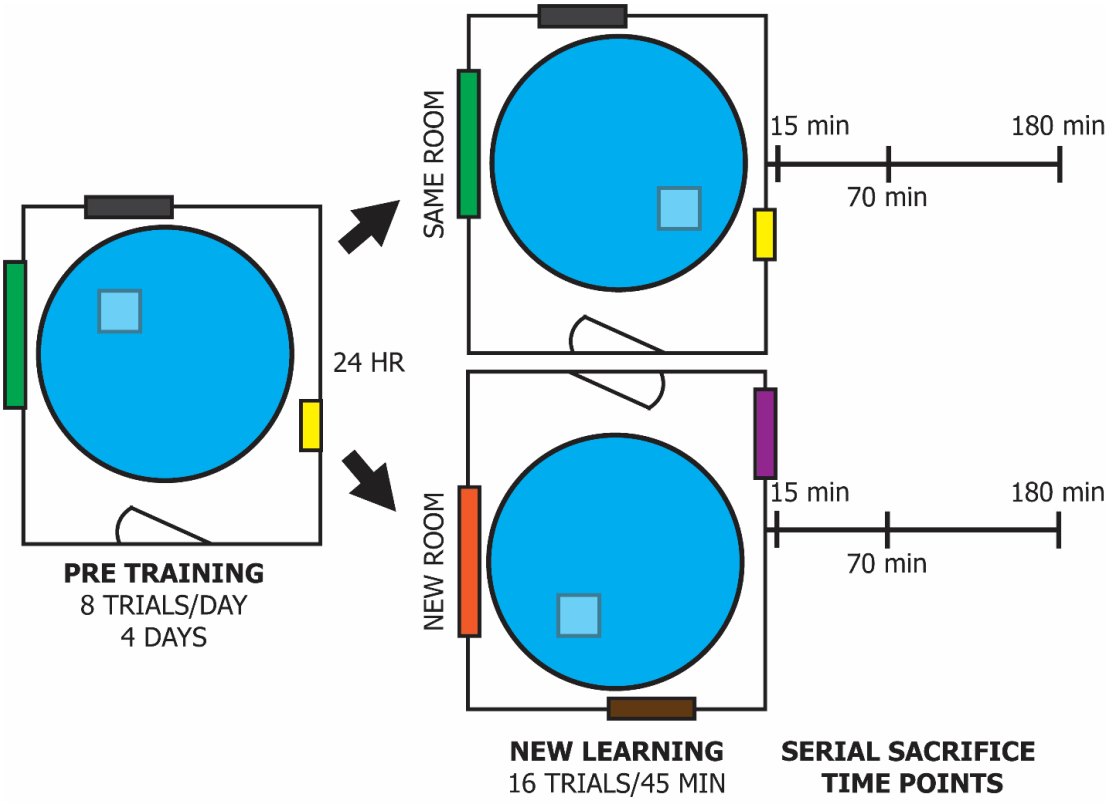

Figure 2.2: Study design for the experiment. All experimental animals underwent pre-training in a hidden platform version of the water maze over 4 days with 8 trials per day. On the 5th day, half of the animals underwent new learning in either the training room (same room) or in a new environment (new room). Animals were sacrificed either 15 (for pCAMKII), 70 (for GluA1, GluA2, and NMDAR), or 180 minutes (for GluA1, GluA2, and pCREB) after new learning. Cage control animals were not subject to any behavioural task.

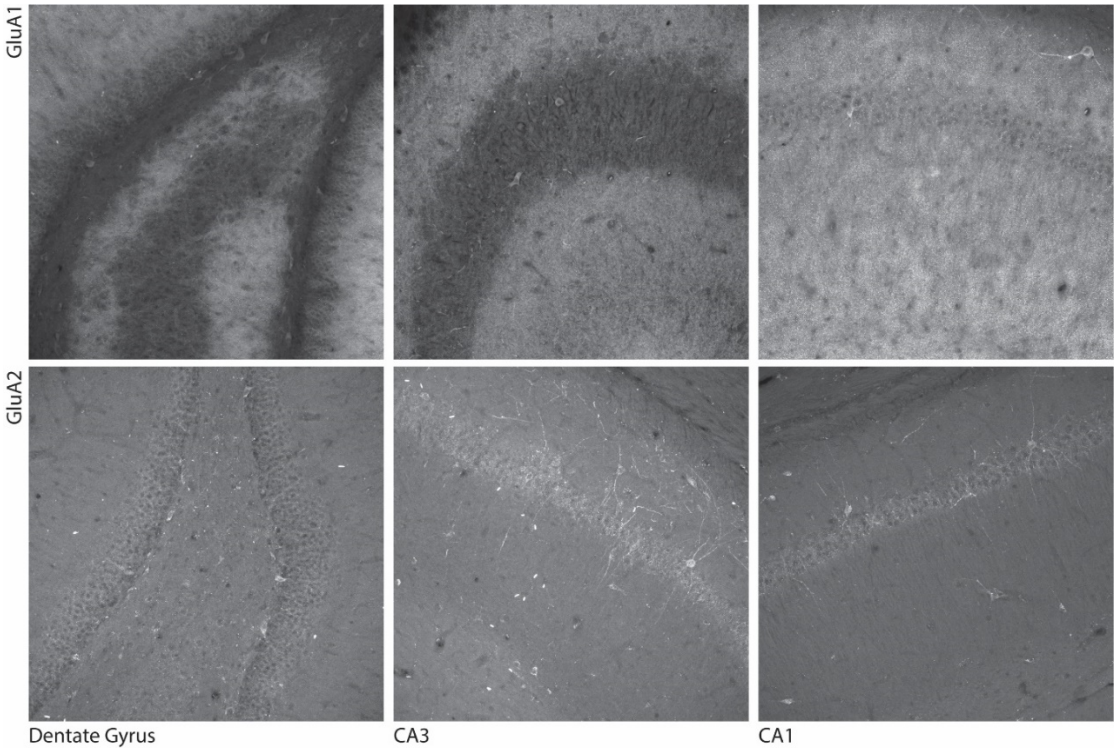

Figure 2.3: Representative images of GluA2 and GluA1 immunohistochemistry in subfields of the hippocampus.

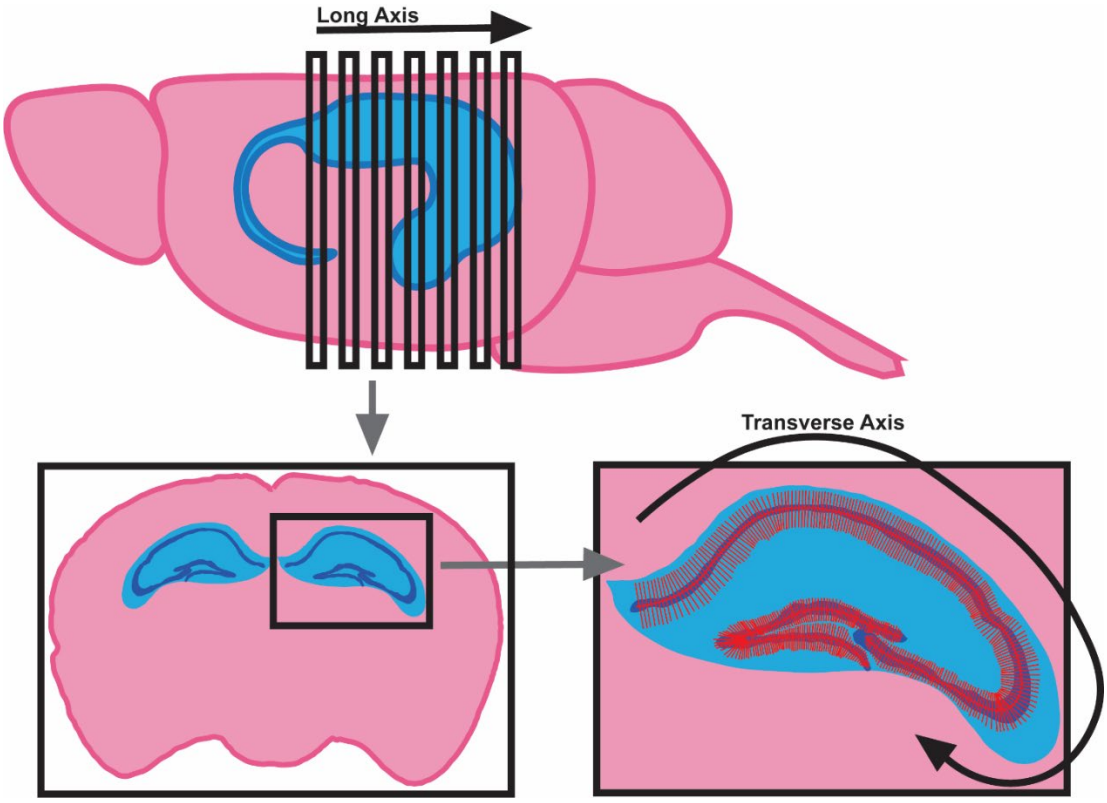

Figure 2.4: Schematic of analysis used to measure average pixel fluorescence along long and transverse axes. Rat brains were sliced in 12 series to capture a representative sample along the long axis. A line was mapped along the molecular layer of the hippocampus and within each subfield was split into 20 bins, with 20 random lines were distributed within each bin, perpendicular to the axis. Average pixel fluorescence was calculated along each line and averaged within each bin.

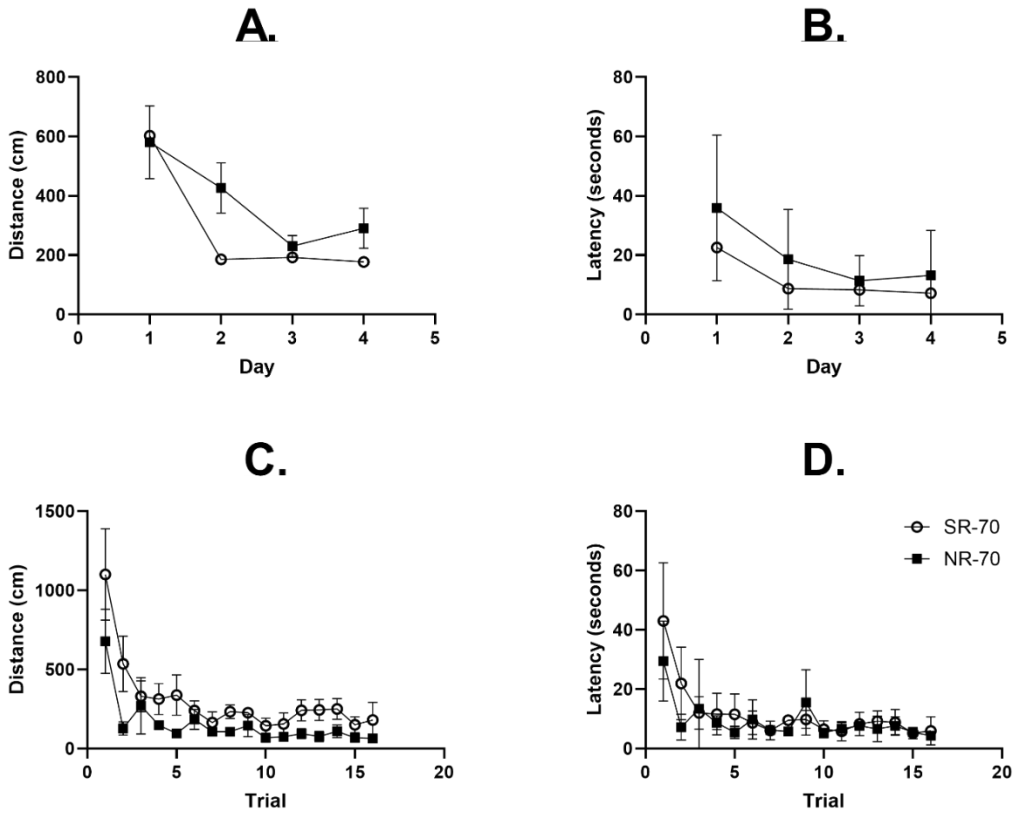

Figure 2.5: Mean path length and latency during pre-training over days and over new learning over trials in same room and new room conditions of animals sacrificed 70 minutes after new learning (NMDAR). A. Average path length across trials per training day. A significant learning effect was observed ($F_{3, 246} = 12.52$, $p < 0.0001$). No significant interaction ($F_{3, 246} = 1.317$, $p = 0.2693$) and effect of room were found ($F_{1, 246} = 3.532$, $p = 0.0614$). Post-hoc comparisons showed that significant differences not observed on any days (Day 1: $p = 0.9991$; Day 2: $p = 0.0582$; Day 3: $p = 0.9917$; Day 4: $p = 0.6802$). B. Average latency across trials per training day. A significant learning effect ($F_{3, 246} = 26.12$, $p < 0.0001$) and room condition ($F_{1, 246} = 20.42$, $p < 0.0001$) effect were observed. No significant interaction ($F_{3, 246} = 1.587$, $p = 0.1932$) was found. Post-hoc comparisons showed that significant differences between room conditions were only

observed on days 1 and 2 (Day 1: $p = 0.0011$; Day 2: $p = 0.0236$; Day 3: $p = 0.8653$; Day 4: $p = 0.3247$). C. Average path length during new learning. A significant learning effect ($F_{15, 96} = 7.926$, $p < 0.0001$) and room effect ($F_{1, 96} = 20.66$, $p < 0.0001$) were observed. No significant interaction ($F_{15, 96} = 0.7356$, $p = 0.7429$) was observed. Post-hoc comparisons showed that significant differences were only observed between room conditions in trials 1 and 2 (Trial 1: $p = 0.0332$; Trial 2: $p = 0.0455$; Trial 3: $p > 0.9999$; Trial 4: $p = 0.9813$; Trial 5: $p = 0.7005$; Trial 6: $p > 0.9999$; Trial 7: $p > 0.9999$; Trial 8: $p = 0.9989$; Trial 9: $p > 0.9999$; Trial 10: $p > 0.9999$; Trial 11: $p > 0.9999$; Trial 12: $p = 0.9936$; Trial 13: $p = 0.9780$; Trial 14: $p = 0.9962$; Trial 15: $p > 0.9999$; Trial 16: $p = 0.9996$). D. Average latency during new learning. A significant learning effect ($F_{15, 96} = 9.632$, $p < 0.0001$), and room effect ($F_{1, 96} = 4.036$, $p = 0.0474$) were observed. No significant interaction ($F_{15, 96} = 1.199$, $p = 0.2857$) was found. Post-hoc comparisons showed that significant differences were only observed between room conditions in trial 2 (Trial 1: $p = 0.0909$; Trial 2: $p = 0.0452$; Trial 3: $p > 0.9999$; Trial 4: $p > 0.9999$; Trial 5: $p = 0.9748$; Trial 6: $p > 0.9999$; Trial 7: $p > 0.9999$; Trial 8: $p = 0.9999$; Trial 9: $p = 0.9858$; Trial 10: > 0.9999; Trial 11: $p > 0.9999$; Trial 12: $p > 0.9999$; Trial 13: $p > 0.9999$; Trial 14: $p > 0.9999$; Trial 15: $p > 0.9999$; Trial 16: $p > 0.9999$).

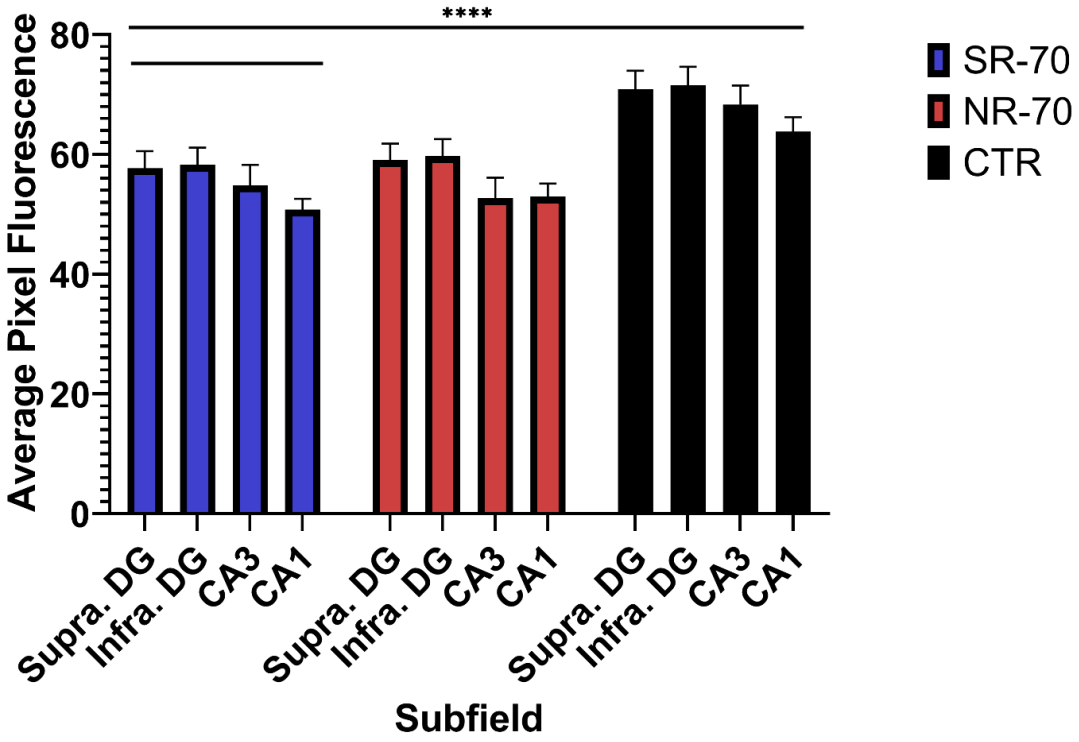

Figure 2.6: Within group comparison of NMDAR expression across hippocampal subfields in new learning. A significant effect of subfield was observed ($F_{3, 36} = 4.333$, $p = 0.0105$), as well as a significant effect of room condition ($F_{2, 36} = 27.06$, $p < 0.0001$). No significant interaction was found ($F_{6, 36} = 0.1692$, $p = 0.9834$). Significant differences between subfields were not observed in post hoc analyses in any conditions. ROUT tests (Q = 1%) identified no outliers.

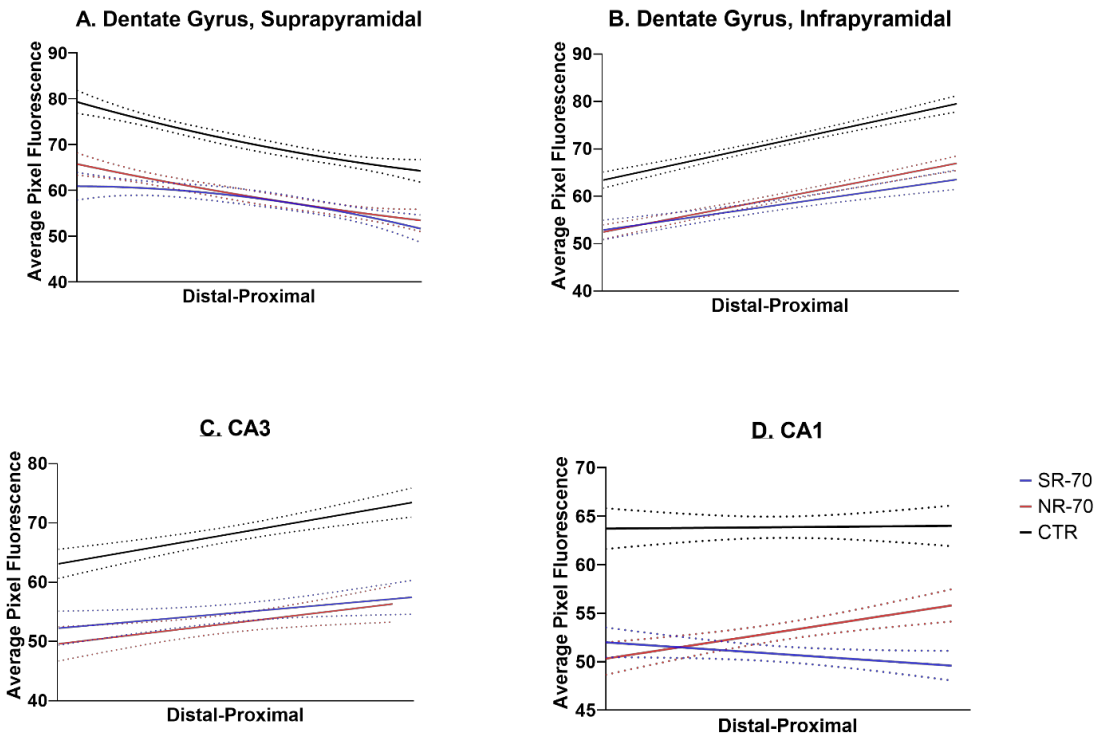

Figure 2.7: NMDAR expression 70 minutes post new-learning in either same-room or new-room conditions across the transverse axis of HPC subfields. A. In the suprapyramidal blade, a concave trend was observed in same-room animals (R square = 0.2640, $Y = 60.92 - 0.02124X – 0.024569X^2$), while a convex trend was observed in new-room (R square = 0.4740, $Y = 65.76 - 0.8335X + 0.009814X^2$) and cage controls (R square = 0.5635, $Y = 79.31 – 1.113X + 0.01697X^2$). B. In the infrapyramidal blade, significant positive expression patterns were observed in all 3 groups (same room: R square = 0.3153, , $F_{1, 78} = 35.92$, $p < 0.0001$; new room: R square = 0.6077, $F_{1, 78} = 120.8$, $p < 0.0001$; cage CTR: R square = 0.6105, , $F_{1, 78} = 122.3$, $p < 0.0001$). C. In CA3, significant positive expression patterns were observed in all 3 groups (same room: R square = 0.05510, , $F_{1, 77} = 4.490$, $p = 0.0373$; new room: R square = 0.08936, $F_{1, 70} = 6.869$, $p = 0.0108$; cage CTR: R square = 0.2384 , $F_{1, 77} = 24.11$, $p < 0.0001$). D. In CA1,

a significant positive trend was found in the new room condition (R square = 0.1633, $F_{1, 76} = 14.83$, $p = 0.0002$). Insignificant trends were observed in the same-room and cage CTR groups (same room: R square = 0.04264, $F_{1, 76} = 3.385$, $p = 0.0697$; cage CTR: R square = 0.0003395, $F_{1, 76} = 0.02581$, $p = 0.8728$).

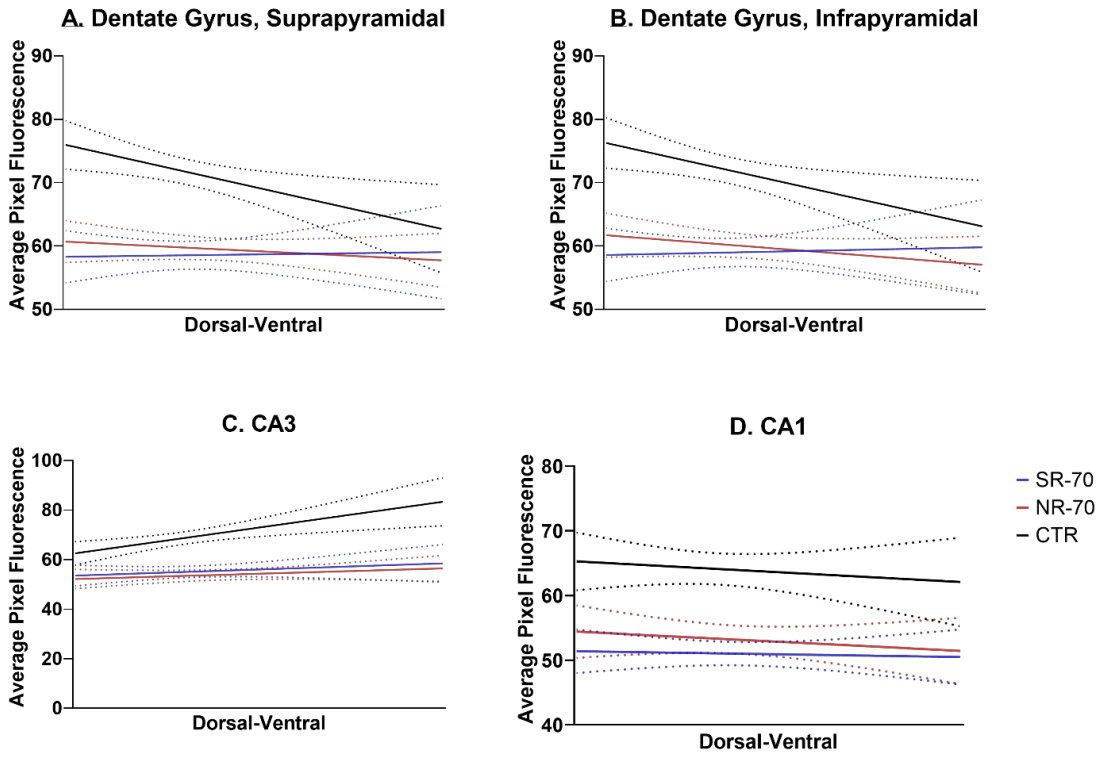

Figure 2.8: NMDAR expression 70 minutes post new-learning in either same-room or new-room conditions across the long axis of HPC subfields. A. In the suprapyramidal blade, significant trends were only observed in the cage CTR group (cage CTR: R square = 0.07816, $F_{1, 83}$ = 7038, p = 0.0096). Insignificant trends were observed in both experimental groups (same room: R square = 0.0002359, $F_{1, 82}$ = 0.01935, p = 0.8897; new room: R square = 0.007335, $F_{1, 103}$ = 0.7610, p = 0.3850). B. In the infrapyramidal blade, no significant trends were observed in experimental conditions (same room: R square = 0.0006205, $F_{1, 82}$ = 0.05091, p = 0.8220; new room: R square = 0.01639, $F_{1, 103}$ = 1.716, p = 0.1931). A significant negative pattern of NMDAR expression was observed from dorsal to ventral (R square = 0.07158, $F_{1, 83}$ = 6.399, p = 0.0133). C. In CA3, no significant trends were observed in experimental conditions (same room: R square = 0.01520, $F_{1, 55}$ = 0.8487, p = 0.3609; new room: R square = 0.01627, $F_{1, 68}$ = 1.124, p =

0.2927). A significant positive trend was observed in cage CTRs (R square = 0.1583, $F_{1, 52} = 9.781$, p = 0.0029). D. In CA1, no significant patterns were observed in NMDAR expression along the long axis (same room: R square = 0.0009873, $F_{1, 72} = 0.07116$, p = 0.7904; new room: R square = 0.007468, $F_{1, 72} = 0.5418$, p = 0.4641; cage CTR: R square = 0.00304, $F_{1, 62} = 0.3933$, p = 0.5329).

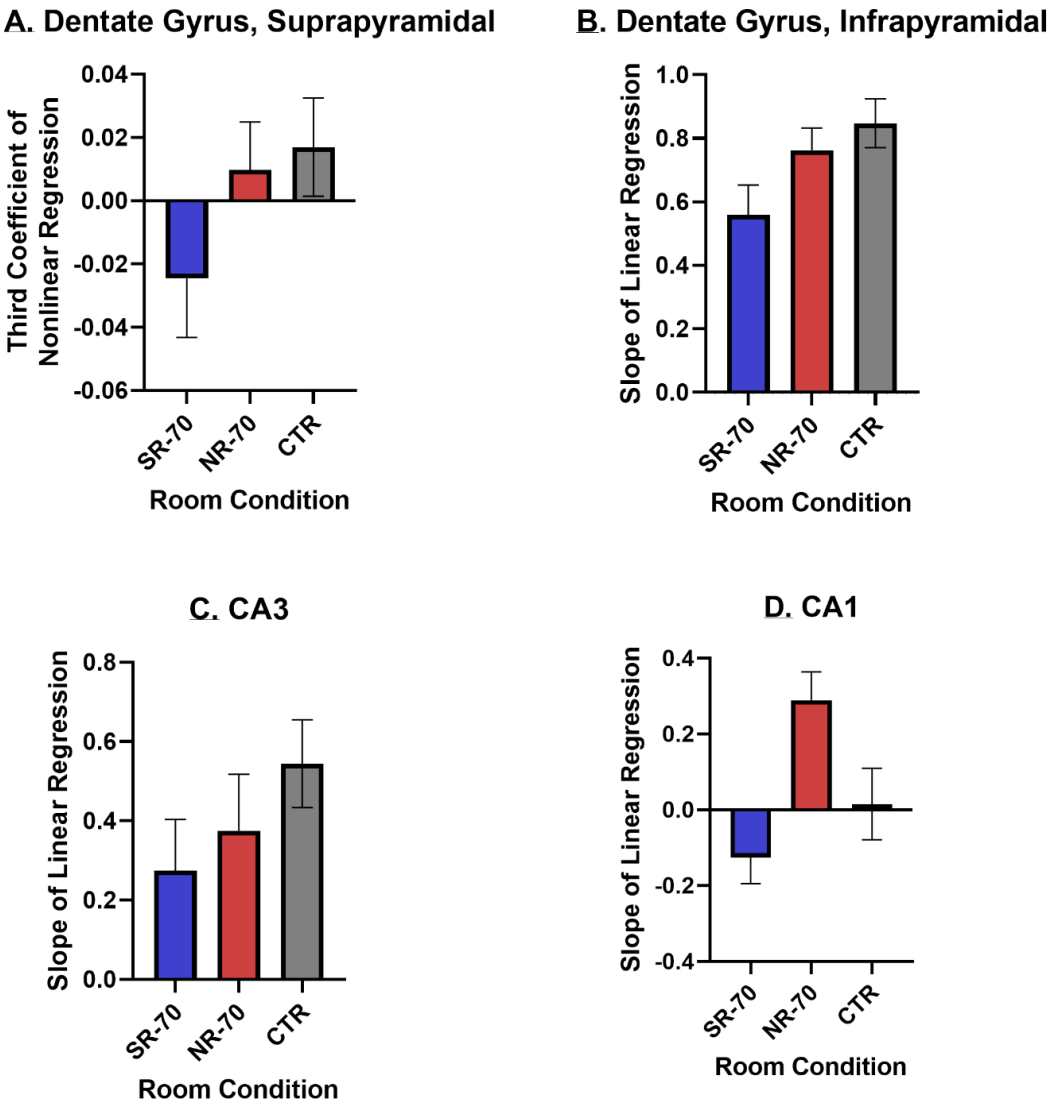

Figure 2.9: Trend analysis of NMDAR expression between room conditions along the transverse axis. A. In the suprapyramidal blade, no significant differences were observed between non-linear regressions of NMDAR expression between any groups. B. In the infrapyramidal blade, the only significant differences were observed between the same room and control groups (SR-70 vs. CTR: mean difference = -0.2877, p = 0.0323). C. In CA3, no significant differences were observed between any groups. D. Significant differences were observed in the trends of CA1 NMDAR expression along the transverse

axis between the new room group and all other groups (SR-70 vs. NR-70: mean difference = -0.4152, p = 0.0009; NR-70 vs. CTR: mean difference = -0.2735, p = 0.0435.

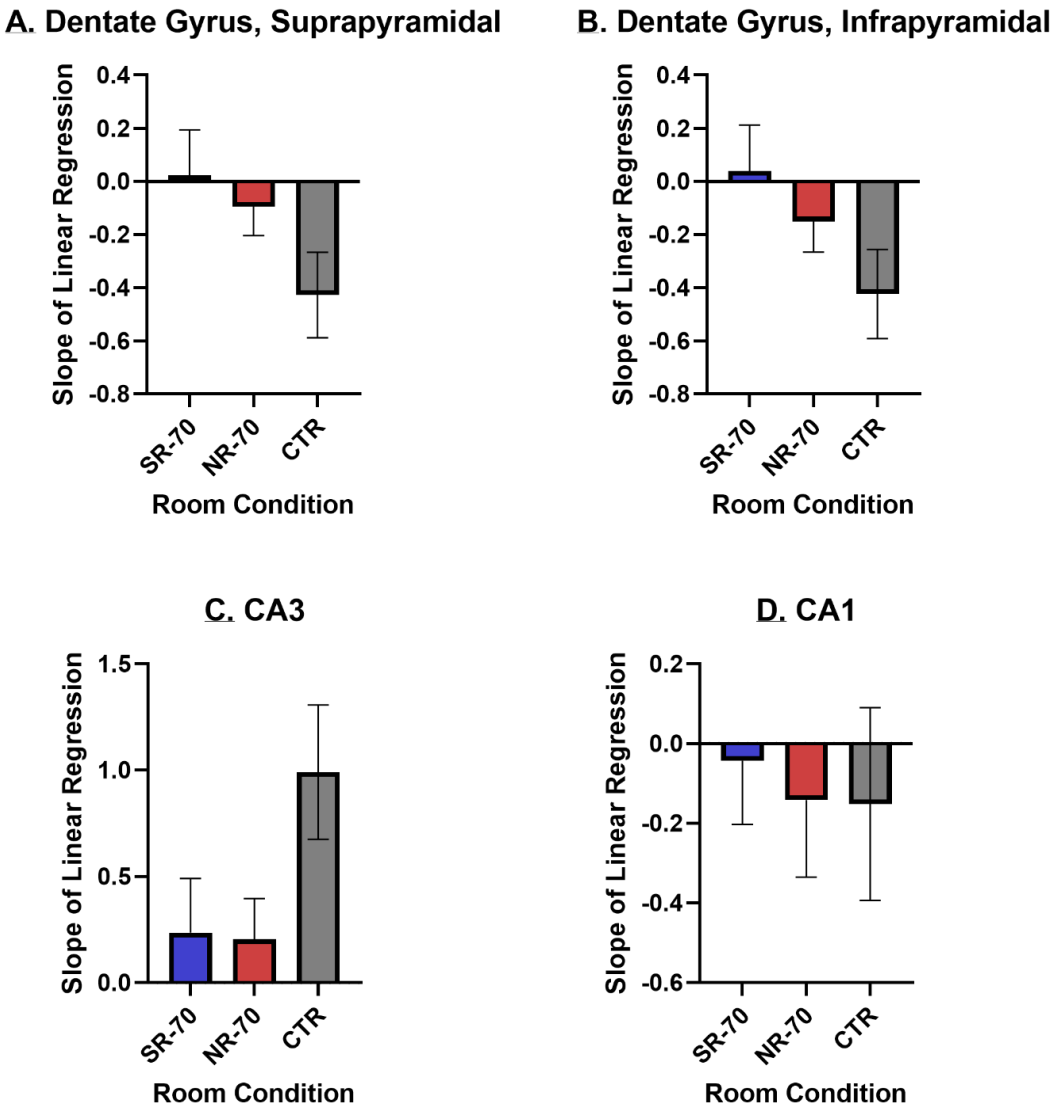

Figure 2.10: Trend analysis of NMDAR expression between room conditions along the long axis. A. In the suprapyramidal blade, no significant differences were observed between any of the groups. B. In the infrapyramidal blade, no significant differences were observed between any of the groups. C. In CA3, no significant differences were observed between any groups. D. In CA1, no significant differences were observed between any of the groups.

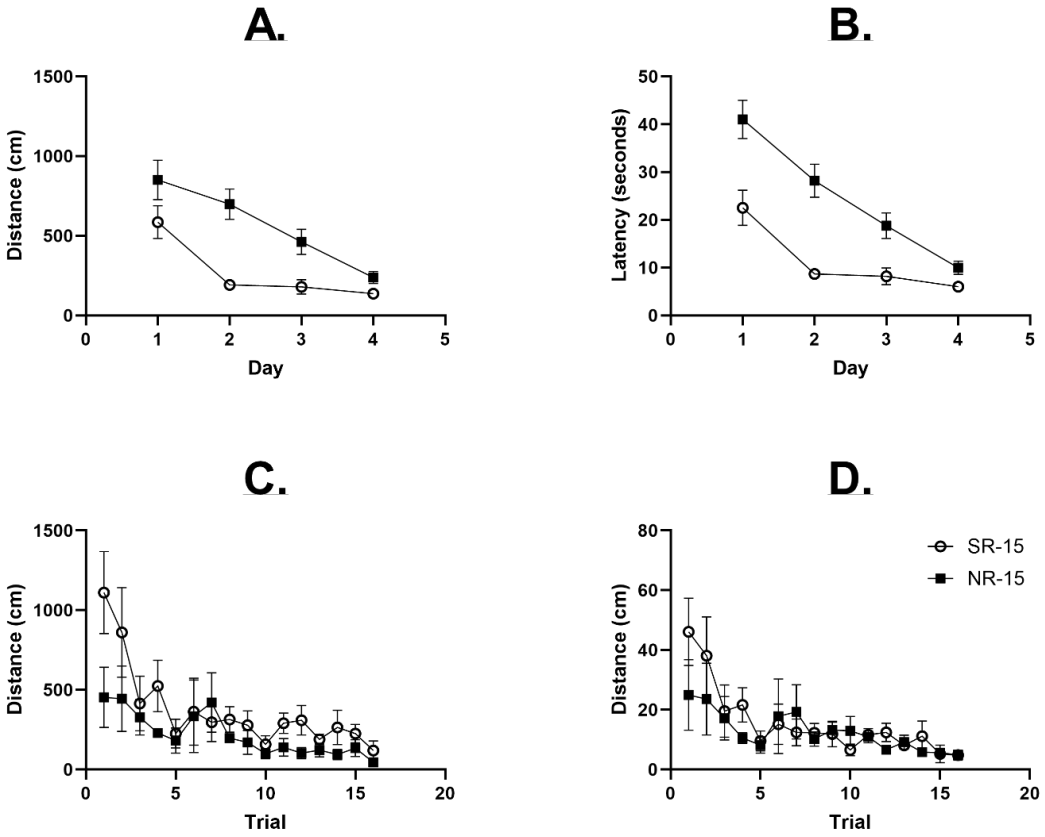

Figure 2.11: Mean path length and latency during pre-training over days and over new learning over trials in same room and new room conditions of animals sacrificed 15 minutes after new learning (pCaMKII). A. Average path length across trials per training day. A significant learning effect ($F_{3, 248} = 17.91$, $p < 0.0001$) and room condition effect ($F_{1, 248} = 29.18$, $p < 0.0001$) were observed. No significant interaction ($F_{3, 248} = 2.431$, $p = 0.0658$) was found. Post-hoc comparisons showed that significant differences were only observed on days 2 and 3 between groups (Day 1: $p = 0.0535$; Day 2: $p < 0.0001$; Day 3: $p = 0.0344$; Day 4: $p = 0.8193$). B. Average latency across trials per training day. A significant learning effect was observed ($F_{3, 248} = 30.09$, $p < 0.0001$). A significant interaction ($F_{3, 248} = 3.867$, $p = 0.0099$) and effect of room were also found ($F_{1, 248} = 50.23$, $p < 0.0001$). Post-hoc comparisons showed that significant differences between

room conditions were observed on days 1, 2, and 3 (Day 1: $p < 0.0001$; Day 2: $p < 0.0001$; Day 3: $p = 0.0186$; Day 4: $p = 0.7370$). C. Average path length during new learning. A significant learning effect ($F_{15, 96} = 4.371$, $p < 0.0001$) and room effect ($F_{1, 96} = 11.50$, $p = 0.0010$) were observed. No significant interaction was observed ($F_{15, 96} = 0.9960$, $p = 0.4658$) were observed. Post-hoc comparisons showed that significant differences were only observed between room conditions in trial 1 (Trial 1: $p = 0.0069$; Trial 2: $p = 0.3115$; Trial 3: $p > 0.9999$; Trial 4: $p = 0.8318$; Trial 5: $p > 0.9999$; Trial 6: $p > 0.9999$; Trial 7: $p > 0.9999$; Trial 8: $p > 0.9999$; Trial 9: $p > 0.9999$; Trial 10: $p = 0.318 > 0.99991$; Trial 11: $p = 0.9997$; Trial 12: $p = 0.9911$; Trial 13: $p > 0.9999$; Trial 14: $p = 0.9990$; Trial 15: $p > 0.9999$; Trial 16: $p > 0.9999$). D. Average latency during new learning. A significant learning effect ($F_{15, 96} = 3.810$, $p < 0.0001$) was observed. No significant room effect ($F_{1, 96} = 1.725$, $p = 0.1922$) or interaction ($F_{15, 96} = 3.199$, $p = 0.7544$) was observed. Post-hoc comparisons showed no significant differences between room conditions in any of the trials (Trial 1: $p = 0.2406$; Trial 2: $p = 0.8048$; Trial 3: $p > 0.9999$; Trial 4: $p = 0.9760$; Trial 5: $p > 0.9999$; Trial 6: > 0.9999; Trial 7: $p = 0.9999$; Trial 8: $p > 0.9999$; Trial 9: $p > 0.9999$; Trial 10: > 0.9999; Trial 11: $p > 0.9999$; Trial 12: $p > 0.9999$; Trial 13: $p > 0.9999$; Trial 14: $p > 0.9999$; Trial 15: $p > 0.9999$; Trial 16: $p > 0.9999$).

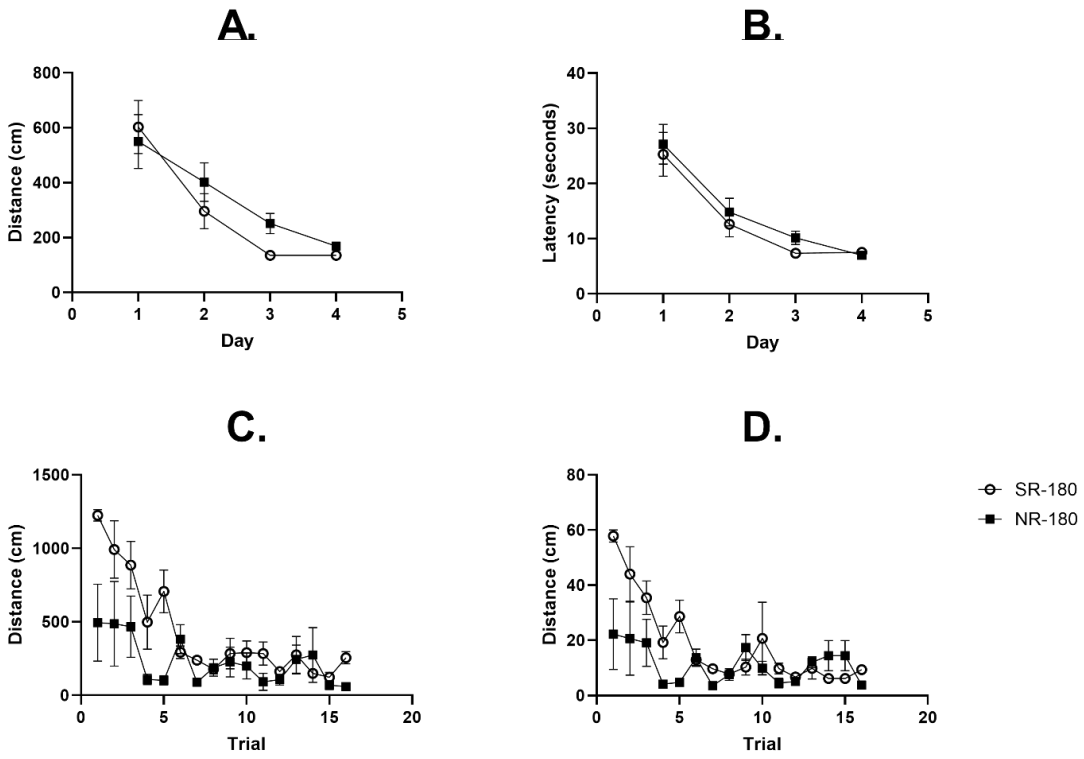

Figure 2.12: Mean path length and latency during pre-training over days and over new learning over trials in same room and new room conditions of animals sacrificed 180 minutes after new learning (pCREB). A. Average path length across trials per training day. A significant learning effect ($F_{3, 248} = 19.86$, $p < 0.0001$) was observed. No significant effect of room condition ($F_{1, 248} = 1.386$, $p = 0.2401$) or interaction ($F_{3, 248} = 0.8202$, $p = 0.4838$) was found. Post-hoc comparisons showed no significant differences on any days between groups (Day 1: $p = 0.9559$; Day 2: $p = 0.6288$; Day 3: $p = 0.5487$; Day 4: $p = 0.9914$). B. Average latency across trials per training day. A significant learning effect was observed ($F_{3, 248} = 27.86$, $p < 0.0001$). No significant interaction ($F_{3, 248} = 0.1990$, $p = 0.8970$) or effect of room were found ($F_{1, 248} = 0.9239$, $p = 0.3374$). Post-hoc comparisons showed no significant differences between room conditions on any days (Day 1: $p = 0.9680$; Day 2: $p = 0.9373$; Day 3: $p = 0.8663$; Day 4: $p = 0.9997$). C.

Average path length during new learning. A significant learning effect ($F_{15, 96} = 7.632$, $p < 0.0001$), room effect ($F_{1, 96} = 23.67$, $p < 0.0001$), and interaction were observed ($F_{15, 96} = 2.299$, $p = 0.0078$) were observed. Post-hoc comparisons showed that significant differences were only observed between room conditions in trials 1, 2, and 5 (Trial 1: $p = 0.0005$; Trial 2: $p = 0.0498$; Trial 3: $p = 0.2000$; Trial 4: $p = 0.2923$; Trial 5: $p = 0.0074$; Trial 6: $p > 0.9999$; Trial 7: $p = 0.9994$; Trial 8: $p > 0.9999$; Trial 9: $p > 0.9999$; Trial 10 $p > 0.9999$; Trial 11: $p = 0.9905$; Trial 12: $p > 0.9999$; Trial 13: $p > 0.9999$; Trial 14: $p > 0.9999$; Trial 15: $p > 0.9999$; Trial 16: $p = 0.9884$). D. Average latency during new learning. A significant learning effect ($F_{15, 96} = 6.721$, $p < 0.0001$), room effect ($F_{1, 96} = 14.53$, $p = 0.0002$), and interaction ($F_{15, 96} = 2.729$, $p = 0.0016$) were observed. Post-hoc comparisons showed that significant differences were only observed between room conditions in trials 1, 2, and 5 (Trial 1: $p = 0.0002$; Trial 2: $p = 0.0476$; Trial 3: $p = 0.4446$; Trial 4: $p = 0.5752$; Trial 5: $p = 0.0399$; Trial 6: > 0.9999; Trial 7: $p = 0.9999$; Trial 8: $p > 0.9999$; Trial 9: $p = 0.9992$; Trial 10: = 0.9434; Trial 11: $p > 0.9999$; Trial 12: $p > 0.9999$; Trial 13: $p > 0.9999$; Trial 14: $p = 0.9955$; Trial 15: $p = 0.9999$; Trial 16: $p > 0.9999$).

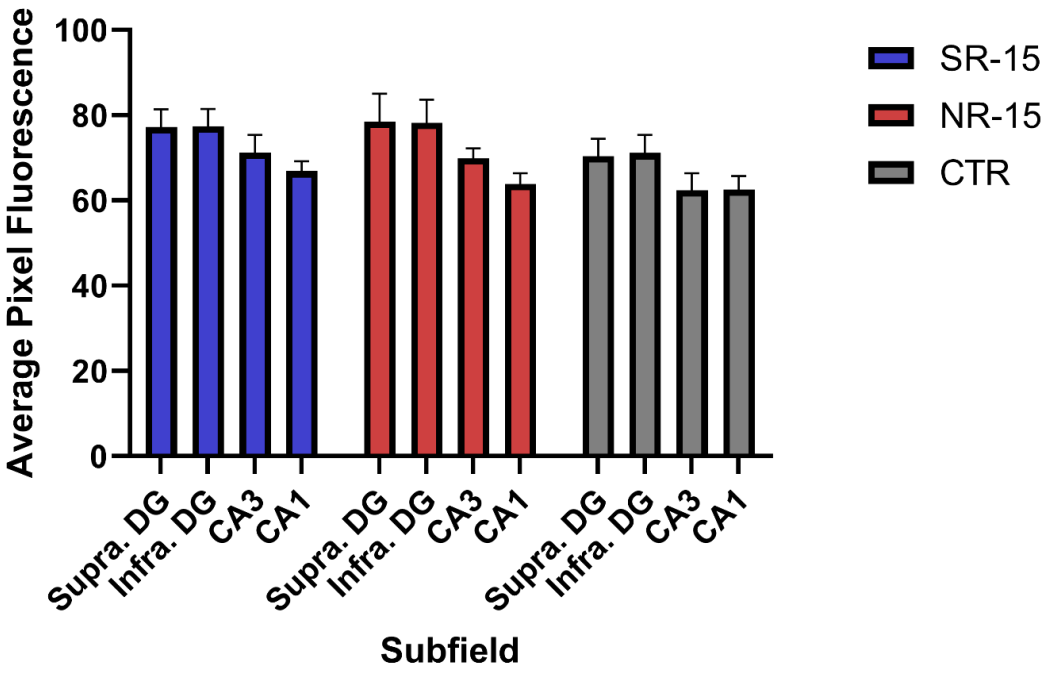

Figure 2.13: Within group comparison of pCaMKII expression across hippocampal subfields in new learning. A significant effect of subfield was observed ($F_{3, 36} = 5.451$, $p = 0.0034$), but no significant effect of room condition ($F_{2, 36} = 3.103$, $p = 0.0571$), and no significant interaction ($F_{6, 36} = 0.1696$, $p = 0.9833$). Significant differences between subfields were not observed in post hoc analyses in any conditions. ROUT tests (Q = 1%) identified no outliers.

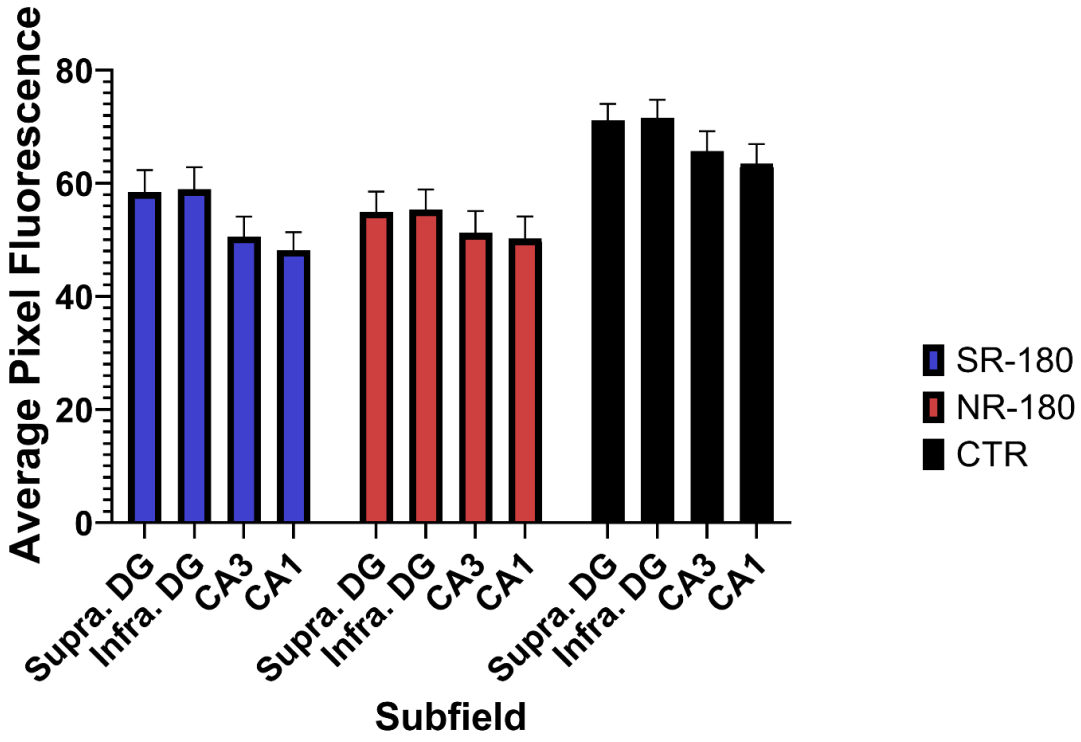

Figure 2.14: Within group comparison of pCREB expression across hippocampal subfields in new learning. A significant effect of subfield ($F_{3, 36} = 3.844$, $p = 0.0174$) and room condition ($F_{2, 36} = 22.27$, $p < 0.0001$) were observed. No significant interaction ($F_{6, 36} = 0.1669$, $p = 0.9840$) was shown. Significant differences between subfields were not observed in post hoc analyses in any conditions. ROUT tests (Q = 1%) identified no outliers.

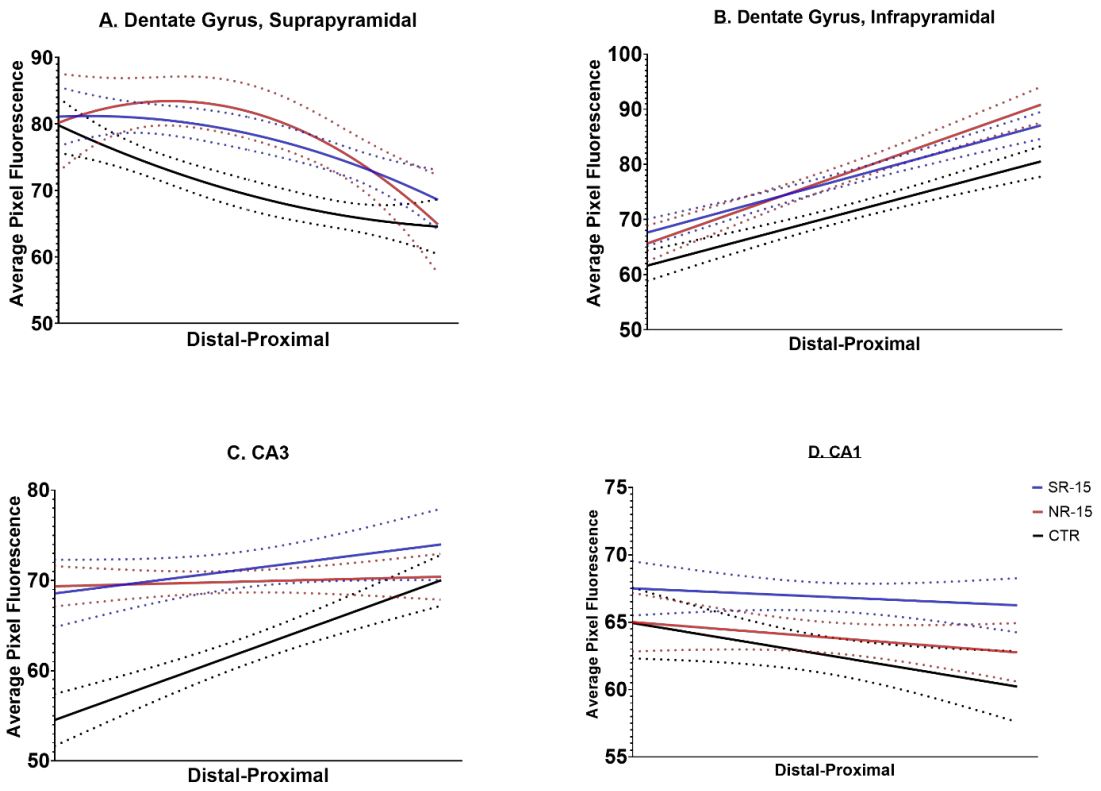

Figure 2.15: pCaMKII expression 15 minutes post new-learning in either same-room or new-room conditions across the transverse axis of HPC subfields. A. In the suprapyramidal blade, a concave trend was observed in both experimental groups (same room: R square = 0.2333, $Y = 2.242 - 0.5469X - 0.02779X^2$; new room: R square = 0.1776, $Y = 3.712 - 0.9055X + 0.04601X^2$). A convex trend was observed in cage controls (R square = 0.3328, $Y = 2.073 - 0.5058X + 0.02570X^2$). B. In the infrapyramidal blade, significant positive expression patterns were observed in all 3 groups (same room: R square = 0.5227, , $F_{1, 78} = 85.44$, $p < 0.0001$; new room: R square = 0.5126, $F_{1, 78} = 82.05$, $p < 0.0001$; cage CTR: R square = 0.4479, $F_{1, 78} = 63.27$, $p < 0.0001$). C. In CA3, insignificant patterns of pCaMKII expression were observed in experimental conditions

(same room: R square = 0.03828, , $F_{1, 68} = 2.707$, $p = 0.1045$; new room: R square = 0.004109, $F_{1, 63} = 0.2599$, $p = 0.6120$). In cage controls, a significant positive trend was observed (cage CTR: R square = 0.3767, $F_{1, 68} = 41.10$, $p < 0.0001$). D. In CA1, insignificant trends were observed in experimental conditions (same room: R square = 0.006822, $F_{1, 77} = 0.5289$, $p = 0.4693$; new room: R square = 0.01887, $F_{1, 76} = 1.462$, $p = 0.2304$). A significant negative trend was observed in cage controls (cage CTR: R square = 0.05391, $F_{1, 77} = 0.0395$, $p = 0.0395$).

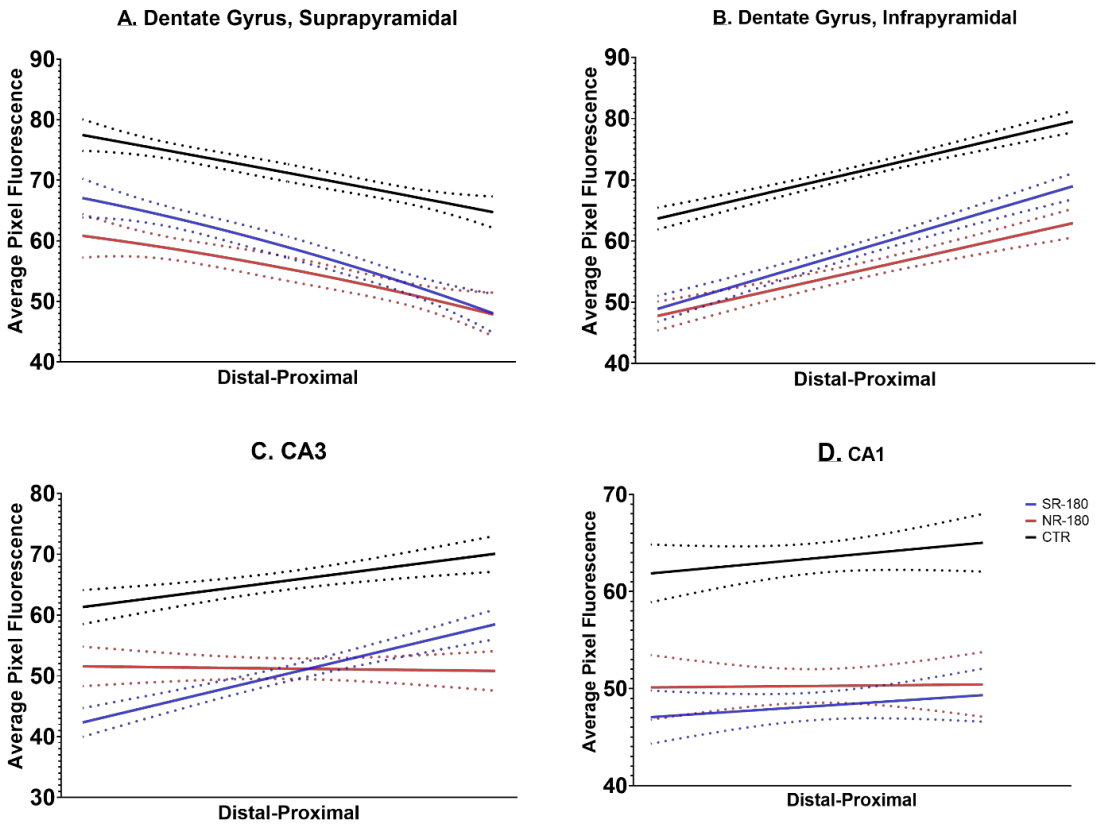

Figure 2.16: pCREB expression 180 minutes post new-learning in either same-room or new-room conditions across the transverse axis of HPC subfields. A. In the suprapyramidal blade, all groups showed a concave trend (same room: R square = 0.5545, $Y = 67.77 - 0.6793X - 0.01539X^2$; new room: R square = 0.3152, $Y = 61.28 - 0.4437X - 0.01143X^2$; cage CTR: R square = 0.4573, $Y = 78.12 - 0.6444X - 0.001266X^2$). B. In the infrapyramidal blade, significant positive expression patterns were observed in all 3 groups (same room: R square = 0.6067, $F_{1, 78} = 120.3$, $p < 0.0001$; new room: R square = 0.4192, $F_{1, 78} = 56.29$, $p < 0.0001$; cage CTR: R square = 0.5808, $F_{1, 78} = 108.1$, $p < 0.0001$). C. In CA3, insignificant patterns of expression were observed in the new room condition (new room: R square = 0.0009170, $F_{1, 78} = 0.07159$, $p = 0.7897$). A significant positive trend was observed in same room and cage controls groups (same room: R square

= 0.4728, $F_{1, 69}$ = 61.88, p < 0.0001; cage CTR: R square = 0.1492, $F_{1, 72}$ = 12.63, p = 0.0007). D. In CA1, insignificant trends were observed in all conditions (same room: R square = 0.01182, $F_{1, 78}$ = 0.9326, p = 0.3372; new room: R square = 0.0001450, $F_{1, 78}$ = 0.01131, p = 0.9156; cage CTR: R square = 0.01925, $F_{1, 78}$ = 1.531, p = 0.2197).

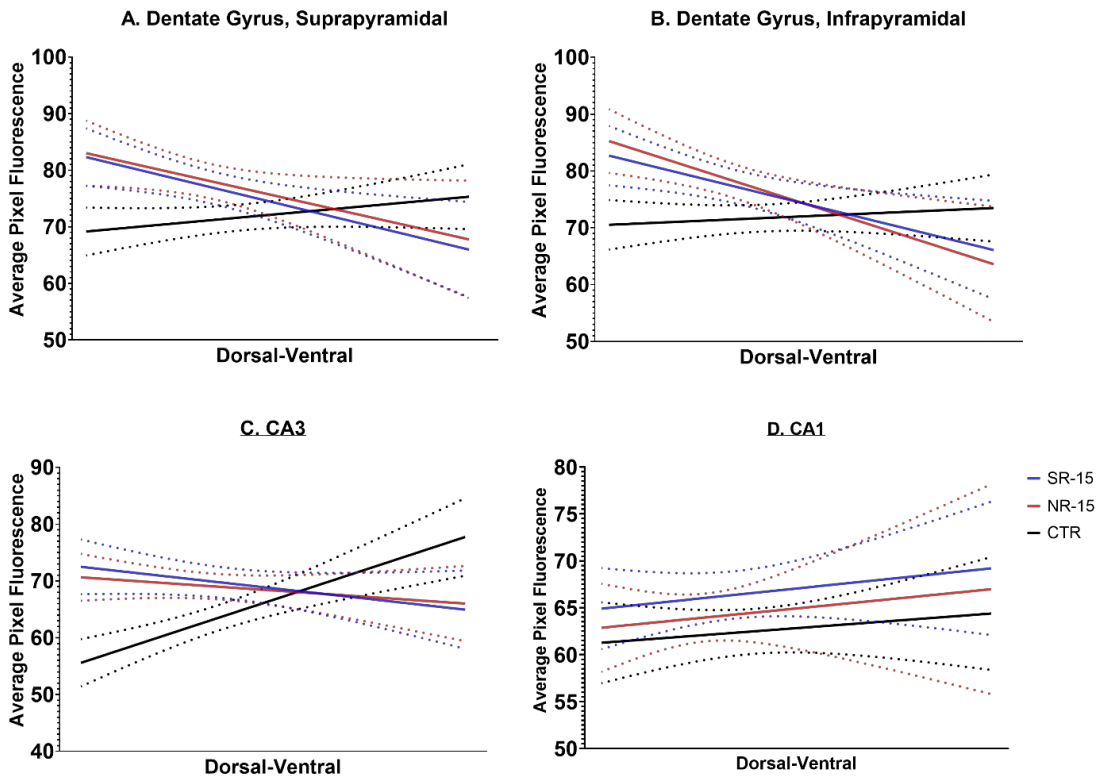

Figure 2.17: pCaMKII expression 15 minutes post new-learning in either same-room or new-room conditions across the long axis of HPC subfields. A. In the suprapyramidal blade, significant negative trends were observed in experimental groups (same room: R square = 0.09113, $F_{1, 72} = 7.219$, p = 0.0090; new room: R square = 0.05531, $F_{1, 72} = 4.216$, p = 0.0437). Insignificant patterns of expression were observed in cage control groups (cage CTR: R square = 0.02192, $F_{1, 86} = 1.928$, p = 0.1686) B. In the infrapyramidal blade, significant negative expression patterns were observed in both experimental groups (same room: R square = 0.08939, $F_{1, 72} = 7.067$, p = 0.0097; new room: R square = 0.1107, $F_{1, 72} = 8.962$, p = 0.0038). In cage controls, an insignificant effect was observed (cage CTR: R square = 0.004840, $F_{1, 86} = 0.4183$, p = 0.5195). C. In CA3, insignificant patterns of expression were observed in both experimental conditions (same room: R square = 0.03743, $F_{1, 55} = 2.139$, p = 0.1493; new room: R square =

0.01733, $F_{1, 52} = 0.9172$, $p = 0.3426$). A significant positive trend was observed in the cage controls group (R square = 0.2775, $F_{1, 52} = 19.97$, $p < 0.0001$). D. In CA1, insignificant trends were observed in all conditions (same room: R square = 0.01223, $F_{1, 58} = 0.7183$, $p = 0.4002$; new room: R square = 0.006155, $F_{1, 50} = 0.3096$, $p = 0.5804$; cage CTR: R square = 0.006615, $F_{1, 70} = 0.4661$, $p = 0.4970$).

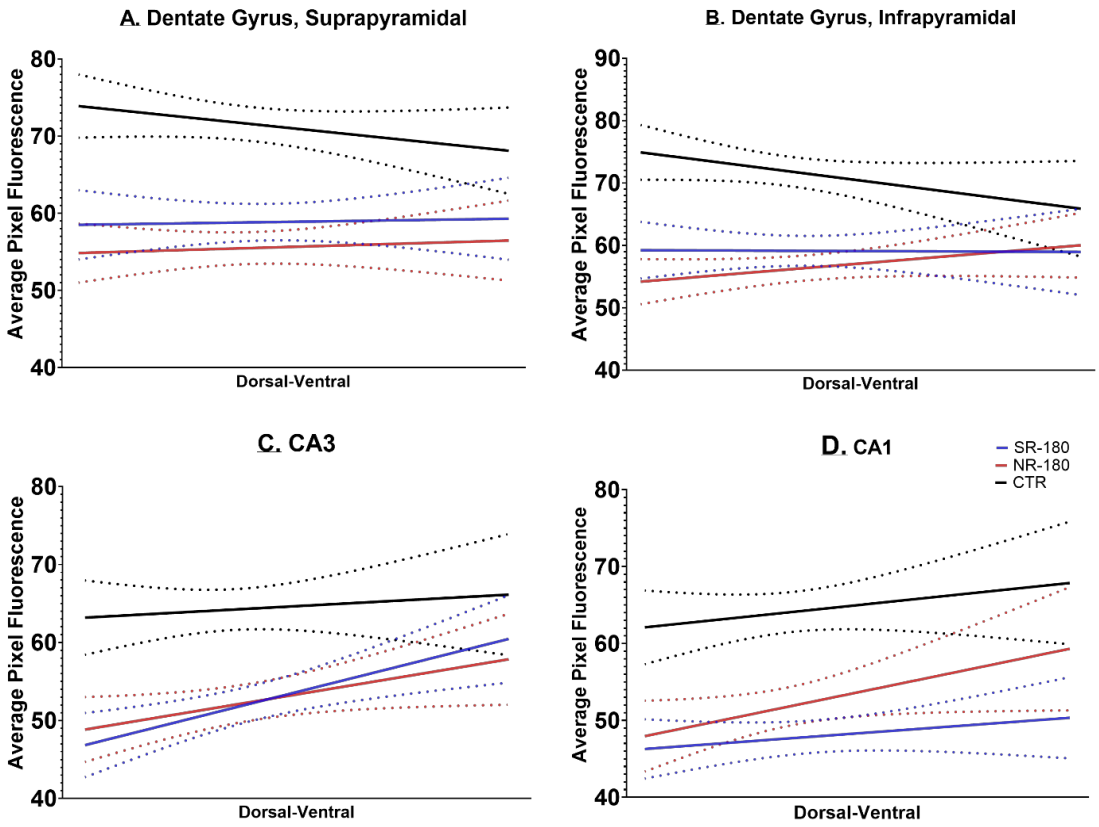

Figure 2.18: pCREB expression 180 minutes post new-learning in either same-room or new-room conditions across the long axis of HPC subfields. A. In the suprapyramidal blade, insignificant trends were observed in all groups (same room: R square = 0.0003526, $F_{1, 93}$ = 0.03280, p = 0.8567; new room: R square = 0.001981, $F_{1, 82}$ = 0.1628, p = 0.6877; cage CTR: R square = 0.02108, $F_{1, 83}$ = 1.788, p = 0.1849). B. In the infrapyramidal blade, insignificant trends were observed in all groups (same room: R square = 3.140e-005, $F_{1, 93}$ = 0.002920, p = 0.9570; new room: R square = 0.02410, $F_{1, 90}$ = 2.223, p = 0.1395; cage CTR: R square = 0.03117, $F_{1, 83}$ = 2.670, p = 0.1060). C. In CA3, significant positive patterns of expression were observed in both experimental conditions (same room: R square = 0.1416, $F_{1, 61}$ = 10.06, p = 0.0024; new room: R square = 0.073333, $F_{1, 54}$ = 4.273, p = 0.0435). Insignificant trends were observed in the

cage control group (R square = 0.005017, $F_{1, 54} = 0.2723$, p = 0.6040). D. In CA1, insignificant trends were observed in all conditions (same room: R square = 0.01352, $F_{1, 73} = 1.000$, p = 0.3206; new room: R square = 0.05940, $F_{1, 62} = 3.915$, p = 0.0523; cage CTR: R square = 0.01530, $F_{1, 64} = 0.9942$, p = 0.3225).

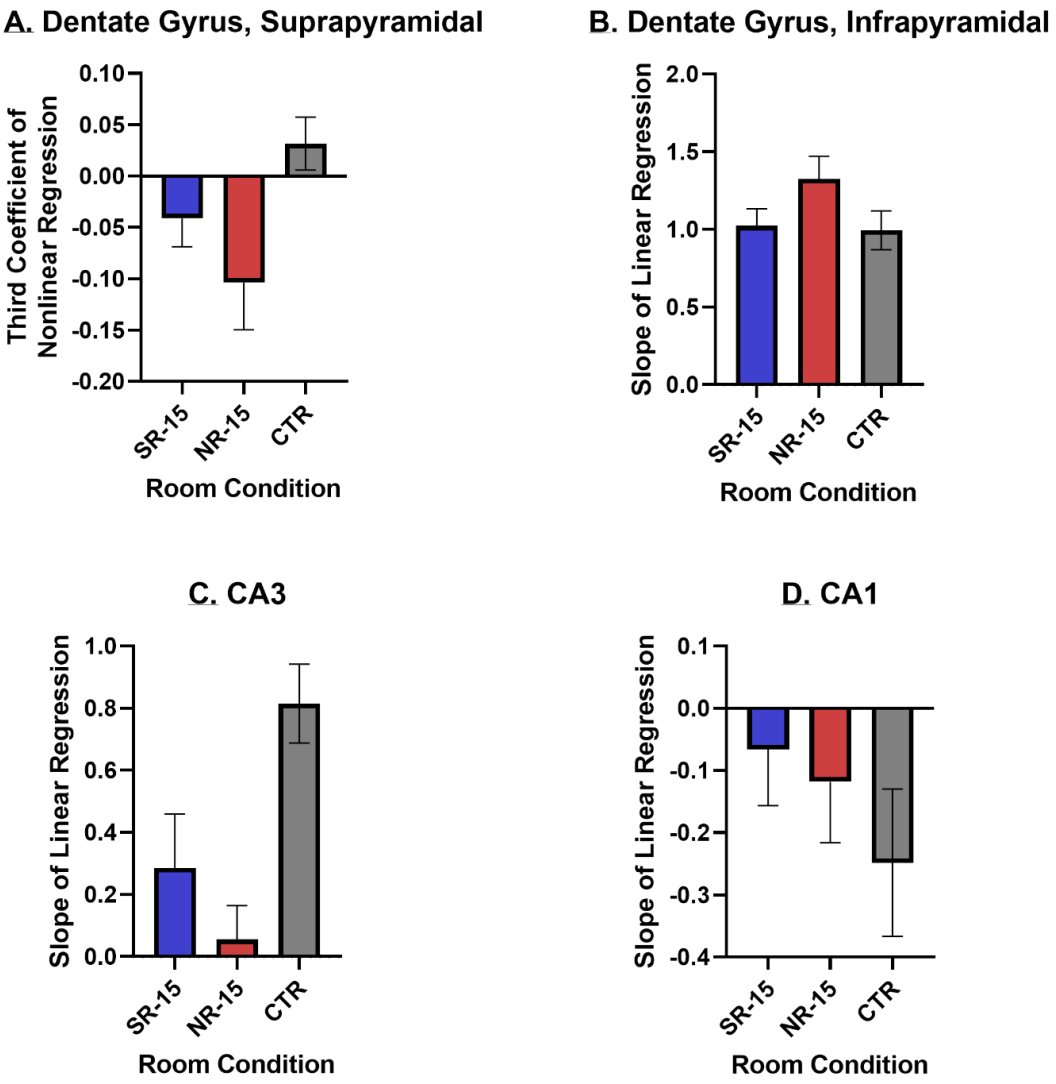

Figure 2.19: Trend analysis of pCaMKII expression between room conditions along the transverse axis. A. The only significant differences observed in pCaMKII expression patterns was between new room and control groups (NR-15 vs. CTR: mean difference = -0.1352, p = 0.0162). B. In the infrapyramidal blade, no significant differences were observed between any of the groups. C. In CA3, significant differences were observed the control group and the two experimental groups (SR-15 vs. CTR: mean difference = -0.5294, p = 0.0208; NR-15 vs. CTR: mean difference = -0.7595, p = 0.0006). D. No

significant differences were observed in pCaMKII expression trends along the transverse axis between any of the groups.

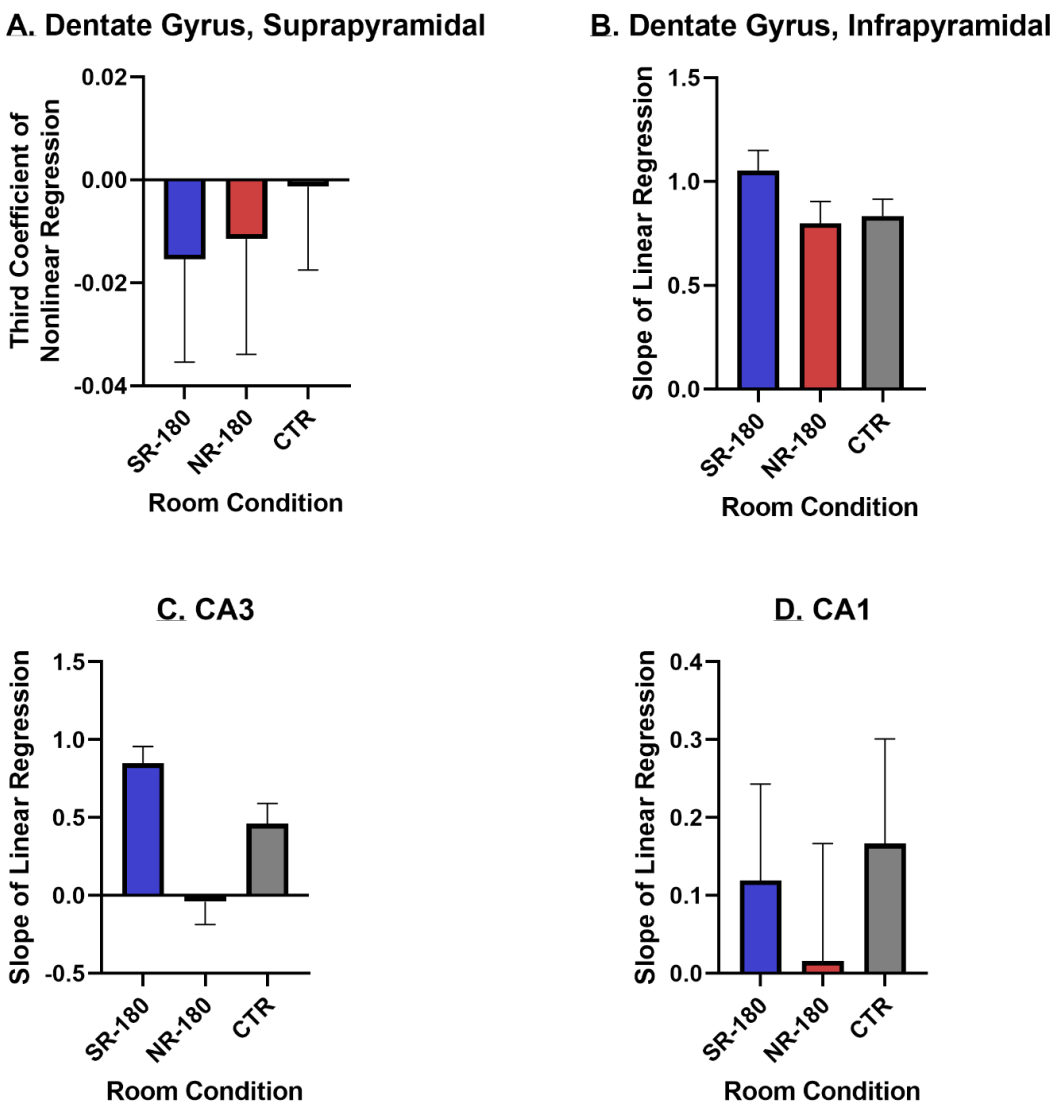

Figure 2.20: Trend analysis of pCREB expression between room conditions along the transverse axis. A. In the suprapyramidal blade, no significant differences were observed between any of the groups. B. In the infrapyramidal blade, no significant differences were observed between any of the groups. C. In CA3, significant differences were observed between the new room group and both other groups (SR-180 vs. CTR: mean difference = 0.8890, $p < 0.0001$; NR-180 vs. CTR: mean difference = -0.5007, $p = 0.0184$). D. No

significant differences were observed in pCREB expression trends along the transverse axis between any of the groups.

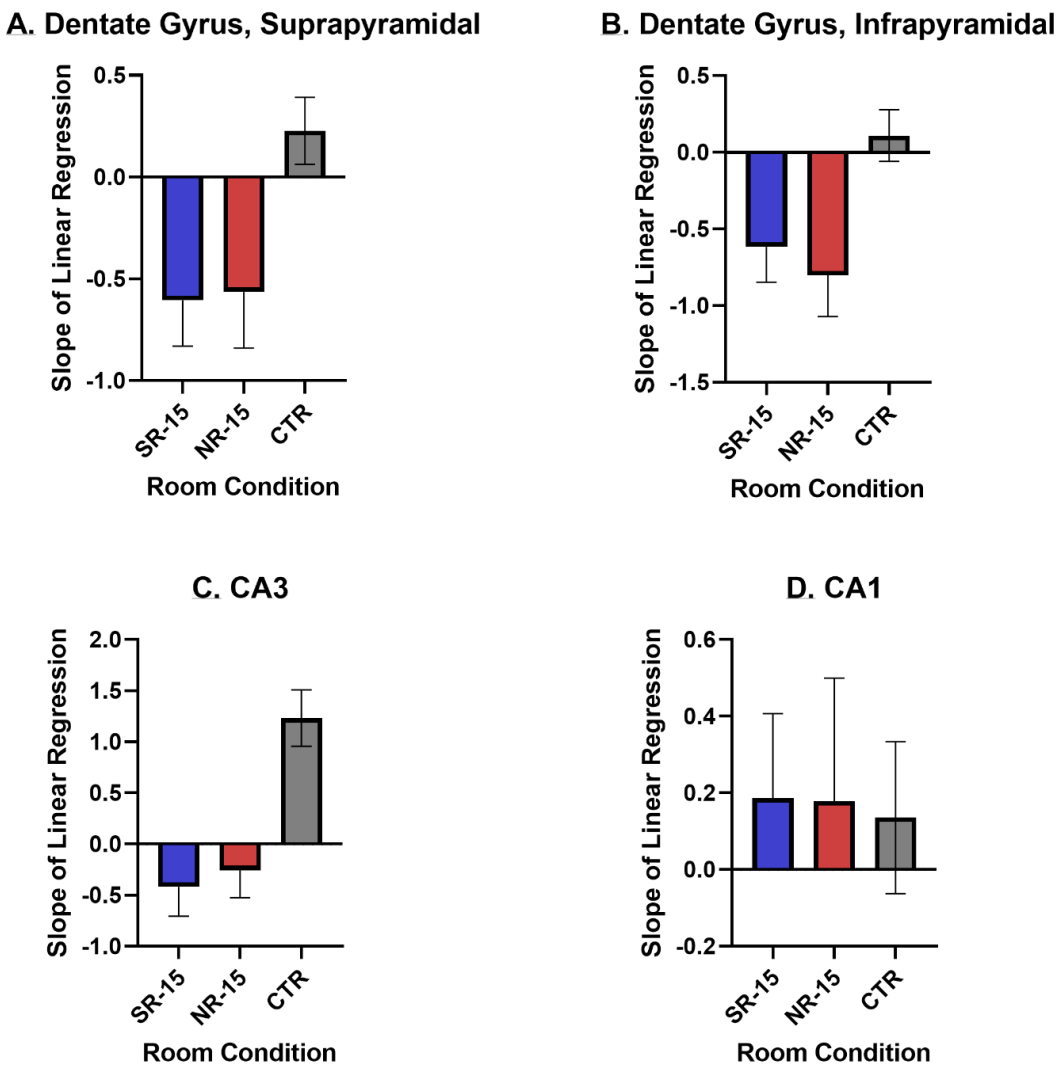

Figure 2.21: Trend analysis of pCaMKII expression between room conditions along the long axis. A. In the suprapyramidal blade, significant differences were observed between the control group and both experimental groups (SR-15 vs. CTR: mean difference = -0.8334, p = 0.0200; NR-15 vs. CTR: mean difference = -0.7924, p = 0.0288). B. In the infrapyramidal blade, significant differences were only observed between the new room and control groups (NR-15 vs. CTR: mean difference = -0.9117, p = 0.0098). C. In CA3, significant differences were observed between the control group and both experimental

groups (SR-15 vs. CTR: mean difference = -1.651, p = 0.0001; NR-15 vs. CTR: mean difference = -1.489, p = 0.0006). D. No significant differences were observed in pCaMKII expression trends along the long axis between any of the groups.

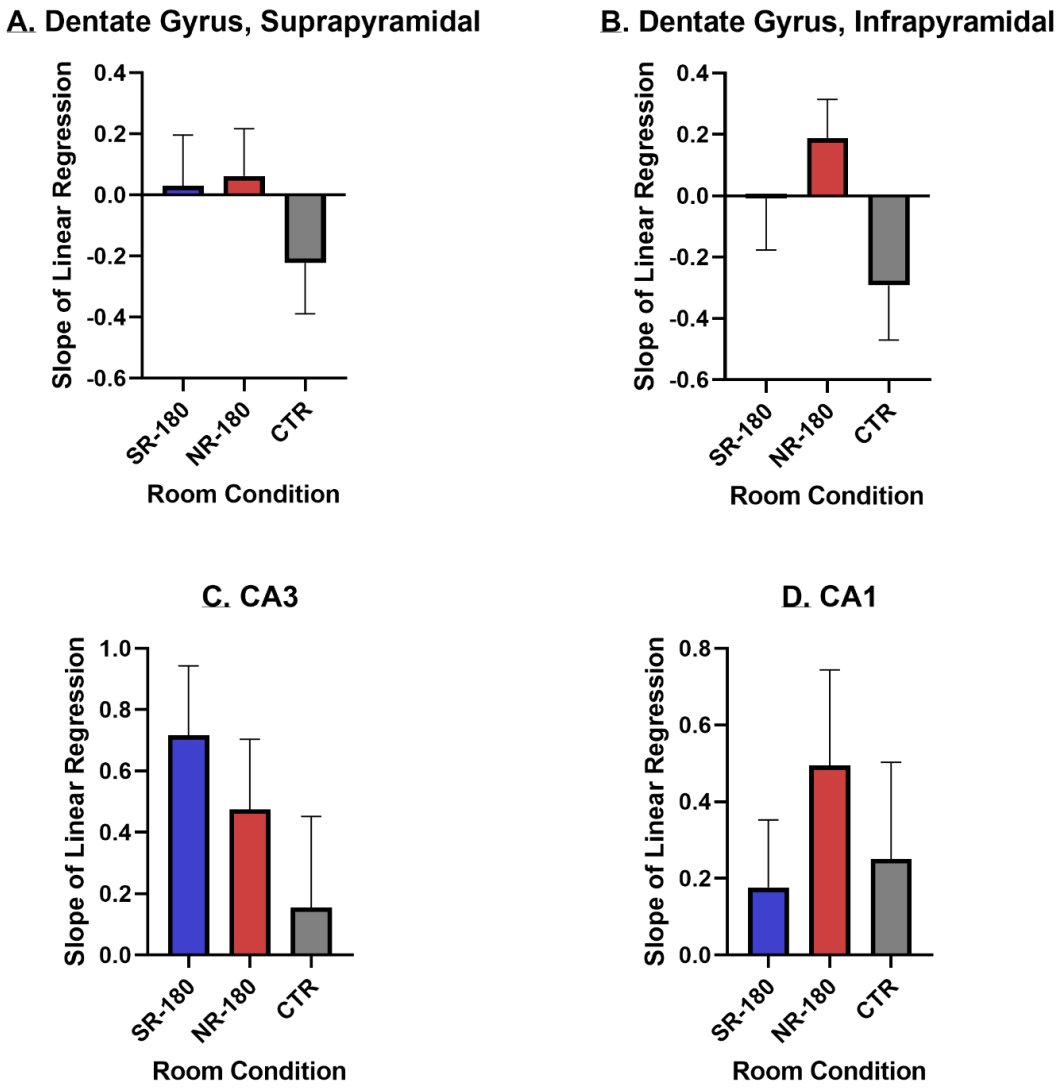

Figure 2.22: Trend analysis of pCREB expression between room conditions along the long axis. A. In the suprapyramidal blade, no significant differences were observed between any groups. B. In the infrapyramidal blade, no significant differences were observed between any of the groups. C. In CA3, no significant differences were observed between any of the groups. D. No significant differences were observed in pCREB expression trends along the long axis between any of the groups.

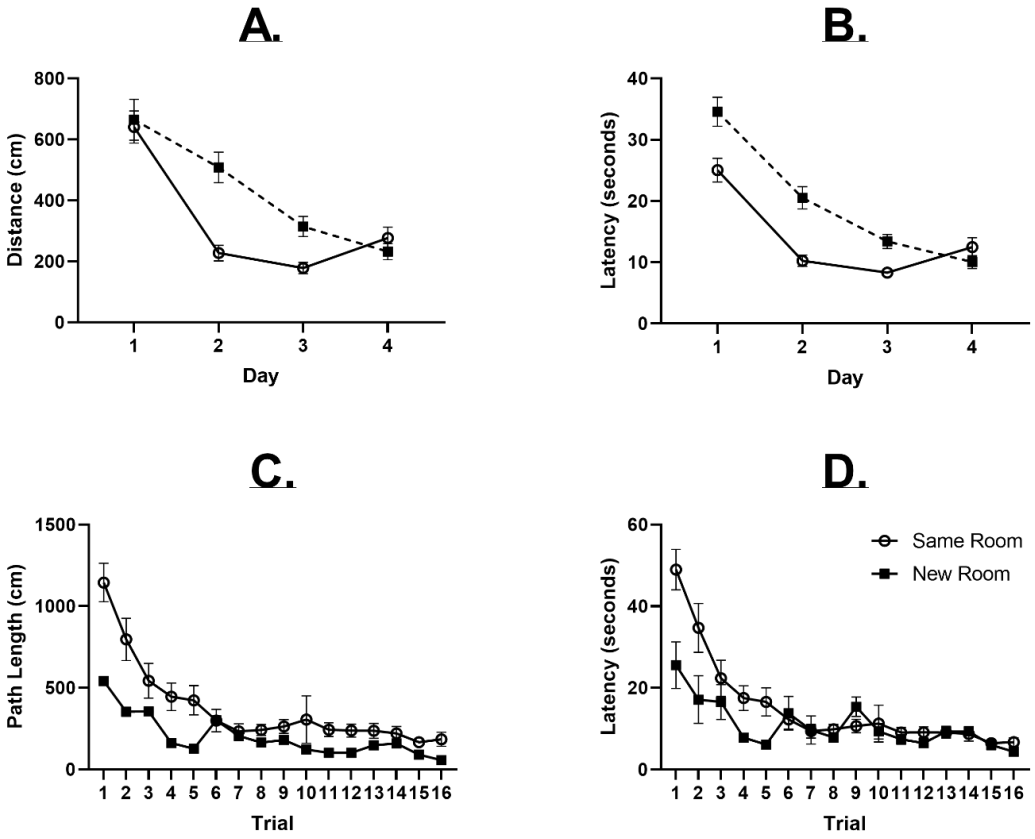

Figure 2.23: Mean path length and latency during pre-training over days and over new learning over trials in same room and new room conditions of animals sacrificed 70 and 80 minutes after new learning (GluA2:GluA1). A. Average path length across trials per training day. A significant learning effect was observed ($F_{3, 820} = 43.08$, $p < 0.0001$). A significant interaction ($F_{3, 820} = 6.057$, $p = 0.0004$) and effect of room were also found ($F_{1, 820} = 11.73$, $p = 0.0006$). Post-hoc comparisons showed that significant differences were only observed on day 2 between groups (Day 1: $p > 0.9999$; Day 2: $p < 0.0001$; Day 3: $p = 0.0748$; Day 4: $p > 0.9999$). B. Average latency across trials per training day. A significant learning effect was observed ($F_{3, 820} = 68.69$, $p < 0.0001$). A significant interaction ($F_{3, 820} = 7.383$, $p < 0.0001$) and effect of room were also found ($F_{1, 820} =$

27.34, $p < 0.0001$). Post-hoc comparisons showed that significant differences between room conditions were only observed on days 1 and 2 (Day 1: $p < 0.0001$; Day 2: $p < 0.0001$; Day 3: $p = 0.0727$; Day 4: $p > 0.9999$). C. Average path length during new learning. A significant learning effect ($F_{1, 352} = 23.42$, $p < 0.0001$), room effect ($F_{15, 352} = 80.79$, $p < 0.0001$), and interaction ($F_{15, 352} = 4.217$, $p < 0.0001$) were observed. Post-hoc comparisons showed that significant differences were only observed between room conditions in trials 1, 2, 4, and 5 (Trial 1: $p < 0.0001$; Trial 2: $p < 0.0001$; Trial 3: $p = 0.2713$; Trial 4: $p = 0.0054$; Trial 5: $p = 0.0028$; Trial 6: $p > 0.9999$; Trial 7: $p > 0.9999$; Trial 8: $p > 0.9999$; Trial 9: $p > 0.9999$; Trial 10: $p = 0.3181$; Trial 11: $p > 0.9999$; Trial 12: $p > 0.9999$; Trial 13: $p > 0.9999$; Trial 14: $p > 0.9999$; Trial 15: $p > 0.9999$; Trial 16: $p > 0.9999$). D. Average latency during new learning. A significant learning effect ($F_{1, 352} = 15.71$, $p < 0.0001$), room effect ($F_{15, 352} = 18.03$, $p < 0.0001$), and interaction ($F_{15, 352} = 3.199$, $p < 0.0001$) were observed. Post-hoc comparisons showed that significant differences were only observed between room conditions in trials 1 and 2 (Trial 1: $p < 0.0001$; Trial 2: $p = 0.0005$; Trial 3: $p > 0.9999$; Trial 4: $p = 0.3236$; Trial 5: $p = 0.1945$; Trial 6: $p > 0.9999$; Trial 7: $p > 0.9999$; Trial 8: $p > 0.9999$; Trial 9: $p > 0.9999$; Trial 10: > 0.9999; Trial 11: $p > 0.9999$; Trial 12: $p > 0.9999$; Trial 13: $p > 0.9999$; Trial 14: $p > 0.9999$; Trial 15: $p > 0.9999$; Trial 16: $p > 0.9999$).

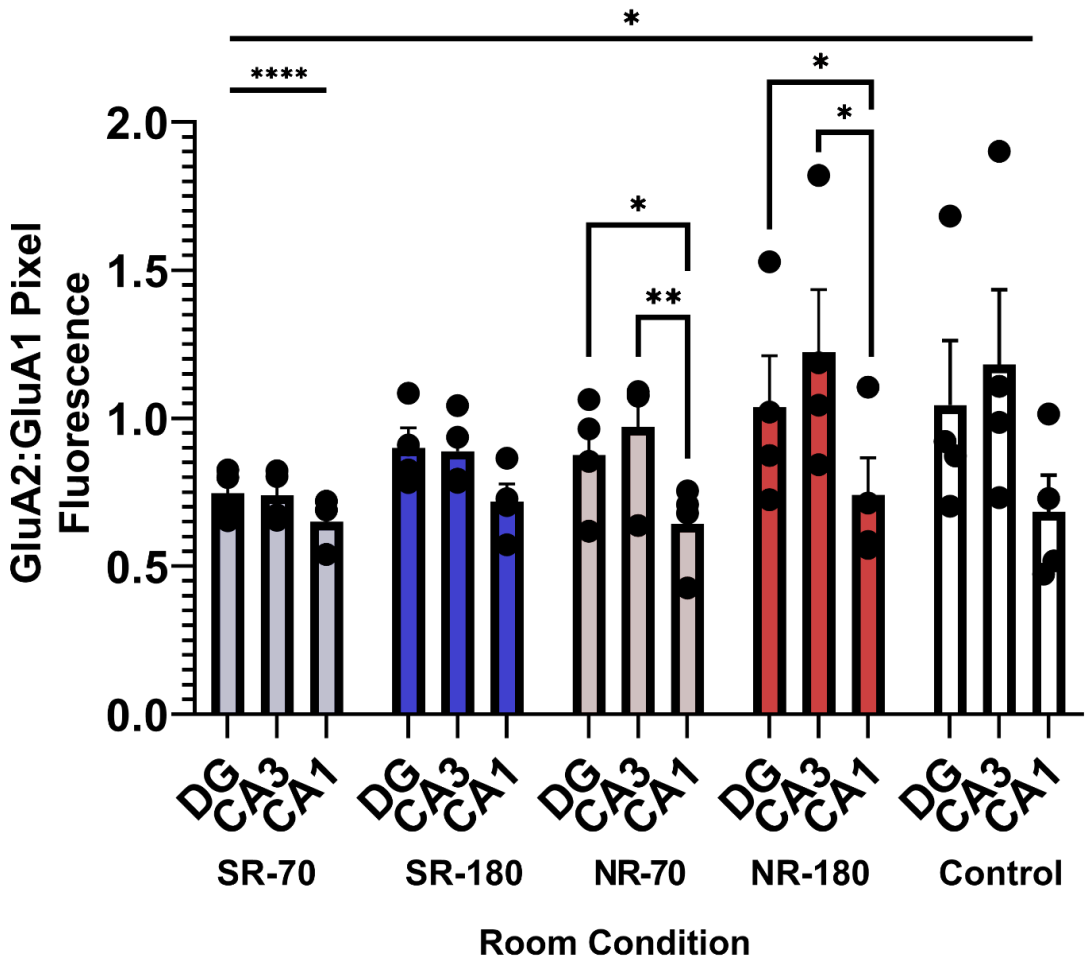

Figure 2.24: Within group comparison of GluA2:GluA1 expression across hippocampal subfield in new learning. A significant effect of subfield was observed ($F_{1.1378,\ 19.98}$ = 52.86, $p < 0.0001$), as well as a significant effect of subfield by animal group (room condition and sacrifice time) ($F_{8,\ 29}$ = 2.957, p = 0.0151). Significant differences between subfields were observed in post hoc analyses in the new room groups, but not same room animals (NR-70: DG vs. CA1, p = 0.0223, CA3 vs. CA1, p = 0.0089; NR-180: DG vs. CA1, p = 0.0229, CA3 vs. CA1, p = 0.0387). ROUT tests (Q = 1%) identified no outliers.

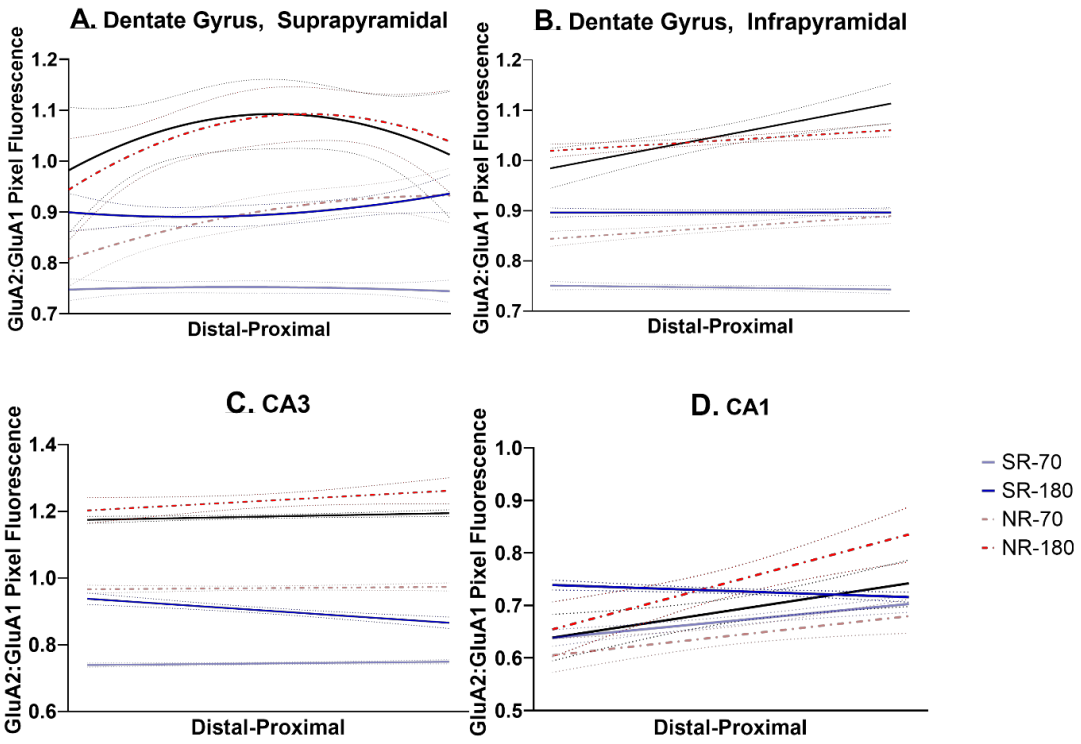

Figure 2.25: GluA2:GluA1 Expression at 180 or 70 minutes post-new learning in either same-room or new-room conditions across the transverse axis of HPC subfields. A. In the suprapyramidal DG, a concave trend from distal to proximal was observed at both time periods in new room animals as well as cage controls (70 minutes: R square = 0.1670, Y = 0.7942 + 0.01374X – 0.0003419X^2; 180 minutes: R square = 0.06406, Y = 0.9174 + 0.02720X – 0.001058X^2; CTR: R square = 0.02546, , Y = 0.9590 + 0.02367X – 0.001050X^2). In same room animals, 70 minute animals demonstrated a very slight concave trend, while 180 minute animals demonstrated a convex trend (70 minutes: R square = 0.004501, , Y = 0.7460 + 0.001370X – 7.312e-005X^2; 180 minutes: R square = 0.04783, , Y = 0.9026 - 0.003634X + 0.0002648X^2). B. In the infrapyramidal DG, a positive trend from distal to proximal was observed at both time periods in new room animals, as well as control animals (70 minutes: R square = 0.4373, $F_{1, 18}$ = 13.99, p =

0.0015; 180 minutes: R square = 0.4498, $F_{1, 18} = 14.72$, $p = 0.0012$; CTR: R square = 0.4702, $F_{1, 18} = 15.97$, $p = 0.0008$). In same room animals, no significant effect was observed at either time point (70 minutes: R square = 0.06732, $F_{1, 18} = 1.299$, $p = 0.2693$; 180 minutes: R square = 3.149e-005, $F_{1, 18} = 0.0005668$, $p = 0.9813$). C. In CA3, no significant trends were observed at either time period in new room animals (70 minutes: R square = 0.5312, $F_{1, 18} = 0.5312$, $p = 0.4755$; 180 minutes: R square = 0.1637, $F_{1, 18} = 3.524$, p = 0768). In same room animals, no significant effect was observed at 70 minutes, but a significant negative relationship was observed at 180 minutes, and a significant positive relationship was observed (70 minutes: R square = 0.1725, $F_{1, 18} = 3.753$, $p = 0.0686$; 180 minutes: R square = 0.5974, $F_{1, 18} = 26.71$, $p < 0.0001$; CTR : R square = 0.2366, $F_{1, 18} = 5.579$, $p = 0.0296$). D. In CA1, significant positive trends were observed from distal to proximal at both time periods in new room animals and controls (70 minutes: R square = 0.3084, $F_{1, 18} = 8.027$, $p = 0.0110$; 180 minutes: R square = 0.5007, $F_{1, 18} = 18.05$, $p = 0.0005$; CTR: R square = 0.3140, $F_{1, 18} = 8.240$, $p = 0.0102$). In same room animals, significant effect was observed at both time points (70 minutes: R square = 0.5825, $F_{1, 18} = 25.12$, $p < 0.0001$; 180 minutes: R square = 0.3301, $F_{1, 18} = 8.868$, $p = 0.0081$).

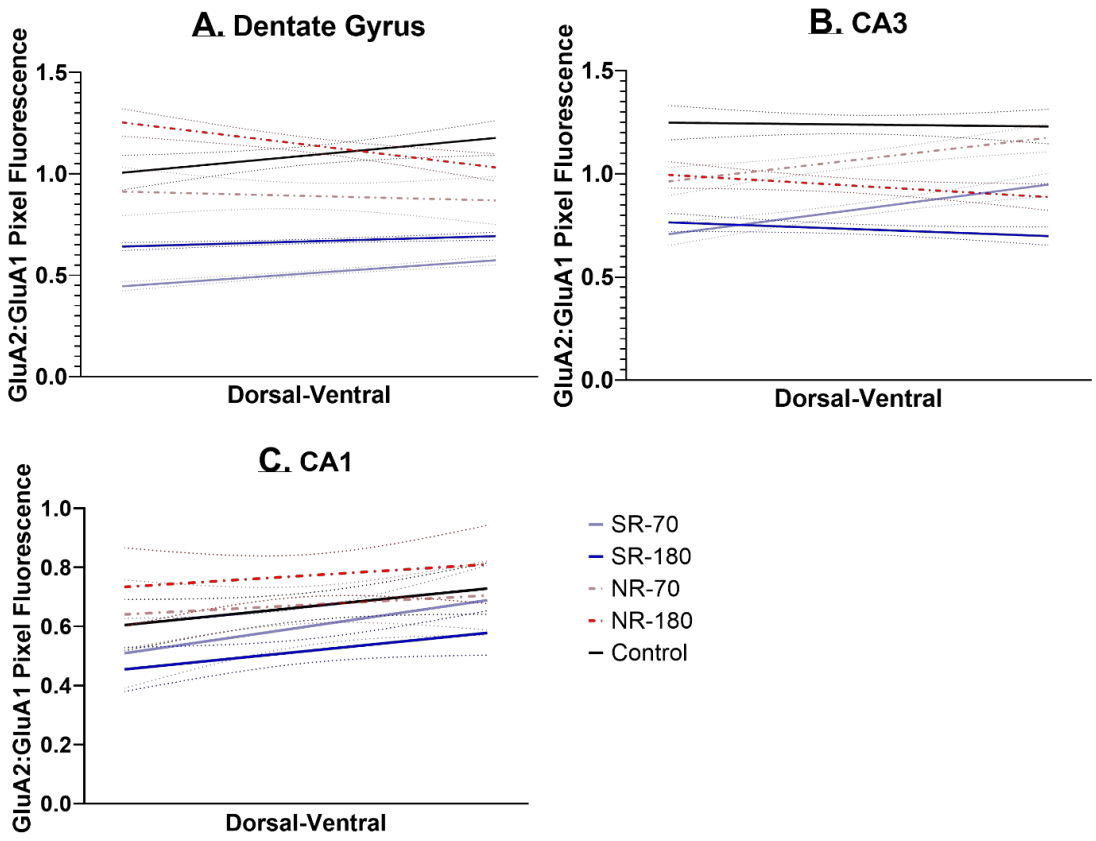

Figure 2.26: GluA2:GluA1 Expression at 180 or 70 minutes post-new learning in same room or new room conditions across the long axis of HPC subfields. A. In the DG, significant negative trends were observed at 180 minutes, but not 70 minutes (70 minutes: R square = 0.0340, $F_{1, 8} = 0.2509$, p = 0.6300; 180 minutes: R square = 0.7165, $F_{1, 8} = 20.22$, p = 0.0020). In same room animals and controls, significant positive effects were observed at both time points from dorsal to ventral (70 minutes: R square = 0.8853, $F_{1, 8} = 61.77$, $p < 0.0001$; 180 minutes: R square = 0.6167, $F_{1, 8} = 12.87$, p = 0.0071; CTR: R square = 0.4869, $F_{1, 8} = 7.592$, p = 0.0249). B. In CA3, a significant positive trend from distal to proximal was observed in new room animals at 70 minutes, but no significant trends were observed at 180 minutes (70 minutes: R square = 0.6926, $F_{1, 8} = 18.03$, p = 0.0028; 180 minutes: R square = 0.3965, $F_{1, 8} = 5.256$, p = 0.0511). In same room

animals, a significant positive effect was observed at 70 minutes, but no significant trends were observed at 180 minutes or in controls (70 minutes: R square = 0.8185, $F_{1, 8} = 36.06$, $p = 0.0003$; 180 minutes: R square = 0.3459, $F_{1, 8} = 4.230$, $p = 0.0737$; CTR: R square = 0.01138, $F_{1, 8} = 0.09209$, $p = 0.7693$). C. In CA1, no significant trends were observed at any time point in any room condition (new room 70 minutes: R square = 0.06583, $F_{1, 8} = 0.5637$, $p = 0.4743$; new room 180 minutes: R square = 0.07164, $F_{1, 8} = 0.6173$, $p = 0.4547$; same room 70 minutes: R squared = 0.3507, $F_{1, 8} = 4.320$, $p = 0.0713$; same room 180 minutes: R squared = 0.3881, $F_{1, 8} = 5.074$, $p = 0.0544$; CTR: R square = 0.3212, $F_{1, 8} = 3.786$, $p = 0.0876$).

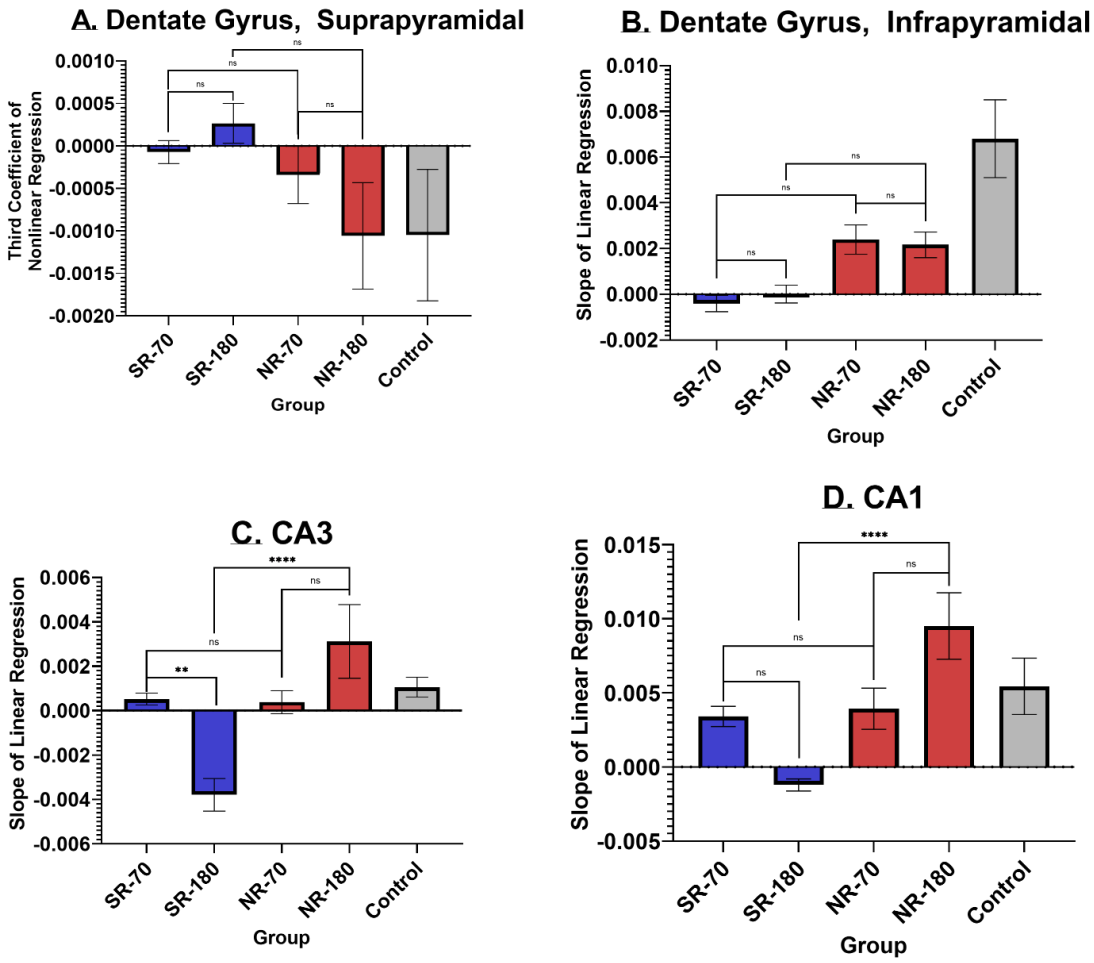

Figure 2.27: Trend analysis of GluA2:GluA1 expression between time points and room conditions along the transverse axis. A. In the suprapyramidal blade, no significant differences were observed between non-linear regressions of GluA2:GluA1 expression. B. In the infrapyramidal blade, the only significant differences were observed in the trends of GluA2:GluA1 expression between the control group and all other groups (SR-70 vs. CTR: mean difference = -0.007206, $p < 0.0001$; SR-180 vs. CTR: mean difference = -0.006791, $p < 0.0001$; NR-70 vs. CTR: mean difference = 0.004406, $p = 0.0059$; NR-180 vs. CTR: mean difference = -0.004641, $p = 0.0032$). C. In CA3, significant differences were observed in the trends of GluA2:GluA1 expression along the transverse axis

between the same room 180 minute group and all other groups (SR-70 vs. SR-180: mean difference = 0.004312, $p = 0.0068$; SR-180 vs. NR-70: mean difference = -0.004171, $p = 0.0096$; SR-180 vs. NR-180: mean difference = -0.006907, $p < 0.0001$; SR-180 vs. CTR: mean difference = -0.004845, $p = 0.0016$). D. Significant differences were observed in the trends of CA1 GluA2:GluA1 expression along the transverse axis between the same room 70 minute group and the new room 180 group, the same room 180 minute group and the new room 180 minute group, and the same room 180 minute group and controls (SR-70 vs. NR-180: mean difference = -0.006107, $p = 0.0379$; SR-180 vs. NR-180: mean difference = -0.01073, $p < 0.0001$; SR-180 vs. CTR: mean difference = -0.006659, $p = 0.0183$).

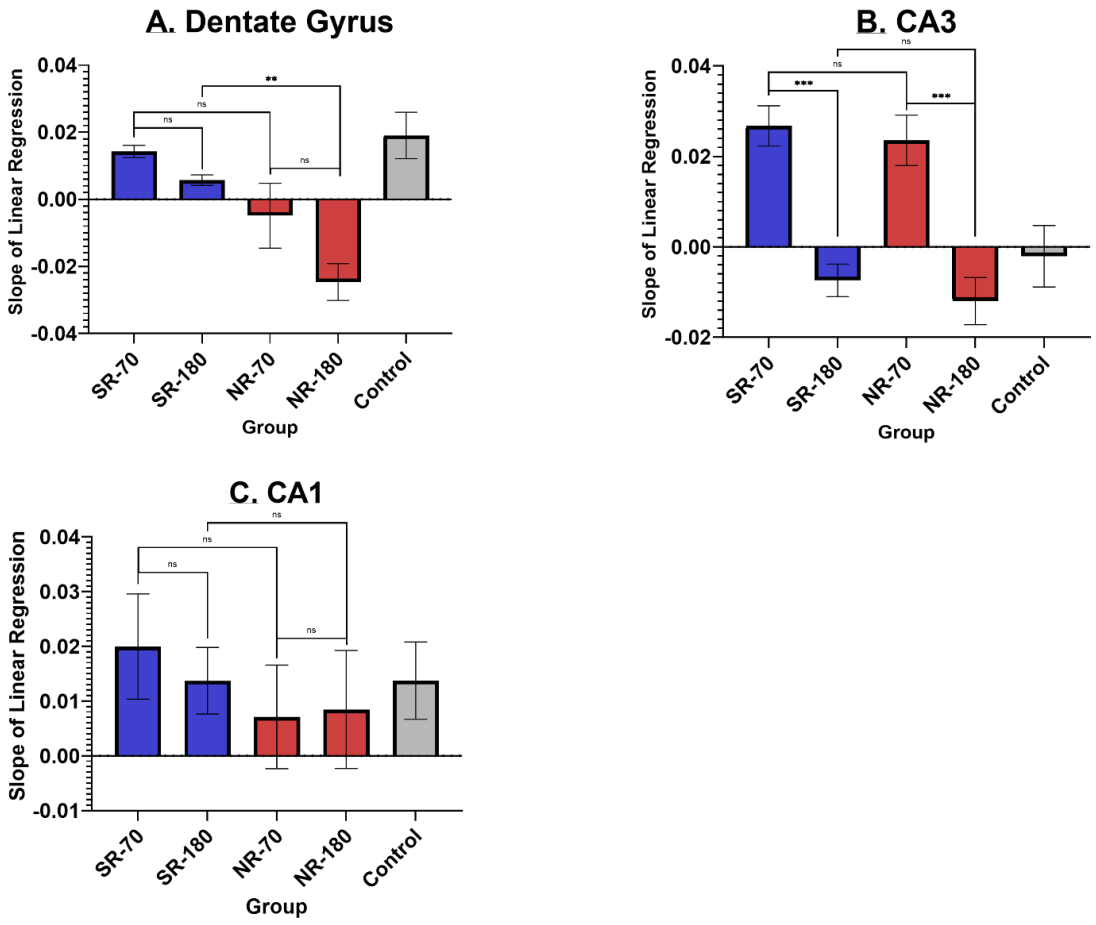

Figure 2.28: Trend analysis of GluA2:GluA1 expression between time points and room conditions along the long axis. A. In the dentate gyrus, significant differences were observed in the trends of GluA2:GluA1 expression along the long axis between the new room 180 minute group, and the same room 70, same room 180, and control groups (SR-70 vs. NR-180: mean difference = 0.3893, $p = 0.0004$; SR-180 vs. NR-180: mean difference = 0.03038, $p = 0.0072$; NR-180 vs. CTR: mean difference = -0.04371, $p < 0.0001$). B. In CA3 significant differences were found in the trends of GluA2:GluA1 expression along the long axis between the same room 70 minute group and same room 180 minute, new room 180 minute, and CTR groups (SR-70 vs. SR-180: mean difference = 0.03415, $p = 0.0004$; SR-70 vs. NR-180: mean difference = 0.03873, $p < 0.0001$; SR-70

vs. CTR: mean difference = 0.02880, p = 0.0032). Significant differences were also found between the new room 70 minute group and same room 180 minute, new room 180 minute, and control groups (SR-180 vs. NR-70: mean difference = -0.03099, p = 0.0014; NR-70 vs. NR-180: mean difference = 0.03557, p = 0.0002; NR-70 vs. CTR: mean difference = 0.02564, p = 0.0107). C. No significant differences were found in the trends of GluA2:GluA1 expression along the long axis of CA1.

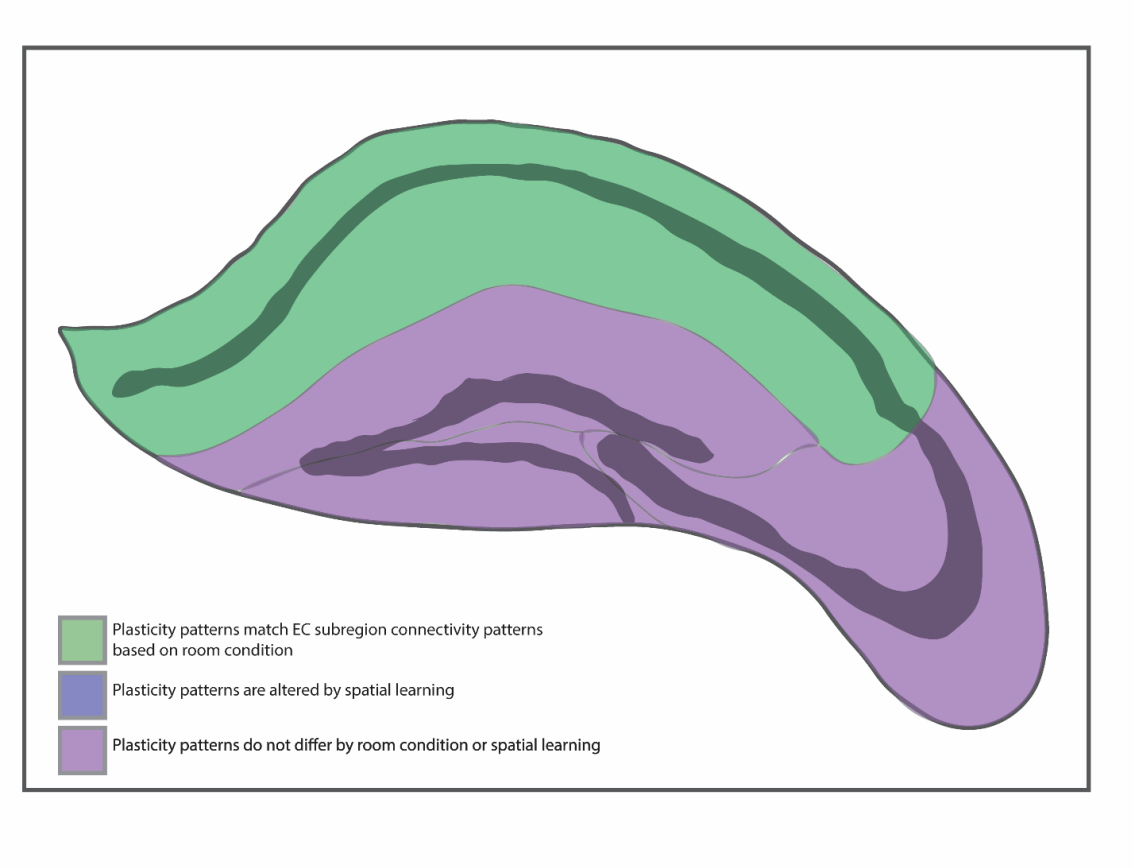

Figure 2.29: Summary of NMDAR expression trends relative to transverse MEC and LEC connectivity patterns to the HPC. In CA1, NMDAR expression patterns differed between room conditions and matched LEC and MEC connectivity patterns. In CA3 and both blades of the DG there was no effect of either room condition or spatial learning in NMDAR expression patterns.

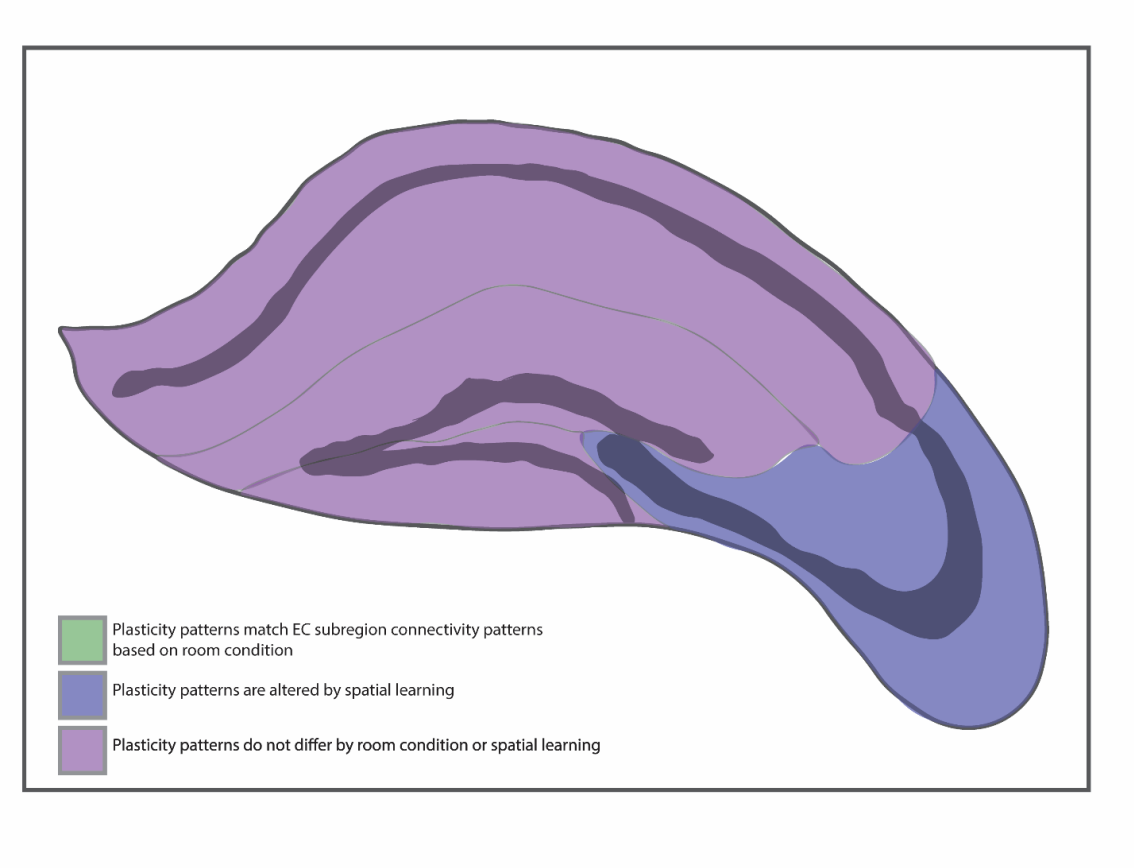

Figure 2.30: Summary of pCaMKII expression trends relative to transverse MEC and LEC connectivity patterns to the HPC. In CA3, pCaMKII expression patterns differed between experimental and control conditions and matched LEC and MEC connectivity patterns. In CA1 and both blades of the DG there was no effect of either room condition or spatial learning in pCaMKII expression patterns.

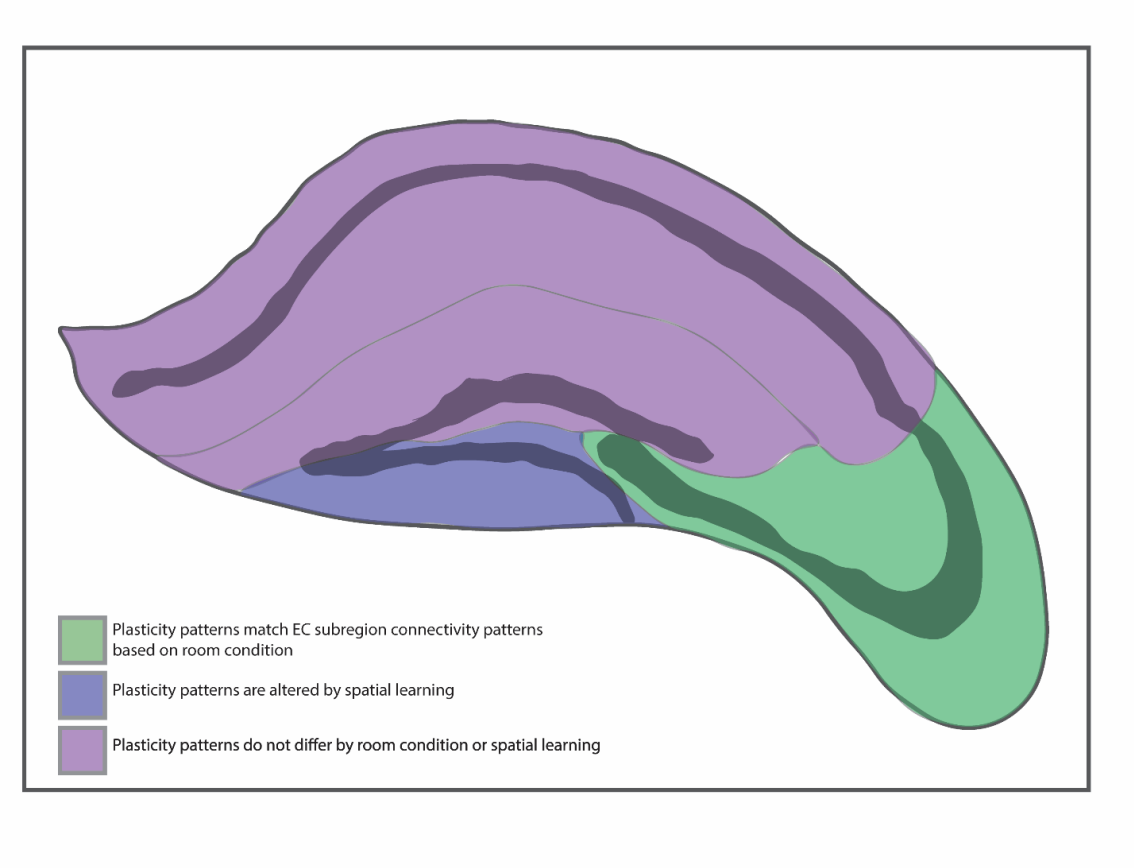

Figure 2.31: Summary of pCREB expression trends relative to transverse MEC and LEC connectivity patterns to the HPC. In CA3, pCREB expression patterns differed between room conditions and matched LEC and MEC connectivity patterns. In CA1 and the suprapyramidal blade of the DG there was no effect of either room condition or spatial learning in pCREB expression patterns. In the infrapyramidal blade, there was an effect of spatial learning that favored MEC-connected regions but no effect of room condition.

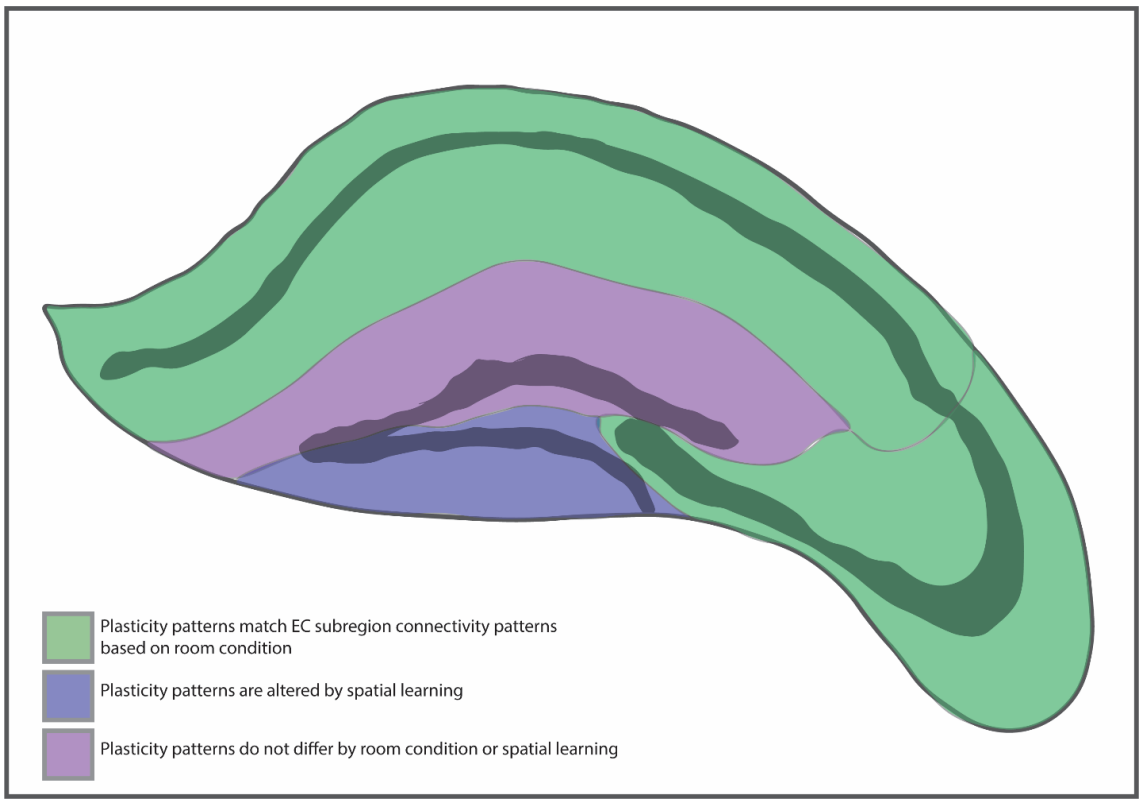

Figure 2.32: Summary of GluA2:GluA1 expression trends relative to transverse MEC and LEC connectivity patterns to subfields of the HPC. In CA1 and CA3, GluA2:GluA1 expression patterns in the same room and new room conditions matched LEC and MEC connectivity patterns, respectively. In the infrapyramidal blade, these expression patterns did not differ by room condition, but they did differ between learning animals and cage controls. In the suprapyramidal blade, there was no effect of either room condition or spatial learning in GluA2:GluA1 expression patterns.

Chapter 3 Figures:

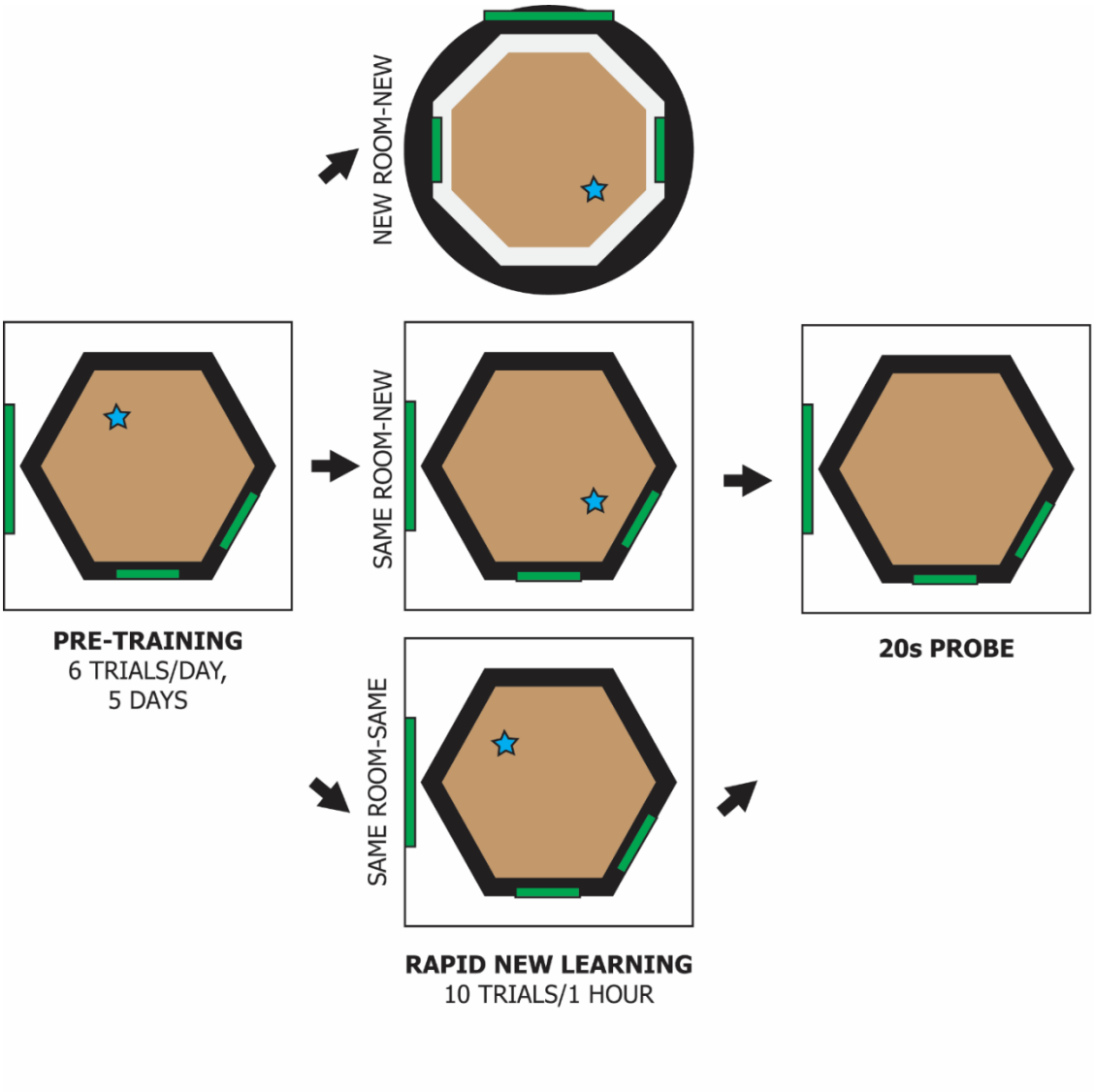

Figure 3.1: Dry land contextual navigation task. All mice underwent pretraining for the DCNT over 5 days with 6 trials per day. During pretraining they learned to find a water reward in an open field spatial navigation task in a consistent location. On the 6th day, the mice were split into three different conditions for rapid new learning: same room same location, same room new location, or new room new location. These conditions varied in the environment that mice learned in and the location of the water reward. In the same

room groups, they underwent new learning in the same room as pretraining, and in the new room group it was a new environment. In the same location group, the water reward was located in the same location as pretraining, and in the new location groups it was moved. On the 7th day, same room same location and same room new location mice underwent a 20 second probe.

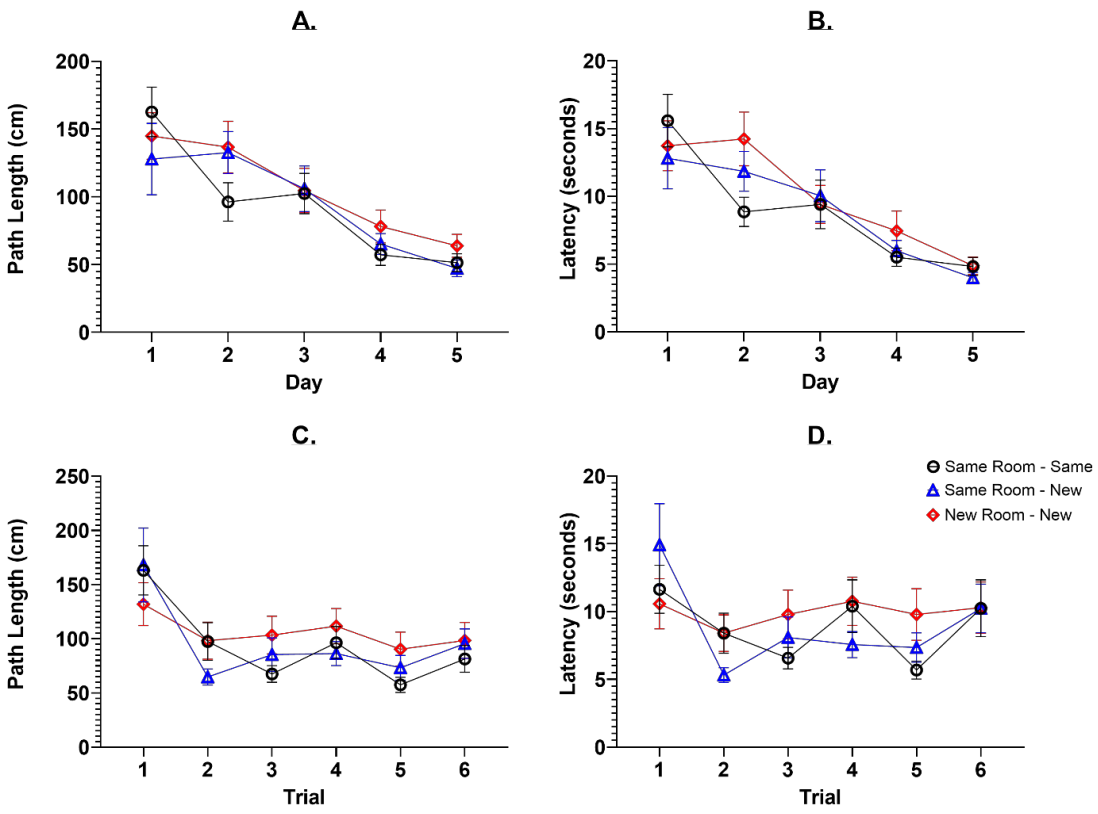

Figure 3.2: Mean path length and latency during pre-training over days or trials in the dry land contextual navigation task. A. Average path length over days of pre-training. A significant effect of days but not room conditions was observed (Day: $F_{4, 733} = 19.26$, $p < 0.0001$; room condition: $F_{2, 733} = 0.9197$, $p = 0.3991$). B. Average latency over days of pre-training. A significant effect of days but not room conditions was observed (Day: $F_{4, 733} = 20.27$, $p < 0.0001$; room condition: $F_{2, 733} = 0.8800$, $p = 0.4152$). C. Average path length over trials of pre-training. A significant effect of trials but not room conditions was observed (Trials: $F_{5, 730} = 8.775$, $p < 0.0001$; room condition: $F_{2, 730} = 0.9080$, $p = 0.4038$). D. Average latency over trials of pre-training. A significant effect of trials but not room conditions was observed (Trials: $F_{5, 730} = 3.847$, $p = 0.0019$; room condition: $F_{2, 730} = 0.8335$, $p = 0.4349$).

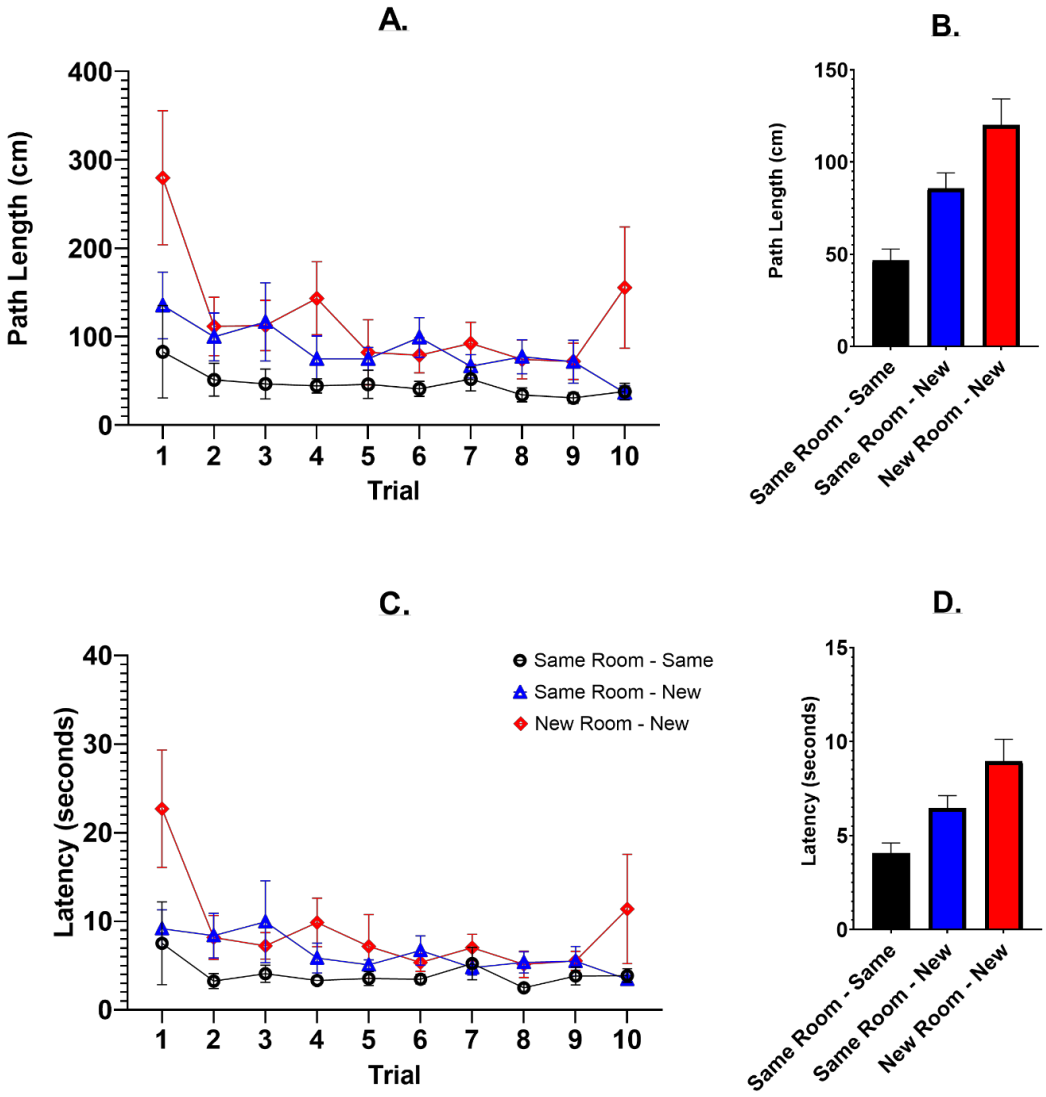

Figure 3.3: Mean path length and latency during new learning over trials or averaged in the dry land contextual navigation task new learning. A. Average path length over trials of new learning. A significant effect of both trial and room condition were observed (Trial: $F_{9, 219} = 2.820$, $p = 0.0037$; room condition: $F_{2, 219} = 13.58$, $p < 0.0001$). No significant interaction was observed. B. Average path length during new learning between groups. Significant differences were observed between the same room same location group and both other groups (SR-S vs. SR-N: mean difference = -39.17, $p = 0.0266$; SR-S

vs. NR-N: mean difference = -73.56, $p < 0.0001$). C. Average latency over trials of new learning. A significant effect of both trial and room condition were observed (Trial: $F_{9, 219} = 2.677$, $p = 0.0057$; room condition: $F_{2, 219} = 8.877$, $p = 0.0002$). D. Average latency during new learning between groups. A significant difference was observed between the same room same location and the new room new location group (SR-S vs. NR-N: mean difference = -4.898, $p = 0.0002$).

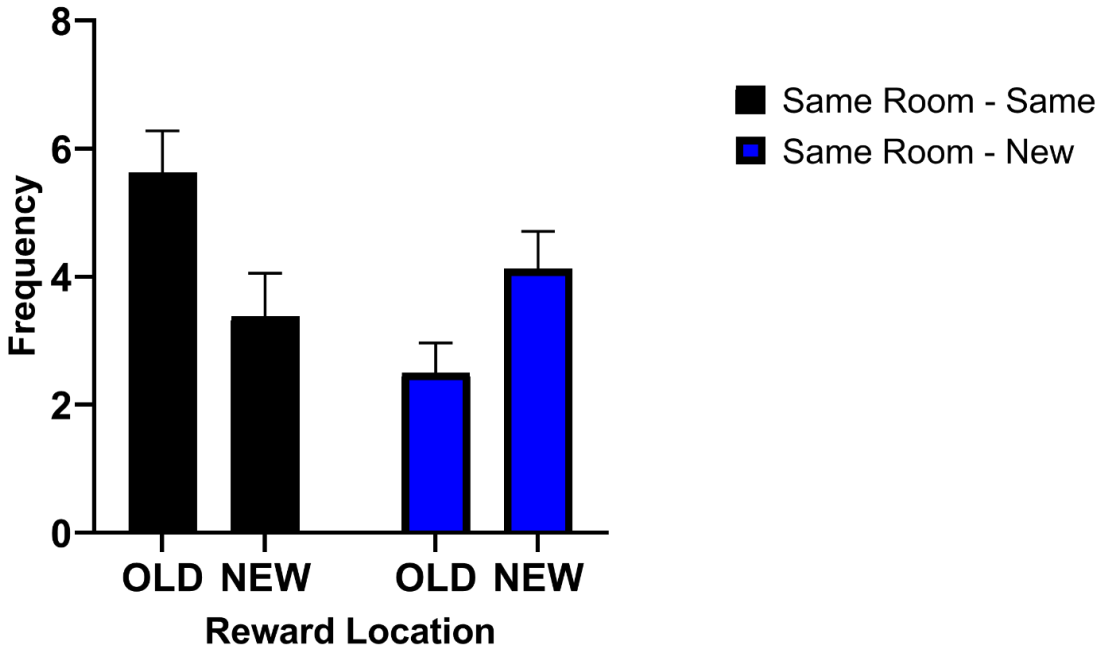

Figure 3.4: Average frequency of reward zone visit during probe trial of the dry land contextual navigation task. We observed a significant interaction between conditions ($F_{1, 28} = 10.43$, $p = 0.0032$), and a significant difference in the frequency of old location visits between conditions (mean difference = 3.125, $p = 0.0058$).

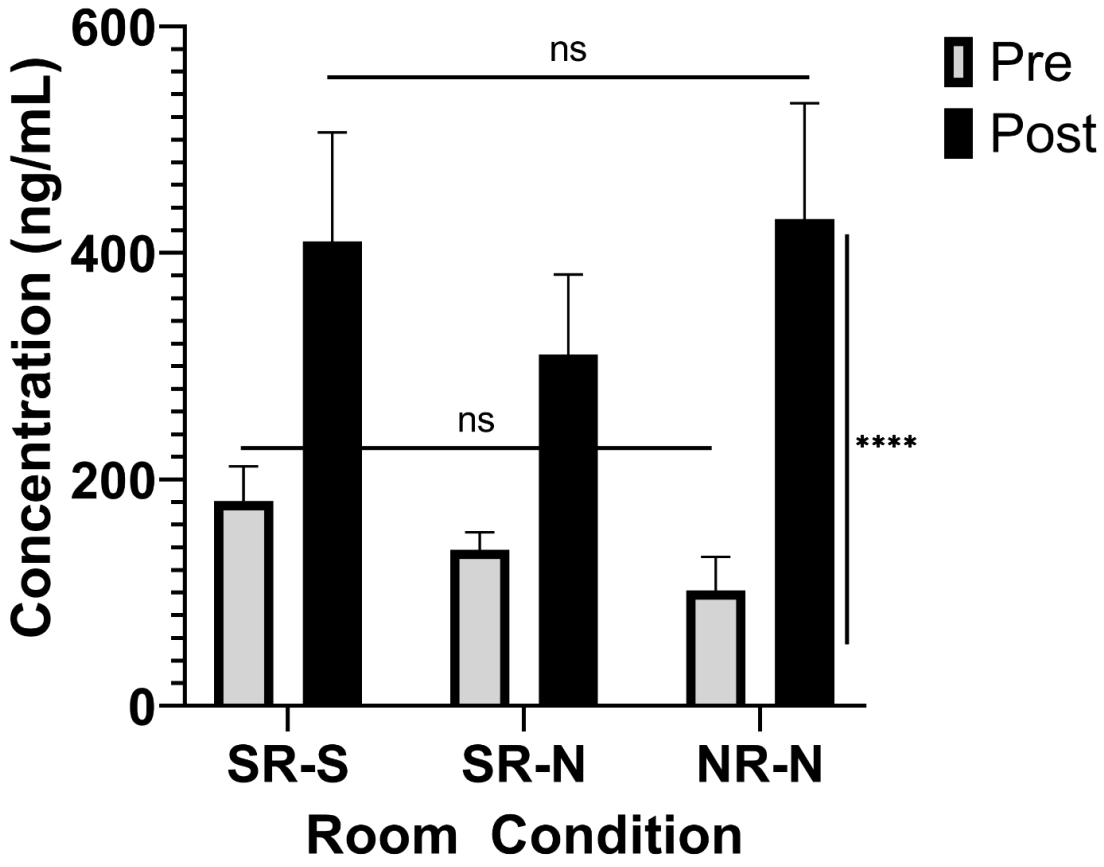

Figure 3.5: Plasma corticosterone levels in mice who underwent the dry land contextual navigation task before pre-training and after new learning. We observed no significant effect of room condition, but we did observe a significant effect of task (Task: $F_{1, 50} = 26.40$, $p < 0.0001$).

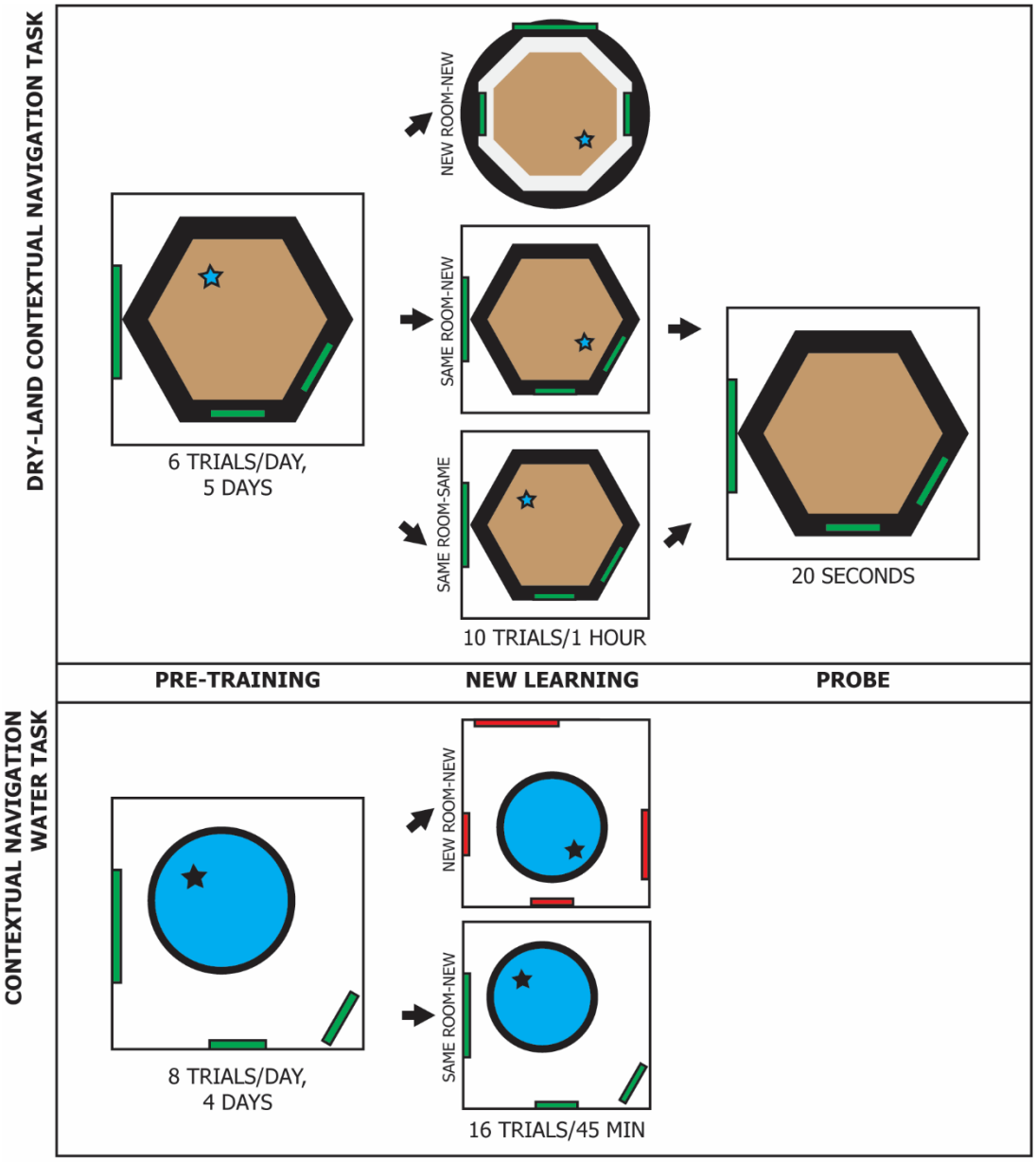

Figure 3.6: Experiment design comparison between DCNT and CNWT. Both tasks have pre-training and new learning phases. They differ in the length of these phases and the conditions during new learning. Furthermore, while we have data for the probe phase of the DCNT, the rats who underwent the CNWT were sacrificed prior to this phase. In the Bye and McDonald version of this task (2019), probe trials are conducted.

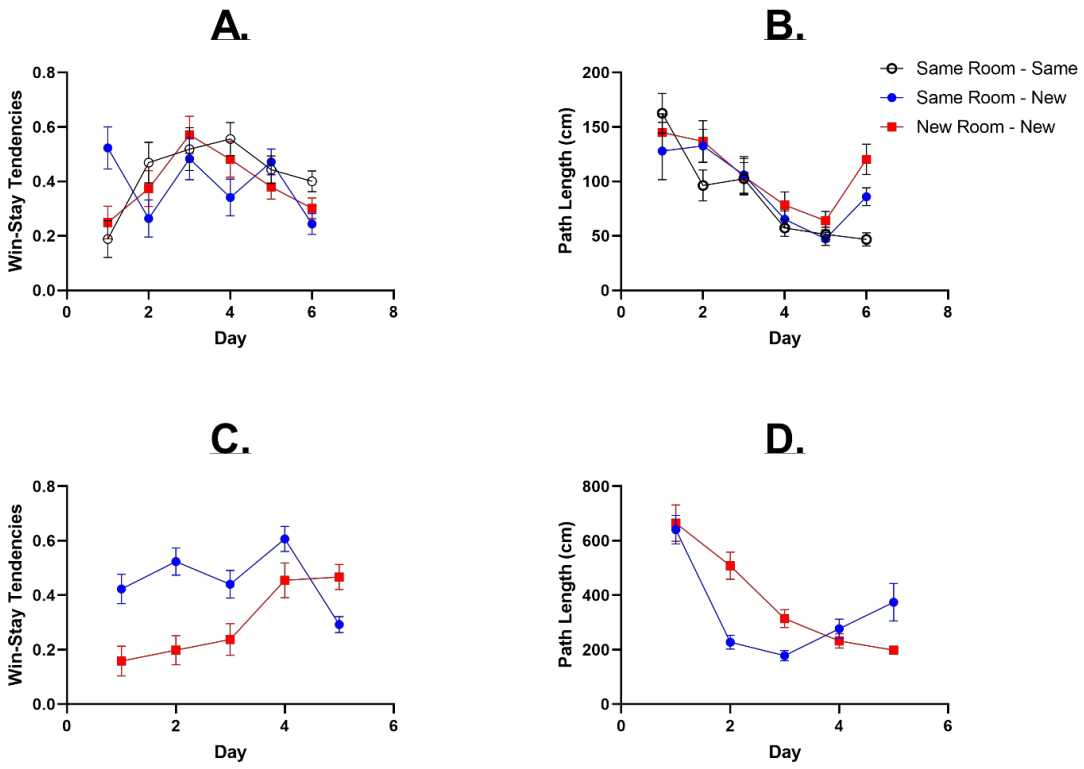

Figure 3.7: Win-stay tendencies and path length between dry land contextual navigation task and contextual navigation water task. A. Average win-stay over days in mice who underwent the DCNT. We observed an effect of day, but no effect of room condition (Day: $F_{5, 718} = 6.173$, $p < 0.0001$; room condition: $F_{2, 718} = 26.40$, $p = 0.4396$). We also observed a significant interaction ($F_{10, 718} = 3.156$, $p = 0.0006$). B. Average path length over days in mice who underwent the DCNT. We observed significant effects of room condition and days (Day: $F_{5, 979} = 16.87$, $p < 0.0001$; room condition: $F_{2, 979} = 3.957$, $p = 0.0215$). We also observed a significant interaction ($F_{10, 979} = 0.0435$, $p = 0.0435$). C. Average win-stay over days in rats who underwent the contextual navigation water task. We observed significant effects of day, room condition, and a significant interaction (Day: $F_{4, 756} = 5.058$, $p = 0.0005$; room condition: $F_{1, 756} = 20.44$, $p < 0.0001$; interaction: $F_{4, 756} = 9.685$, $p < 0.0001$). B. Average path length over days in mice who underwent the

DCNT. We observed significant effects of room condition and days (Day: $F_{5, 979} = 16.87$, $p < 0.0001$; room condition: $F_{2, 979} = 3.957$, $p = 0.0215$). D. Average path length over days in rats who underwent the contextual navigation water task. We observed significant effects of day and significant interaction (Day: $F_{4, 842} = 33.33$, $p < 0.0001$; interaction: $F_{4, 842} = 5.298$, $p = 0.0003$). No significant effect of room condition was found.

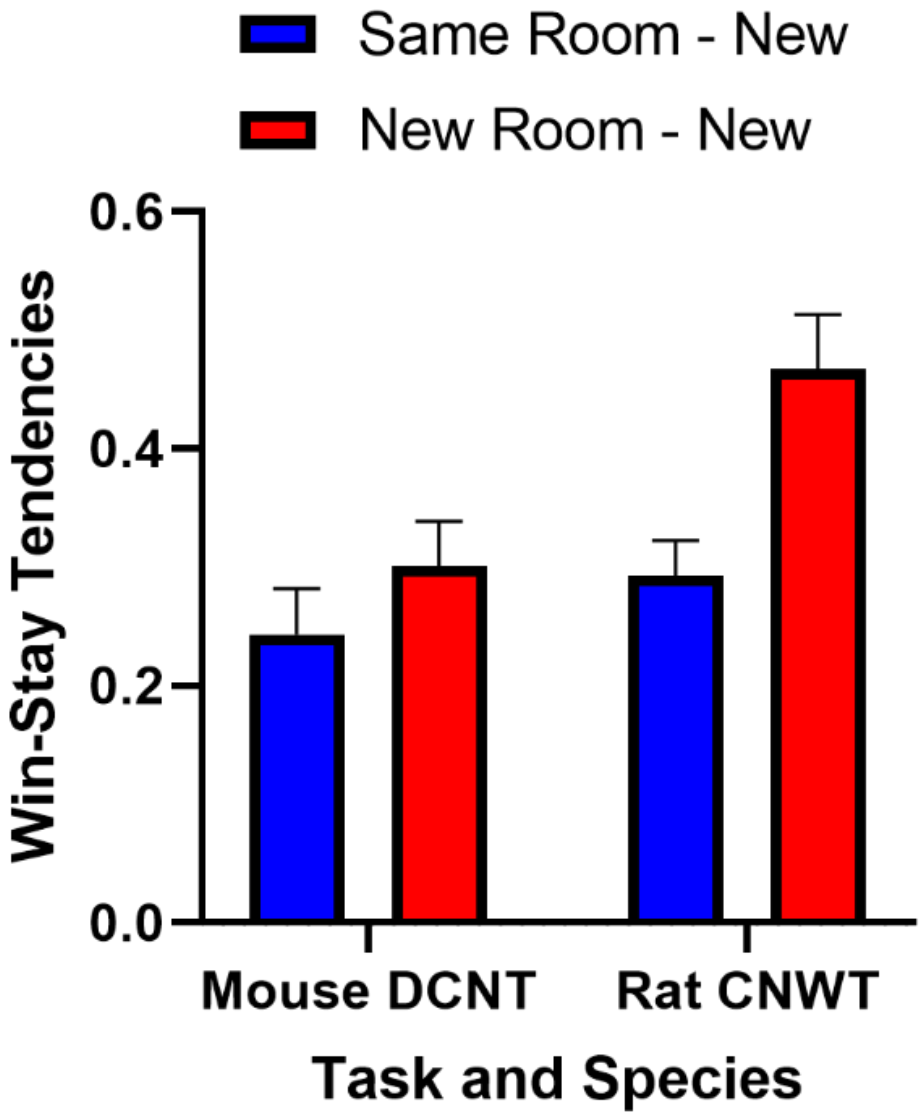

Figure 3.8: Average win-stay tendency in the dry land contextual navigation task or contextual navigation water task during new learning. We observed a significant effect of both task/species, and room condition (Task/species: $F_{1, 400} = 6.816$, $p = 0.0094$; room condition: $F_{1, 400} = 7.910$, $p = 0.0052$). No significant interaction was observed ($F_{1, 400} = 2.005$, $p = 0.1575$).

Chapter 4 Figures:

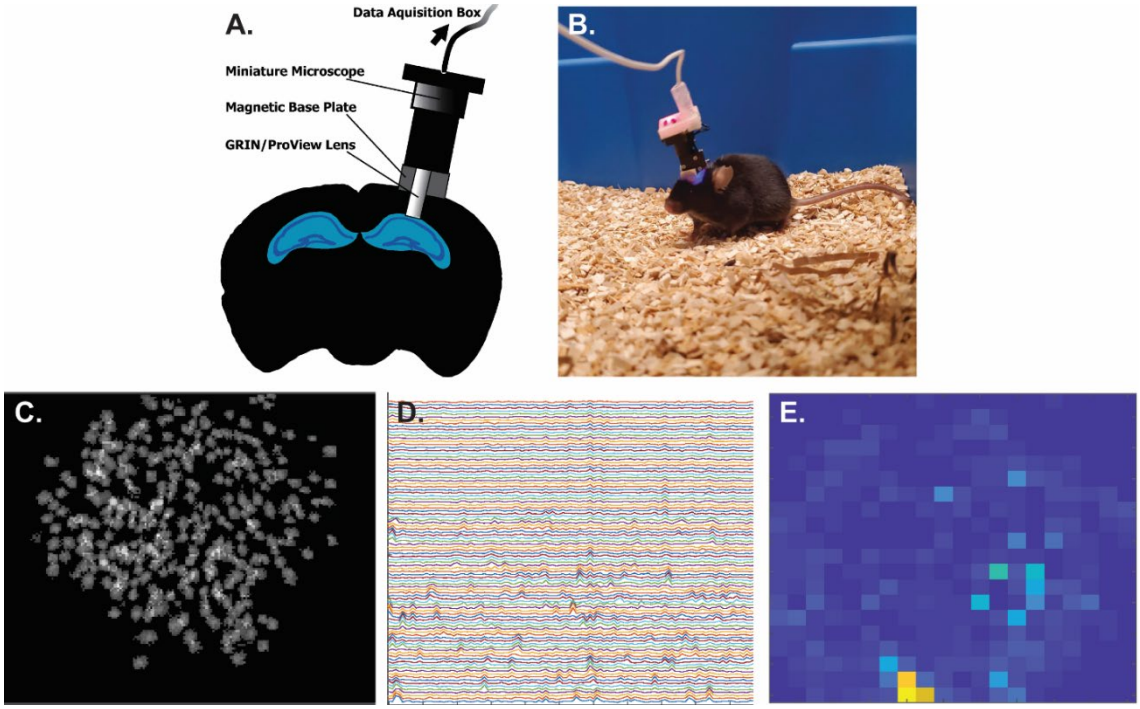

Figure 4.1: Miniaturized microscope imaging samples. A. Schematic of miniscope imaging for dorsal CA1 of the hippocampus. B. Photo of adult mouse outfitted with miniaturized microscope in intertrial context. C. Sample field of view image of cell population active throughout one trial of the DCNT. D. Sample cell traces. E. Sample place field.

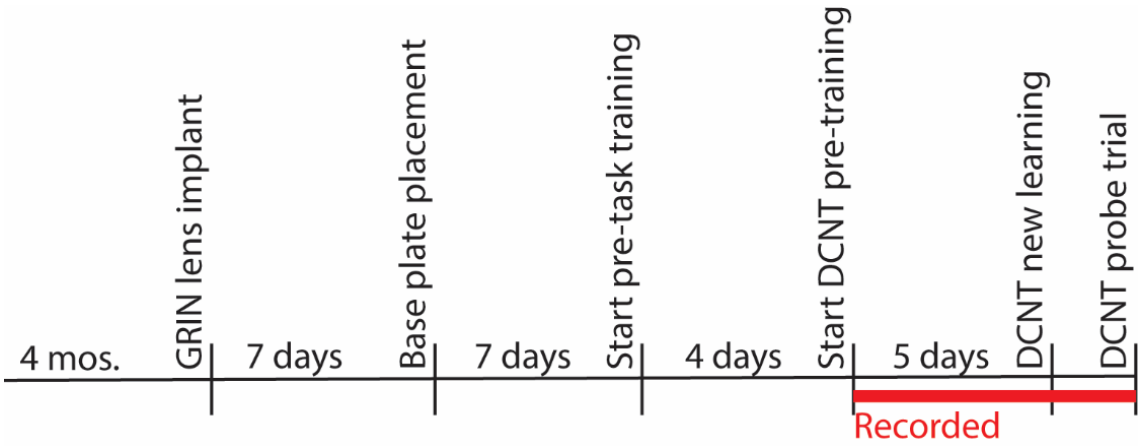

Figure 4.2: Experimental design of the DCNT with miniaturized microscope imaging. Once mice had aged 4 month, they underwent surgery to implant a GRIN lens to image dorsal CA1. 7 days later, they underwent anesthesia again to be outfitted with base plates. 7 days later, pre-task training commenced for 4 days, followed by the DCNT. Recording took place for the entirety of the DCNT.

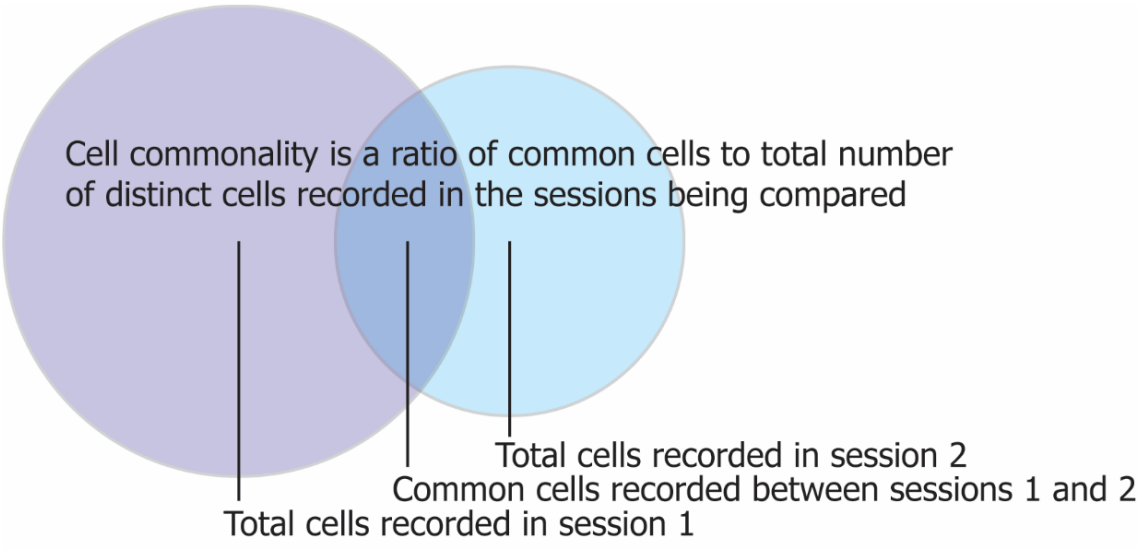

Figure 4.3: Cell commonality ratio schematic. Cell commonality is a ratio of common cells to the total number of distinct cells recorded in the sessions being compared. Cell commonality was calculated as: Cell commonality = (common cells recorded between sessions 1 and 2)/(total cells recorded in session 1 + total cells recorded in session 2 – common cells recorded between sessions 1 and 2). This means that if there was total overlap between two sessions but 1 had a greater number of cells active than 2, then cell commonality = (cells active in session 1)/(cells active in session 2) and would be less than 1. Furthermore, if there was no overlap, cell commonality = 0.

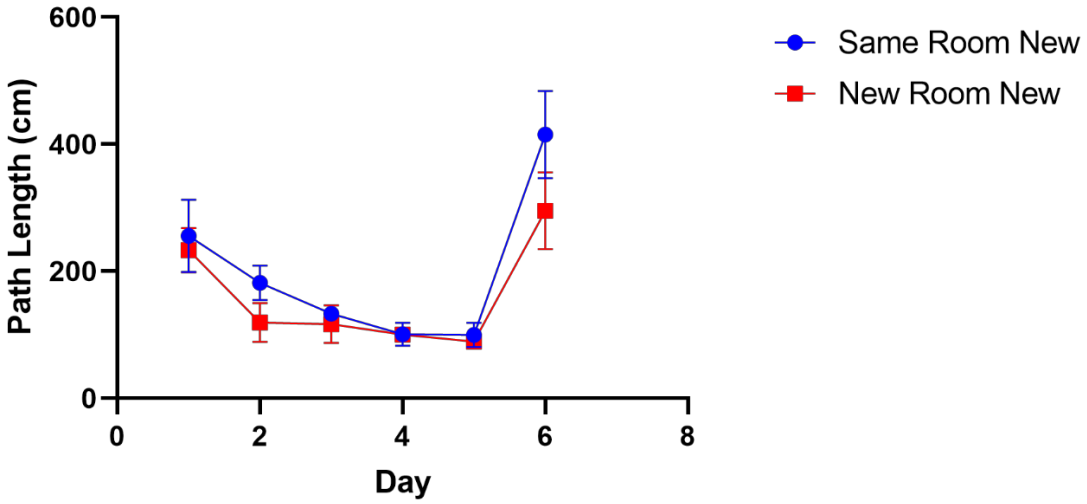

Figure 4.4: Mean path length during all days of dry-land contextual navigation task. A significant effect of days but not room condition was observed (Day: $F_{5, 148} = 11.96$, $p < 0.0001$; room condition: $F_{1, 148} = 2.017$, $p = 0.1577$).

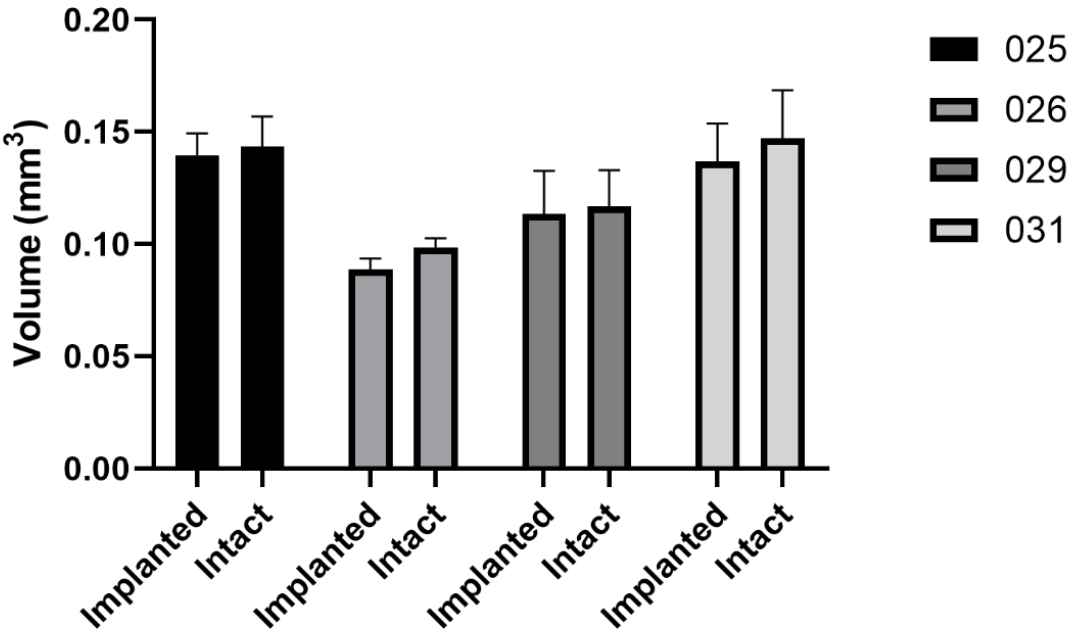

Figure 4.5: Volumetric analysis of implanted and intact hemispheres of the hippocampus. Average volume of slices within the implanted region are reported here. No effect of implantation was observed ($F_{3, 56} = 41.36$, $p < 0.0001$).

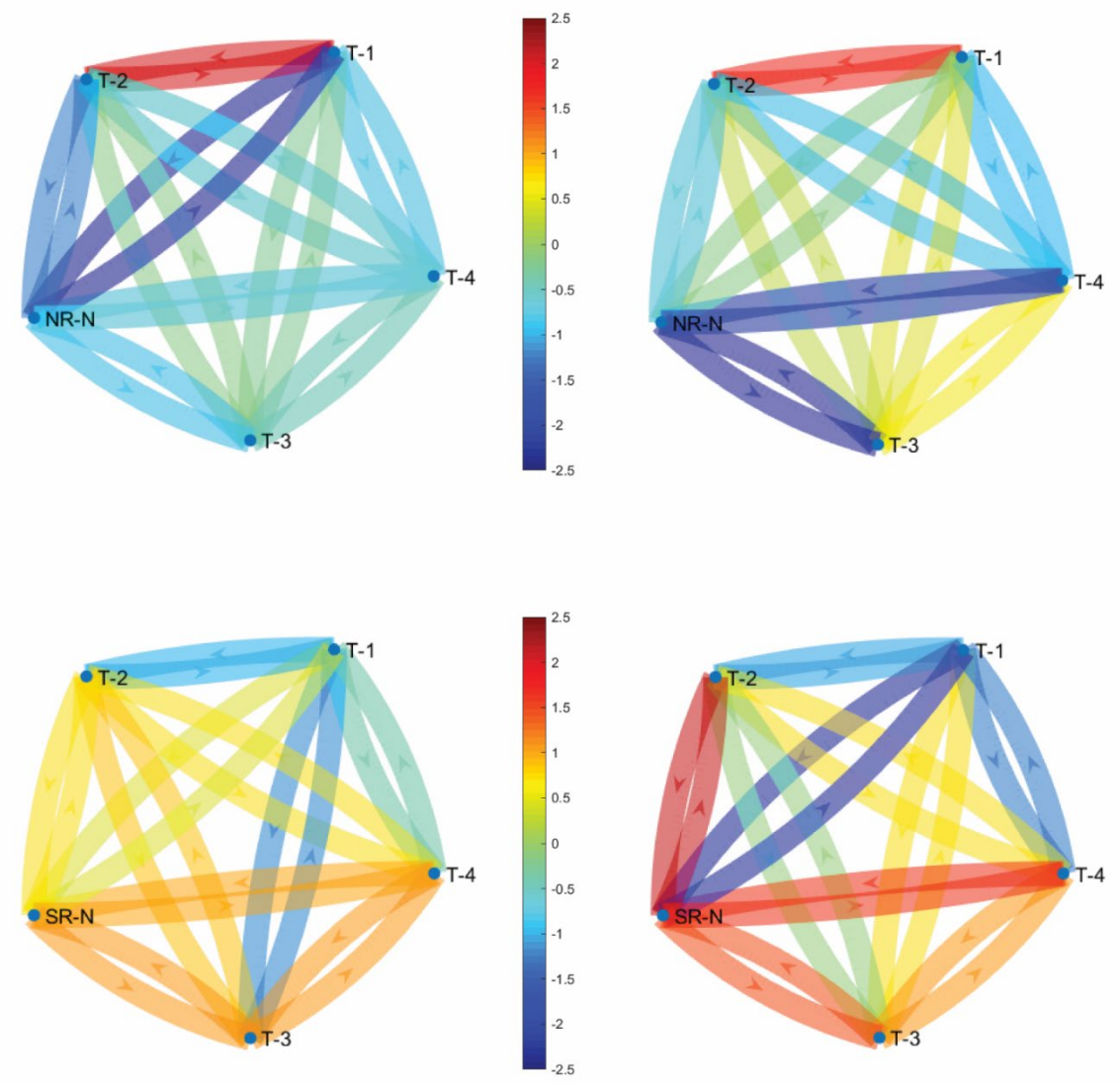

Figure 4.6: Network diagram of cell commonality z scores between days of dry-land contextual navigation task in each animal recorded. Each network diagram is a different animal. The coloured lines show a Z-score of the cell commonality, and blue is less common and red is more common. Each node is a day of the task, from pretraining (T-1, T-2, T-3, T-4) to new learning (NR-N or SR-S). The new learning condition can be identified as either new room (NR-N) or same room (SR-S). In the new room condition

(upper two panels) we observed significantly less commonality between new learning and pre-training days. In the same room condition (lower two panels) we observed either no significant or significantly more commonality between new learning and pre-training days.

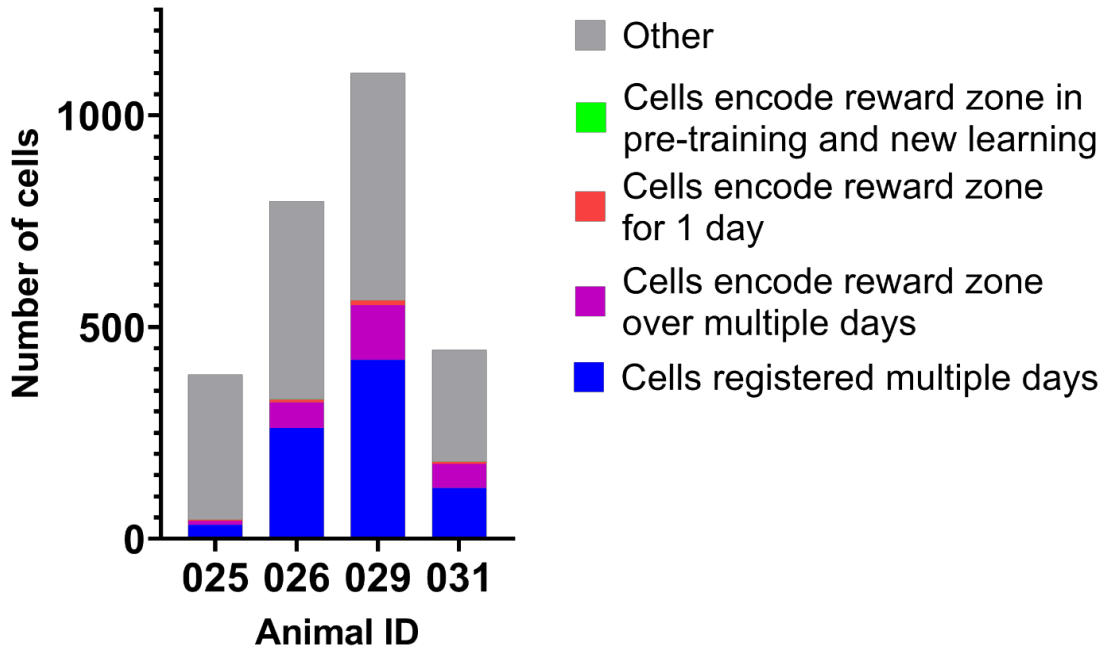

Figure 4.7: Distribution of cellular representations in recorded animals. Here we show the distribution of place cells registered over multiple days, and cells whose place fields overlap with the pre-training reward region. On average, 30.7% of total cells were registered over multiple days (mean = 209.5, SEM = 85.39), 9.33% of total cells had place fields that overlapped with the reward zone during multiple days of pre-training (mean = 63.75, SEM = 24.69), 0.952% of total cells had place fields that overlapped with the reward zone for 1 day (mean = 6.5, SEM = 1.707), and only 0.037% of total cells had place fields that overlapped with both the pre-training and new learning reward zone (mean = 0.25, SEM = 0.25).

APPENDIX 2: SUPPLEMENTARY FIGURES FROM CHAPTER 2, EXPERIMENT 3

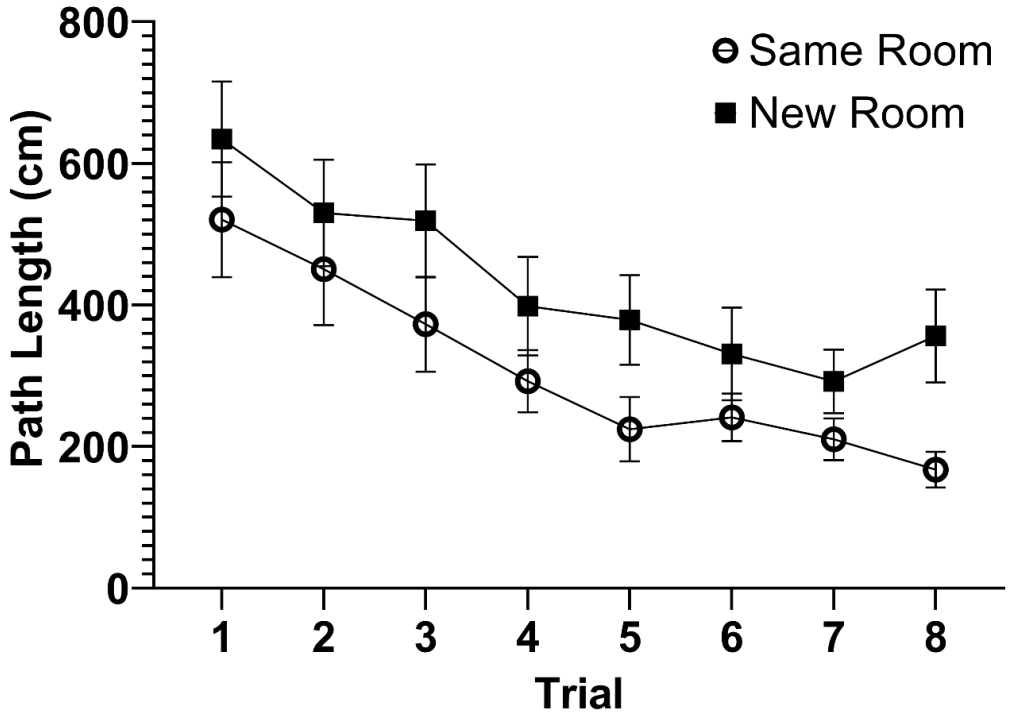

Figure S1: Average path length across training days per trial during training. A significant decrease in latency to platform over trials of training was observed ($F_{7, 752} = 7.473$, $p < 0.0001$). A significant effect of group was also found ($F_{7, 752} = 8.768$, $p = 0.0001$), however multiple comparisons did not show significant differences between the groups at any of the trials.

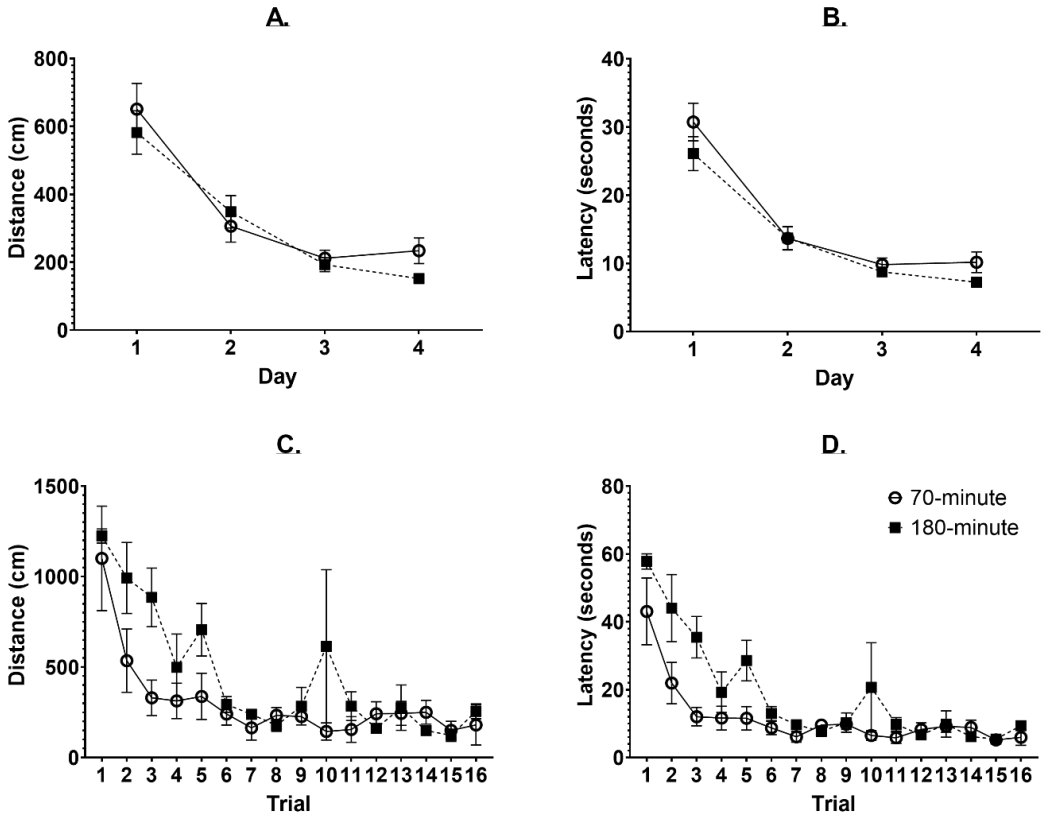

Figure S2: Pre-training and new learning behaviour in animals sacrificed at either 70 or 180 minutes. A. Average path length across trials per training day. A significant learning effect was observed ($F_{3, 514} = 8.768$, $p < 0.0001$). No effect of group was found ($F_{1, 514} = 0.9190$, $p = 0.3382$). B. Average latency across trials per training day. A significant learning effect was observed ($F_{3, 514} = 57.11$, $p < 0.0001$). No effect of group was found ($F_{1, 514} = 2.973$, $p = 0.0853$). C. Average path length during new learning. A significant learning effect was observed ($F_{15, 96} = 8.861$, $p < 0.0001$). While there was an effect of group ($F_{1, 96} = 9.998$, $p = 0.0021$), multiple comparisons only showed significant differences in trial 3 ($p = 0.0490$). D. Average latency during new learning. A significant learning effect was observed ($F_{15, 96} = 14.86$, $p < 0.0001$. While there was an effect of

group ($F_{1, 96} = 19.36$, $p < 0.0001$), multiple comparisons only showed significant differences in trials 2 and 3 (Trial 2: $p = 0.0096$; Trial 3: $p = 0.0046$).